

A Thesis Submitted for the Degree of PhD at the University of Warwick

Permanent WRAP URL:

<http://wrap.warwick.ac.uk/134056>

Copyright and reuse:

This thesis is made available online and is protected by original copyright.

Please scroll down to view the document itself.

Please refer to the repository record for this item for information to help you to cite it.

Our policy information is available from the repository home page.

For more information, please contact the WRAP Team at: wrap@warwick.ac.uk

STEREOCHEMICAL AND TRAPPING STUDIES OF BIRADICALS

A thesis submitted for the degree of
Doctor of Philosophy

by

Andrew John Francis Edmunds

Department of Chemistry
University of Warwick

December 1986

To my parents

Chapter 1

1.1	Introduction	1
1.2	Theoretical description of biradicals	1
1.3	Photochemistry	5
1.3.1	Photophysical processes	5
1.3.2	Photochemical reactions	7
1.3.3	Photochemistry and biradicals	10
1.4	Detection and characterisation of biradicals	12
1.4.1	Spectroscopic studies	13
1.4.2	Chemical trapping	20
1.4.3	Stereochemical studies (1)	24
1.4.4	Thermokinetic and theoretical studies	29
1.4.5	Stereochemical studies (2). Biradical commonality	36
1.4.6	Stereochemical studies (3). Factors affecting biradical stereochemical behaviour	41
1.4.6.1	Effect of spin state	41
1.4.6.2	Effect of substitution	44
1.4.6.3	Effect of temperature	46
1.5	Summary	47

Chapter 2

2.1	Introduction	49
2.2	Bicyclic and polycyclic azoalkanes that generate 1,3-biradicals	49
2.3	Bicyclic and polycyclic azoalkanes that generate 1,4-biradicals	58
2.4	2,3-Diazabicyclo[2.2.2]oct-2-ene (DBO).	64
2.4.1	Pyrolysis of bicyclohexane	64
2.4.2	Thermal decomposition of DBO	76
2.4.2.1	Application of the Ramsperger criterion to DBO decomposition	76
2.4.2.2	Stereochemical studies	79
2.4.3	Photochemical decomposition of DBO	86
2.4.3.1	Photophysical studies	86
2.4.3.2	Application of the Ramsperger criterion to direct photochemical decomposition of DBO's.	88
2.4.3.3	Stereochemical studies	90
2.5	Summary	92
2.6	Scope of this work: General strategy involved in studying the stereochemistry of DBO decomposition.	93

Chapter 3

3.1	Synthesis and stereochemical assignments of DBO and its precursor	97
3.1.1	^1H NMR stereochemical assignments	98
3.1.2	Synthesis of stereoselectively labelled d_2 -DBO (1).	102
3.2	Synthesis of stereoselectively labelled d_2 -DBO (2).	105
3.3	Determination of deuterium content	115
3.4	Summary	122

Chapter 4

4.1	Introduction	124
4.2	Hydrocarbon products. Stereochemical assignments	124
4.3	Stereochemistry of the direct photolysis	126
4.4	Double inversion of BCH stereochemistry. Confirmation of results	129
4.5	Stereochemistry of the photosensitised decomposition	135
4.6	Discussion	137
4.7	Synthesis of 1,4-dimethyl-2,3-diazabicyclo[2.2.2]oct-2-ene (DMDBO).	141
4.8	Stereochemical assignments in DMDBO	143
4.9	Synthesis of stereoselectively labelled d ₂ -DMDBO	147
4.10	Photophysics of the direct and sensitised photolysis of DMDBO	148
4.11	Product stereochemical assignments	148
4.12	Direct and sensitised photolysis of stereoselectively labelled d ₂ -DMDBO	150
4.13	Discussion	154
4.14	Summary	157

Chapter 5

5.1	Introduction	158
5.2	Cleavage kinetic isotope effects	158
5.2.1	Discussion	160
5.2.2	Bicyclohexane pyrolysis. Measurement of intramolecular KIE's	163
5.2.2.1	Synthesis of 2,2,3,3-[² H] ₄ -bicyclo[2.2.0]hexane (d ₄ -BCH)	163
5.2.2.2	Isolation of 2,3-[² H] ₂ -bicyclo[2.2.0]hexane from d ₂ -DBO photolysis mixtures	166
5.2.2.3	Discussion	169
5.3	Proportions of EE-, EZ-, and ZZ- 1,6-[² H] ₂ -hexa-1,5-dienes from photochemical decomposition of d ₂ -DBO	170
5.3.1	Method of analysis	170
5.3.2	Synthesis of EE-1,6-bis-phenylsulphonylhexa-1,5-diene	175
5.3.3.1	Determination of disulphone deuterium content	177
5.3.3.2	Relationship of disulphone deuterium content to hexa-1,5-diene stereochemistry	178
5.4	Results	180
5.4.1	Control experiments. Secondary KIE's	182
5.4.2	Control experiments. Deuterium wash-out	183
5.5	Discussion	189

5.6	Comparison of DBO photochemical decomposition with BCH pyrolysis	193
5.6.1	Preparation of stereoselectively labelled d ₂ -BCH	195
5.6.2	Pyrolysis of d ₂ -BCH	196
5.6.3	Discussion	197
5.6.4	BCH pyrolysis and DBO photolysis. Common biradical intermediates	199
5.6.5	The cyclohexane-1,4-diyl potential energy surface	200
5.6.5.1	Through-bond and through-space interactions in biradicals	200
5.6.5.2	Stereoselective cleavage; chair or 90°-twist diyl intermediates	205
5.7	Summary	208
5.8	The Cope rearrangement of hexa-1,5-diene	209
5.8.1	Concerted versus stepwise mechanisms. Thermokinetic studies	210
5.8.2	Concerted versus stepwise mechanisms. Use of secondary KIE's to locate transition states	211
5.8.3	Summary	213

Chapter 6

6.1	Introduction	215
6.2	Occurrence of cyclohexenes	215
6.2.1	Direct photochemical decomposition of DBO and DMDBO	216
6.2.2	Photosensitised decomposition of DBO and DMDBO	217
6.2.3	Pyrolysis reactions	217
6.3	Discussion	218
6.3.1	Different electronic states of a biradical. TS and TB interactions	221
6.4	Stereochemistry and mechanism of formation	222
6.4.1	Discussion	226
6.5	Summary	228

Chapter 7

7.1	Introduction	229
7.2	Photochemical rearrangement of 3,3-dimethyl-6-methylenecyclohexa-1,4-diene (153)	229
7.3	Trimethylenemethanes (TMM's)	232
7.3.1	Strain protected TMM's	233
7.3.1.1	Singlet 2-alkylidene-cyclopentane-1,3-diyls	234
7.3.1.2	Trapping of singlet diyls	235
7.4	Involvement of TMM biradicals in the photochemical rearrangement of (153)	237
7.4.1	Synthesis of 3,3-dimethyl-6-methylenecyclohexa-1,4-diene (153)	237
7.4.2	Photolysis of 3,3-dimethyl-6-methylenecyclohexa-1,4-diene in the presence of biradical traps	238
7.4.3	Discussion	240
7.4.4	Detailed analysis of photoadduct mixtures	242
7.4.4.1	Independent synthesis of Diels-Alder adducts	243
7.4.4.2	Analysis of photoadduct mixtures	246
7.4.5	Discussion	248

Chapter 8

Experimental

General notes	250
Experimental for Chapter 3	250
Experimental for Chapter 4	260
Experimental for Chapter 5	268
Experimental for Chapter 6	280
Experimental for Chapter 7	284

<u>References</u>	291
-------------------	-----

Appendices

Appendix 1	306
Appendix 2	309
Appendix 3	312
Appendix 4	315
Appendix 5	316
Appendix 6	320

SUMMARY

The work in this thesis can be divided into two parts.

1) Stereochemical studies

Irradiation of cis-anti-5,6- $[\text{}^2\text{H}]_2$ -2,3-diazabicyclo[2.2.2]oct-2-ene

(d_2 -DBO) leads to bicyclo[2.2.0]hexane (BCH) in which the deuterium is predominantly exo, i.e. double inversion of configuration, and hexa-1,5-diene (HD) with equal amounts of cis and trans deuterium. In addition, direct photolysis affords small amounts of cyclohexene formed via a stereoselective 1,3-shift. The proportions of EE-, EZ-, and ZZ- d_2 -HD's were not accessible by direct spectroscopic methods but could be obtained by a chemical method combined with mass spectrometry. Stereoselective substitution at the 1,6-positions, in which Z-deuterium was lost and E-deuterium retained, translated stereochemical information into deuterium content. The results of the analysis showed that the EZ-isotopomer was formed predominantly, but significant amounts of EE- and ZZ-isotopomers were also present. The results are compared to the pyrolysis stereochemistry of stereoselectively labelled d_2 -BCH and the known stereochemistry for the deazetation of DBO. A mechanism is proposed that accounts for all the observations.

2) Trapping studies

While triplet biradicals have been intercepted by a wide range of biradical traps only one case of singlet biradicals, 2-alkylidenecyclopentane-1,3-diyls, are sufficiently long-lived to undergo intermolecular reactions. Related singlet biradicals have been proposed as intermediates in the photochemical rearrangement of a cyclic triene, 6-methylene-3,3-dimethylcyclohexa-1,4-diene. When the triene was irradiated in the presence of olefins, 1:1 triene:olefin adducts could be isolated. Their structure was established by X-ray diffraction, spectroscopy, and independent synthesis. The mechanism of their formation is discussed.

ACKNOWLEDGEMENTS

I wish to express my sincere gratitude to my supervisor, Dr. Christopher J. Samuel, for his continued advice and encouragement throughout the course of this study.

My thanks are also due to Dr. O.W. Howarth and Dr. E.H. Curzon for the measurement of high field NMR spectra.

Thanks are also due to the technical staff of the Chemistry Department and Mrs Sandra Beaufoy for her excellent typing of this thesis.

I am indebted to the S.E.R.C. for the award of a studentship.

Finally, I wish to thank my parents for all the help they have given me over the years of my education.

Abbreviations

1. ABHI 7-Azabicyclo[2.2.1]heptane N-imide
2. BCH Bicyclo[2.2.0]hexane
3. BCP Bicyclo[2.1.0]pentane
4. DBD 7,8-Diazabicyclo[4.2.2]dec-7-ene
5. DBN 6,7-Diazabicyclo[3.2.2]non-6-ene
6. DBO 2,3-Diazabicyclo[2.2.2]oct-2-ene
7. DEAD Diethylazodicarboxylate
8. DIAD Diisopropylazodicarboxylate
9. DMBCH 1,4-Dimethylbicyclo[2.2.0]hexane
10. DMCHD 1,4-Dimethylcyclohexa-1,3-diene
11. DMDBO 1,4-Dimethyl-2,3-diazabicyclo[2.2.2]oct-2-ene
12. ISC Inter system crossing
13. LFP Laser flash photolysis
14. PTAD 4-Phenyl-1,2,4-triazoline-3,5-dione
15. SCE Spin correlation effect
16. VFP Vacuum flash pyrolysis

CHAPTER 1

1.1 Introduction

Traditionally, the organic chemists' symbolism and thinking have been closely correlated with the treatment of closed shell molecules, that is, molecules with electrons paired in low lying molecular orbitals. This attitude has broadly changed with the development of mechanistic organic photochemistry, and the introduction of orbital symmetry considerations in the treatment of organic reactions.¹ The importance of high energy intermediates in the form of biradicals, with two "unpaired" electrons, was recognised. Biradicals have therefore taken a central role as (hypothetical) intermediate stages in the description of photochemical reactions, as well as those ground state reactions that, on the basis of symmetry or geometry, have been classed as thermally disallowed.

In this Chapter we develop the meaning of the term biradical. This includes a theoretical description and formal definition. Since most, if not all, unimolecular photochemical reactions involve intermediate stages in the form of biradicals, we reiterate some basic photochemical principles and consider the relationship between photochemical excited states and biradicals. We also give examples of some techniques used to study these elusive species, and evidence for their existence as true reaction intermediates. We conclude the Chapter with some of the factors that affect their reactivity.

1.2 Theoretical description of biradicals

Biradicals can be considered to arise from the one bond homolysis of, for example, a closed shell molecule in its ground

state. Salem and Rowland² have discussed how the biradical properties can be derived by consideration of the interaction between the two electrons in two nearly degenerate orbitals.

The ultimate biradical would be a bifunctional system in which the two radical centres (electrons in, for example, atomic orbitals with wavefunctions ϕ_A and ϕ_B) behave quite independently of each other. If the radical centres interact, molecular orbitals (with wavefunctions ψ_1 and ψ_2) embracing both centres develop. For weak interactions, the energy separation of the molecular orbitals is small (they are essentially non-bonding) and the electrons can be distributed between the two orbitals to give a triplet (T) and three singlet states (S_0 , S_1 , and S_2). This situation is represented diagrammatically in Figure 1.1(a). The wavefunctions of the singlet states can only properly be described by superposition of the three states shown in Figure 1.1(a). For such weak interactions, the molecular orbital energy difference ($E\psi_2 - E\psi_1$) is small, and a ground state triplet would be expected on the basis of Hund's rule. If the interaction between the radical centres increases, the molecular orbitals obtain some bonding and anti-bonding character, and the electrons pair off in ψ_1 . This situation is represented in Figure 1.1(b).

Figure 1.1a) Weakly interacting radical centres

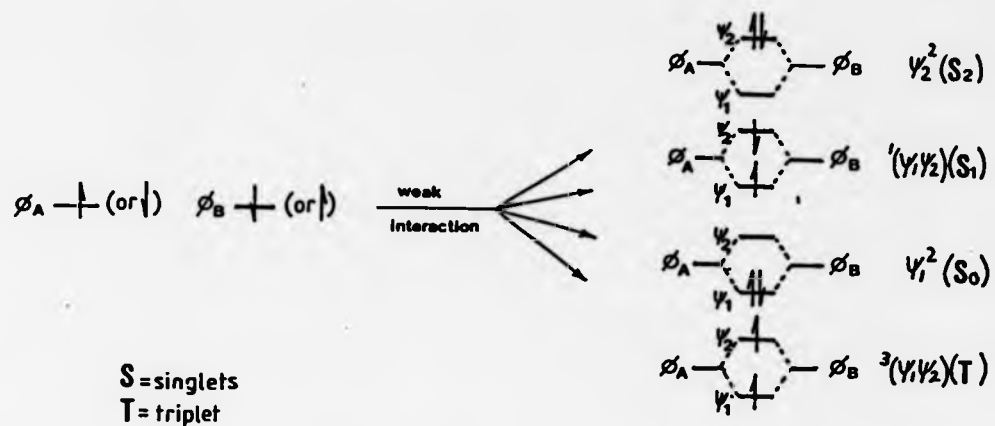
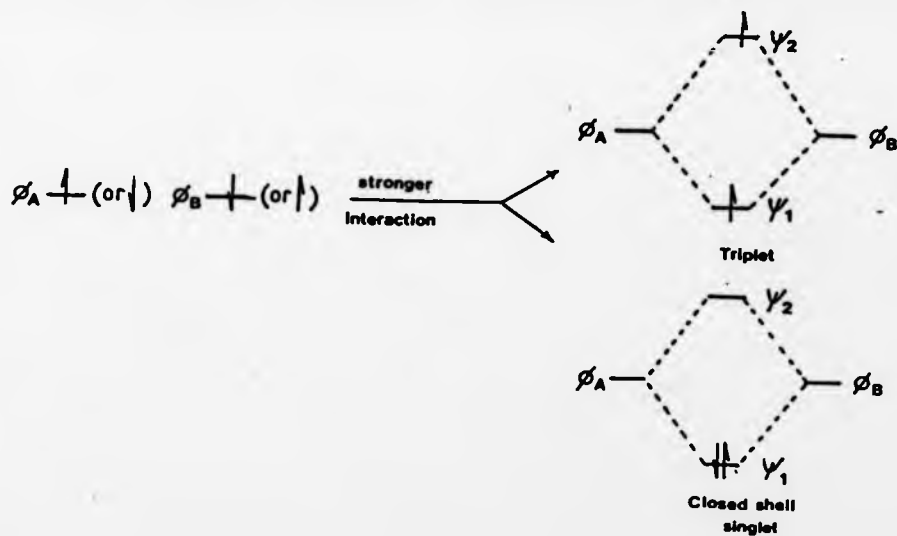


Figure 1.1b) Strongly interacting radical centres



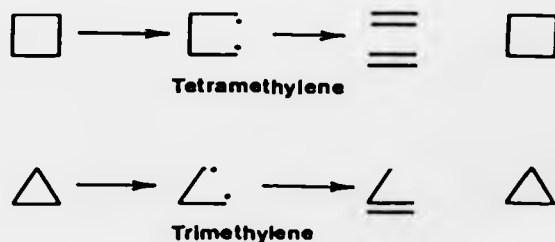
ϕ_A, ϕ_B : Wavefunctions of localised atomic orbitals

$\psi_1\psi_2$: Wavefunctions of orbitals formed by linear combination of ϕ_A and ϕ_B .

The singlet state now has closed shell character and is lower in energy than the triplet state. Thus, the energetic ordering of the states is reversed as the interaction between the radical centres increases. The point where this reversal of state energies occurs is ill-defined. Salem and Rowland² suggested that the term "biradical" should be restricted to the case where interaction between the radical centres is weak. This led to Salem and Rowland defining a biradical as "a species containing two unpaired electrons in two nearly degenerate and non-bonding molecular orbitals".

A wide variety of superficially different species can be classified as biradicals under this definition. These include carbenes³ (1,1-biradicals) and antiaromatic annulenes⁴, such as cyclobutadiene. Biradicals of particular interest to this work are conjugated hydrocarbons for which no classical Kekulé structures can be written, such as trimethylenemethane, and intermediates or transition states in reactions that are non-concerted by virtue of geometry or symmetry considerations. This latter class of compounds includes biradicals such as trimethylene and tetramethylene, the proposed intermediates in the pyrolysis of cyclopropane and symmetry forbidden cycloreversion of cyclobutane, respectively (Scheme 1.1).

Scheme 1.1



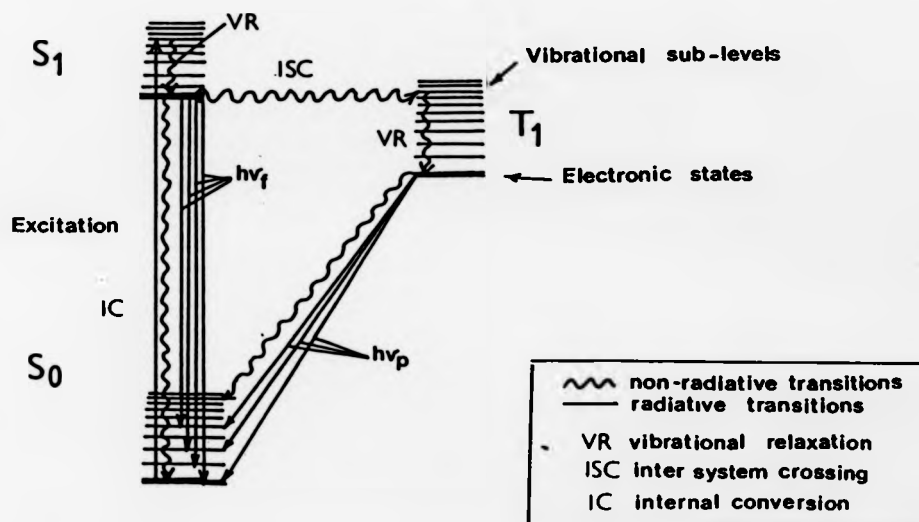
1.3 Photochemistry⁵

Absorption of a photon of sufficient energy will promote an electron from, for example, the electronic ground state of a closed shell molecule (S_0) to a higher electronic state (S_1). The electron is promoted with conservation of electron spin and usually has an excess of vibrational energy. This excess vibrational energy is dissipated very rapidly (ca. 10^{-11} s) in solution as thermal energy (a process known as vibrational relaxation) until a Boltzmann distribution of the lowest vibrational level of S_1 is achieved. This excited state can decay by various photophysical processes, or be transformed to a different molecule in a photochemical reaction.

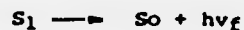
1.3.1 Photophysical processes⁵

Photophysical processes are most easily explained with reference to the simplified Jablonski diagram shown in Figure 1.2.

Figure 1.2 Simplified Jablonski diagram (modified from Streitweiser and Heathcock).

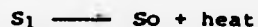


The vibrationally relaxed singlet excited state (S_1) can undergo an electronic transition to the ground state (S_0) with emission of radiation:

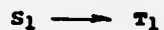


The wavelength of the emitted light, known as fluorescence (f), is generally⁶ longer (lower energy) than the wavelength of the excitation light. This is because the excited state has vibrationally relaxed prior to fluorescence, and also because electronic transitions can occur to higher vibrational sub-levels of S_0 .

The excited state can also undergo several non-radiative decay processes. It may return to S_0 by electronic and vibrational deactivation, a process known as internal conversion (IC). The absorbed energy of the photon is dissipated as thermal energy;



The S_1 state can also intersystem cross to the excited triplet surface (T_1), resulting in a net spin inversion of the excited state species;



Intersystem crossing (ISC) is forbidden by the principle of spin conservation. That it occurs at all is a consequence of spin orbit coupling. When the singlet-triplet energy separation is small, ISC is generally efficient and the triplet state can be extensively, or completely, populated.

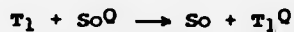
The triplet state (T_1) itself has several modes of deactivation available. It may undergo an electronic transition to the singlet ground state with emission of radiation (phosphorescence);



Due to the spin inversion required, phosphorescence is a slow process. The emitted light has a longer wavelength than fluorescent light because T_1 is lower in energy than S_1 . Non-radiative decay modes include ISC and subsequent vibrational relaxation to S_0 ;



A particularly important triplet deactivation mode is triplet energy transfer. This process involves a suitable molecule in its ground state (S_0^Q) interacting with the triplet, resulting in generation of the triplet state of the quenching molecule (T_1^Q):



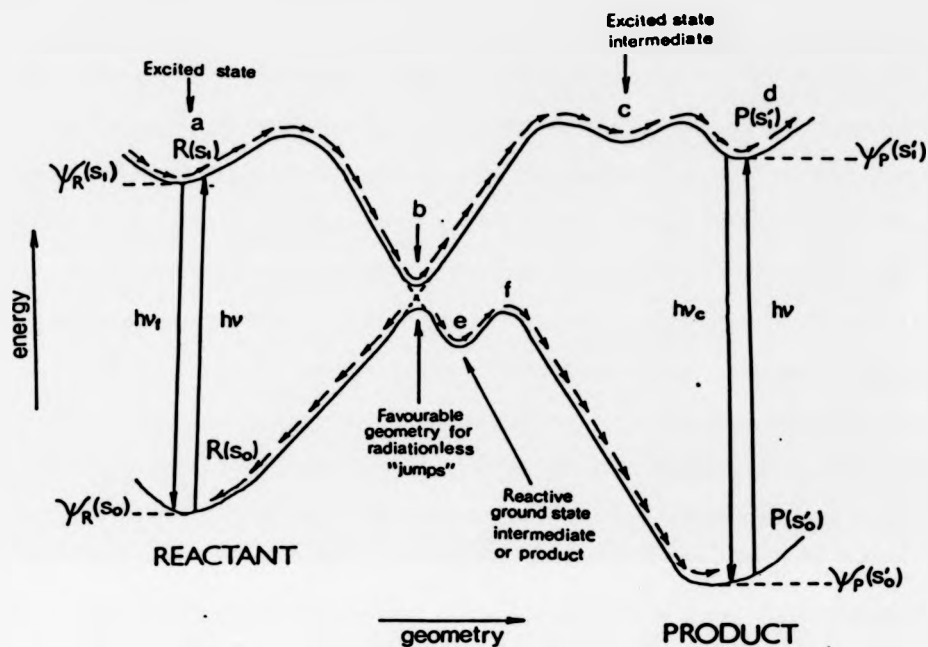
This quenching process forms the basis for photosensitised generation of triplet states.

In general, triplet excited states are longer-lived than the corresponding singlet excited states. One of the reasons for this is that electronic transitions between T_1 and S_0 are spin forbidden. Inter system crossing between T_1 and S_0 is much slower than inter system crossing between S_1 and T_1 (energy gap law), explaining why T_1 may be long-lived, but readily populated from S_1 .

1.3.2 Photochemical reactions⁵

A qualitative picture of photochemical reaction pathways can be obtained by considering the ground and excited state potential energy surfaces, or more simply, potential energy curves. Ground and excited singlet state potential energy curves for a typical unimolecular photochemical reaction ($R + h\nu \rightarrow P$) are shown in Figure 1.3.

Figure 1.3 Potential energy diagram for the unimolecular reaction $R+h\nu\rightarrow P$ (modified from ref. 5).



Each point on the curves represents a particular molecular geometry and energy, except for region b where the two surfaces are "close" together. In this region state mixing occurs so the molecular geometry and energy are ill-defined.

Absorption of a photon of sufficient energy promotes an electron from a minimum on the ground state surface, $R(S_0)$, to the excited state surface. The first formed excited state vibrationally relaxes until a Boltzmann distribution of the excited state vibrational sub-levels is achieved. The excited state, $R(S_1)$, can then decay by a radiative transition (fluorescence, $h\nu_f$) or proceed along the surface (the movement represented by arrows in Figure 1.3) until it reaches point d. This represents the excited state of product, $P(S_1')$. Emission of light from this state is known as chemilumines-

cence ($h\nu_c$). There is an alternative route for the excited state molecule when it reaches point b. The geometry at this point is very similar to that of a high energy ground state molecule. In this region the Born-Oppenheimer approximation breaks down and electronic-vibrational coupling occurs. Electronic-vibrational coupling allows an electronic transition, or "jump", to occur to the ground state surface. The dotted lines in Figure 1.3 represent zero order crossing (which occurs with unit probability). Thus, the small energy gap between the excited and ground state potential energy surfaces represents a weakly avoided crossing (ie the geometry at which surface "jumps" are most favourable). Once the molecule has "jumped" onto the ground state surface, it may "spill" back into the minimum of the reactant (corresponding to internal conversion)



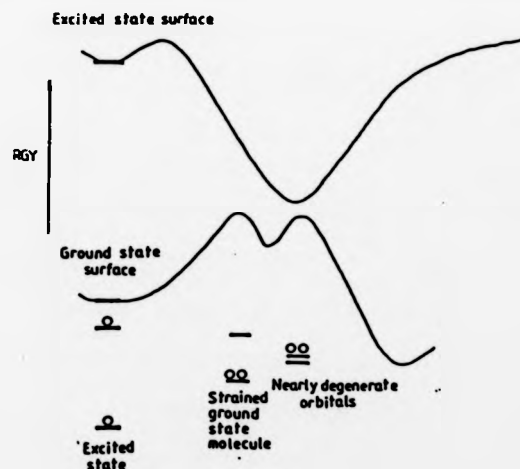
or proceed to region e which is a ground state minimum. This minimum may be an isolable product or a reactive intermediate of the ground state. Such an intermediate would be inaccessible in a ground state reaction due to the high energy barrier that must be surmounted to reach it. If the intermediate has sufficient thermal energy, and this energy is not rapidly removed, it may move past e, over f, and come to rest at P(S₀) after thermally equilibrating with its environment. This constitutes a typical photochemical reaction involving an intermediate. Part of the nuclear motion is controlled by the excited state surface and part by the ground state surface in the reaction



1.3.3 Photochemistry and biradicals

The majority of known organic photochemical reactions are probably not concerted in nature but involve intermediates between the excited state molecule and product. The most common intermediates are species which are not fully bonded (i.e. biradicals). Whether or not a photochemical excited state is classed as a biradical depends upon definition. Figure 1.4 shows the potential energy curves of an excited state and ground state molecule, and the relationship between excited state molecules, ground state molecules, and biradicals.

Figure 1.4 Relationship between ground and excited state potential energy surfaces (modified from ref. 5)

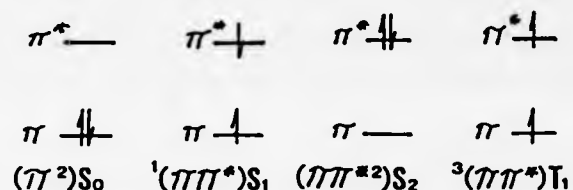


The excited state molecule can generally be viewed in terms of two characteristic half filled orbitals. Motion along the reaction co-ordinate, such as stretching a σ -bond or twisting a π -bond, may bring the representative point to a geometry where the orbitals are

nearly degenerate. The excited state could then be defined as a biradical by strict application of Salem and Rowland's definition².

As an example, consider the excited states of ethylene.⁵ Absorption of a photon promotes an electron from a π -orbital to the antibonding π^* -orbital. Electronic transitions are faster than nuclear motion (Franck-Condon principle) so the excited state is formed with the same planar geometry as the ground state. The ground state and possible excited states of ethylene, together with their spectroscopic notations, are shown in Figure 1.5.

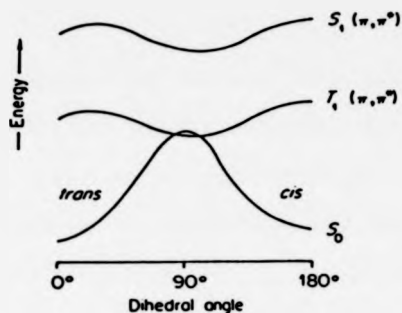
Figure 1.5 Ground and excited states of ethylene (from Barltrop and Coyle)



These planar excited states are not biradicals under Salem and Rowland's definition as the energy separation between the π and π^* orbitals is large (c.f. Figure 1.1(b) p.3). If twisting occurs about the terminal methylene groups the π -bond uncouples and becomes completely non-bonding when the methylene groups are orthogonal. This has the effect of reducing the energy of states where π -bonding is not important (the excited states) and increasing the energy of the ground state. At 90°-twist, the two electrons occupy two degenerate p-orbitals and can be classified as a biradical according to Salem and Rowland's definition.² In summary, the planar excited states of ethylene are not biradicals but the orthogonal excited states (normally ${}^1(\pi\pi^*)$ and ${}^3(\pi\pi^*)$) and orthogonal ground state

geometries can be classified as such. Figure 1.6 illustrates the effect of methylene twisting on the energy of the various states.

Figure 1.6 State correlation diagram for twisting of an ethylene π -bond (from Bartrop and Coyle)



We have shown that the region near weakly avoided crossing of ground and excited state potential energy surfaces (i.e. where the surfaces "come-close") in photochemical reactions enables excited states to be defined as a biradical. This would imply that biradicals are transition states with no barriers to reactions such as coupling of the radical centres or cleavage. If there are small barriers to such reactions, the biradical will be in a potential energy minimum and may be defined as a reaction intermediate. What is the evidence for the existence of biradicals as reaction intermediates?

1.4 Detection and characterisation of biradicals

The existence of triplet biradicals as intermediates in organic reactions, as well-defined minima on potential energy surfaces, is firmly established in many cases. Since they must undergo inter system crossing before formation of molecular products they may be sufficiently long-lived to be observed and scrutinised spectroscopi-

cally or intercepted by radical traps. This is especially true if conjugation or incipient ring strain in the products increases the triplet biradical lifetime. The existence of singlet biradicals as energy minima, on the other hand, still lacks experimental verification. This is because there are no spin restrictions to formation of molecular products and activation energies for reactions such as coupling and cleavage are expected to be very small. Consequently they are very short-lived species (lifetimes probably $< 10^{-9}$ s) and their credibility as intermediates is based on inference from thermokinetic and theoretical arguments, and experiments involving product stereochemistry.

1.4.1 Spectroscopic studies

A wide variety of spectroscopic techniques have been applied to detect and characterise biradical intermediates. The most common techniques are:

- a) Low temperature electron spin resonance (ESR)
- b) Chemically induced dynamic nuclear polarization (CIDNP)
- c) Laser flash photolysis (LFP)
- d) Infra-red spectroscopy (IR)

For the reasons stated in Section 1.4, spectroscopic techniques have been used almost exclusively in the study of triplet biradicals (the exceptions are discussed in Chapter 7).

Probably the single most informative technique is ESR spectroscopy.⁷ Analysis of ESR spectra can yield kinetic, structural, and ground state multiplicity information of triplet biradicals (singlet biradicals have net zero spin-angular momentum and are not ESR-active).

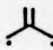


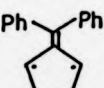
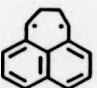
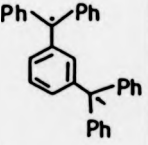
Low temperatures (4-77K) and highly viscous matrices are used almost exclusively in the ESR of triplet biradicals. These conditions of temperature and phase severely restrict the motion available to the triplet biradical and thus increase its lifetime. The ESR spectrum of a triplet is dominated by the dipole-dipole interactions of the two unpaired electrons, which gives rise to large magnetic splittings. As such, it is readily distinguished from the ESR of a free radical where the much weaker electron nuclear interactions give rise to much smaller magnetic splittings. The triplet spectrum can be analysed in terms of the zero field splitting parameters ($|D|$ and $|E|$) which are measures of the interaction between the radical centres. The $|D|$ parameter is a measure of the radical centre separation. It is proportional to $1/R^3$, where R is the average distance between the radical centres. The $|E|$ parameter is related to the molecular symmetry and is zero if the triplet possess a three fold, or higher, axis of symmetry.

Although only triplet biradicals are ESR active, observation of an ESR signal does not require that the triplet is the ground state. It is possible that the triplet is a higher state which has been thermally populated from a low lying singlet. However, determination of ground state multiplicity can be obtained from a study of the ESR signal intensity temperature dependence (Curie law analysis).⁸ In favourable cases, Curie law analysis can provide a measure of a biradical's singlet - triplet energy separation.

Some typical examples of triplet biradicals studied by solid phase ESR are shown in Table 1.1. The high $|D|$ parameters of the carbene illustrates the closeness of the unpaired electrons in 1,1-biradicals, while the low $|D|$ parameters of the phenyl derivatives

are consistent with spin delocalisation. All the biradicals shown in Table 1.1, with the exception of methylene, were shown to have triplet ground states by Curie law analysis.

Table 1.1 ESR $|D|$ and $|E|$ parameters of some typical biradicals
(modified from ref. 5).

Biradical	$ D /hc \text{ cm}^{-1}$	$ E /hc \text{ cm}^{-1}$	Class	Ref.
$:\text{CH}_2$	0.6881	0.00346	1,1	9
	0.0248	< 0.001	1,3	10
	0.0265	0.0055	1,3	11
	0.0256	0.00340	1,3	11
	0.0180	0.0013-0.0032	1,3	11
	0.0180	< 0.003	1,4	12
	0.0079	≤ 0.0005	1,5	13

A major advance in biradical chemistry was signified by Closs and Buchwalter's detection of the first non-conjugated biradical.¹⁴ They observed a well defined triplet ESR spectrum on irradiating 2,3-diazabicyclo[2.2.1]hept-2-ene (DBH) in a solid matrix at 5.5K. The large zero field splitting parameter ($|D|/hc = 0.084\text{cm}^{-1}$) was consistent with the proposed planar 1,3-biradical intermediate (Scheme 1.2) and could be qualitatively reproduced theoretically.¹⁴

Scheme 1.2



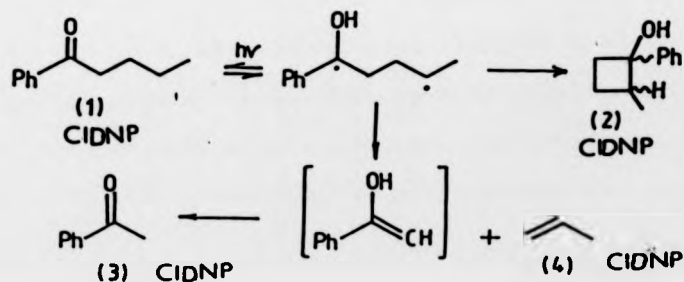
The signal decayed when the irradiation was discontinued and so a Curie law analysis was not applicable in this case. However, a triplet ground state was assigned to the biradical on the basis of the signal decay rate at 5.5K which was too slow to be caused by radiationless conversion to a lower lying singlet.¹⁴ (This has since been confirmed by CIDNP studies).¹⁵ The rate of ESR signal decay showed an Arrhenius temperature dependence between 5.5K and 21K. This enabled the activation energy (E_a) for the biradical cyclization reaction to be determined ($E_a = 2.3\text{kcalmol}^{-1}$).¹⁵ This value (which represents the depth of a triplet cyclopentane-1,3-diyl potential energy minima) has been qualitatively reproduced by the SCF calculations of Pitzer *et al.*¹⁶

A somewhat less direct but often more simple way of detecting biradicals is provided by the CIDNP method.¹⁷ The method of CIDNP

has been coined to define systems for which the chemical reactions lead to non-equilibrium populations of nuclear sub-levels. The observation of enhanced absorption or of emission in an NMR experiment, and the magnetic field dependence thereof, give information on the intermediacy of biradicals and their dynamic behaviour (e.g. deduction of rates of inter-system crossing). The details of a CIDNP spectrum also allow deduction of a biradical ground state multiplicity. A detailed account of CIDNP is beyond the scope of this discussion as its application has so far been limited mainly to the study of triplet biradicals.

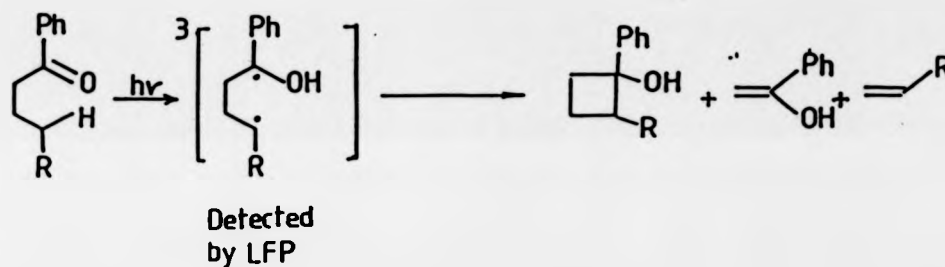
For example, Buchwalter and Closs have reported the intermediacy of triplet cyclopentane-1,3-diyl in the photochemical decomposition of DBH.¹⁵ This was deduced on the observation that photosensitised decomposition of DBH enhanced absorption for all ^1H NMR transitions of the product bicyclopentane. The theory of CIDNP also allowed Buchwalter and Closs to deduce that the biradical had a triplet ground state,¹⁵ a result not available from ESR studies.¹⁴ Kaptein and Kanter¹⁸ have also used the CIDNP method to deduce the intermediacy of triplet 1,4-biradicals in the Norrish II-type reaction of valerophenones, since polarisations (absorption and emission) were observed in the ^1H NMR of the products (Scheme 1.3).

Scheme 1.3



Like ESR, Laser flash photolysis (LFP) enables direct detection of biradicals. In typical experiments biradical precursors are irradiated with a pulsed laser and the resultant transients observed by electronic absorption spectroscopy. The rate of decay of the transient spectrum can be used to determine the solution phase lifetime of the transient. For example, Small and Sciaino¹⁹ observed transient absorption in the Norrish type-II reaction of phenyl alkyl ketone derivatives, (Scheme 1.4).

Scheme 1.4

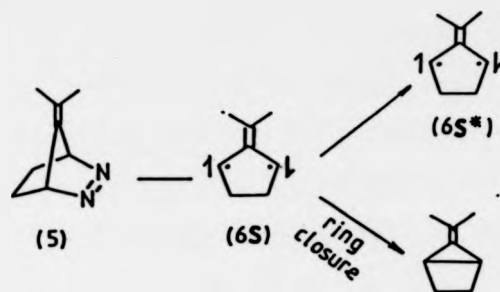


The transients had absorption spectra and extinction coefficients similar to those of related ketyl radicals and were presumed to be the triplet 1,4-biradicals shown in Scheme 1.4. First order decay of the observed signals suggested the triplet biradical had a lifetime of 40-100ns.

Due to the very short lifetimes of singlet biradicals, LFP studies are usually confined to triplets. However, the advent of picosecond LFP has enabled the excited state of a singlet biradical to be detected. Berson *et al.*²⁰ reported that picosecond excitation of the azo precursor(5) gave rise to transient species which could be detected by their fluorescence. Fluorescence decay led to an

estimated transient lifetime of 280ps at ambient temperature. It was suggested that (5) loses nitrogen leading to a planar singlet biradical (6S) in its ground state. Absorption of a second laser photon generates the excited singlet state (6S*) which was believed to be the species responsible for fluorescence (Scheme 1.5).

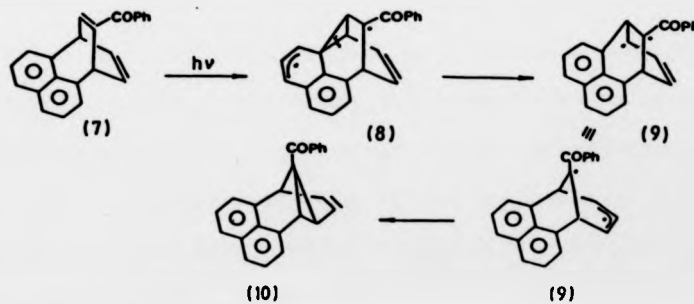
Scheme 1.5



This type of biradical is a member of a special class of compounds (trimethylenemethanes) which are discussed in more detail in Chapter 7.

Infra-red spectroscopy has been used less widely for the detection and characterisation of biradicals. However, Schaffner *et al*²¹ have reported IR detection of triplet biradicals in the di- π -methane rearrangement illustrated in Scheme 1.6.

Scheme 1.6



Irradiation of (7) at 77K led to new carbonyl stretching frequencies in the IR. These were assigned to the triplet biradical (8). On warming from 77K to 182K in the dark, the carbonyl stretching frequencies of the triplet biradical (9) were observed prior to those of the product (10).

In summary, spectroscopic methods can be very useful for the detection and characterisation of "stable" triplet biradicals but give little information on non-conjugated triplet biradicals and (with the exception of trimethylenemethanes) singlet biradicals. This is a consequence of the extremely short lifetimes of non-conjugated triplet biradicals and singlet biradicals.

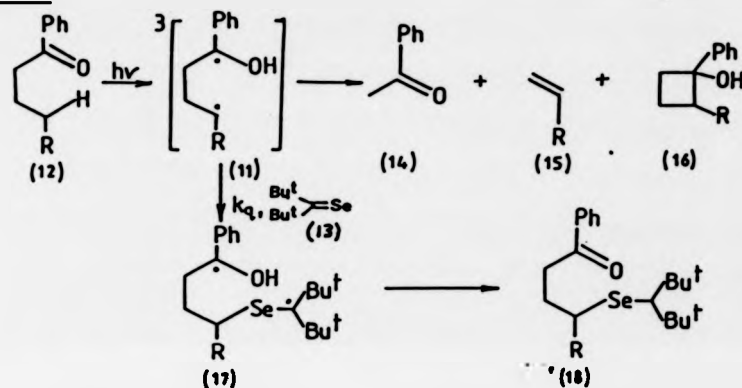
1.4.2 Chemical trapping

Biradicals that exist as true reaction intermediates in well defined potential energy surface minima may be sufficiently long-lived to undergo reactions that compete with the unimolecular reactions of the biradical. This rationale forms the basis of chemical trapping experiments. If a biradical may be intercepted by some chemical reagent (known as the biradical trapping agent) it is regarded as a credible reaction intermediate. Furthermore, trapping studies can give information regarding the structure and lifetime of the species being intercepted. At the present time there is only one class of singlet biradicals sufficiently long-lived to be chemically trapped. This special case will be discussed in Chapter 7. Triplet biradicals, on the other hand, have been captured by a wide variety of chemical reagents. With the exception of trimethylenemethane biradicals generated thermally at low temperatures (see Chapter 7), trapping studies are usually confined to photochemical reactions

since high temperatures reduce the biradical lifetime. Some representative photochemical trapping studies are discussed here.

Triplet 1,4-biradicals (11) in the Norrish Type-II reaction of phenyl alkyl ketones (12) have been trapped with a variety of chemical reagents.²² A typical example²³ involving ditertiary-butylselenoketone (13) is shown in Scheme 1.7.

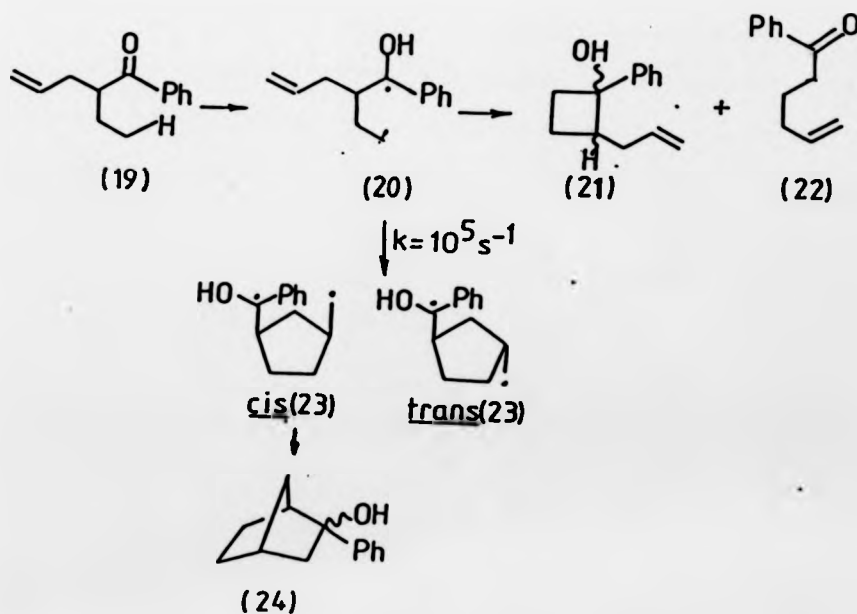
Scheme 1.7



The formation of Norrish Type-II products ((14), (15) and (16)) was quenched by the addition of selenoketone (13). Stern-Volmer analysis of the quenching led to a value for $k_q \tau$, where k_q is the rate constant for the quenching reaction and τ is the lifetime of the triplet biradical (11). Estimation of the value of k_q suggested a lifetime for (11) of ca 100ns. This value shows good agreement with the lifetime measured directly in LFP studies (40-100ns).¹⁹ The organoselenium compound (18) was isolated and thought to arise by an intermolecular reaction at the alkyl radical site of (11) followed by an intramolecular hydrogen transfer from the hydroxyl group of the 1,6-biradical (17).²³

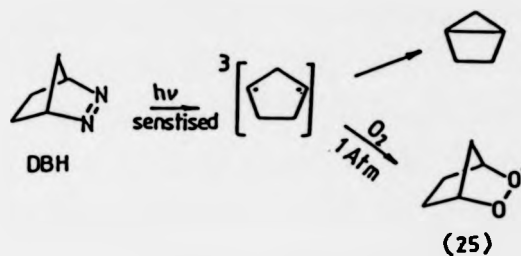
Wagner and Liu²⁴ employed an intramolecular trapping technique to estimate the lifetime of a similar 1,4-biradical, Scheme 1.8. Photolysis of (19) led to intramolecular oxetane formation and Norrish Type-II products ((21) and (22)) via the (assumed) intermediate (20). The biradical can also rearrange to cis - and trans - cyclopentylmethyl biradicals (23). Coupling occurs for cis - (23) to give the trapping product, 2-phenyl-2-norborneol (24). Since the rate of 5-hexenyl to cyclopentylmethyl radical cyclisations are known,²⁵ analysis of the product distribution allowed the lifetime of the 1,4-biradical (20) to be estimated. The estimated lifetime (ca 300ns) was of similar magnitude to the lifetimes of other Norrish Type-II biradicals measured directly (by LFP)¹⁹ and by trapping studies.²²

Scheme 1.8



The first chemical trapping of a non-conjugated biradical was reported by Wilson and Geiser.²⁶ They found that benzophenone photosensitised decomposition of DBH under 10Atm of oxygen led to the endoperoxide (25), consistent with oxygen trapping of a cyclopentane-1,3-diyl, (Scheme 1.9).

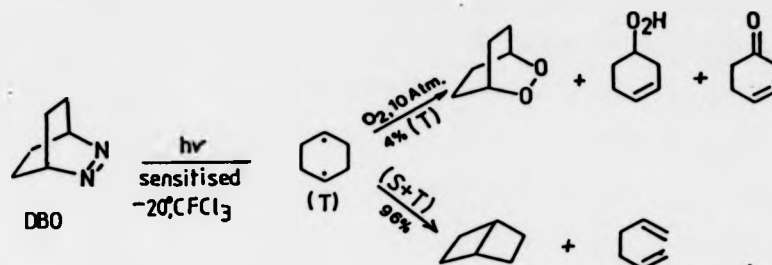
Scheme 1.9



In a more recent study,²⁷ the photosensitized decomposition of DBH was carried out under 10Atm of oxygen using a UV-laser. Under these conditions the formation of bicyclopentanes was completely quenched and the lifetime of triplet cyclopentane-1,3-diyl was estimated to be ca 900ns at 280K.²⁷

Adam, Wilson and Hanneman²⁷ used identical conditions (10Atm of oxygen UV-laser photolysis) to intercept the assumed cyclohexane-1,4-diyl intermediate in the photosensitized decomposition of 2,3-diazabicyclo[2.2.2]oct-2-ene (DBO). Oxygen containing products were formed with much lower efficiency than in DBH, the major reaction pathway being unimolecular decomposition to bicyclo[2.2.0]hexane and hexa-1,5-diene (Scheme 1.10).

Scheme 1.10



The difference in trapping efficiencies between DBH and DBO (100% and 4%, respectively) reflects the difference in triplet lifetimes of cyclopentane-1,3-diyl and cyclohexane-1,4-diyl. Adam *et al.*²⁷ estimated these to be ca 900ns at 280K (cyclopentane-1,3-diyl) and 0.1ns at 253K (cyclohexane-1,4-diyl). The very short triplet lifetime of the 1,4-diyl is expected by analogy to the parent system (tetramethylene) for which a singlet ground state and small singlet - triplet energy gap (ca 1.6kcal mol⁻¹) have been estimated theoretically.²⁸

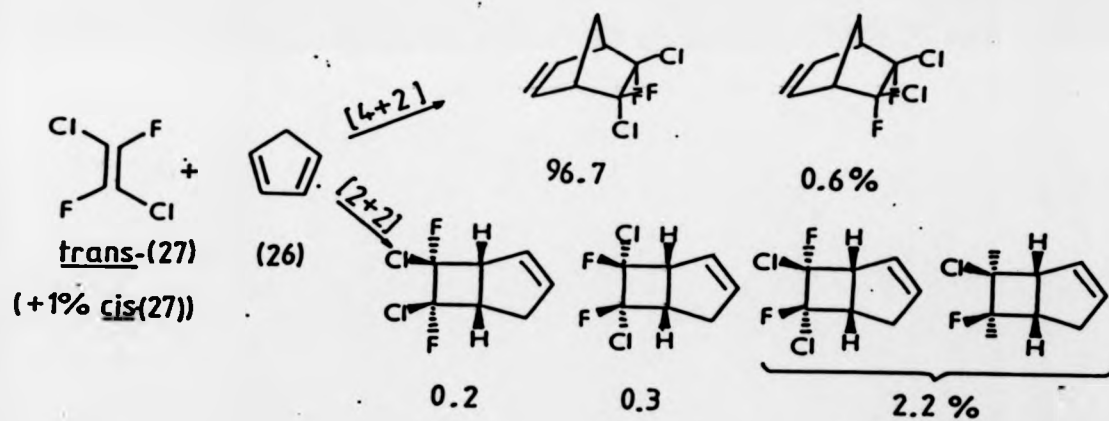
1.4.3 Stereochemical studies (1)

The organic chemist generally perceives a biradical reaction as one that proceeds with loss of stereochemical integrity, and a concerted reaction as one that proceeds with exclusive stereoselectivity. This is because a biradical is generally thought to undergo bond rotation faster than bond formation or cleavage. A concerted reaction, on the other hand, does not involve intermediates but proceeds through a transition state to products whose stereochemistry can be predicted from principles of orbital symmetry conservation.¹ Using such stereochemical criteria it should be

possible to distinguish between concerted and biradical pathways.

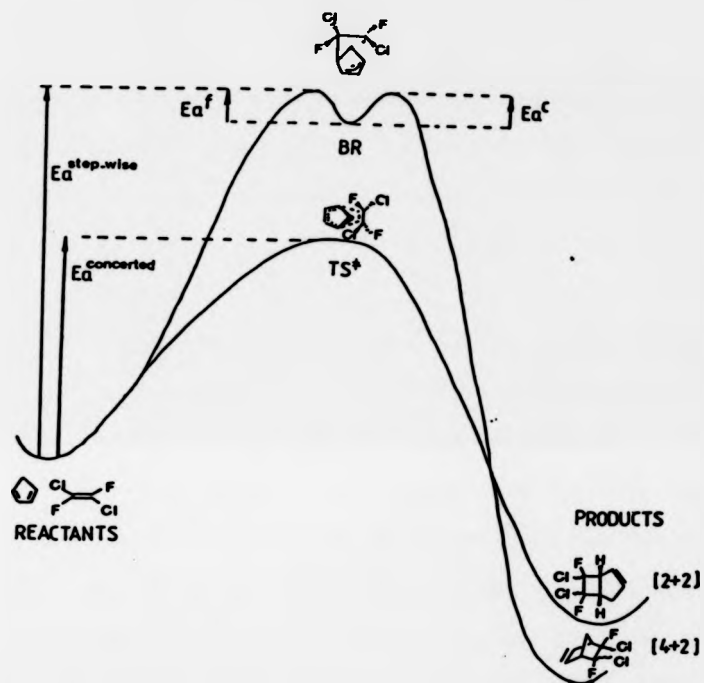
Bartlett and Wheland²⁹ used just such criteria to distinguish between biradical and concerted pathways in the thermal gas phase reaction between cyclopentadiene (26) and trans-1,2-dichloro-1,2-difluoroethylene (27) (contaminated with 1% of cis-fluoroalkene). The observed product distribution is shown in Scheme 1.11.

Scheme 1.11



The results are most easily explained with reference to Bartlett's schematic representation of the reaction potential energy surface³⁰ shown in Figure 1.7.

Figure 1.7 Potential energy surface for [4+2] and [2+2] reactions of cis- and trans-(27) with cyclopentadiene (modified from ref. 30).

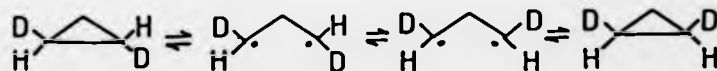


Given that the fluoroalkene was contaminated with 1% of cis-(27), the [4 + 2] adduct was formed with complete retention of fluoroalkene configuration. The high proportion of [4 + 2] product

and its retained stereochemistry is evidence that it is formed by the lower energy, concerted $\pi 4s + \pi 2s$ pathway (Figure 1.7). The [2 + 2] adducts were formed with 18% loss of trans-fluoroalkene configuration which was too large to be accounted for by the presence of 1% cis- (27). This loss of configuration was rationalised by invoking a biradical intermediate. As an intermediate the biradical lies in a shallow potential energy minimum with small activation energies for cleavage (E_a^f) and coupling (E_a^c). The loss of configuration implied that bond rotation occurred prior to formation of the [2 + 2] adduct (i.e. the energy barrier to bond rotation in the biradical is comparable to E_a^f or E_a^c).

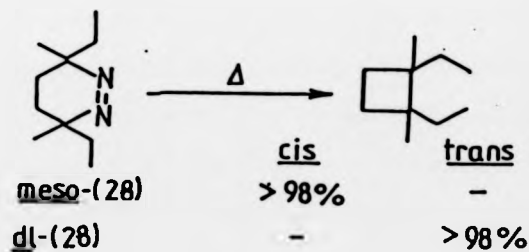
Loss of stereochemical integrity has been used similarly as evidence for the involvement of trimethylene in the pyrolysis of cyclopropane. Rabinovitch *et al.*³¹ examined the thermal isomerisation of trans-1,2-[²H]₂-cyclopropane and found that the cis-isomer was present in recovered cyclopropane. This demonstrated that a pathway existed which was capable of producing rotation about at least one of the cyclopropane C-C bonds i.e. exactly the sort of behaviour expected of an intermediate deuterated trimethylene biradical (Scheme 1.12).

Scheme 1.12



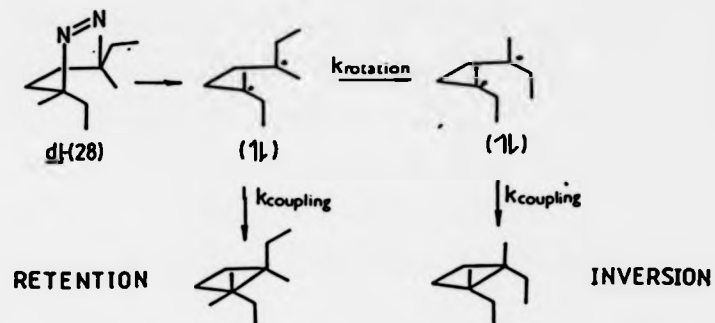
If a biradical does exist in an energy minimum its stereochemical behaviour will depend on barriers to rotation compared with the depth of the minimum (or, alternatively, the relative rates of cleavage, coupling, and rotation). In the previous two examples it was suggested that biradicals were involved in which bond rotation occurs at comparable rates to its unimolecular reactions. However, if the depth of the minimum is such that cleavage or coupling occur before bond rotation, the biradical could behave stereoselectively. A striking example of this point has been reported by Bartlett and Porter.³² They studied the thermal and direct photochemical decomposition of meso- and dl-3,6-diethyl-3,6-dimethyltetrahydropyridazine (28) and found that the cyclobutane products were formed with > 98% retention of configuration (Table 1.2).

Table 1.2 Stereochemistry of cyclobutane products from pyrolysis of (28).



The results were rationalised in terms of a singlet 1,4-biradical intermediate that coupled in its original conformation before bond rotation could occur.³² The mechanism is illustrated for the dl-isomer in Scheme 1.13.

Scheme 1.13



Clearly, the concept of a biradical as a "freely rotating" species is oversimplified and loss of configuration, though frequently observed, is not required in biradical reactions. If biradical potential energy minima could be located, it would be possible to readily distinguish between stepwise (biradical) and concerted reaction pathways. Furthermore, if the depth of the minima and barriers to bond rotation could be measured it would be possible to predict the stereochemical behaviour of the biradical. Unfortunately, potential energy minima cannot be measured experimentally. However, thermokinetic and theoretical studies allow their existence to be postulated and their depth to be estimated.

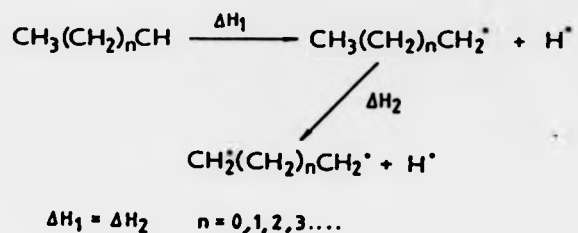
1.4.4 Thermokinetic and theoretical Studies

In principle, if a biradical lies energetically below the

transition states for cleavage and coupling it is a permitted (but not required) reaction intermediate while if it lies substantially above it is largely excluded as an intermediate from the reaction in question. The aim of thermokinetic³³ (and theoretical studies) is to estimate the energies of the possible intermediates and transition states. This allows distinction between non-concerted and concerted reaction pathway and also affords a qualitative representation of the reaction potential energy surface. Once the depth of the potential energy minimum has been estimated, comparison with energy barriers to bond rotation allows the stereochemical behaviour of the biradical to be predicted.

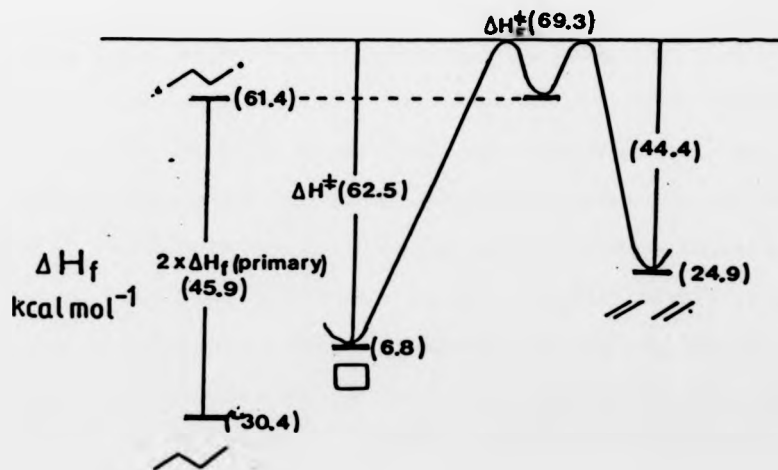
As an example, consider the reversible interconversion of cyclobutane and two molecules of ethylene.³⁴ The reaction could involve a tetramethylene biradical or a four membered transition state. Is the tetramethylene biradical an energetically feasible reaction intermediate?

The enthalpy of formation of the transition state (ΔH_F^\ddagger) can be estimated by summing the experimental activation energy for cyclobutane decomposition ($\Delta H^\ddagger = 62.5 \text{ kcal mol}^{-1}$) and the enthalpy of formation of cyclobutane ($\Delta H_F^\circ = 6.8 \text{ kcal mol}^{-1}$). The enthalpy of formation of tetramethylene from n-butane cannot be measured directly. Its value can, however, be estimated from group additivity arguments.³³ These assume that the enthalpy required to produce a primary monoradical from a saturated hydrocarbon is identical to that required to produce a biradical from the monoradical;



This assumption is valid only if the radical centres are non-interacting. Benson and O'Neal have obtained the centrally important value for the heat of formation of primary monoradicals from kinetic studies.³⁴ Their value of $+45.9 \text{ kcal mol}^{-1}$ when added to the heat of formation of n-butane ($\Delta H_f = -30.4 \text{ kcal mol}^{-1}$) led to an estimated value for ΔH_f^\cdot (tetramethylene) of $+61.4 \text{ kcal mol}^{-1}$ (assuming the radical centres are non-interacting). These relations are collected in the energy diagram of Figure 1.8.

Figure 1.8 Energy diagram for cyclobutane pyrolysis (modified from ref. 36).



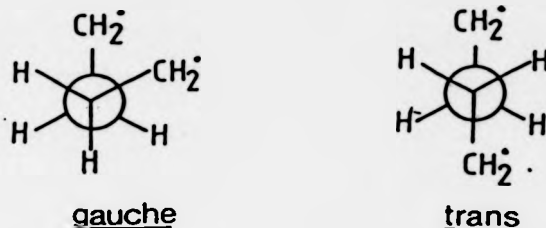
Inspection of Figure 1.8 shows that tetramethylene is a feasible reaction intermediate in the pyrolysis of cyclobutane, lying in a potential energy minimum of 6 - 8 kcalmol⁻¹. Barriers to rotation in primary (and substituted) alkyl monoradicals are < 1.2kcalmol⁻¹.³⁵ Thus, assuming that the tetramethylene radical centres are non interacting, Benson and O'Neal predicted that cyclobutane pyrolysis involves a "freely-rotating" 1,4-biradical intermediate.³⁴ Stereochemical studies, discussed in the following Section, are inconsistent with this concept since ethylenes are produced with partially retained configuration. This implies that barriers to bond rotation are much higher than expected (i.e. 6 - 8kcalmol⁻¹) or Benson and O'Neal's estimate of the potential energy minimum is too high.

Doering³⁶ has discussed the importance of primary, secondary, and tertiary biradical ΔH_f values in such estimates. All the values up until 1981 were considered allowing Doering to update the ΔH_f values of primary, secondary, and tertiary biradicals. Using the updated value for ΔH_f of primary biradicals the depth of the tetramethylene minimum is reduced to < 2kcalmol⁻¹.³⁶ If this value represents the true minimum, the thermokinetic model of cyclobutane pyrolysis predicts that a tetramethylene biradical is involved which cleaves, couples, and rotates at comparable rates (i.e. may show some preference for retained stereochemistry, in accord with the stereochemical studies discussed in the following Section).

Proceeding on the supposition that the most recent calculations are more credible than earlier ones, there is theoretical support for the thermokinetic model. The most recent ab initio calculations

(MC-SCF with 4 - 31G basic sets) find two potential minima in the cycloaddition reaction of two ethylenes.³⁷ These correspond to the gauche and trans conformations of tetramethylene (Scheme 1.14) which have barriers to cleavage of 0.62 and 0.38 kcal mol⁻¹, respectively.

Scheme 1.14



Similar considerations apply to the involvement of trimethylene in cyclopropane pyrolysis. Before Doering's updated values for primary biradicals were reported³⁶ Benson and co-workers thermokinetic arguments suggested that cyclopropane pyrolysis involved a trimethylene intermediate some 9-10 kcal mol⁻¹ below the transition states for ring closure and 1,2-hydrogen migration. Benson's hypothesis³³ indicates that cyclopropane pyrolysis involves reversible C-C bond cleavage to a biradical which resides in a potential energy minimum so deep that randomisation of stereochemical labels at C-1 and C-2 by bond rotation occurs faster than ring closure. Using Doering's updated value for ΔH_f^\ddagger of primary mono-radicals the depth of the minimum falls to some 3-5 kcal mol⁻¹,³⁶ still consistent with a 'freely rotating' trimethylene intermediate. However, this is not the only pathway suggested for the geometric isomerisation of cyclopropane.³⁸ Smith³⁹ and Kollmar⁴⁰ have proposed a mechanism involving reversible C-C bond cleavage with

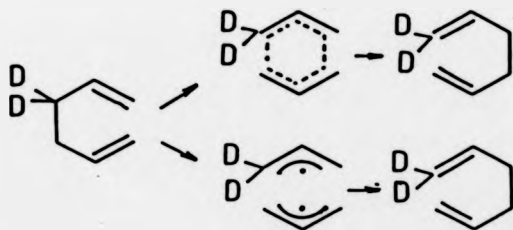
rotation of only one methylene group while Hoffman⁴¹ has proposed a mechanism involving C-C bond cleavage and conrotating motions around both remaining C-C bonds to a π -cyclopropane which recloses to cyclopropane by conrotation. Stereochemical studies have not been able to resolve the mechanistic ambiguity as double inversion, partial and complete randomisation of stereochemistry have all been observed in pyrolysis of 1,2-disubstituted cyclopropanes.⁴² Theoreticians are unable to agree upon the existence (or depth) of a trimethylene potential energy minimum in the pyrolysis of cyclopropane.^{38,42} Clearly, an understanding of cyclopropane geometric isomerisation is not yet possible. This is also the case for thermal decompositions of monocyclic pyrazolines (which can be envisaged to lose nitrogen to generate the same trimethylene intermediates) as formation of cyclopropanes with double inversion, single inversion, and double retention of stereochemistry have all been observed.⁴²

It should be emphasised that thermokinetic arguments are based on the critical assumption of non-interacting radical centres. Referring to Section 1.2, it is immediately apparent that such an assumption is not justified. Interactions between degenerate non-bonding orbitals at radical centres are required to give a biradical a small amount of bonding character so it can exist as a 'stable' entity. The effects of such interactions will be reduced the greater the separation of the radical centres. Consequently, it is not surprising that 1,4-biradicals behave more predictably (thermokinetically and stereochemically) than 1,3-biradicals. The chemical effects of interactions between the radical centres are discussed in Chapter 6.

There is a further oversimplification involved in thermokinetic arguments. The estimated enthalpy of a biradical is of unspecified spin state. While this is less important if the singlet-triplet energy gap is small (as in tetramethylene) a large singlet-triplet energy gap confuses the thermokinetic conclusions. An example of such a system where the proposed biradical intermediate (trimethylenemethane) has a large singlet-triplet energy gap is the pyrolysis of methylenecyclopropane. This will be discussed in more detail in Chapter 7.

There are reactions in which thermokinetic arguments unambiguously distinguish between concerted or non-concerted pathways. One such reaction is the Cope rearrangement of hexa-1,5-diene.⁴³ In principle, this reaction could proceed intramolecularly through a six-membered transition state or involve initial C-C bond cleavage and resultant recombination of allyl radicals (Scheme 1.15).

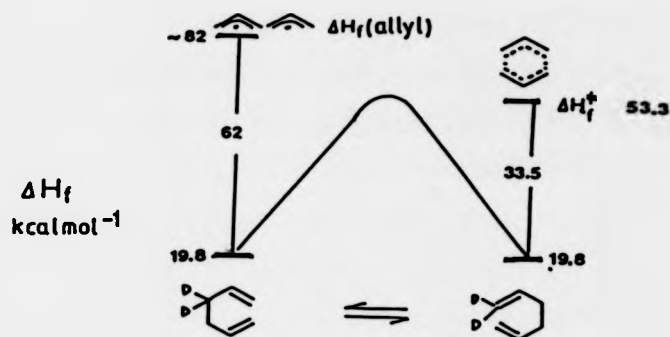
Scheme 1.15



There is a third possibility involving initial C-C bond formation and a cyclohexane-1,4-diyl but discussion of this mechanism is deferred until Chapter 5. The enthalpy diagram for the two former

pathways (using Doering's³⁶ updated values for the ΔH_f value of allyl radicals) is shown in Figure 1.9.

Figure 1.9 Partial energy diagram for degenerate Cope rearrangement (modified from ref. 36).



Clearly, dissociation into two allyl radicals is an energetically inaccessible mechanism for the Cope rearrangement of hexa-1,5-diene even when one considers the uncertainties in the enthalpy values.

1.4.5 Stereochemical studies (2). Biradical commonality

The existence of biradicals as true reaction intermediates lacks experimental verification in many cases. In such cases their existence is inferred from thermokinetic studies or by loss of stereochemical integrity. However, we have seen that biradicals can behave stereoselectively if energy barriers to bond rotation are greater than those for cleavage or closure and thermokinetic arguments, while attractive in theory, can be frustrating in their application (frustration develops when the magnitude of the difference between the enthalpies of activation of the hypothetical non-concerted model is comparable to or less than the combined

uncertainties.) If a biradical does exist as a true reaction intermediate lying in a well-defined energy minimum, its stereochemical behaviour should be identical (or very similar) independent of the point of entry onto the surface. In other words, biradicals generated from different precursors should show identical stereochemical behaviour. Stereochemical commonality is a powerful criterion of biradical identity. Since many factors can affect the stereochemical behaviour of biradicals (see following Sections) comparisons should be carried out where possible under identical conditions of temperature, phase, spin state, etc.

Dervan and co-workers⁴² have used this criterion to show that 1,4-biradicals are the common intermediates in the decompositions of 1,1- and 1,2-diazenes, 2 + 2 cycloadditions of ethylenes, and cyclobutane pyrolyses (Scheme 1.16).

Scheme 1.16

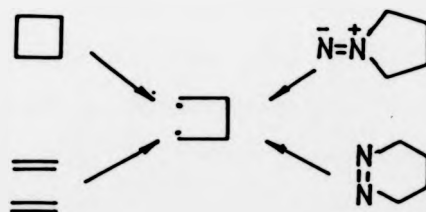


Table 1.3 summarises the results comparing thermal decomposition of cis and trans-3,4-dimethyltetrahydropyridazines (29)⁴⁴ with the [2 + 2] additions of the appropriate olefins.⁴⁵ The properties of the assumed 1,4-biradical intermediates were measured in terms of relative rates of cleavage (k_F), coupling (k_C), and rotation (k_R), deduced from steady state analysis of the reaction product distributions.

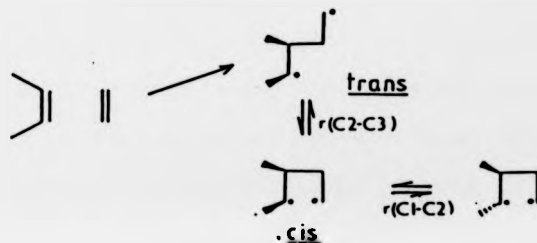
Table 1.3 Comparison of biradical reactivities in the thermal decomposition of (29) and the [2+2] additions of olefins.

PRECURSOR	CONDITIONS	<u>cis</u> isomer		<u>trans</u> -isomer	
		k_f/k_r	k_c/k_r	k_f/k_r	k_c/k_r
	430°/Gas	1.5 ^a	1.9	1.8	0.7
	430°/Gas	1.6	1.4	1.2	0.8

- a. The relative rates were calculated after subtraction of a component of stereoselective cleavage.

The relative rates show good qualitative agreement, indicating a common 1,4-biradical intermediate. Dervan *et al*⁴⁴ noted that it was perhaps curious that the [2 + 2] addition data fit so well. Loss of nitrogen from (29) would be expected to lead to a 1,4-biradical in a cis (or gauche) conformation. The [2 + 2] addition could, in principle, lead to the same intermediate in cis/trans conformations. One explanation is that the olefins dimerise in a cis (or gauche) conformation for some unknown reason. Alternatively, if both cis and trans conformations are formed, either the trans-conformer cleaves back to olefins faster than C₂-C₃ bond rotation (Scheme 1.17) such that it loses mechanistic importance (a no-reaction reaction), or the trans-conformer rotates about C₂-C₃ faster than loss of stereochemical integrity at the radical centres (rotation about C₁-C₂).

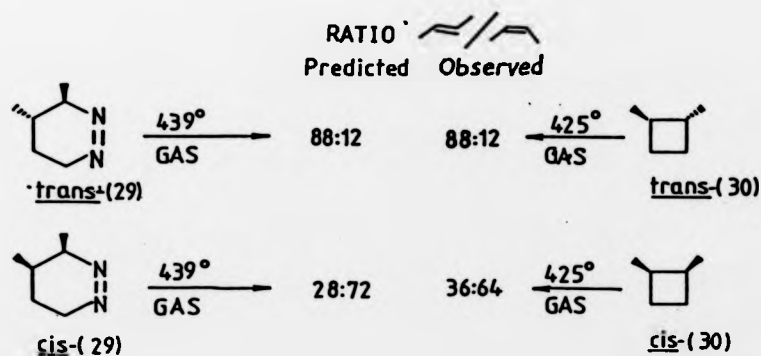
Scheme 1.17



Dervan *et al*⁴⁴ noted that if the latter situation occurs, an estimate of the C₂-C₃ bond rotation barrier (ca 3kcalmol⁻¹) puts a lower limit on C₁-C₂ bond rotational barriers in 1,4- biradicals. This value is higher than expected (rotational barriers are < 1.2kcal mol⁻¹ in alkyl radicals),³⁵ and is possible evidence for interactions between the radical centres.

A similar analysis cannot be performed for pyrolysis of 1,2-dimethylcyclobutanes (30) as the ring opening is reversible, and the cleavage reaction is complicated by the involvement of two different sets of 1,4-biradicals. However, Dervan *et al*⁴⁴ showed that the kinetic ratio of 2-butenes obtained experimentally from (30)⁴⁶ was in good agreement with the ratio predicted from the thermal decomposition of (29), after subtraction of 2-butene formed from (29) in a stereoselective cleavage reaction (Figure 1.9).

Figure 1.9 Ratio of cis and trans-but-2-enes from pyrolysis of (29) and (30) (modified from ref. 42).

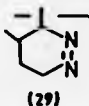
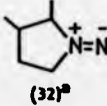
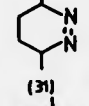
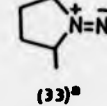


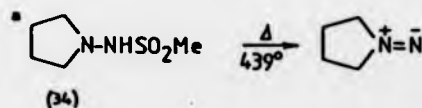
Dervan and Uyehara have also shown that the thermal decomposition of 1,2-diazenes such as (29) and (31), lead to very similar product distributions to those obtained from the thermal

decomposition of the corresponding 1,1-diazenes (32) and (33).⁴⁴ Table 1.4 compares the stereochemistry of the cyclobutane products for the decompositions. The excellent agreement is consistent with a common 1,4-biradical intermediate. It should be noted that the 1,1-diazenes are the assumed intermediates from the unimolecular thermal decomposition of the appropriate N-methylsulphonamido dimethylpyrrolidines (34).

Unlike the 1,4-biradical systems, there is no series of experiments showing that 1,3-biradicals generated from different precursors show identical stereochemical behaviour.⁴²

Table 1.4 Stereochemistry of cyclobutanes from pyrolysis of 1,2- and 1,1-diazenes (from ref. 47).

Precursor	Conditions	Cyclobutane	
		Retention / Inversion	
 (29)	<u>cis</u> <u>trans</u>	439°/Gas	2.29
			7.76
 (32) ^a	<u>cis</u> <u>trans</u>	439°/Gas	3.94
			6.75
 (31)	<u>cis</u> <u>trans</u>	439°/Gas	1.68
			1.67
 (33) ^a	<u>cis</u> <u>trans</u>	439°/Gas	1.70
			1.84



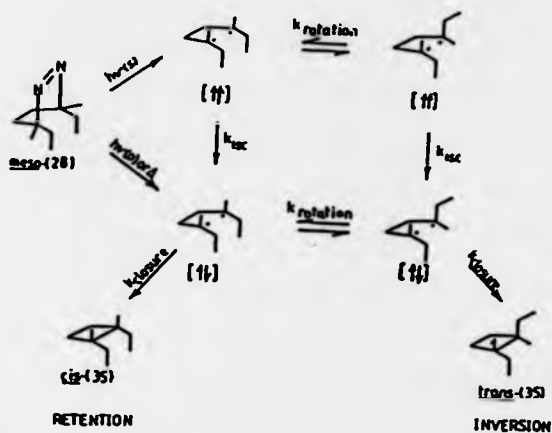
1.4.6 Stereochemical studies (3). Factors affecting biradical stereochemical behaviour.

In previous Sections we have discussed the evidence (direct and indirect) for the existence of biradicals as true reaction intermediates. In this Section we discuss how factors such as temperature, spin state, and substitution affect their reactivity by looking at their effect on product stereochemistry. The effect of interactions between the radical centres on biradical reactivity is deferred until Chapter 6. Since interactions are expected to be more pronounced in 1,3-biradicals than in 1,4-biradicals, this discussion is restricted to 1,4-biradicals.

1.4.6.1 Effect of spin state

The principle of spin conservation requires that biradicals generated thermally, or from singlet photochemically excited states, are singlets while those generated from triplet excited states are triplets. Since triplet biradicals can be selectively generated from sensitised photochemical reactions, the effect of spin state on the reactivity of a biradical can be assessed. In a classic report, Bartlett and Porter³² studied the stereochemistry of the thermal, direct, and sensitised photochemical decomposition of meso - and - dl - 3,6 - diethyl -3,6 - dimethyltetrahydropyridazines (28), which should decompose to give substituted 1,4-biradicals (1,4- diyls). The stereochemistry of the diyl coupling product (35) and the proposed mechanistic Scheme are given in Figure 1.10.

Figure 1.10 SCE's in the decomposition of (28)



	Δ	% RETENTION	
		$h\nu_{\text{dir}}$	$h\nu_{\text{sen}}$
meso-(28)	> 98	95	61
dl-(28)	> 98	97	65

s; sensitised
 d; direct

Thermal and direct photochemical decomposition leads to cyclobutanes with essentially retained configuration. The results were rationalised in terms of a generated singlet ($\uparrow\uparrow$) diyl coupling from its initial conformation before bond rotation occurs (i.e. $k(\text{closure}) \gg k(\text{rotation})$.) In other words, the singlet biradical must reside in a potential energy minimum with an energy barrier to coupling that is less than that of bond rotation. Sensitised photolysis, on the other hand, generates triplet ($\uparrow\downarrow$) diyls which must undergo spin inversion (ISC) before coupling can occur. The substantial loss of configuration in the sensitised decomposition is consistent with bond rotation occurring prior to ISC (i.e. $k(\text{rotation}) > k(\text{ISC})$). This suggests that the triplet biradical has a lower A factor for reaction than the singlet.

Bartlett and Porter³² called this phenomenon, in which biradicals of different multiplicities give rise to different product distributions, a spin correlation effect (SCE). Similar SCE's are observed in many other biradical systems.

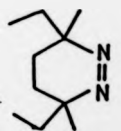
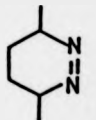
While SCE's may be a consequence of different rotational barriers in singlet versus triplet biradicals, they are generally regarded to be a reflection of rate limiting ISC in triplet biradicals.

An alternative explanation of Bartlett and Porter's results has been proposed by Stephenson and Brauman.⁴⁸ They suggested SCE's arose because the vibrationally excited, or "hot", triplet biradical produced from photosensitized decomposition is deactivated and undergoes ISC to the singlet biradical which mostly loses stereochemistry. Thermolysis and direct photolysis, on the other hand, were said to generate "hot" singlet biradicals which could readily overcome the barrier to stereoselective closure. If SCE's were due to "hot" molecule effects rather than differences in barriers to rotation, coupling, and cleavage, substitution would have no effect on product stereochemistry. The observation that less substituted biradicals behave less stereoselectively (see following Section) is in full accord with Bartlett and Porter's interpretation and contradicts Stephenson and Brauman's rationale. Furthermore, SCE's are also observed when both singlet and triplet biradical are generated in solution. It is extremely unlikely that "hot" singlet biradicals could be generated in solution so Bartlett and Porter's explanation is to be preferred.

1.4.6.2 Effect of substitution

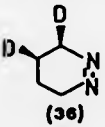
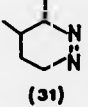
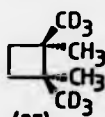
The high retention of configuration in the cyclobutane product obtained from thermal and direct photochemical decompositions of (28) reflects a much faster rate of diyl coupling compared with rotation of the tertiary radical centres. If the radical centres were less substituted, faster rotation rates would be expected on the basis of a reduced moment of inertia (leading to an increase in the activation entropy for rotation) and, in this case, reduced steric hindrance. Thus, biradicals with primary, secondary, and tertiary radical centres can lead to products with different stereochemistries. Dervan and Uyehara⁴⁴ have compared the thermal decomposition of (28) with that of 3,6-dimethyltetrahydropyridazine (29), which should decompose to give a 1,4-biradical with secondary radical centres. The cyclobutane products from (29) did indeed show a much lower stereoselectivity (Table 1.5) suggesting the rate of rotation has increased, and is competitive with diyl coupling (i.e. $k(\text{closure}) \approx k(\text{rotation})$).

Table 1.5 Cyclobutane stereochemistry from pyrolysis of (28) and (29) (from ref. 44).

	T, °C	Phase	Cyclobutane Ret/Inv
 meso-(28) dl-(28)	148	Solution	49 49
 cis-(29) trans-(29)	306	Gas	1.9 2.2

As phase and temperature may also affect the product stereochemistry, the differences in retention/inversion ratios could arise from the different reaction conditions used for (28) and (29). Dervan *et al*^{44,49} have shown that increasing substitution at radical centres does truly slow rotation rates by comparing systems under identical conditions. The relative rates of rotation to cleavage and coupling for primary, secondary, and tertiary biradicals, derived from the precursors shown in Table 1.6, were obtained from a steady state analysis of the product distributions. Although the reduced ratios for increasing substitution may be due to an increased coupling or cleavage rate, it is more plausible to ascribe at least the qualitative direction of the effects to a reduced rate of internal rotation.

Table 1.6 Effect of substitution on 1,4-biradical reactivity (from refs. 44 and 49).

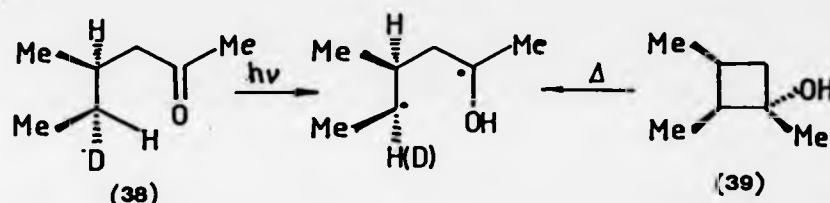
Precursor	Temp/Phase	k_r/k_f^a	k_r/k_c^b	Ref.
 (36)	439°/Gas	5.5	12.0	44,49
 (31)	439°/Gas	0.33 ^c 0.79 ^c	0.54 1.39	44,49
 (37)	401°/Gas	0.02	d	50

- Rotation/fragmentation rate
- Rotation/coupling rate
- Relative rates calculated after subtraction of a stereoselective component of cleavage
- Not accessible.

1.4.6.3 Effect of temperature

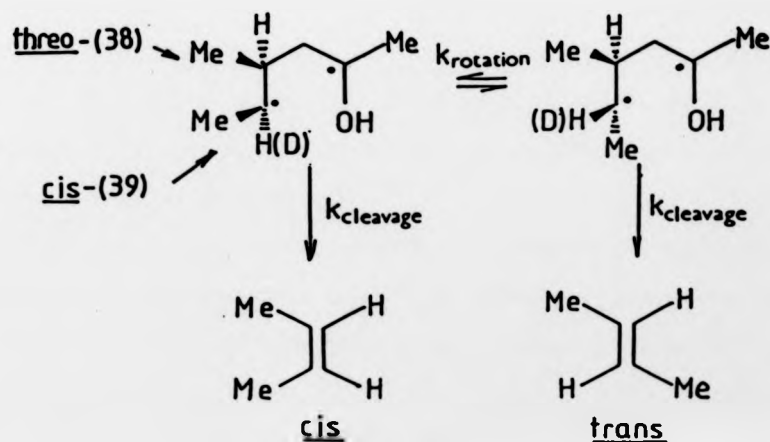
Due to the temperature dependence of rate constants, differences in the stereochemical behaviour of biradicals generated under different conditions can often be ascribed to temperature effects. This will be particularly important when comparing the product distributions of singlet biradicals generated thermally and by direct photolysis. For example, the Norrish type II reaction of threo-5-[²H]-4-methyl-2-hexanone (38) and pyrolysis of the appropriately substituted cyclobutanol (39) should generate the same (or very similar) 1,4-biradical (Scheme 1.18).

Scheme 1.18





Cleavage of this biradical leads to 2-butenes whose stereochemistry is controlled by the relative rates of cleavage and internal rotation (Scheme 1.19).

Scheme 1.19



The stereochemistry of the 2-butenes obtained from the decomposition of (38)⁵⁰ and (39)⁵¹ (see Table 1.7) indicate that rotation is much more competitive with cleavage in (39) than (38). It seems certain that the increased internal rotation is due, at least in part,⁵⁰ to the higher temperature required to generate the biradical from (39).

Table 1.7 Effect of temperature on 1,4-biradical reactivity

COMPOUND	METHOD	temp/phase	%	
				
<u>threo</u> -(38)	hν	25°/Solution	91	9
<u>cis</u> -(39)	Δ	585°/Gas	70	30

1.5 Summary

In this Chapter we have given a brief theoretical description of biradicals and shown that the formal definition covers a wide variety of superficially different species. A brief survey of some of the techniques used to investigate their chemistry and existence showed that triplet biradicals can truly be classed as reaction intermediates. They are longer-lived than the corresponding singlet biradicals largely due to the fact that they must undergo ISC before formation of ground state products. Singlet biradicals, and short-lived triplet biradicals on the other hand, have only been investigated by inferential methods, such as trapping, thermokinetic, and stereochemical studies.

The work in this thesis concerns the (assumed) biradical intermediates in the decomposition of an azoalkane (Chapters 3-6) and photochemical rearrangement of a cyclic triene (Chapter 7). We are

principally concerned with singlet biradicals and thus the methods used to study their chemistry (and in the case of azoalkanes, mechanism of formation) are largely inferential.

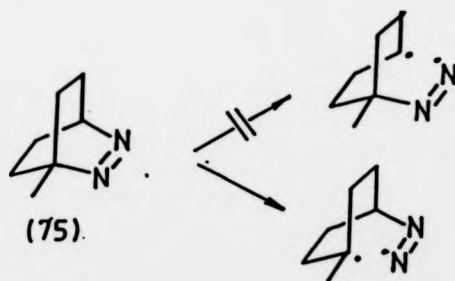
CHAPTER 2

2.1 Introduction

Bicyclic azoalkanes lose nitrogen thermally and photochemically under a wide variety of conditions. As such, they are generally regarded as the cleanest and most convenient source of cyclic biradicals of nearly any desired structure.¹

Stereochemical studies of their decomposition (nitrogen loss) gives an insight into both the mechanism of nitrogen loss, and nature of the assumed biradical intermediates. The key question regarding the mechanism of decomposition is whether the two C-N bonds cleave synchronously, with direct extrusion of nitrogen, or sequentially with the production of an intermediate diazenyl biradical (Scheme 2.1).

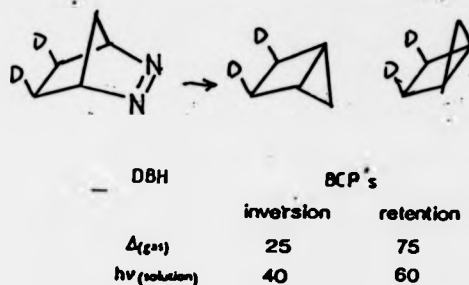
Scheme 2.1



2.2. Bicyclic and polycyclic azoalkanes that generate 1,3-biradicals

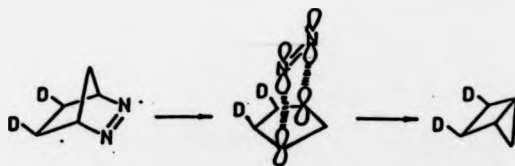
In 1967, Roth and Martin² reported that thermal and direct photochemical decomposition of anti-5,6-[²H]₂-2,3-diazabicyclo[2.2.1]hept-2-ene (DBH) leads to bicyclo[2.1.0.]pentanes (BCP's) with predominant double inversion of configuration (Scheme 2.2).

Scheme 2.2



The double inversion could be rationalised in terms of a concerted $\sigma_{2a} + \sigma_{2a}$ C-N bond cleavage with concurrent C-C bond formation. This mechanism requires a transition state with a planar five membered ring (Scheme 2.3).

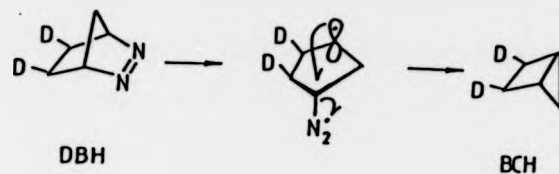
Scheme 2.3



However, a concerted mechanism is unlikely since the $\sigma_{2a} + \sigma_{2a}$ process is thermally forbidden³, and yet thermal decomposition gives quantitatively more doubly inverted BCP than photochemical decomposition.

Roth and Martin⁴ chose to interpret the predominant double inversion in terms of a mechanism involving initial cleavage of only one C-N bond. Backside attack of the radical centre at the remaining nitrogen bound carbon in the diazenyl biradical affords the inverted product. It is important to note that such a mechanism requires a planar five membered ring (Scheme 2.4).

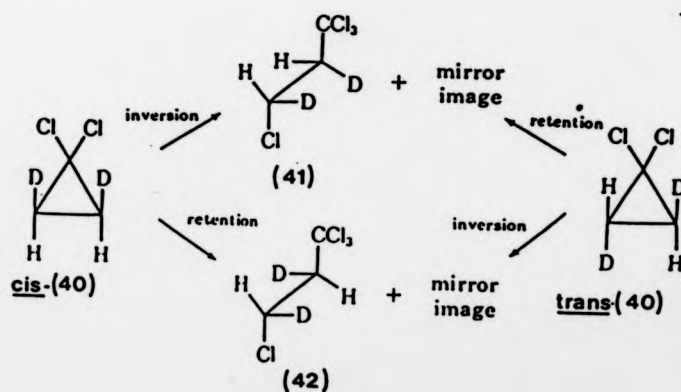
Scheme 2.4



Since Roth and Martin's original reports^{2,4} evidence has come to light which suggests this mechanism is essentially an S_H2 -type reaction with inversion.

Incremona and Upton⁵ have reported evidence which shows that S_H2 -type reactions do proceed with inversion of configuration. Photochlorination of cis- and trans-2,3-[²H]₂-1,1-dichlorocyclopropane (40) led to products ((41) and (42)) with > 96% inversion of configuration⁵ (Scheme 2.5).

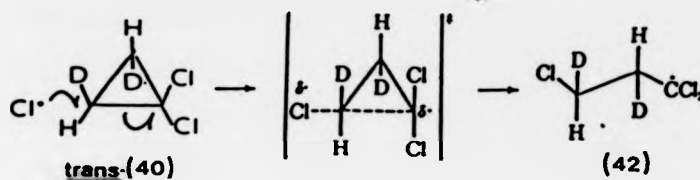
Scheme 2.5



Starting material	%Products	
	(41)	(42)
<u>cis</u> -(40)	96.6	3.4
<u>trans</u> -(40)	3.9	96.1

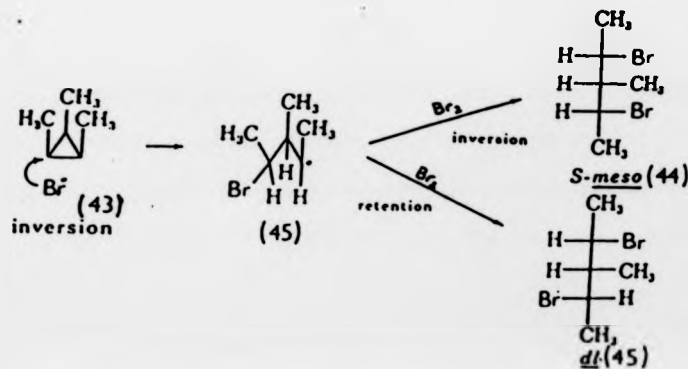
Incremona and Upton⁵ proposed a mechanism involving backside attack of a chlorine free radical and a transition state similar to that normally envisioned for S_N2 reactions. The mechanism is outlined for the trans-isomer in Scheme 2.6.

Scheme 2.6



A similar rationale can be used to explain the results from Mayes and Applequist's study of bromine free-radical induced ring opening of cis-1,2,3-trimethylcyclopropane (43)⁶. Equal proportions of S-meso- and dl-3-methyl-2,4-dibromopentane (44) were observed⁶, consistent with initial S_H2-type attack of bromine with inversion, followed by non-stereoselective bromination of the monoradical intermediate (45), (Scheme 2.7).

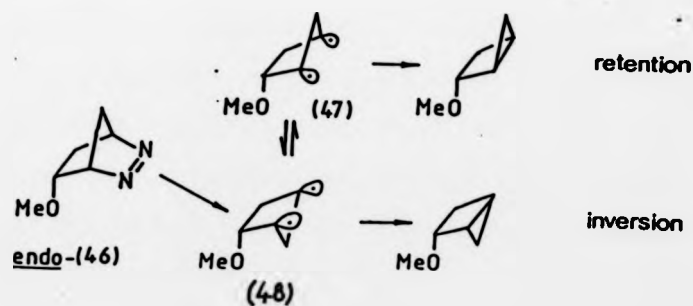
Scheme 2.7



If the initial attack of bromine had occurred with retention of configuration, equal proportions of *R*-meso-(44) and *dl*-(44) would have been observed. Since *R*-meso-(44) was not detected in the product mixture, the results implied that the initial S_H2 -type attack of bromine proceeded with complete inversion of configuration⁶. Thus, the S_H2 -type mechanism with inversion of configuration is a plausible rationale for the decomposition stereochemistry of DBH.

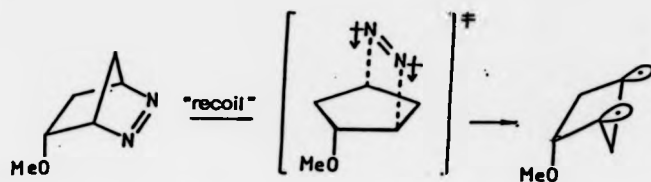
Allred and Smith⁷ also observed BCP's with predominant double inversion of configuration in their study of thermal and photochemical decomposition of exo- and endo-5-methoxy DBH derivatives (46). They rationalised the results in terms of a mechanism involving partially equilibrated cyclopentane-1,3,-diyls (Scheme 2.8).

Scheme 2.8



Their mechanism requires that a diyl with inverted configuration (48) is produced directly from endo-(46). Partial equilibration and ring closure would then lead to the observed stereochemistry. Allred and Smith⁷ suggested that (48) arises from endo-(46) because the departing nitrogen atoms exert a "recoil force" on the bridgehead carbons (Scheme 2.9).

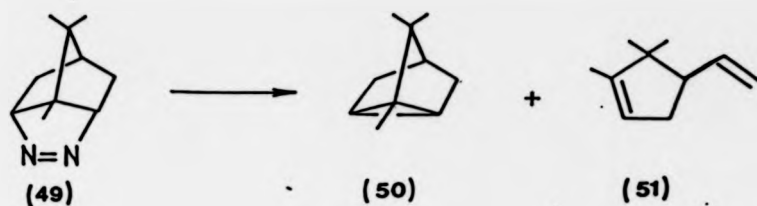
Scheme 2.9



They suggested that the "recoil" is caused by the energy released from the synchronous C-N bond cleavage.⁷ However, Engel *et al*⁸ have noted that thermal generation of a cyclopentane-1,3-diyl from DBH is endothermic with most of the exothermicity only being released after ring closure. Consequently the "recoil" mechanism has not been received favourably.⁹

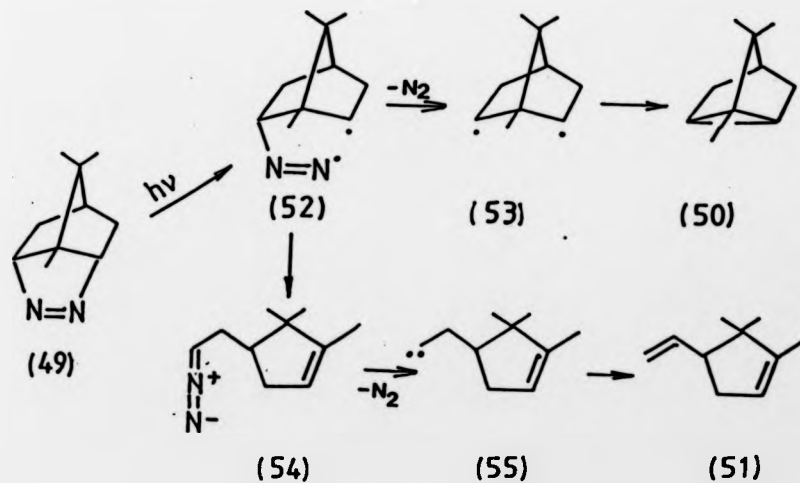
Recent studies by Adam and co-workers are in support of a mechanism involving stepwise C-N bond cleavage.^{10,11} They have repeated Roth and Martin's analysis of *anti*-5,6-[²H]₂-DBH and rationalised the predominant double inversion by a mechanism involving initial formation of a diazenyl biradical.¹⁰ This then loses nitrogen to give an inverted diyl conformer which preferentially ring closes to inverted bicyclopentane.¹⁰ In studies of tricyclic systems, Adam *et al*¹¹ have been able to detect nitrogen containing species presumed to arise from diazenyl biradical intermediates. For example, thermal and direct photochemical decomposition of (49) led to a tricycloheptane (50) as major product and trace amounts of vinylcyclopentene (51)¹¹, (Scheme 2.10).

Scheme 2.10

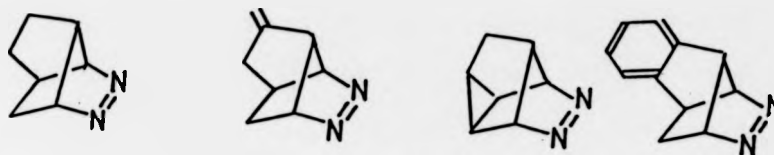


A mechanism was proposed¹¹ involving stepwise C-N bond cleavage and formation of a diazenyl biradical (52). This loses nitrogen to generate a 1,3-biradical (53), and subsequently (50), or rearranges to the diazoalkane (54). The diazoalkane was independently synthesised and shown to decompose to (51), presumably via the carbene intermediate (55).¹¹ On preparative LFP, appreciable amounts of the diazoalkane could be detected by UV-Vis and IR spectroscopy.¹¹ The mechanistic pathways are summarised in Scheme 2.11.

Scheme 2.11



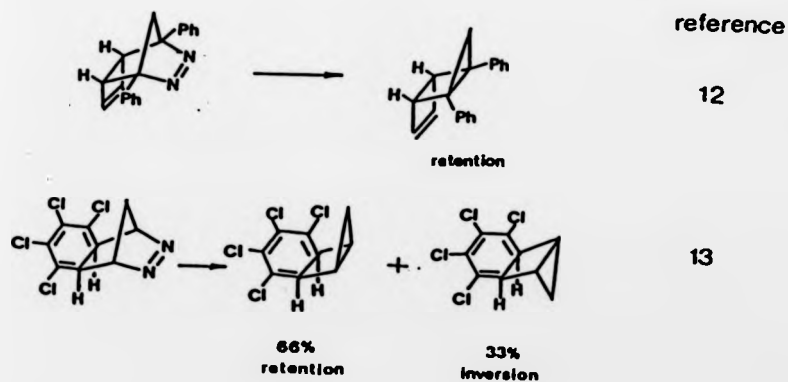
Diazoalkanes similar to (54) were also detected in the photochemical decomposition of tricyclic azoalkanes containing the DBH skeleton¹¹,



It is important to emphasise that all DBH decomposition mechanisms require the five-membered carbon ring to be planar at some point along the reaction co-ordinate. While this is acceptable for DBH systems (angle strain is minimal in planar five-membered carbon rings) it may not be energetically permissible for other bicyclic azoalkanes.

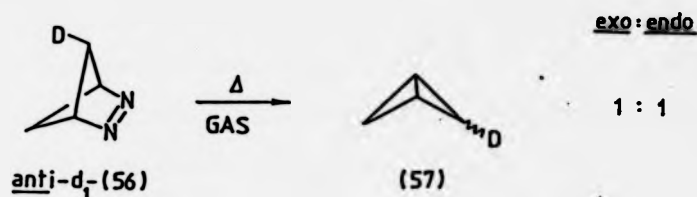
Predominant double inversion of configuration is a general phenomenon in decompositions of DBH and its derivatives. Exceptions occur only when the products are sterically biased in favour of the more thermodynamically stable isomer (Scheme 2.12).

Scheme 2.12



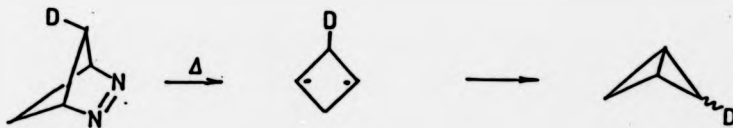
Stereochemical studies of other bicyclic azoalkanes suggest that the double inversion of configuration observed in DBH and its derivatives is unique. The next lower homologue, 2,3-diazabicyclo[2.1.1.]hex-2-ene (56) decomposes thermally to give bicyclo[1.1.0.]butanes (57) with complete loss of configuration (Scheme 2.13)¹⁴

Scheme 2.13



Since thermal decomposition of (57) is known to occur without exo/endo isomerisation¹⁵, the result was explained¹⁴ in terms of synchronous (or stepwise) C-N bond cleavage leading to a planar, or rapidly inverting, cyclobutane-1,3-diyl intermediate (Scheme 2.14).

Scheme 2.14



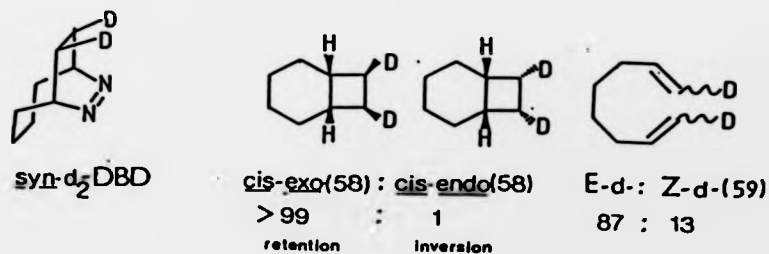
It should be noted that the stereochemistry of monocyclic pyrazoline decompositions is extremely complex and double inversion, double retention and single inversion have all been observed¹⁶, sometimes in the same system!¹⁷

In summary, decompositions of azoalkanes that generate 1,3-biradicals are incompletely understood as evidenced by the wide range of mechanisms used to rationalise the diverse stereochemical data.

2.3 Bicyclic and polycyclic azoalkanes that generate 1,4-biradicals

Unlike the preceding discussion, azoalkanes that generate 1,4-biradicals have, so far, given stereochemical results consistent with production of a nitrogen-free biradical with retained azoalkane configuration, which leads to products whose stereochemistry can be predicted by consideration of relative rates of rotation, cleavage, and coupling. Stepwise C-N bond cleavage may be involved in these decompositions, but a diazenyl biradical is not required to rationalise stereochemical data since double inversion of stereochemistry is only observed in sterically biased systems. For example, Samuel¹⁸ has carried out a detailed stereochemical investigation of 7,8-diazabicyclo[4.2.2.]dec-7-ene (DBD) decomposition using deuterium as stereochemical labels. The results obtained from the thermal decomposition are given in Table 2.1.

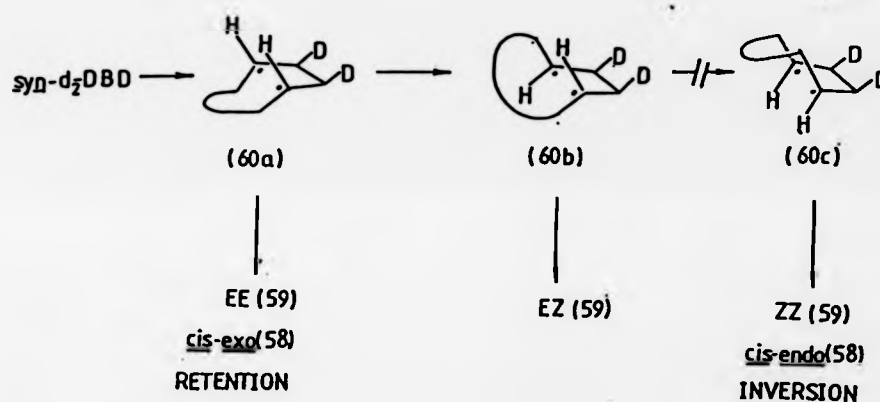
Table 2.1 Partial decomposition stereochemistry of DBD.



The results showed that bicyclo[4.2.0]octane (58) was formed with complete double retention of configuration, so mechanisms involving "recoil" or backside attack in a diazenyl biradical were not involved.¹⁸

Samuel¹⁸ rationalised the stereochemical data in terms of conformations of a cyclooctane-1,4-diyl (60), (Scheme 2.15).

Scheme 2.15

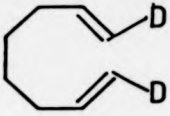
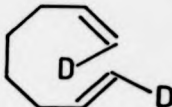
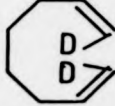


Loss of nitrogen (by stepwise or synchronous C-N bond cleavage) leads to diyl conformer (60a) which can couple or cleave to give products with retained configuration. If (60a) is converted to conformer (60b) this can only cleave since trans-(58) was shown to be absent, but stable under the reaction conditions. Conformational equilibration can not be complete as cis-endo-(58) was absent, so (60c) which would lead to it is not involved.

One of the consequences of the proposed mechanism is that all the 2-deuterium in (59) should be present as EZ-(59) with ZZ-(59) being absent. This has recently been confirmed by Samuel¹⁹, who has

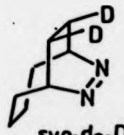
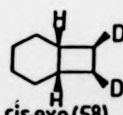
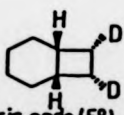



determined the proportions of EE-, EZ- and ZZ-(59) obtained from the thermolysis of DBD (Table 2.2).

Table 2.2 Stereochemistry of the cleavage products from thermal decomposition of *syn*-[^2H]₂-DBD

				NET E-d
%	79	20	1	89

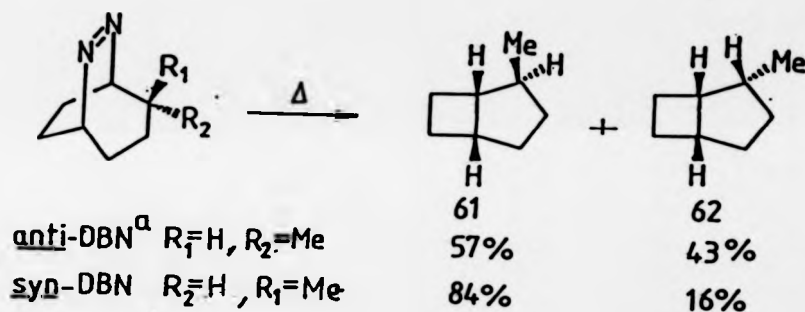
Direct photochemical decomposition of DBD gave qualitatively similar results (i.e. predominant retention of stereochemistry)¹⁹ and was rationalised by invoking singlet cyclooctane-1,4-diyls similar to those involved in the thermal decomposition.¹⁹ Photosensitised decomposition of DBD led to products less stereoselectively, as expected if a SCE operates.¹⁹ The results are summarised in Table 2.3, which also contains the thermolysis results for comparison.

Table 2.3 Complete decomposition stereochemistry of DBD

	→					
<i>syn</i> -d ₂ -DBD		<i>cis-exo</i> (58)	<i>cis-endo</i> (58)	EE	EZ	ZZ
MODE		Retention	Inversion			
Δ		> 99:1		79	20	1
hν(Direct)		90	10	64	33	3
hν(Sensitised)		73	27	45	53	4

A mechanism involving partial equilibration of a diyl (in this case, cycloheptane-1,4-diyl) can be used to rationalise the stereochemical observations of Ueyhara *et al*²⁰. They reported that thermal decomposition of methyl labelled bicyclo[3.2.2.]non-6-ene (DBN) leads to bicyclo[3.2.0.]heptanes with a preference for retained stereochemistry (Table 2.4).

Table 2.4 Thermal decomposition stereochemistry of DBN



^a For steric reasons, the methyl group prefers to be *exo* so both azo compounds give excess double retention compared with an equilibrium mixture.




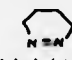
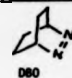
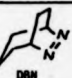

Although stereochemical tests of the cleavage reaction are lacking²¹, the results indicate that decomposition leads to a cycloheptane-1,4-diyl with retained configuration which closes (or cleaves?) before conformational equilibration.

Tetrahydropyridazines (monocyclic azoalkanes) also lead to product distributions that can be rationalised by a mechanism

involving partial equilibration (i.e. bond rotation) of a 1,4-biradical formed from the azoalkane with retained stereochemistry¹⁶ (see Chapter 1, Sections 1.5, 1.6 and 1.7 for examples).

In summary, thermal and photochemical decompositions of azoalkanes that generate 1,4-biradicals do not require mechanisms involving diazenyl biradical intermediates as, unlike pyrazoline decompositions, predominant double inversion of configuration has not been reported. The various stereochemical consequences of saturated, cyclic, and polycyclic azoalkanes are summarised in Table 2.5.

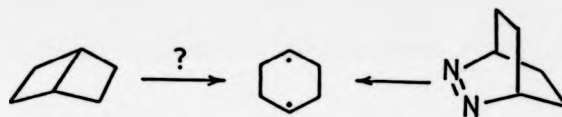
Table 2.5: Summary of azobenzene decomposition stereochemistries

AZOBENZENE	MODE OF DECOMPOSITION ^a	STEREOCHEMISTRY	RATIONALE
 pyrazidines	Δ , hv(D)	DOUBLE INVERSION, SINGLE INVERSION, DOUBLE RETENTION.	Incompletely understood. May involve trimethylene biradicals or diazenyl biradicals
 diazabicyclohexene		RANDOM	Planar cyclobutane-1,3-diyI or rapidly interconverting biradical
 DBH	Δ , hv(D)	PREDOMINANT DOUBLE INVERSION	Several rationales including stepwise C-N bond cleavage and/or cyclopentane-1,3-diyIs
 tetrahydropyridazine	Δ , hv(D)	PARTIALLY RETAINED	Partial equilibration (rotation) of a tetramethylene biradical formed with retained stereochemistry
 DBO		SEE BELOW	
 DBH	Δ	PREDOMINANT RETENTION	Partial conformational equilibration of a cycloheptane-1,4-diyI formed with retained stereochemistry.
 DDB	Δ , hv(D)	NEARLY COMPLETE RETENTION	Partial equilibration of a cyclooctane-1,4-diyI formed with retained stereochemistry

^a The stereochemical outcome of photosensitized decompositions are complicated by SCE's and are not included. In all cases, sensitized photolyses lead to products less stereoselectively.

2.4 2,3-Diazabicyclo[2.2.2.]oct-2-ene (DBO)

Thermal and photochemical decomposition of DBO leads to bicyclo[2.2.0.]hexane (BCH) and hexa-1,5-diene via an assumed intermediate cyclohexane-1,4-diyl.¹ Before considering the decomposition mechanism, and the stereochemical behaviour of the diyl intermediate, it is important to consider some stereochemical studies of BCH pyrolyses. This bicyclic hydrocarbon is also a potential precursor to cyclohexane-1,4-diyl. If pyrolysis of BCH involves a diyl intermediate similar to that involved in the decomposition of DBO, the stereochemistries of their decompositions should be nearly identical;



2.4.1. Pyrolysis of bicyclohexane

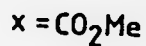
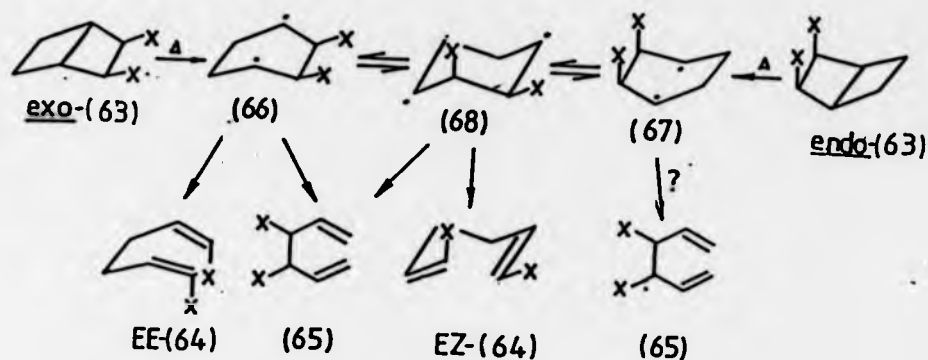
In 1960, Srinivasan and Cramer²² reported that pyrolysis of BCH led to an isomeric C_6H_{10} hydrocarbon, hexa-1,5-diene. Steel and Zand²³ studied the kinetics of the isomerisation and found $E_a = 36.0$ kcal mol⁻¹. We consider that this low activation energy could be consistent with a concerted cleavage. The orbital symmetry allowed cleavage reaction is a $\sigma_{2a} + \sigma_{2s}$ process³ which should lead to stereoselective formation of *EZ*-hexa-1,5-dienes from pyrolysis of cis-exo- or cis-endo-2,3-disubstituted BCH's. Paquette and Schwartz²⁴ observed such stereoselective cleavage in the pyrolysis of both cis-isomers of (63), Table 2.6.

Table 2.6 Decomposition stereochemistry of bicyclo[2.2.0.]hexane-2,3-dicarboxylic acid dimethyl ester.

PRECURSOR	% PRODUCTS			
	EE(64)	EZ(64)	ZZ(64)	(65)
<u>cis-exo</u> (63)	10	80	0	10
<u>cis-endo</u> (63)	9	79	0	12

Although the stereoselective cleavage to EZ-(64) could be explained in terms of a concerted $\sigma_{2a} + \sigma_{2s}$ process, Paquette and Schwartz²⁴ considered the strain required in the transition state would be too great for the mechanism to be energetically feasible.²⁵ Furthermore, small amounts of EE-(64) were observed which would require symmetry forbidden cleavage reactions. Consequently a biradical mechanism was proposed (Scheme 2.16).

Scheme 2.16

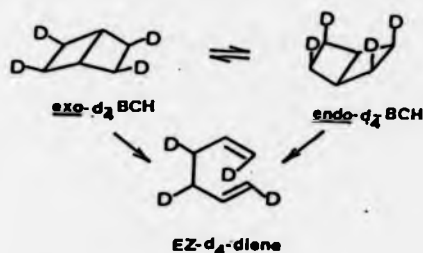


Cleavage of the central C-C bond in the BCH's leads to cyclohexane-1,4-diyloxy ((66) or (67)) in boat conformations. Paquette and Schwartz assumed²⁴ that the boat diyls rapidly convert to the more thermodynamically stable chair diyl conformation (68), which cleaves to give EZ-(64) as major product. They suggested that the near identity of product distributions from cis-exo-(63) and cis-endo-(63) was due to conformational equilibration of boat and chair diyls. The small amount of EE-(64) suggests that cleavage can occur from a boat diyl.

One of the consequences of a mechanism involving stereochemically equilibrated boat-chair conformers of a cyclohexane-1,4-diyl is that exo/endo isomerisation (skeletal inversion) will be observed in recovered BCH if similar activation

energies are involved in chair to boat conversion, cleavage of the chair diyl, and coupling of the boat diyl. This has been found for the parent system. Goldstein and Benzon²⁶ reported that pyrolysis of all-exo-d₄-BCH led exclusively to EZ-hexa-1,5-diene, while all-endo-d₄-BCH was present in the recovered BCH (Scheme 2.17).

Scheme 2.17



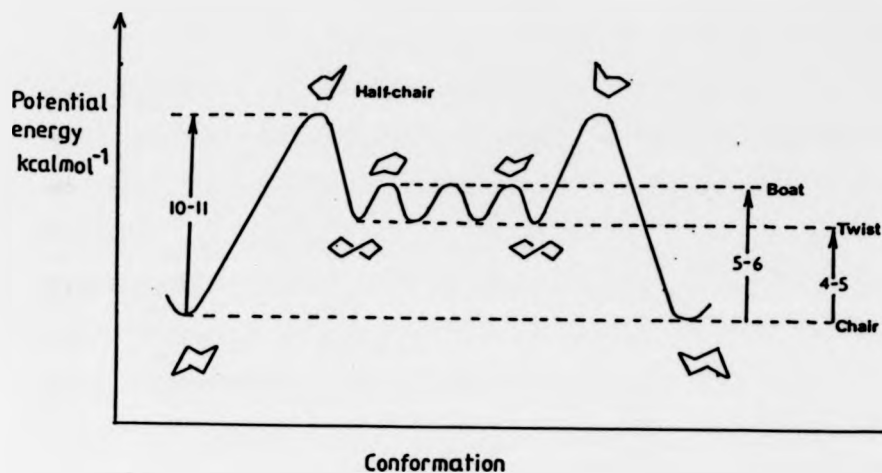
A study of the reaction kinetics²⁶ showed that the activation energies for skeletal inversion and cleavage were similar (E_a (inversion) = 35.0 ± 0.3 kcal mol⁻¹, E_a (cleavage) = 36.0 ± 0.3 kcal mol⁻¹). The skeletal inversion could, in principle, be a concerted reaction (formally a [1,1] antarafacial, antarafacial sigmatropic rearrangement). However, we do not consider that a concerted mechanism is energetically feasible since it would involve a transition state with a planar six-membered ring. The skeletal inversion and stereoselective cleavage could be explained by a mechanism involving stereochemically equilibrated boat and chair conformations of a cyclohexane-1,4-diyl (cf Scheme 2.16). The exclusive formation of EZ-diene only requires that cleavage does not occur from boat diyl conformers.

It is generally accepted that pyrolysis of BCH occurs in a stepwise manner involving biradical intermediates.²⁵ Our discussion so far has only considered the involvement of stereochemically equilibrated boat and chair conformers. However, if the diyl shows similar conformational preferences to cyclohexane, a chair diyl is not required for skeletal inversion or stereoselective cleavage. This can be illustrated by considering conformations of cyclohexane.²⁷

It is well known that there are two forms of cyclohexane; a chair form, which is rigid, and a boat form which is flexible and hence really corresponds to one of a continuous manifold of twist and boat forms. The rigidity of the chair form and the flexibility of the boat form are both immediately apparent from a study of models e.g. Dreiding Models, in which bond angles are held more or less constant but rotation about bonds is not restricted. Any deformation of the chair form is associated with a deviation of the tetrahedral bond angles from their standard value (ca 109°). On the other hand, very little bond-angle distortion is required in passing from a boat form to a twist form and vice versa. This is reflected in the potential energy curve for interconversion of cyclohexane conformers (Figure 2.1).

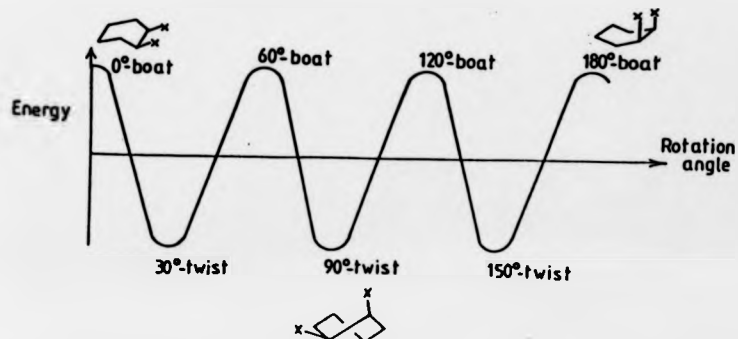
Inspection of Figure 2.1 shows that the conversion of chair to boat requires some 10-11 kcal mol⁻¹ due to deviation from the normal tetrahedral bond angles. Since this is not required in converting boat and twist forms, the energy required is much less (1-2 kcal mol⁻¹). If cyclohexane-1,4-diyl shows similar conformational preferences to cyclohexane, it is more energetically economical for skeletal inversion (which requires interconversion of boat conformers) to occur via boat and twist forms rather than boat and chair forms.

Figure 2.1 Cyclohexane potential energy surface (modified from Ref.27)



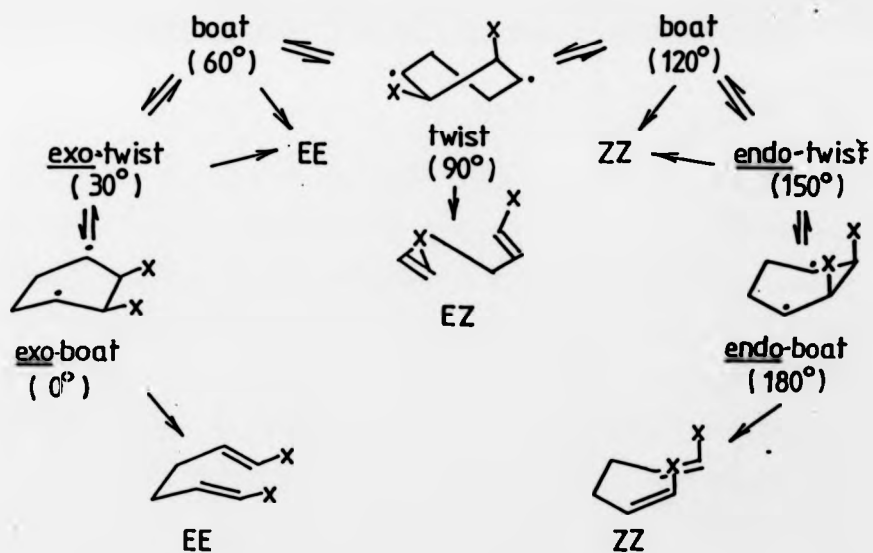
Could the flexible form also be involved in the stereoselective cleavage reaction of BCH? The flexible form of cyclohexane keeps bond angles constant but allows rotation about bonds. If we define a 0° -boat as one having two pseudo-equatorial substituents, inspection of Driending Models reveals that a 180° rotation is required to generate the inverted (di-axially substituted) boat, required for skeletal inversion. There are also several intermediate boat and twist arrangements, as shown in Figure 2.2.

Figure 2.2 Rotation about bonds in the flexible form of 1,2-disubstituted cyclohexanes.



If cyclohexane-1,4-diy1 shows similar conformational preferences (as the calculations (Gaussian 70 at STO-3G level) of Lloyd *et al*²⁸ suggest) then at 90° rotation a conformer is reached which could ring open to EZ-diene. This is illustrated in Scheme 2.18, which also shows the other stereochemical consequences of diene formation by ring opening of flexible diyls as a function of rotation about bonds.

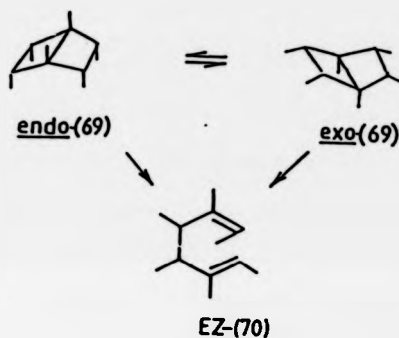
Scheme 2.18 Stereochemistry of hexa-1,5-dienes formed from non chair conformations of cyclohexane-1,4-diyls as a function of pseudorotation. Angle of pseudorotation is given in brackets.



Thus, the 90° -twist conformer is a possible intermediate in both skeletal inversion and stereoselective cleavage of BCH.

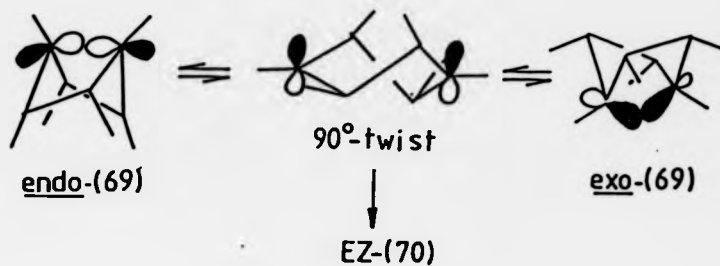
Rantwijk *et al*²⁹ invoked non-chair conformations of a cyclohexane-1,4-diyl to rationalise the skeletal inversion and exclusive stereoselective cleavage observed in the pyrolysis of the all-endo hexamethyl BCH (69), (Scheme 2.19).

Scheme 2.19



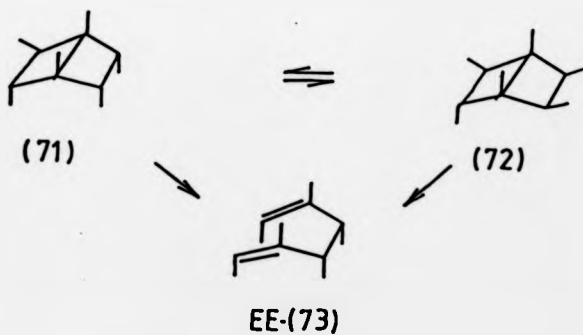
They suggested that the [2.2.0.] skeleton twists, leading to cleavage of the central C-C bond and entry onto the twist-boat potential energy surface of the diyl.²⁹ This twisting of the [2.2.0.] skeleton was considered reasonable as the gas phase structure of the parent (unsubstituted) BCH is somewhat skewed.³⁰ At 90° pseudorotation a conformation is reached which can ring open to EZ-(70). Rantwijk *et al*²⁹ suggested that the 90° -twist conformer is stabilised relative to other possible twist-conformers by a 1,4- π -bond (Scheme 2.20).

Scheme 2.20



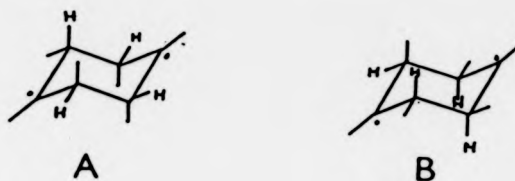
The involvement of a chair biradical was ruled out for the following energetic reasons;²⁹ Pyrolysis of the isomeric hexamethyl BCH's, (71) and (72), yielded predominantly the EE-diene (73) (Scheme 2.21).

Scheme 2.21



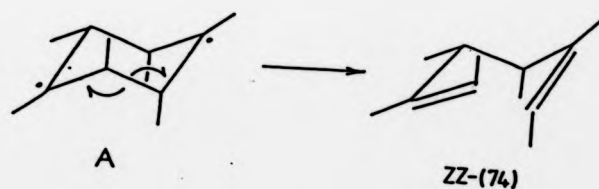
Rantwijk *et al*²⁹ noted that if a chair diyl were involved it could have two possible conformations. Both of these were assumed to have planar radical centres (Figure 2.3).

Figure 2.3 Possible chair conformations of a hexamethyl cyclohexane-1,4-diyl



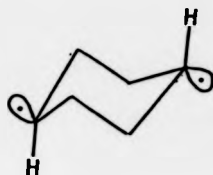
Conformer B has three eclipsing methyl groups whereas conformer A has only two. Therefore, it was reasoned that conformer A was the more stable of the two. Cleavage of the C₅-C₆ bond in A would lead to a ZZ-diene (Scheme 2.22).

Scheme 2.22



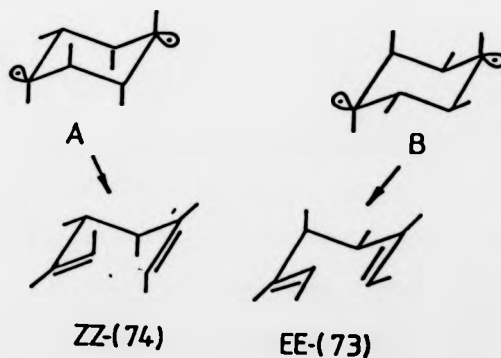
Since pyrolysis of (71) and (72) yielded predominantly the EE-diene (Scheme 2.21), Rantwijk *et al.*²⁹ concluded that cleavage must occur mainly *via* a 90°-twist diyl conformer. However, it is not certain that conformer A is more stable than conformer B. Dewar *et al.*³¹ have carried out a MINDO/3 study of the C₆H₁₀ system and found that the lowest energy geometry of the chair diyl is one which is distorted in the manner shown in Figure 2.4.

Figure 2.4 Distortion of the cyclohexane-1,4-diyl chair conformation (from ref. 31).



If conformers A and B had similarly pyrimidalised radical centres, we suggest that conformer B will be the more stable of the two (neither conformers has eclipsed methyls but conformer A has three axial methyls and B only has one). Since conformer B will ring open to yield EE-diene (Scheme 2.23), a chair diyl is a feasible intermediate in the cleavage of hexamethyl BCH's, contrary to the arguments of Rantwijk *et al*²⁹.

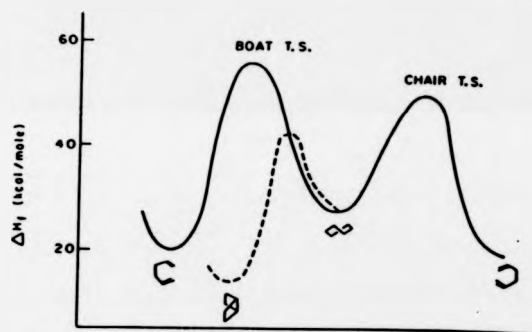
Scheme 2.23



In summary, stereoselective cleavage of BCH's may occur from a chair or a 90°-twist conformer.

Theoretical studies agree that pyrolysis of BCH involves biradical intermediates but do not distinguish between the involvement of boat and chair or flexible cyclohexane-1,4-diyls. In the most advanced theoretical study to date, Dewar *et al*³¹ used MINDO/3 with configuration interaction to calculate the various energies of intermediates and transition states involved in the pyrolysis of BCH. Their calculated potential energy surface is illustrated in Figure 2.5.

Figure 2.5 MINDO/3 potential energy surface for BCH pyrolysis (from ref. 31).



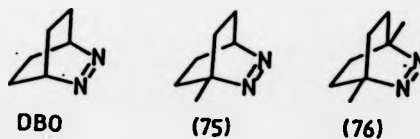
The accuracy of the MINDO/3 calculations with configuration interaction was insufficient to allow the relative energies of the chair, boat, and twist diyl conformations to be determined. However, the depth of the minimum (ca 15 kcal mol⁻¹) is such for the qualitative prediction to be that all diyl conformational interconversions occur faster than cleavage or coupling.³¹ This prediction is consistent with stereochemical studies of the pyrolysis but does not distinguish between mechanisms involving boat and chair or flexible diyl conformers.

2.4.2. Thermal decomposition of DBO

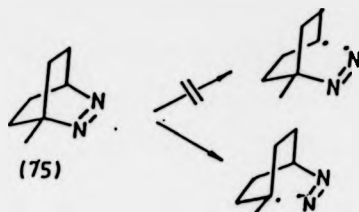
Thermal decomposition of DBO proceeds through an assumed cyclohexane-1,4-diyl intermediate.¹ Consequently, stereochemical studies of the azoalkane decomposition should be identical (or very similar) to those of BCH pyrolysis (i.e. biradical commonality). Different stereochemical behaviour may arise if the diyl is generated from DBO by stepwise C-N bond cleavage. If the generated diazenyl biradical is sufficiently long-lived it may show stereochemical behaviour quite different from that of the diyl in BCH pyrolysis. Is there evidence that decomposition of DBO involves stepwise C-N bond cleavage?

2.4.2.1. Application of the Ramsperger Criterion to DBO decomposition

In order to test stepwise versus synchronous C-N bond cleavage mechanisms, Engel et al⁸ have applied the Ramsperger criterion³² to DBO and the bridgehead methyl substituted derivatives (75) and (76);

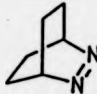
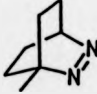
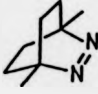


According to this criterion, successive addition of radical stabilising groups to the bridgehead positions should cause equal rate enhancement factors (n) if C-N bond cleavage occurs synchronously. In the stepwise mechanism, initial C-N bond cleavage in (75) would be expected to occur at the C-N bond leading to the more stable radical centre, viz;



Thus, the rate constant for the decomposition of (76) should be identical (or very similar) to that of (75) if an irreversible stepwise mechanism is involved. Assigning a value of 1.0 to the first order rate constant of DBO, the synchronous mechanism predicts the relative rate constants (k_{rel}) for (75) and (76) to be n and n^2 , respectively. If decomposition occurs by a stepwise mechanism, the k_{rel} values for (75) and (76) should be n and $(2n-1)^{33}$, respectively. The experimental rate constants for three different decomposition temperatures are given in Table 2.7.⁸

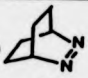
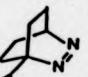
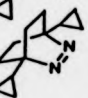
Table 2.7 Rate constants for thermolysis of some DBO's (modified from ref. 8)

Azoalkane	$k \times 10^4, s^{-1}$	temperature, °C
	0.635	230.22
	1.500	239.93
	2.495	245.96
	1.388	230.22
	3.193	239.93
	5.182	245.96
	3.382	230.22
	7.595	239.93
	12.500	245.96

The average k_{rel} values from these data are 1.0, 2.13 and 5.13 for DBO, (75), and (76), respectively. The predicted k_{rel} values are 1.0, 2.13, and 3.26 for the stepwise mechanism, and 1.0, 2.13, and 4.54 for the mechanism involving synchronous C-N bond cleavage. Thus, the second methyl group was found to enhance the rate more than predicted by either mechanism. Engel *et al*⁸ suggested the results were more consistent with the synchronous C-N bond cleavage mechanism, and attributed the discrepancy between k_{rel} observed and k_{rel} predicted (ca 10%) to experimental error. This conclusion is not unambiguous because the rate enhancements caused by methyl groups on DBO decomposition are extremely small (in acyclic azoalkanes, methyl groups enhance the rate approximately 15 fold⁸). Such small rate enhancement factors (attributed to reduction of ground state strain in (75) and (76)) magnify the errors in the observed k_{rel} values.⁸

The Ramsperger criterion has, however, been applied to numerous other DBO derivatives where the bridgehead substituents cause a much greater rate enhancement. For example, the series of azoalkanes consisting of DBO, (77), and (78) gave an observed k_{rel} value for (78) that was in excellent agreement with that predicted for the synchronous C-N bond cleavage mechanism (Table 2.8).³⁴

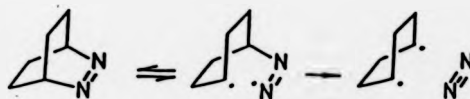
Table 2.8 Observed and predicted relative rate constants for thermolysis of DBO's

Azoalkane	k_{rel} predicted		k_{rel} observed
	stepwise mechanism	synchronous mechanism	
DBO 	1.0	1.0	1.0
(77) 	4.27	4.27	4.27
(78) 	7.54(2n-1)	18.23(n ²)	18.4

The rate enhancement caused by addition of bridgehead cyclopropyl groups to the bridgehead carbons of DBO is considerably greater than the rate enhancement caused by addition of methyl groups. Consequently, differences in ground state strain between DBO, (77), and (78) (ca. 1.5 kcal mol⁻¹ for each added cyclopropyl) are less significant than differences in ground state strain for the methyl substituted derivatives ((75) and (76)).³⁴

Application of the Ramsperger criterion only affords mechanistic information on the bridgehead disubstituted member of the series. The previous two examples have indicated that (76) and (78) lose nitrogen by synchronous C-N bond cleavage. This implies that symmetric azoalkanes (including the parent compound) denitrogenate by synchronous C-N bond cleavage. However, Engel *et al*³⁴ have noted that such kinetic arguments can't distinguish between synchronous and stepwise C-N bond cleavage mechanisms in symmetric DBO's if the stepwise mechanism is reversible (Scheme 2.24).

Scheme 2.24



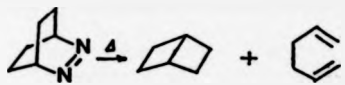
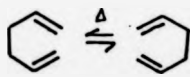
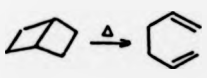
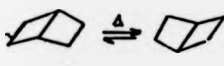
2.4.2.2. Stereochemical studies

There are very few stereochemical studies of DBO derivatives thermal decomposition. This is because the products, BCH's and hexa-1,5-dienes, can undergo secondary reactions at the temperature required to decompose the azoalkane. The possible secondary reactions are:

- (a) Skeletal inversion of BCH's
- (b) Cleavage of BCH's
- (c) Cope rearrangement of hexa-1,5-dienes.

The thermal stability of BCH and hexa-1,5-diene can be assessed by comparing the relative rates (or reaction half-lives) of the various reactions at the temperature required (ca 220°) to decompose DBO (Table 2.9).


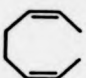
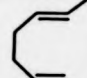
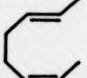

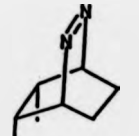
Table 2.9 Rate parameters for the decomposition of DBO and BCH, and the Cope rearrangement of hexa-1,5-diene.

Reaction	Rate parameters ^a	$t_{1/2}^{220^\circ}$	Ref.
	$\ln k_D = 36.1 - \frac{45,700}{RT}$	2.5×10^4	34
	$\ln k_{\text{Cope}} = 23.9 - \frac{34,300}{RT}$	4.5×10^4	31
	$\ln k_{\text{Cleavage}} = 31.6 - \frac{36,800}{RT}$	260	26
	$\ln k_{\text{Inversion}} = 31.5 - \frac{35,900}{RT}$	115	26

a) Rate parameters expressed in natural logarithm form of Arrhenius equation with E_a in J mol^{-1}

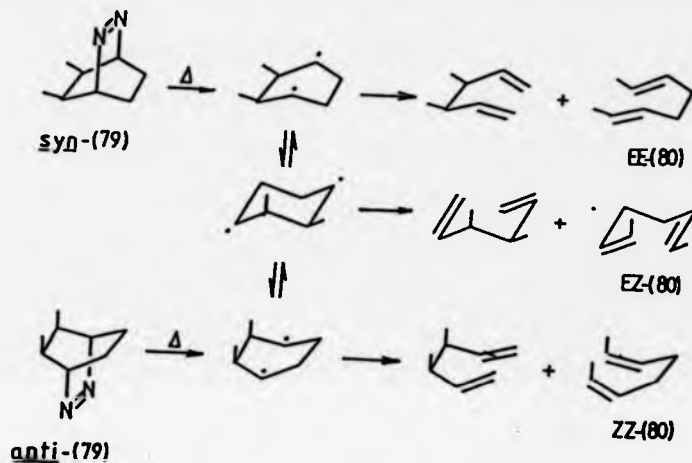
Inspection of the data in Table 2.9 reveals that BCH is particularly unstable at the temperature required to decompose DBO (BCH undergoes skeletal inversion and cleavage faster than loss of nitrogen from the azoalkane). Furthermore, if the azoalkane decomposition were to be carried out under static conditions, the hexa-1,5-dienes would also undergo a Cope rearrangement. Roth and Martin³⁵ appreciated these complications in their study involving the thermal decomposition of both cis isomers of 5,6-dimethyl-2,3-diazabicyclo[2.2.2]oct-2-ene (79). In an attempt to obtain the kinetic hydrocarbon product distributions, the decompositions were carried to only 5% conversion under vacuum flash pyrolysis (VFP) conditions (under VFP conditions the product residence time is ca ls).³⁵ The product distributions obtained are shown in Table 2.10.

Table 2.10 Thermal decomposition stereochemistry of 5,6-dimethyl-DBO (from Ref. 35).

REACTANT	% PRODUCTS			
				
 syn-(79)	33.0	<0.1	8.7	58.3
 anti-(79)	33.0	<0.1	3.0	64.0

The results were rationalised³⁵ by invoking stereochemically equilibrated conformations of a cyclohexane-1,4-diy1 and assuming predominant cleavage occurs from a chair conformer (Scheme 2.25).

Scheme 2.25



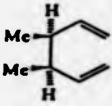
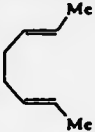
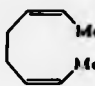
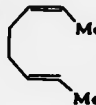
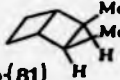
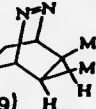

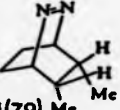
It was noted that an identical mechanism had been used to explain the results from stereochemical studies of BCH pyrolyses. This implies that pyrolysis of BCH and thermal decomposition of DBO involve a common biradical intermediate. Roth later compared the thermal decomposition of both cis isomers of (79) with the appropriate BCH pyrolyses under identical VFP conditions.³⁶ The product distributions observed are shown in Table 2.11.

Several points are to be noted from the data in Table 2.11.

Firstly, all the decompositions lead to near identical product distributions implying a common biradical intermediate.

Secondly, the cleavage reaction is stereoselective leading to predominantly EZ-diene.

Table 2.11 Product distributions from the thermolysis of 2,3-dimethyl BCH's and 2,3-dimethyl DBO's (modified from ref. 36)

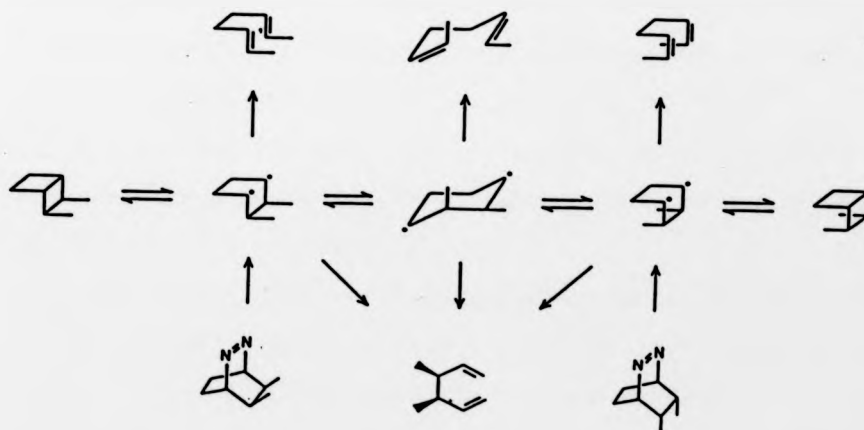
Reactant	Products (%)				<u>exo</u> (81)	<u>endo</u> (81)
						
 <u>exo</u> (81)	37.4	3.1	0	54.9	*	4.6
 <u>syn</u> (79)	28.7	6.3	2.5	51.5	*	7.1
 <u>endo</u> (81)	33.1	1.4	0	47.6	17.9	*
 <u>anti</u> (79)	31.1	2.3	0	47.2	17.1	*

- a These decompositions were carried to only 5% conversion; The percentages listed are the percentages of other compounds kinetically formed from exo-(81) and endo-(81).
- b The percentages listed have been calculated excluding endo-(81) formed from anti-(79) (7.0%) and exo-(81) from syn-(79) (11.7%) in order to compare precisely the azocompound and hydrocarbon thermolysis product distributions.

Thirdly, decomposition of both cis azoalkane isomers leads to a predominance of the exo-BCH. However, our calculations based on the data in Table 2.11³⁷ show that ring closure is stereorandom as both cis isomers of (79) give a very similar ratio of stereoisomeric BCH's.

These results were explained by invoking a common biradical intermediate.³⁶ Loss of nitrogen from (79) leads to a cyclohexane-1,4-diyl in a boat (or nearby twist) conformation. The same intermediate can be generated by cleavage of the central C-C bond in BCH. Roth assumed³⁶ that the first formed boat-diyl then undergoes conformational boat-chair equilibration before coupling to BCH's stereorandomly, and cleaving preferentially from the chair diyl (as we have noted previously, stereoselective cleavage does not require involvement of a chair diyl. Cleavage from a 90°-twist conformer would also lead to EZ-diene). Roth's proposed mechanism³⁶ is shown in Scheme 2.26.

Scheme 2.26 (from ref. 16)



Note that this mechanism affords no information on whether loss of nitrogen occurs by stepwise or synchronous C-N bond cleavage. More importantly, all Roth's conclusions are based on the crucial assumption that the product distributions in Table 2.11 represent those kinetically formed from the azoalkanes.³⁶ It is not certain that the latter assumption is valid, even though the decompositions were only carried to 5% conversion. VFP conditions reduce the product residence time to ca 1s. In order to achieve this the temperature must be considerably greater than the minimum temperature required to decompose the azoalkane (ca 220°). As BCH is considerably more thermally labile than DBO (see Table 2.9) the use of higher temperatures may lead to secondary reactions (cleavage and skeletal inversion) of BCH's formed kinetically from the azoalkane, even at low conversion. If this were the case it would not be surprising that the product distributions from the azoalkanes and BCH's (see Table 2.11) were so similar! It is perhaps significant that Roth and Martin did not report the temperature at which the azoalkane decompositions were carried out.^{35,36}

In summary, it would appear that any conclusions based on stereochemical studies of DBO decomposition are somewhat ambiguous due to product thermal lability. This problem could be overcome if loss of nitrogen from DBO could be carried out at a temperature at which the hydrocarbon products were thermally stable. Photochemical decomposition of DBO offers this opportunity. The key questions in the photochemical decomposition are:

- (a) does loss of nitrogen occur by a similar mechanism (stepwise versus synchronous C-N bond cleavage) to that involved in thermal decomposition of DBO?

(b) does the assumed cyclohexane-1, 4-diyl show similar stereochemical behaviour to the assumed intermediate generated by thermal decomposition of DBO (or BCH)?

2.4.3 Photochemical decomposition of DBO

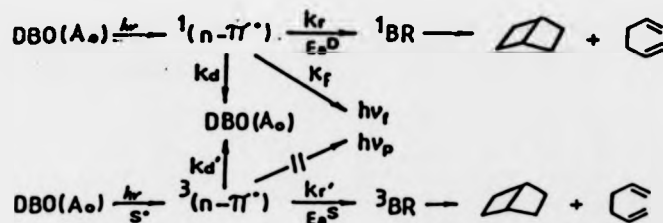
There is considerable evidence from trapping, kinetic, and product studies that solution phase photochemical decomposition of DBO and its derivatives involves an intermediate cyclohexane-1,4-diyl.¹ Is the diyl generated by synchronous or stepwise C-N bond cleavage?

We have previously noted the kinetic evidence which suggests that symmetrically bridgehead substituted DBO's lose nitrogen thermally by synchronous C-N bond cleavage (see Section 2.4.2.1). Is there kinetic evidence that photochemical decomposition involves a similar mechanism?

2.4.3.1. Photophysical studies

The photochemistry of the parent azoalkane was originally reported by Clark and Steel³⁸ but has recently been summarised by Engel et al³⁹ (Scheme 2.27).

Scheme 2.27

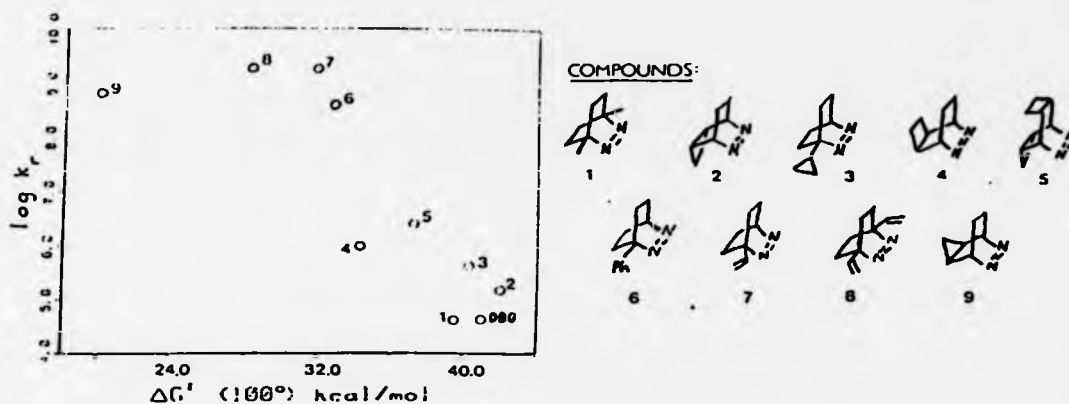


Direct irradiation of ground state (A_0) DBO populates the $^1(n-\pi^*)$ state which decays, fluoresces or decomposes to a singlet biradical (1BR) with rate constants k_d , k_f and k_r , respectively. Triplet sensitisation (S^3) behaves analogously except the $^3(n-\pi^*)$ state does not phosphoresce. The $(n-\pi^*)$ states surmount different energy barriers ($E_a^D = 8.6 \text{ kcal mol}^{-1}$, $E_a^S = 9.0 \text{ kcal mol}^{-1}$) to generate the biradical, accounting for the different temperature dependences of the two photolysis modes.³⁹ No evidence was found to suggest that the $^3(n-\pi^*)$ state is populated from direct irradiation (i.e. lack of transient absorption in LFP) so ISC is probably very inefficient. This is expected on the basis of the 20 kcal mol^{-1} singlet-triplet energy gap, and the forbidden nature of the process. Quantum yields for decomposition (ϕ_r), in terms of nitrogen evolution, and the long fluorescence lifetimes (τ_f) of DBO and its derivatives

were measured directly. From Scheme 2.27 this enabled the rate constants for decomposition (k_r) to be calculated ($k_r = \phi_r^D / \tau_f$). In this manner, Engel *et al*³⁹ obtained k_r values for direct photochemical decomposition of DBO and several of its derivatives. These values were compared to rate parameters for the thermal decomposition, and showed that direct photochemical and thermal decomposition of DBO's have similar substituent dependences (Figure 2.7).³⁹

The correlation shown in Figure 2.7 is frustratingly crude and far from conclusive. Nevertheless, it suggests that thermal and direct photochemical decomposition of DBO and its derivatives proceed by a similar mechanism.

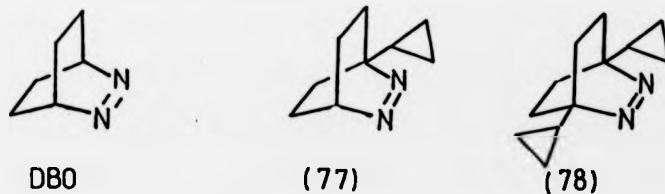
Figure 2.7 Correlations of photochemical with thermal stability of DBO derivatives (from ref. 39)



2.4.3.2. Application of the Ramsperger criterion to direct photochemical decomposition of DBO's

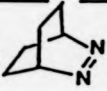
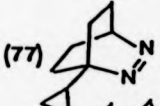
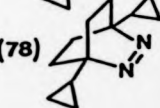
Application of the Ramsperger criterion to thermal decomposition of the series of azoalkanes shown in Scheme 2.28 led to an observed rate constant for (78) that was in excellent agreement with that predicted by a synchronous C-N bond cleavage mechanism (see Section 2.4.2.1).

Scheme 2.28



Since Engel *et al*³⁹ have reported Φ_r^D and τ_f values for (77) and (78), we can calculate k_r values and apply the Ramsperger criterion to the direct photochemical decomposition. The calculated and predicted rate constants for the series are shown in Table 2.12.

Table 2.12 Observed and predicted relative rate constants for photochemical decomposition of DBO's

Azoalkane	$k_r \times 10^{-4} \text{ s}^{-1}$	k_{rel} predicted		k_{rel} observed
		stepwise mechanism	synchronous mechanism	
DBO 	4.13	1.0	1.0	1.0
(77) 	39.80	9.64	9.64	9.64
(78) 	25.32	18.27(2n-1)	92.93(n ²)	6.13

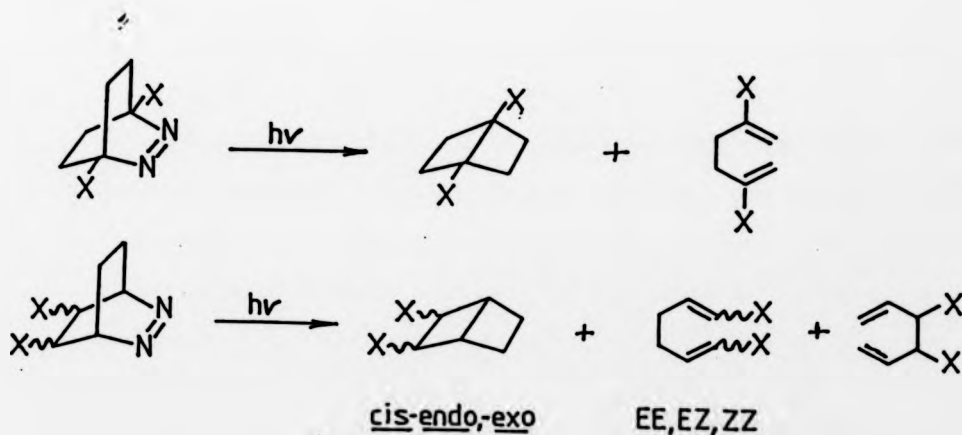
Inspection of the data in Table 2.12 shows that addition of the second cyclopropyl group enhances the rate less than expected by either mechanism. However, the results are more consistent with a stepwise C-N bond cleavage mechanism. The results should be compared with the thermal decomposition in which for the synchronous C-N bond cleavage mechanism the k_{rel} predicted and k_{rel} observed values show excellent agreement (see Section 2.4.2.1.). This contradicts the tentative conclusion of Engel *et al*³⁴ that thermal and photochemical

decomposition of DBO's proceed by a similar mechanism. These studies show that conclusive evidence is not yet available to determine whether loss of nitrogen from DBO occurs by stepwise or synchronous C-N bond cleavage.

2.4.3.3. Stereochemical studies




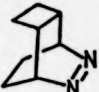

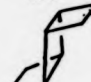
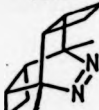

Stereochemical behaviour of the assumed cyclohexane-1,4-diyl intermediate has, to date, received little consideration. Substituents of the bridgehead positions are known to affect diyl cleavage/coupling ratios but give no indication of the exo/endo ratio of BCH's, or diene stereochemistry.³⁹ This information can only be obtained from DBO derivatives with cis substituents at the 5,6-positions (Scheme 2.29).

Scheme 2.29



Photolysis of certain polycyclic azoalkanes has yielded stereochemical information on the coupling reaction. The product distributions are shown in Table 2.13.

Table 2.13 Photochemical decomposition stereochemistry of some DBO derivatives

AZOALKANE	Conditions	Retention	Inversion	Ref.
 (82)	$h\nu$ (direct) -20° , Et_2O	 0	 100	40
 (83)	$h\nu$ (direct) 25° , a	 0	 100	41
 (84)	$h\nu$ (direct) -10° , Et_2O	 100	b	42

- a. Various other solutions were used which did not affect the stereoselectivity of ring closure but did lead to different cleavage/coupling ratios.
- b. There are two possible inversion products, neither of which was observed.

Inspection of the data in Table 2.13 reveals that the tricyclic azoalkanes, (82)⁴⁰ and (83)⁴¹, stereoselectively ring close with double inversion of configuration. However, these decompositions were sterically biased and gave the more thermodynamically stable isomers. The tetracyclic azoalkane (84) led to a diyl closure product with complete retention of stereochemistry.⁴² Examination of Drieding

models shows that double inversion is very hindered so retention of configuration was the only possible stereochemical outcome.

2.5 Summary

In this Chapter we have discussed some of the mechanisms proposed for the decomposition of azoalkanes. We have seen that azoalkanes that generate 1,3-biradicals can lead to products with doubly retained, doubly inverted, or scrambled stereochemistry. In the case of products being formed with doubly inverted stereochemistry (typically from DBH and its derivatives) a variety of mechanisms were proposed with the common feature being that they all required a planar five membered carbon ring at some point along the reaction co-ordinate.

Azoalkanes that generate 1,4-biradicals such as DBD, DBN, and tetrahydropyridazines, decompose to products with partially retained stereochemistry. This suggests the involvement of a 1,4-biradical formed from the azoalkane, initially with retained configuration, that couples or cleaves before complete conformational equilibration.

It would appear from stereochemical studies that thermal decomposition of DBO involves completely stereochemically equilibrated conformers of a cyclohexane-1,4-diyl. However, it is not certain that the product distribution observed in the thermal decomposition represents the kinetic distribution since the hydrocarbon products are thermally unstable under the reaction conditions. Significantly, thermal decomposition of 5,6-dimethyl-DBO and pyrolysis of 2,3-dimethyl BCH lead to near identical product distributions. Does this indicate biradical commonality or the fact that the BCH products are unstable under the reaction conditions used to decompose DBO?

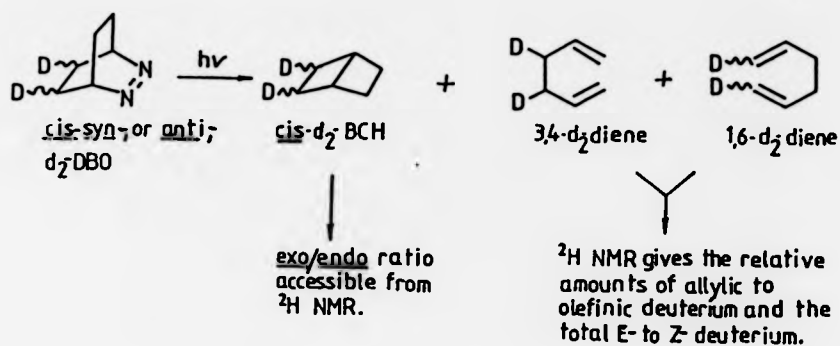
Ideally we should compare the stereochemistry of the photochemical decomposition of DBO with BCH pyrolysis. However, few stereochemical studies of the photochemical decomposition have been reported, and those that have were sterically biased so that the more thermodynamically stable products were formed. Clearly, a stereochemical study of DBO is required using stereochemical labels that do not lead to steric bias in the product distribution. The results, when compared with the stereochemistry of BCH pyrolysis, will indicate whether a common biradical intermediate is involved, and its stereochemical behaviour. The product stereochemistry from the photochemical decomposition may also give information on the mechanism of nitrogen loss (ie stepwise versus synchronous C-N bond cleavage), which kinetic studies (application of the Ramsperger criterion) suggest is stepwise.

2.6 Scope of this work: General strategy involved in studying the stereochemistry of DBO decomposition

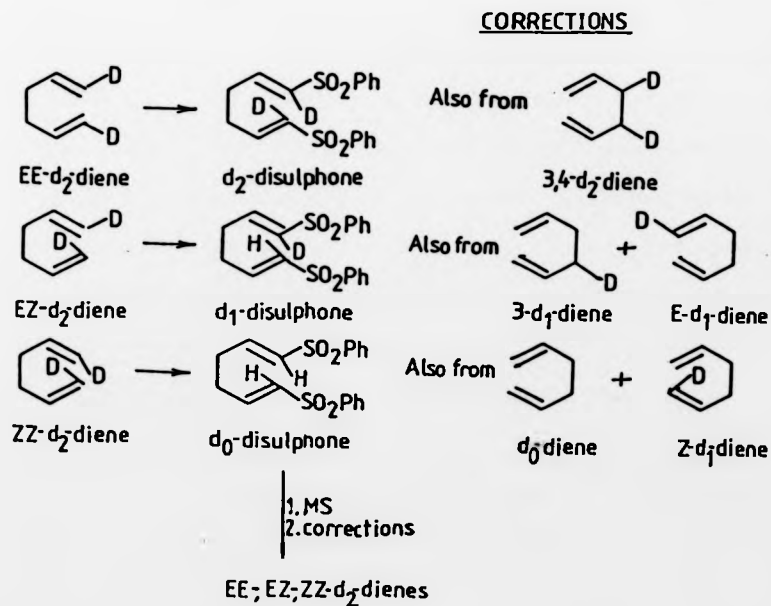
The general strategy of our stereochemical study is outlined in Schemes 2.30 and 2.31. Thus, direct and sensitised solution phase photolysis of stereoselectively cis-deuterium labelled azoalkane (d_2 -DBO) should lead to the deuterated hydrocarbons shown in Scheme 2.30.¹ The stereochemical course of the ring closure reaction can be ascertained directly from 2H NMR analysis. Electronic integration of the signals corresponding to the exo and endo deuterons in the deuterated bicyclohexanes (d_2 -BCH's) affords the exo/endo ratio.

The stereochemistry of the deuterated diene products (d_2 -dienes) cannot be similarly analysed. The 2H NMR of

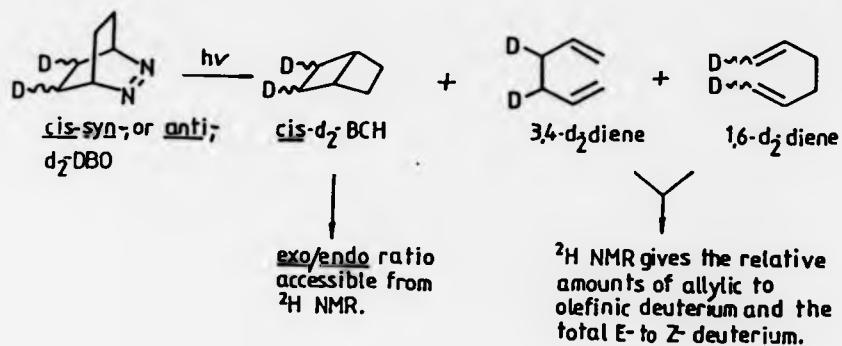
Scheme 2.30



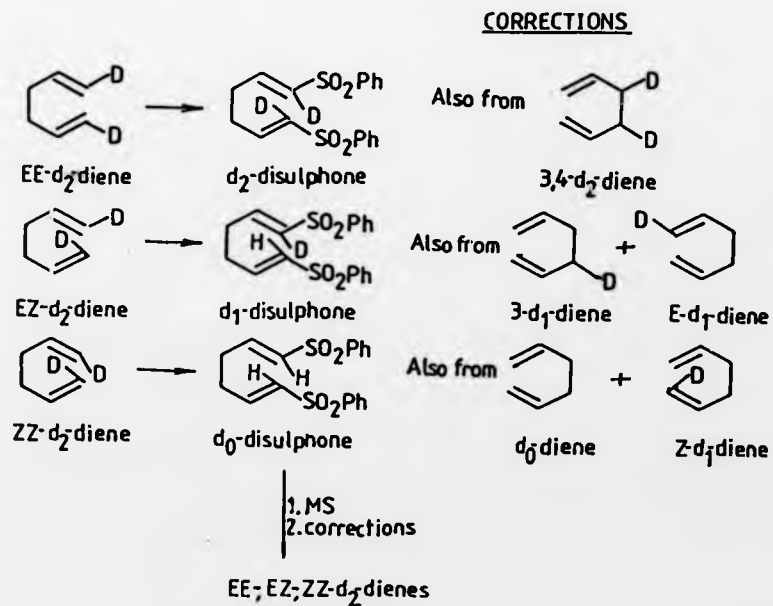
Scheme 2.31



Scheme 2.30



Scheme 2.31



**PAGINATION
ERROR**

d_2 -diene products will only contain three signals corresponding to E-deuterium, Z-deuterium, and allylic deuterium. Integration of these signals will lead to the ratio of E/Z deuterium, and the proportions of allylic to total olefinic deuterium. The proportions of EE, EZ and ZZ isotopomers will be inaccessible. However, similar work in this laboratory¹⁹ has shown that this information can be obtained by an indirect chemical method combined with mass spectroscopy. This involves a stereoselective substitution of phenylsulphonyl groups to the terminal carbons of the product hexadienes. As illustrated in Scheme 2.31, the substitution occurs so that E-deuterium is retained, and Z-deuterium is lost. The required stereochemical information is thus translated into deuterium content of the disulphones. The latter information can be obtained by mass spectroscopy which, after appropriate correction, is directly related to the proportions of EE, EZ and ZZ- d_2 -dienes.

The quality of the results from our stereochemical analysis are dependant on the degree of stereoselectivity and deuterium content in the azoalkane. Consequently we required a sample of d_2 -DBO labelled with high stereoselectivity and with high deuterium content.

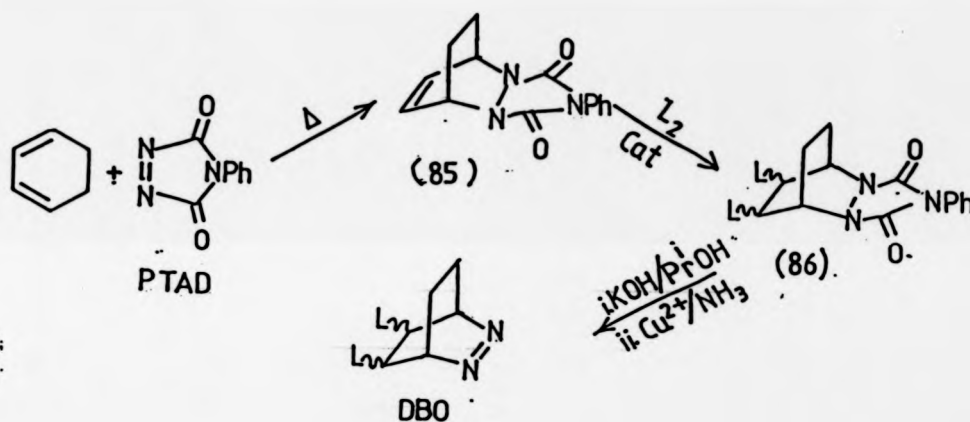
Chapter 3 deals with the synthesis, stereochemical assignments, and determination of deuterium content in samples of d_2 -DBO. Chapter 4 discusses the initial results based on 2H NMR analysis and, in particular the stereochemistry of the BCH's. Chapter 5 gives a detailed account of the diene stereochemical analysis and the results we obtained when applying it to the decomposition of d_2 -DBO. In Chapter 6, a hydrocarbon product previously not reported to be involved in the decomposition is discussed, and the overall results are summarised for a final conclusion.

Throughout, the results are compared with thermal reactions thought to involve intermediate cyclohexane-1,4-diyls such as thermal decomposition of DBO, pyrolysis of BCH, and the Cope rearrangement of hexa-1,5-diene. In the light of the results, several additional experiments were required which are discussed when and where appropriate.

CHAPTER 3

3.1 Synthesis and stereochemical assignments of DBO and its precursor

The synthesis of DBO was accomplished by the previously reported route¹ shown in Scheme 3.1.



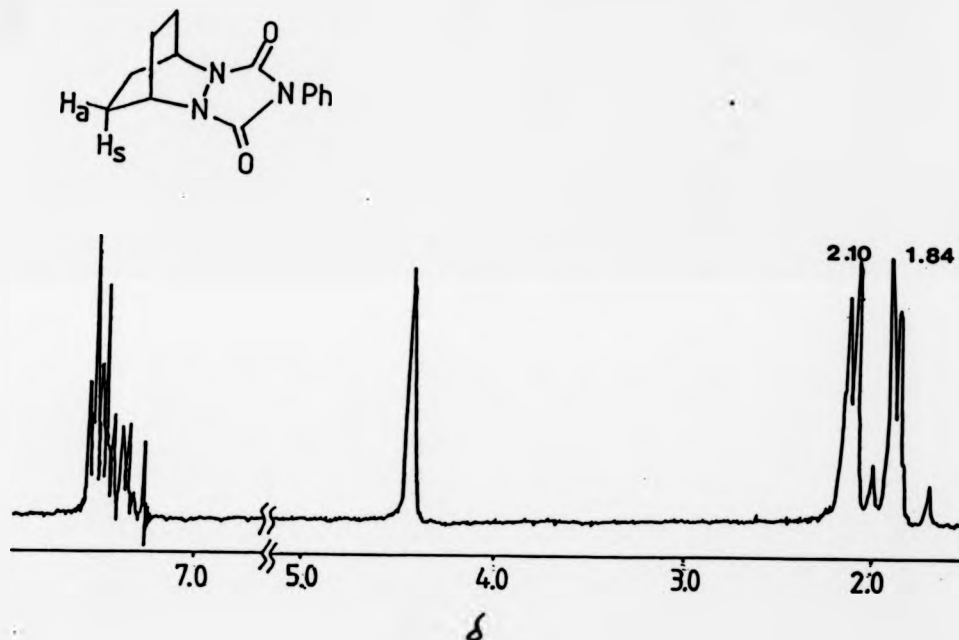
Scheme 3.1 L = H, D

Thus, a Diels-Alder reaction of 4-phenyl-1,2,4-triazoline-3,5-dione (PTAD) with cyclohexa-1,3-diene gave the unsaturated triazolinedione adduct (85). Subsequent catalytic reduction, followed by hydrolysis and copper (II) chloride oxidation of the saturated triazolinedione adduct (86H), gave DBO in moderate yield. Modification of the literature synthesis was found to improve the yields of DBO greatly (ca 80% after purification). The details are given in the experimental.

3.1.1 ¹H NMR stereochemical assignments

The 220MHz ¹H NMR of 4-phenyl-2,4,6-triazatricyclo[5.2.2.0^{2,6}]undecane-3,5-dione (86H) is illustrated in Figure 3.1.

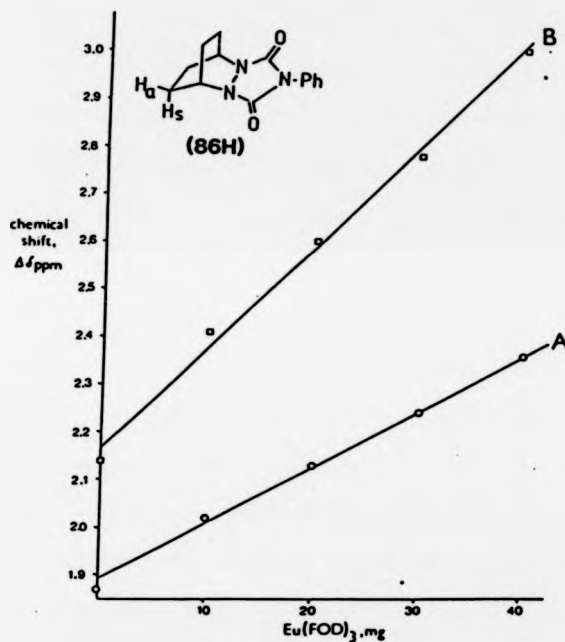
Figure 3.1 220 MHz ¹H NMR of 4-phenyl-2,4,6-triazatricyclo[5.2.2.0^{2,6}]undecane-3,5-dione (86H)



Although the relevant protons (Hs and Ha) are part of a complicated AA'BB'XX' spin-spin system, for simplicity we treated it as a first order spectrum. Thus, we treated the two signals centred at 2.10 ppm and 1.84 ppm as two "doublets", and ignored the small signal in between these "doublets". One of the "doublets" corresponds to the four equivalent syn protons (Hs), and the other to the four

equivalent anti protons (H_a) of (86H). We accomplished their stereochemical assignment using $\text{Eu}(\text{FOD})_3$ lanthanide shift reagent (LSR). The chemical shift dependence of the two "doublets" against added increments of $\text{Eu}(\text{FOD})_3$ is represented graphically in Figure 3.2.

Figure 3.2: Plot of induced chemical shift of H_s and H_a protons in (86H) against added $\text{Eu}(\text{FOD})_3^a$



A: Chemical shift of "doublet" at 1.84 ppm

B: Chemical shift of "doublet" at 2.10 ppm.

a. Tables of results can be found in the experimental section.

Irrespective of whether the europium binds to the N- or O-atoms of (86H), the syn and anti protons are sufficiently isolated from the site of co-ordination for the contact and co-ordination contributions to the downfield shifts to be negligible.² Therefore, the pseudo-contact shift, represented by $(3 \cos^2\theta - 1)r^{-3}$, is dominant.³ Inspection of Drieding models reveals that the angular dependences (θ) of the syn and anti protons are similar. Thus, the induced shift should be dominated by the radial term (r^{-3}). For the low concentrations of $\text{Eu}(\text{FOD})_3$ compared with substrate used in our experiments, the magnitude of the gradients in Figure 3.2 are a measure of the proximity of the co-ordinated europium atom to the syn and anti protons. The signal which shifts the furthest downfield (ie has the larger gradient in the graphs shown in Figure 3.2) corresponds to the signal of the nuclei which are closest to the bound europium atom. Whether the europium is bound near the oxygen or nitrogen atoms, inspection of Drieding models reveals that the syn protons are closest to the europium atom. From inspection of Figure 3.2 we therefore assigned the signal centred at 2.10 ppm to the syn protons and the signal at 1.84 ppm to the anti protons.

The 220 MHz ^1H NMR of DBO is in many ways similar to that of (86H) as the syn and anti protons are also part of an AA'BB'XX' spin-spin system (Figure 3.3).

As in the ^1H NMR of (86H), we can simplify the stereochemical assignment by assuming that the four syn and four anti protons correspond to the two "doublets" centred at 1.55 and 1.27 ppm and ignoring the small signal in between the "doublets". Appropriate use of $\text{Eu}(\text{FOD})_3$ LSR (see experimental section) led to the graphs shown in Figure 3.4.

Figure 3.3: 220 MHz ^1H NMR of DBO

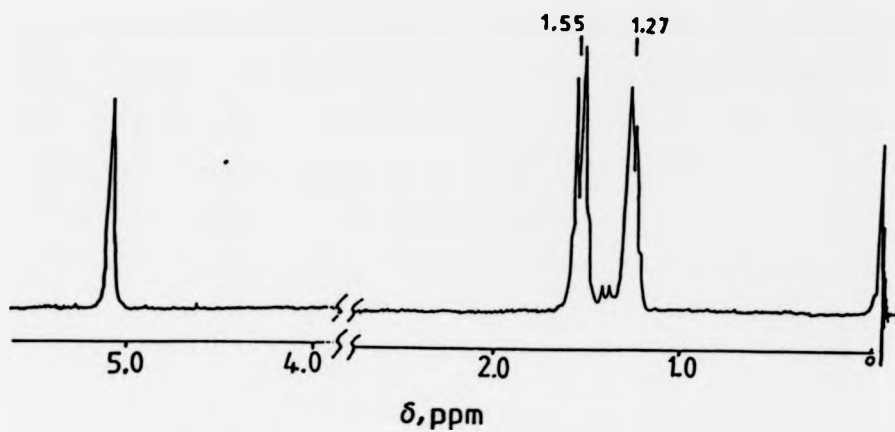
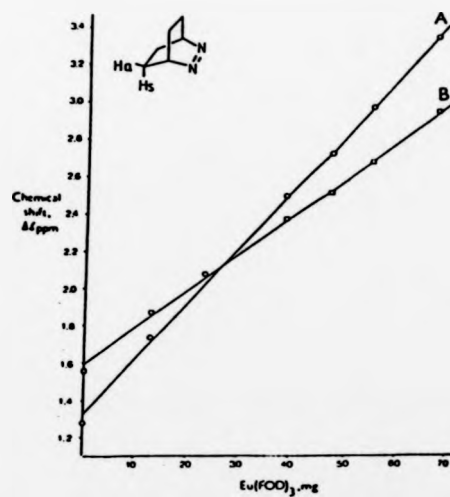


Figure 3.4: Plot of induced chemical shift of Hs and Ha protons in DBO against added $\text{Eu}(\text{FOD})_3$.^a



A: Chemical shift of "doublet" at 1.27 ppm

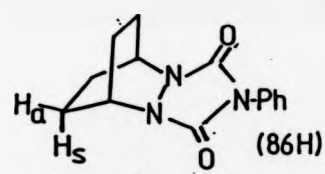
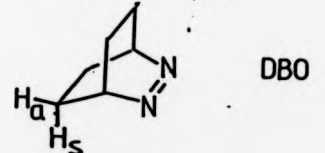
B: Chemical shift of "doublet" at 1.55 ppm

a. Tables of results can be found in the experimental section.

Employing an identical argument to that used to assign the spectrum of (86H), and noting that the europium is bound to the -N=N- function of DBO, requires that the signal showing the larger induced downfield shift (*ie* larger gradient of the two plots in Figure 3.4) is that corresponding to the syn protons. Consequently, the signal centred at 1.27 ppm was assigned to the syn protons while the signal at 1.55 ppm was assigned to the anti protons.

The stereochemical assignments of DBO and (86H) are summarised in Table 3.1.

Table 3.1 Stereochemical assignments in (86H) and DBO.

	¹ H NMR signal	Assignment
 (86H)	1.84 ppm	H _a
	2.10 ppm	H _s
 DBO	1.27 ppm	H _s
	1.55 ppm	H _a

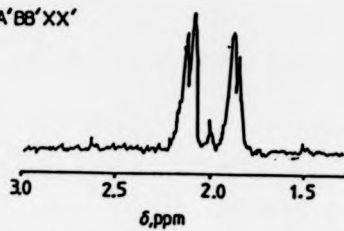
3.12 Synthesis of stereoselectively labelled d₂-DBO (1)

Replacement of hydrogen for deuterium in the synthesis (Scheme 3.1) led to (86D) and subsequently d₂-DBO. Although the proportions of syn and anti deuterium in (86D) and/or d₂-DBO could have been determined by integration of the appropriate ¹H NMR signals, the second order nature of the spectra and the presence of the other

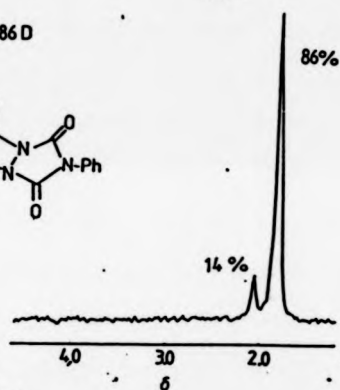
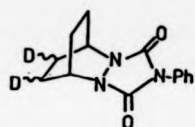
Figure 3.5 ^1H and proton decoupled ^2H NMR's of 86D and DBO derived from catalytic reduction (EtoAc/Adam's catalyst) of (85).

a) ^1H NMR of 86D

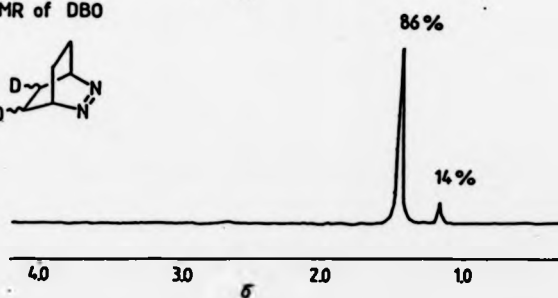
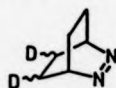
AA'BB' part of AA'BB'XX' spin system



b) ^2H NMR of 86D



c) ^2H NMR of DBO

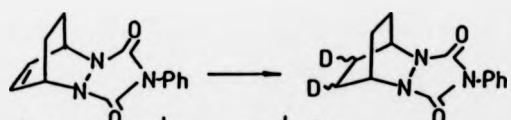


methylene protons limited the accuracy. The deuterium was more quantitatively located by comparison of the ^1H NMR's with the ^2H NMR's. Electronic integration of the latter gave the ratio of syn/anti deuterium. Figure 3.5 shows the ^1H and ^2H NMR's of a sample of (86D) prepared by atmospheric deuteration of the unsaturated adduct (85), using Adam's catalyst in ethyl acetate. Also shown in Figure 3.5 is the ^2H NMR of the d_2 -DBO derived from this sample of (86D).

Inspection of Figure 3.5 reveals that addition of deuterium occurs stereoselectively at the face of the double bond leading to anti-(86D). The sample of d_2 -DBO shows the same ratio of anti/syn deuterium (86:14).

Since we required a sample of d_2 -DBO with stereoisomeric purity, we required a sample of precursor (86D) with a high anti/syn (or syn/anti) ratio of deuterium. As choice of solvent and metal catalyst are known to affect the stereoselectivity of heterogeneous reductions⁴, we deuterogenated (85) under several different conditions. These conditions, together with the quantitative location of deuterium in the resultant samples of (86D), are given in Table 3.2.

Table 3.2 Conditions and stereoselectivities in Deuterogenations of (85)



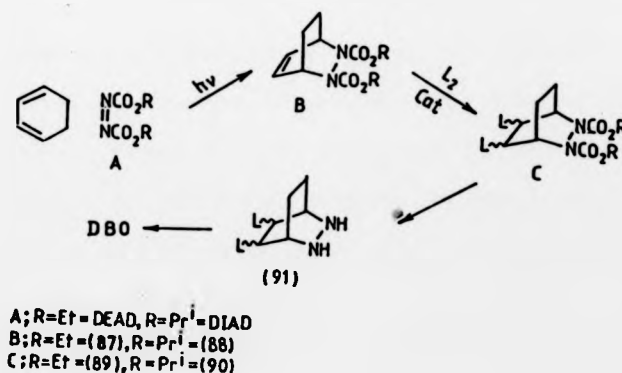
Catalyst	Solvent	^2H NMR signals, ratios syn(2.10ppm):anti(1.84ppm)
PtO_2	EtOH	26 : 74
PtO_2	EtOAc	14 : 86
$\text{Pd}(10\% \text{ on C})$	C_6H_6	32 : 68

The results in Table 3.2 show that all the reductions led to samples of (86D) with a predominance of anti deuterium. As this stereoselectivity is probably a consequence of steric hindrance when the double bond attaches to the catalyst surface, we felt it would be easier to obtain samples of d_2 -DBO with a higher anti/syn (or syn/anti) ratio of deuterium by employing a precursor with a more hindered double bond.

3.2 Synthesis of Stereoselectively Labelled d_2 -DBO (2)

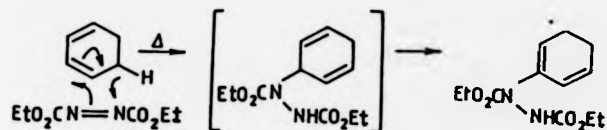
The azoester chosen to synthesise a more hindered DBO precursor was diisopropylazodicarboxylate (DIAD). Although DIAD has not previously been used in Diels-Alder reactions with cyclohexa-1,3-diene, similar reactions with the diethyl analogue (DEAD) are well known.⁵ Furthermore, the adducts obtained from the latter reactions have been used as precursors in the synthesis of DBO⁶ and thus serve as a useful model for our synthesis (Scheme 3.2).

Scheme 3.2



As DEAD is a less reactive dieneophile than PTAD, higher temperatures are required for it to undergo Diels-Alder reactions with cyclohexa-1,3-diene.⁷ The use of higher temperatures has been reported to lead to low yields of the unsaturated diethyl bis carbamate (87) because a thermally allowed $\pi 2s + \pi 2s + \pi 2s$ (or "ene") reaction becomes the major reaction pathway (Scheme 3.3).⁶

Scheme 3.3

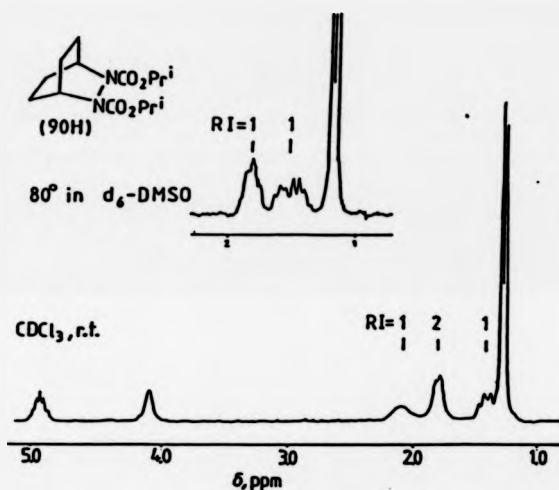


Askani obtained high yields of the Diels-Alder adduct by carrying out the reaction under photochemical conditions at ambient temperature.⁸ Since DEAD is predominantly trans at ambient temperature and photolysis is assumed to cause trans to cis isomerization of DEAD, Askani concluded that the cis-DEAD isomer must be more reactive than the trans. Askani's modification was reported prior to Woodward and Hoffman's discussions of the importance of orbital symmetry in organic reactions.⁹ In the light of Woodward and Hoffman's report, we can rationalise the greater reactivity of the cis-DEAD isomer compared with the trans, on the basis of secondary orbital interaction effects on Diels-Alder reactions.

Using Askani's modification we were able to prepare the unsaturated Diels-Alder adduct (88) in high yield. The synthesis of DBO could then be accomplished from (88) by catalytic reduction to

(90), followed by hydrolysis and oxidation (Scheme 3.2). The ^1H NMR of the precursor (90H) is illustrated in Figure 3.6.

Figure 3.6 220MHz ^1H NMR of (90H) in CCl_4 .
(Inset; 1.3-2.2 ppm at 80° in d_6 -DMSO)

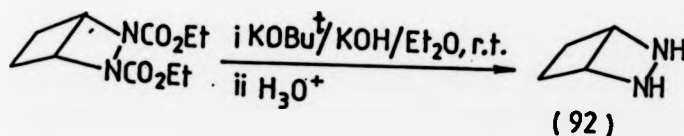


Restricted rotation about the amide bonds doubles the number of signals for the syn and anti protons of (90H). Thus, the three signals at 2.09, 1.78 and 1.39 ppm are due to two pairs of overlapping signals corresponding to the four syn and four anti protons of (90H). We verified that non-equivalence was due to restricted rotation by running the NMR spectrum at elevated temperatures. At 80° in d_6 DMSO, rotation about the amide bond of (90H) occurs. This simplifies the ^1H NMR spectrum since only one signal appears for the four syn protons, and one for the four anti protons of (90H) (inset, Figure 3.6).¹⁰ Due to the fact that the syn and anti protons of (90H) are non-equivalent and are part of a complicated ABCDXY spin

system, we were unable to achieve their stereochemical assignment by LSR studies. However, this is of no importance since we have previously assigned the ^1H and ^2H NMR's of DBO and so were able to determine reduction stereoselectivities.

One of the problems we did encounter using (90) as precursor was finding satisfactory conditions for its hydrolysis and oxidation. Using the procedure we had previously used for (86) (refluxing in potassium hydroxide and isopropyl alcohol for three hours, followed by copper (II) chloride oxidation) gave poor yields of DBO (ca 10% after purification). Consequently we employed several different methods to improve the yields of DBO from (90).

Gassman *et al*¹¹ have reported a mild method for the hydrolysis of amides that has been successfully applied to the analogous preparation of 2,3-diazabicyclo[2.2.0]hexane (92);¹²



However, our attempts to prepare DBO from (90H) in this manner were unsuccessful, possibly due to steric hindrance in the initial nucleophilic attack of base.

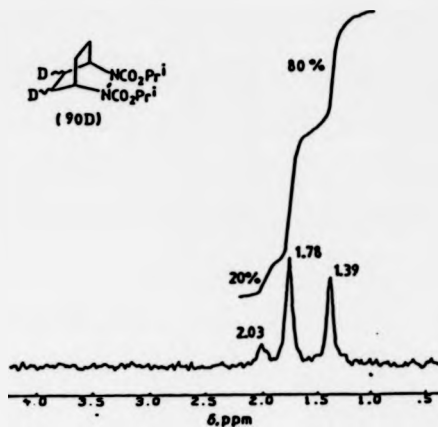
Jung and Lyster¹³ have reported that reaction of alkyl carbamates (of general structure (93)) with trimethylsilyliodide (94) affords high yields of the corresponding amines (Scheme 3.4).

We applied this method to affect the hydrolysis of (90H), using neat liquid trimethylsilyliodide or generating it in situ from trimethylsilylchloride and sodium iodide. The resultant hydrazocompound was not isolated but immediately oxidised with copper (II) chloride. We found the method employing neat trimethylsilyliodide to be superior, leading to moderate yields of DBO (40-50%) after purification.

The most efficient method of preparing DBO from (90H) was eventually found to be a simple variant of that used for the hydrolysis and oxidation of (86), (see Section 3.1). Since (86) is more strained than (90H), more forcing conditions should be required to hydrolyse the latter.⁷ It has previously been assumed that low yields of diazoalkanes obtained from hydrolysis of dialkyl-bis-carbamates are a consequence of these forcing conditions. However, we consistently obtained excellent yields of DBO by refluxing (90H) for 70 hr in strong alcoholic base solution. The details are given in the experimental section.

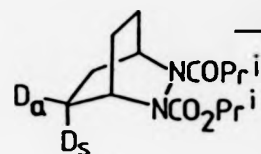
Replacement of hydrogen for deuterium in the synthesis led to the deuterated precursor (90D). As we noted previously, we could not assign the ¹H NMR spectrum of (90D) by LSR studies due to the non-equivalent syn and anti protons being part of a complicated ABCDXY spin-spin system. Analysis of its proton decoupled ²H NMR is more straightforward; If reduction occurs exclusively to one face of the double bond in (88) there will be only two ²H NMR signals ie two syn or two anti deuterium resonances. If deuterium adds randomly, on the other hand, there will be a total of four signals for the syn and anti deuterons of (90D). Figure 3.7 shows the ²H NMR of a sample (90D) we obtained by deuterogenation of (88) in toluene with Wilkinson's catalyst.

Figure 3.7 61.4 MHz Proton decoupled ^2H NMR of (90D) from reduction of (88) in toluene with Wilkinson's catalyst.



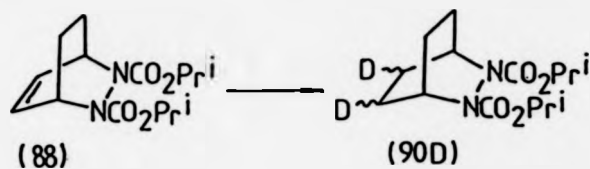
There are three ^2H NMR signals at 1.39, 1.78, and 2.03 ppm. These correspond to the four signals of the syn and anti protons, two of which overlap at 1.78 ppm. In this, and all subsequent ^2H NMR spectra of (90D), the integral of the signal at 1.78 ppm was equal to the summation of the signals at 1.39 and 2.03 ppm. The stereoselectivity of the deuterogenations could be determined simply by comparing the integrals of the signals at 1.39 and 2.03 ppm. Inspection of Figure 3.7 reveals that this sample of (90D) was deuterogenated with 80% stereoselectivity. To determine whether the deuterium was predominantly syn or anti, we compared the ^2H NMR of the sample shown in Figure 3.7 with that of the sample of d_2 -DBO obtained from it. The sample of d_2 -DBO had ^2H NMR signals at 1.52 and 1.23 ppm with an integral ratio of 80:20, respectively ie 80% anti deuterium (see Section 3.1). Back analysis also allowed us to assign the ^2H NMR signals at 1.39 and 1.78 ppm to the non-equivalent anti protons of (90D). The ^2H NMR assignments of (90D) are summarised in Table 3.3.

Table 3.3 ^2H NMR stereochemical Assignments for (90D).

	^2H NMR signals		Assignment
		1.78	1.39 ppm
	1.78	2.03 ppm	Ds

In order to maximise the stereoselectivity, we deuterogenated (88) under several different reaction conditions. Having assigned the ^2H NMR of (90D), we were able to determine the stereoselectivity of the deuterogenations from the ^2H NMR's of the precursors (90D). The various conditions used for the catalytic deuterogenations, together with the quantitative location of deuterium, are given in Table 3.4. Also included in this Table are the results for a reduction employing deuterio-diimide (N_2D_2).

The results in Table 3.4 show that heterogeneous catalysts (Pd and Pt) give cis-anti-(90D) exclusively, or nearly exclusively. Presumably, the face of the double bond in (88) that is anti to the nitrogens is less sterically hindered than the syn face (Figure 3.8). Wilkinson's catalysts, known to cause reduction at the least sterically hindered face of a double bond, also leads to cis-anti-(90D), but with lower stereoselectivity. Steric effects are less important in diimide reductions, as evidenced by the low stereoselectivity of the reaction employing N_2D_2 . Interestingly, the stereoselectivity is reversed in the N_2D_2 reduction ie predominance of syn deuterium. Thus, cis-addition of deuterium must have occurred to the more sterically hindered face of the double bond.

Table 3.4 Stereoselectivity in deutero-genations of (88).

REDUCING CONDITIONS	SOLVENT	H NMR signals, ratios ^a 2.03 ppm, <u>syn</u> : <u>anti</u> , 1.39 ppm
PtO ₂ (Adam's catalyst) 1 Atm D ₂	EtOAc	3 : 97 ^b
Pd/10% on C 1 Atm D ₂	EtOAc	> 99 ^c
Pd/10% on C 1 Atm D ₂	C ₆ H ₆	> 99 ^c
Rh[P(Ph ₃) ₃] Wilkinson's catalyst 1 Atm D ₂	C ₆ H ₅ CH ₃	20 : 80 ^b
N ₂ D ₂	EtOD	60 : 40 ^b

a. $\pm 3\%$

b. Three ²H NMR signals at 1.39, 1.78 and 2.03 ppm.

c. Two ²H NMR signals at 1.39 and 1.78 ppm.

Similar results have been observed in other bicyclic systems containing heteroatoms, and have been explained¹⁴ in terms of electronic interaction of the diimide with the heteroatoms (Figure 3.8).

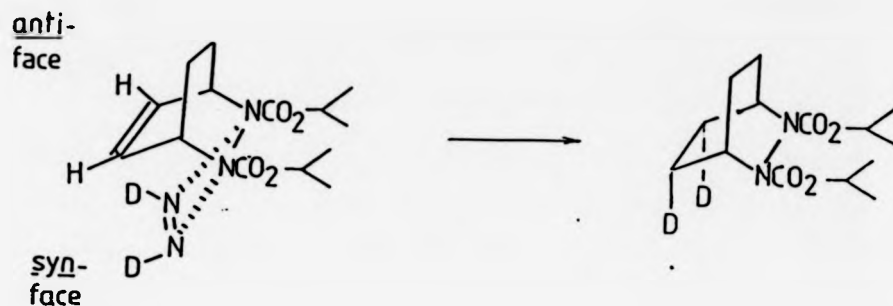
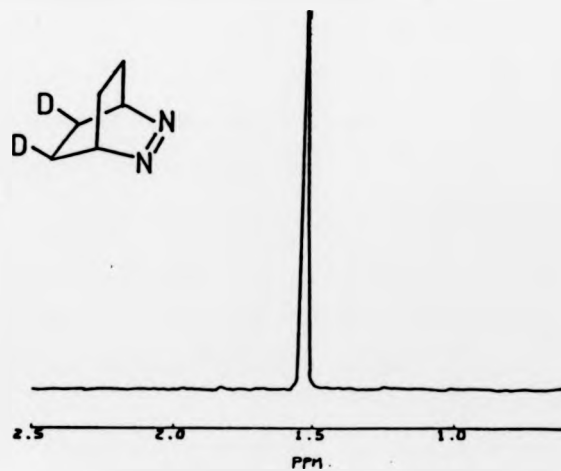


Figure 3.8 N_2D_2 reduction of (88)

In summary, the method employing palladium catalysed deuteration leads to samples of precursors with the required, maximum stereoselectivity. Hydrolysis and oxidation of these samples leads to d_2 -DBO with the deuterium located only at the anti-position (Figure 3.9).

Figure 3.9 2H NMR of d_2 -DBO derived from palladium catalysed reduction of (88) in benzene.



3.3 Determination of deuterium content¹⁵

This section outlines the general method used to determine the deuterium content of samples of d_2 -DBO. We also discuss the possible errors involved, and give the results for all samples of d_2 -DBO prepared.

The deuterated sites in the precursors (86D) and (90D) are sufficiently far removed from the functional groups to be unaffected by base hydrolysis and oxidation. Therefore, we assume that the deuterium content of a sample of d_2 -DBO is identical to that of the precursor from which it is derived. This is important since it is easier to determine mass spectrophotometrically the deuterium content of the precursors than the thermally labile, and volatile, azoalkane.

A particular sample of precursor will be composed of molecules containing; no deuterium atoms (d_0), one deuterium atom (d_1), two deuterium atoms (d_2), etc. For chemical reasons, such as the absence of bridgehead deuterium in the ^2H NMR of (90D), no molecules are expected to be more highly deuterated than d_2 . The relative ion intensities of all peaks in the region of the labelled precursor molecular ions (M) can be determined using electron impact (EI) mass spectroscopy. These intensities must be corrected for natural abundance isotope contributions using the calculated (see Appendix 1), or experimental, ion intensities of unlabelled precursor. The corrected intensities then allow computation of the proportions of d_0 , d_1 , d_2 molecules (see Appendix 2).

The most likely sources of error in the analysis arise from;

- (a) The presence of (M-1) and (M-2) peaks.
- (b) Ion-molecule collisions resulting in proton transfer and the presence of artificial (M+1) peaks.

(c) The presence of background or sample impurities that contribute to the peaks to be measured.

It is not possible to correct arithmetically for natural abundance isotope contributions to the intensities of the labelled (M-1) and (M-2) peaks using the corresponding experimental ion intensities of unlabelled precursor. This is because the deuterated sample may give rise to these peaks by loss of hydrogen or deuterium. However, we were unable to detect any (M-1) or (M-2) peaks in the EI mass spectra of labelled and unlabelled samples of (90) and (86).

The second possible source of error (ie artificial (M+1) peaks) is caused by extraction of a hydrogen radical from another molecule during an ion-molecular collision. If this were reproducible, it would be corrected along with the natural isotope abundances by subtraction of experimental, or calculated, unlabelled sample ion-intensities. However, the intensity of such an (M+1) peak is sensitive to a number of experimental factors, one of which is sample pressure. If self-protonation was occurring in our experiment, the (M+1) peak of the precursors would be artificially high and lead to errors in the determination of d_0 , d_1 and d_2 values. Table 3.5 shows the data for an unlabelled sample of (90). The sample was introduced into the spectrometer on three separate occasions and six scans were recorded each time. The average percentage ion abundances for three separate experimental runs are compared with the calculated ion abundances of (90H).

Table 3.5 Percentage isotope abundances of (90H)

m/z	Experimental ^{a,b}			Calculated ^c
	run 1	run 2	run 3	
284	83.523 ± .113	82.029 ± .220	81.329 ± .259	83.807
285	14.283 ± .180	15.617 ± .186	15.954 ± .172	14.208
286	2.010 ± .162	2.170 ± .060	2.602 ± .115	1.801
287	.170 -	.170 -	.170 -	.170
288	.013 -	.013 -	.013 -	.013
289	.001 -	.001 -	.001 -	.001

- a The experimental values were corrected to take into account the absence of experimental intensities at m/z 287 and above (see Appendix 1).
- b Each run represents an average of six scans. The same sample of precursor was used for each run.
- c See Appendix 1.

The results in Table 3.5 show that the (M+1) peak (m/z 285) was experimentally higher than the calculated value. Furthermore, the experimental runs showed (M+1) peaks of variable intensity. We therefore concluded that self-protonation occurred in (90). Similar analysis showed that self-protonation also occurred in the EI/MS of (86).

We were able to determine the degree of self-protonation and correct the values of d_0 , d_1 , and d_2 . Table 3.6 shows the corrected and uncorrected d-values for a particular sample of precursor (see Appendix 3). The sample had been introduced into the

mass spectrometer on two separate occasions (runs 1 and 2), and scanned six times on each occasion. Note the excellent agreement between the results for the two runs, even though run 2 involved a considerably higher degree of self-protonation than run 1. This proved the validity of our self-protonation corrections.

Table 3.6 Proportions of deuterated material in a sample of (90D) before and after correction for self-protonation.^a

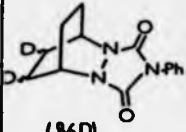
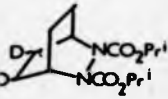
	² H Content ^{b,c}						% Self-protonation ^d
	Uncorrected			Corrected ^d			
	d ₀	d ₁	d ₂	d ₀	d ₁	d ₂	
run 1	0	0.895	99.106	0	0.925	99.075	3.5
run 2	0.15	1.142	98.873	0	1.081	98.919	11.5

- a Sample obtained from Wilkinson's catalyst reduction of (88) in toluene.
- b The sample was analysed on two separate occasions (runs 1 and 2) and scanned six times.
- c The results are quoted to three decimal places to prevent number round off errors in later calculations (see Appendix 5).
- d See Appendix 3.

To eliminate possible errors due to background or sample impurities, the intensities of a particular labelled sample of precursor were recorded before and after recrystallisation, on two separate occasions. Since all samples of precursors gave two sets of d₀, d₁ and d₂ values that agreed to within $\pm 0.5\%$, errors due to

background and sample impurities were minimal (see Table 3.7). The proportions of d_0 , d_1 , and d_2 molecules for all the precursors discussed are given in Table 3.7. The values of d_0 , d_1 and d_2 were calculated for each scan on each run and then averaged. (a complete example of the procedure used to compute the set of data in Table 3.7 is given in Appendix 4). Table 3.7 also contains the precursor anti:syn deuterium ratio for completeness.

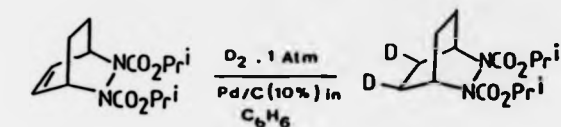
Table 3.7 ^2H incorporation and anti/syn ratio's of DBO precursors

Precursor	Reducing conditions ^a	^2H Incorporation ^b			Stereoselectivity ^c <u>anti: syn</u>
		d_0	d_1	d_2	
 (86D)	PtO_2 in EtOAc	18.479	29.662	51.859	86:14
	PtO_2 in EtOH	< 10% total deuterium content ^d			74:26
	$\text{Pd}(10\% \text{ on C})$ in C_6H_6	0.997	11.287	87.716	68:32
 (90D)	PtO_2 in EtOAc	31.753	41.973	26.270	97:3
	N_2D_2 in EtOD	2.999	26.885	70.142	40:60
	Wilkinson's catalyst in $\text{C}_6\text{H}_5\text{CH}_3$	0	1.081	98.763	80:20
	$\text{Pd}(10\% \text{ on C})$ in EtOAc	0.732	9.471	89.798	>99:1
	$\text{Pd}(10\% \text{ on C})$ in C_6H_6	0.080	6.754	93.208	>99:1

- a. All reductions (except N_2D_2 (EtOD) were carried out using deuterium gas at 1 Atm.
- b. The results are quoted to three significant figures to prevent number round-off errors in later calculations (see Appendix 5).
- c. $\pm 3\%$.
- d. Estimated from ^1H NMR.

The results of deuterium content in Table 3.7 indicate that solvent exchange occurs in the deuterogenations involving platinum (IV) oxide catalysts, particularly in ethanol solvent. Although the usual precautions were observed in the N_2D_2 reduction, Table 3.7 shows that substantial amounts of d_1 material were present. This probably reflects the operation of a large kinetic isotope effect during the reaction of the N_2D_2 . Palladium catalysts on charcoal gave us high deuterium incorporation and anti/syn ratio's of deuterium. The best conditions for deuterium incorporation and stereoselectivity were palladium catalysed deuterogenation in benzene. Thus, all samples of d_2 -DBO with high stereoselectivity and deuterium incorporation were obtained from samples of (90D) prepared in this manner. Several batches of this particular precursor were prepared, each batch being separately analysed for deuterium content and stereoselectivity. The results for all precursors so prepared are given in Table 3.8.

Table 3.8 ^2H Incorporation for samples of d_2 -DBO derived from Precursors (90D) deuterogenated in Benzene catalysed by Palladium.^a



Batch	^2H Content ^b		
	d_0	d_1	d_2
1	0.083	6.754	93.208
2	1.156	11.089	87.797
3	0.753	8.659	90.588
4	0	4.488	95.512
5	0.763	15.673	83.607
6	0.031	5.690	94.279

- a The two ^2H NMR signals (at 1.39 and 1.78 ppm) indicated maximum anti/syn ratio's of deuterium.
- b Each batch was analysed on two separate occasions and six scans recorded each time. The results are given to 3 significant figures to prevent round-off errors in later calculations (see Appendix 5).

3.4 Summary

In this chapter we have discussed two strategies for the synthesis of stereoselectively labelled d_2 -DBO. The method employing (90) as precursor was chosen so that deuterogenations would occur with high stereoselectivity. Suitable deuterogenation

conditions (Palladium catalyst in benzene) did lead to samples of (90D), and subsequently d_2 -DBO, whose deuterium was exclusively anti. We also discussed the determination of deuterium content in precursors (86D) and (90D). This was measured by EIMS and assumed to be identical to that of the d_2 -DBO sample obtained from it.

Chapter 4

4.1 Introduction

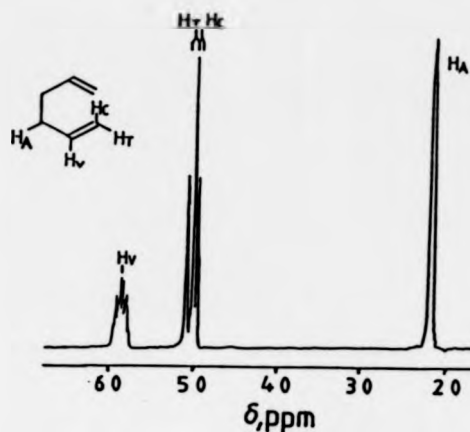
In this Chapter we give the ^2H NMR results locating deuterium in the hydrocarbon products from the photochemical decomposition of d_2 -DBO. Since ^2H NMR analysis reveals the complete stereochemistry of the diyl closure product, the stereochemistry of BCH is considered in detail. Mechanistic conclusions are based on the exo/endo ratios of BCH deuterium and total E- to Z- deuterium in the hexa-1,5-dienes. This Chapter also contains the stereochemistry of photochemical decomposition of 1,4-dimethyl-2,3-diazabicyclo[2.2.2]oct-2-ene (DMDBO). This was carried out to test our preferred mechanism(s) for the photochemical decomposition of d_2 -DBO.

4.2 Hydrocarbon products. Stereochemical assignments

The reported hydrocarbon products from direct and sensitised photochemical decomposition of DBO are bicyclo [2.2.0]hexane and hexa-1,5-diene.¹ It was necessary to assign their ^1H NMR spectra so that deuterium could be located.

The assignment of the allylic (H_A) and vinylic (H_V) signals in the ^1H NMR of hexa-1,5-diene is trivial. The terminal olefinic protons (H_C and H_T) could be assigned on the basis of their vicinal coupling constants to H_V . Since trans vicinal coupling is typically 10-14 Hz, while cis vicinal coupling is 8-10 Hz, the doublet centred at 4.99 ppm was assigned to H_T ($J_{\text{H}_V\text{H}_T}$, 14.6 Hz) and that at 4.93 ppm to H_C ($J_{\text{H}_V\text{H}_C}$, 9.3 Hz). The 220 MHz ^1H NMR of hexa-1,5-diene is shown in Figure 4.1.

Figure 4.1 220 MHz ^1H NMR of authentic hexa-1,5-diene.



The 220 MHz ^1H NMR spectrum of BCH (which we isolated by preparative gas chromatography from a sensitised photolysis mixture) is illustrated in Figure 4.2. The signal at 2.77 ppm may be assigned to the two bridgehead protons (H_B). The crucial assignments are those of the exo (H_X) and endo (H_N) proton signals. These assignments have previously been reported by Goldstein and Benzon in their work on BCH pyrolysis.² The BCH ^1H NMR assignments are summarised in Table 4.1, together with those of hexa-1,5-diene.

Figure 4.2 ^1H NMR of isolated BCH.

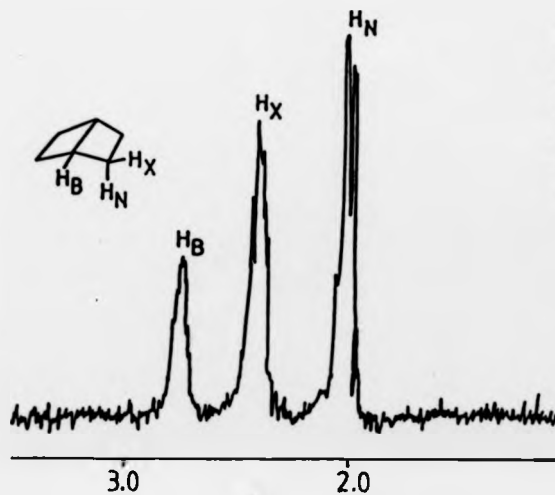
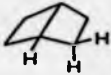
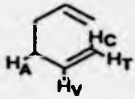


Table 4.1 ^1H NMR spectral assignments for BCH and hexa-1,5-diene

PRODUCT	^1H NMR Chemical shift (δ , ppm)	Assignment
	2.77 2.44 2.04	H _B H _x H _n
	5.85 4.99 4.93 2.12	H _V H _T H _C H _A

4.3 Stereochemistry of the direct photolysis

The first deuterated sample of azoalkane we photolysed was derived from a sample of (86D) containing 68% anti- and 32% syn-deuterium. After photolysis and removal of polar species (e.g. any unreacted d_2 -DBO), the concentrated n-pentane solution gave the proton decoupled ^2H NMR shown in Figure 4.3.

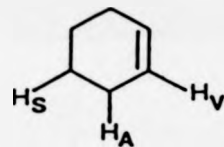
Figure 4.3 ^2H NMR of products from the direct photochemical decomposition of d_2 -DBO^a

^a a 68% anti, 32% syn ^2H .

δ , ppm

Comparison of this ^2H NMR spectrum with the ^1H NMR spectra of hexa-1,5-diene and BCH allowed us to assign all the signals in Figure 4.3 except those at 5.62, 1.94, and 1.58 ppm. We identified these as the vinylic, allylic, and saturated deuterium resonances of cyclohexene by comparison with the ^1H NMR of authentic material (Table 4.2).


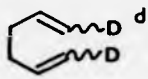
Table 4.2 ^2H and ^1H NMR signal assignments in cyclohexene.

	^1H NMR signals	^2H NMR signals	Assignment
	5.68	5.62	H _v
	1.95	1.94	H _A
	1.61	1.58	H _s

The cyclohexene product, which we envisaged to arise from a 1,3-hydrogen shift in the assumed cyclohexane-1,4-diyl intermediate, had not previously been reported as a product from this decomposition. This became of sufficient mechanistic importance to warrant more detailed study (see Chapter 6).

The location of deuterium in the d_2 -BCH's and d_2 -dienes, together with the appropriate stereochemical ratio's, are given in Table 4.3.

Table 4.3 Location of deuterium in products from the direct photochemical decomposition of d_2 -DBO.²

PRODUCT	^2H NMR signals, assignments	RATIO ^{b,c}
	2.41(<u>exo</u>) 2.03(<u>endo</u>)	64:36
	4.99 (E) 4.93 (Z)	50:50

- a 68% anti; 32% syn ^2H
- b A second run gave identical results
- c Ratio's from ^2H NMR integrals (\pm 3%)
- d A signal was also observed at 2.09 ppm and was assigned to the allylic deuterium.

The data in Table 4.3 reveals that the d_2 -dienes are formed with an E/Z deuterium ratio of 1. This result is analogous to that observed in Goldstein and Benzon's study of BCH pyrolysis² and is consistent with stereoselective formation of EZ- d_2 -diene.

More suprisingly, d_2 -DBO with predominantly anti deuterium led to BCH's in which the deuterium was predominantly exo (i.e. double inversion of configuration). The result was suprising because it was envisaged that the photolysis of DBO would involve a similar diyl intermediate to that involved in the pyrolysis of BCH. We have previously noted that stereochemical studies of BCH pyrolysis suggested the involvement of fully equilibrated conformations of a cyclohexane-1,4-diyl (see Section 2.4.1, p64). We also noted that all

other azoalkanes that generate 1,4-biradicals led to closure products with retained, or partially retained, stereochemistry (see Table 2.5, p.63). Thus, we expected the ring closure to proceed with partial retention, or loss of stereochemistry.

Inversion of configuration is well known in photochemical decompositions of monocyclic and bicyclic pyrazolines. In particular, we have noted that the thermal and photochemical decomposition of DBH and its derivatives led to BCP's with predominant inversion of configuration, a result for which several rationales have been proposed (see Section 2.2, p.49). However, all the mechanisms used to rationalise the stereochemistry of DBH are unlikely to apply to the photochemical decomposition of DBO because they would require the six-membered carbon ring to be planar at some point along the reaction co-ordinate. Before considering alternative mechanisms, we sought confirmation of the BCH stereochemistry.

4.4 Double inversion of BCH stereochemistry. Confirmation of results

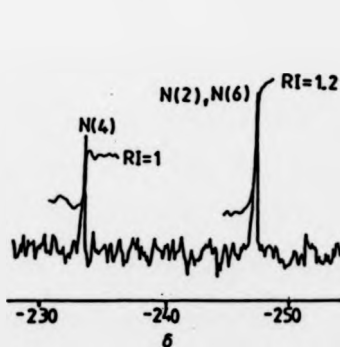
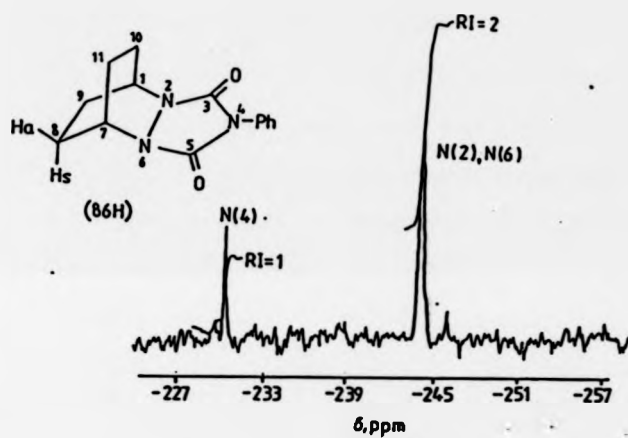
To confirm our results we required proof that;

- (a) the intensity of the signal assigned to exo BCH deuterium was not artificially enhanced by some underlying impurity.
- (b) Our NMR assignments in DBO and BCH were correct.

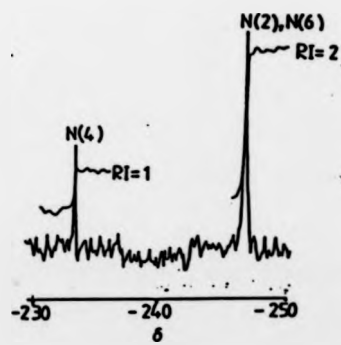
As the photolysates were chromatographed over alumina and eluted with n-pentane before ^2H NMR's were recorded, no oxygen or nitrogen containing species could have been present. To confirm that no deuterium containing non-polar impurities were present, a chromatographed sample obtained from direct photochemical decomposition of d_2 -DBO (68% anti and 32% syn deuterium) was analysed by ^2H NMR before and after isolation of the d_2 -BCH's by

Figure 4.4 ^{15}N NMR's of (86H). Use of $^{15}\text{N}(^1\text{H})$ nOe studies for stereochemical assignments of the syn (H_s) and anti (H_a) protons of (86H).

a) Normal ^{15}N NMR



b) Irradiation at 2.10 ppm



c) Irradiation at 1.74 ppm

preparative gas chromatography (prep. g.c.). Although the cyclohexene and BCH's co-chromatographed, the same ratio of exo/endo BCH deuterium was observed in both spectra (ie 64% exo, 36% endo).

Confirmation of the azoalkane ^1H NMR stereochemical assignments was achieved in the following manner;

We had previously assigned the syn and anti ^2H NMR signals of d_2 -DBO by comparison of its ^1H and ^2H NMR spectra (or those of its precursor (86)) and appropriate use of $\text{Eu}(\text{FOD})_3$ LSR (see Section 3.1.1, p.98). We confirmed the precursor ^1H NMR assignments, and consequently those of DBO, by an $^{15}\text{N}\{^1\text{H}\}\text{nOe}$ study (see Figure 4.4).

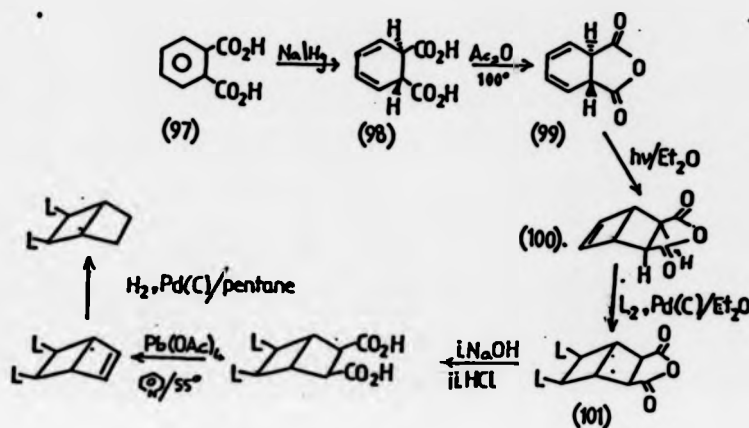
Inspection of Figure 4.4 shows that the signal at ca - 244 ppm (N(2), N(6)) exhibits a 40% negative nOe upon irradiation at 2.10 ppm (Figure 4.4b) but none on irradiation at 1.74 ppm (Figure 4.4c). Since an nOe is expected upon irradiation of the syn protons but not the anti protons, this experiment confirms the earlier assignments.

Such nOe's are maximised if the relevant dipole-dipole interaction dominates the relaxation mechanism.³ Whilst this type of interaction contributes significantly to the relaxation of ^{15}N nuclei, other mechanisms may account for 50-60%. In particular, interaction with paramagnetic species (such as molecular oxygen) provides an extremely efficient mechanism.³ Therefore, the experiment was repeated using deoxygenated solutions of (86H). Identical results were obtained, with the N(2), N(6) ^{15}N NMR signal showing a 40% negative nOe only upon irradiation at 2.10 ppm (H_g). To our knowledge, this is the first time an $^{15}\text{N}\{^1\text{H}\}\text{nOe}$ experiment has been used to aid a stereochemical assignment.

The stereochemical assignments in BCH (Table 4.1) were those reported by Goldstein and Benzon.² They had accomplished these by ^1H NMR analysis of protio and deuterio cis-bicyclo[2.2.0]

hexane-2,3-dicarboxylicanhydride (101), a precursor in their synthesis of BCH (Scheme 4.1).

Scheme 4.1 L = H, D



Thus, the 60 MHz ¹H NMR of (101H) showed complicated multiplets for the bridgehead (H_B), exo (H_X), and endo (H_N) proton resonances, and a singlet for the H_α signal. Replacing hydrogen for deuterium in the synthesis, and subsequent ¹H NMR analysis of (101D), gave a spectrum with three sharp singlets. The singlets were in the ratio of 1:1:1 and the signal centred at 2.74 ppm in (101H) was completely absent. The Karplus equation predicted J_{BN} and J_{BX} to be 3.5 ± 3.5 Hz and 12.5 ± 3.0 Hz respectively. Thus, the deuteration was deduced to have occurred to give exo-(101D), and the signal at 2.74 ppm in the ¹H NMR of (101H) was assigned to H_X. Subsequent hydrolysis, decarboxylation, and reduction of exo-(101D) led to exo-d₂-BCH. Comparison of its ¹H NMR with that of BCH obtained from (101H) enabled assignment of BCH H_X and H_N resonances.²

We confirmed Goldstein and Benzon's assignments² in (101H), and thus BCH, by analysis of ¹H(¹H)NOe difference spectra. A sample of (101H), synthesised as shown in Scheme 4.1, gave the 220 MHz

Figure 4.5 ^1H NMR of *cis*-bicyclo[2.2.0]hexane-2,3-dicarboxylic anhydride.

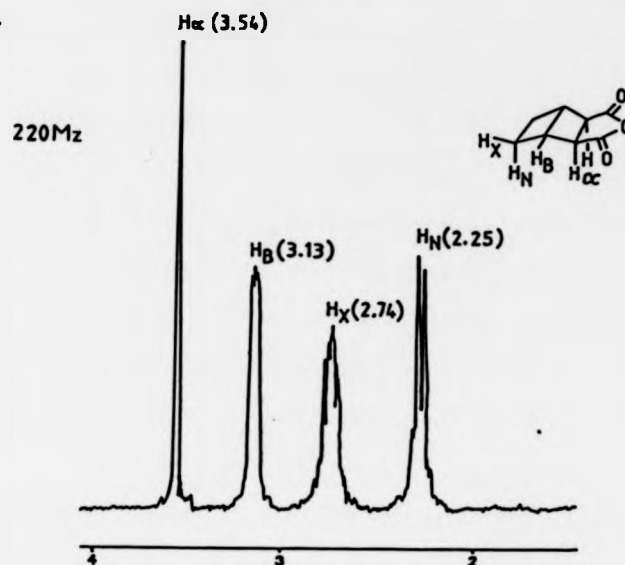


Table 4.4 400 MHz $^1\text{H}\{^1\text{H}\}n\text{Oe}$ difference spectrum of (101H). Percentage signal enhancements.

Irradiated signal ^b	% Signal enhancements ^a			
	3.54	3.13	2.74	2.25
3.54	I	3.1	c	2.6
3.13	1.3	I	1.9	c
2.74	c	4.7	I	10.9
2.25	1.5	c	5.8	I

^a "I" represents irradiated signal

^b Solutions were not de-oxygenated

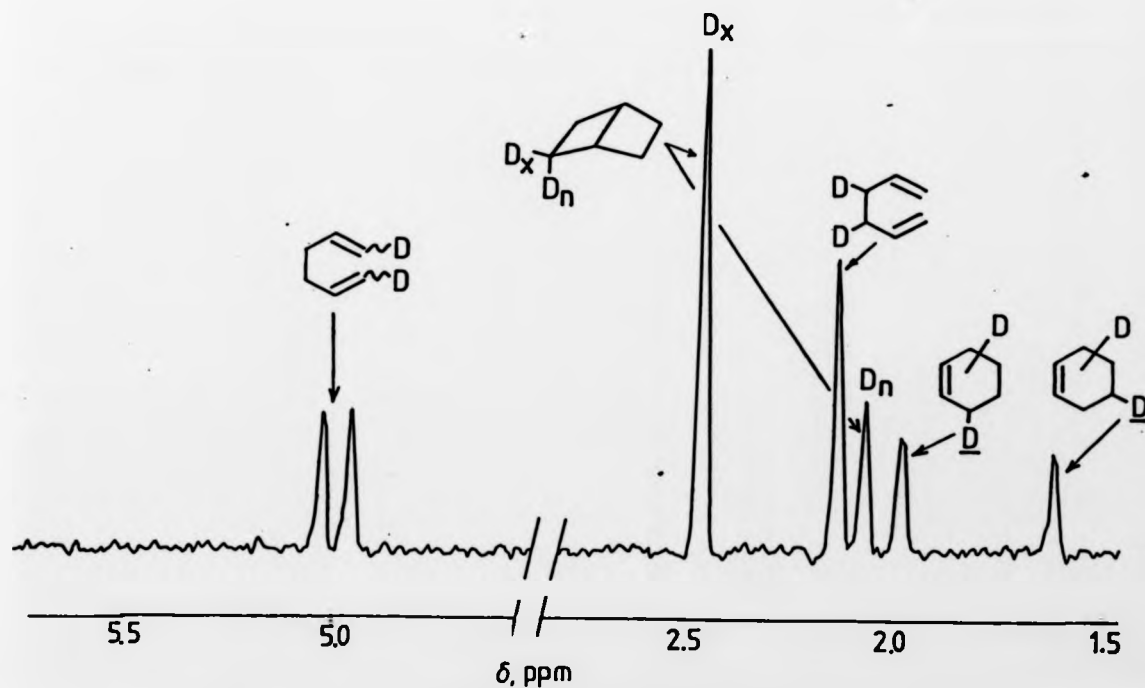
^c < 1%

^1H NMR shown in Figure 4.5. The assignments are those according to Goldstein and Benzon. Table 4.4 shows the 400 MHz $^1\text{H}\{^1\text{H}\}\text{nOe}$ signal enhancements, per proton, for the same sample.

The results in Table 4.4 show that irradiation at 3.54 ppm gave an nOe at 2.25 ppm but not at 2.74 ppm while irradiation at 3.13 ppm gave an nOe at 2.74 ppm but not 2.25 ppm, in full accord with the assignments shown in Table 4.1 and Figure 4.5.

Thus, the predominance of inverted BCH is firmly established. Quantitative analysis of the degree of inversion was complicated because the sample of d_2 -DBO was not stereoisomerically pure. Direct photolysis of d_2 -DBO samples with > 99% anti deuterium gave ^2H NMR spectra such as that shown in Figure 4.6.

Figure 4.6 ^2H NMR of products from direct photolysis of stereoisomerically pure anti- d_2 -DBO.

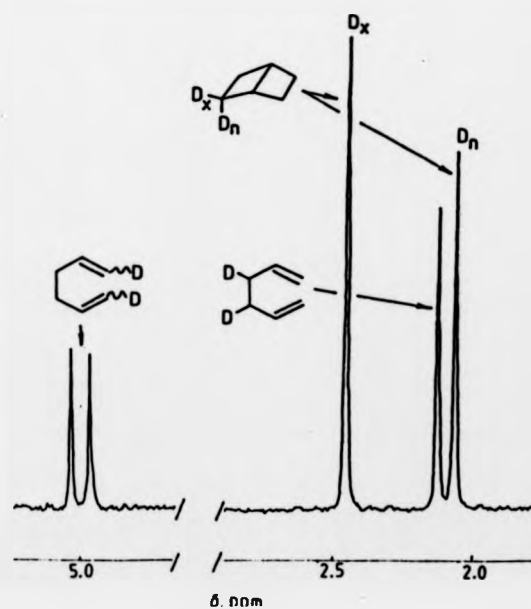


This spectrum is qualitatively similar to the spectrum in Figure 4.3. Thus, the diene is formed with an E/Z deuterium ratio of 1 and cyclohexene resonances are present at 1.95 and 1.61 ppm. The significant differences are the increased ratio of exo/endo BCH deuterium (83:17) and the absence of cyclohexene olefinic resonances. The latter point is a consequence of the mechanism and will be discussed in Chapter 6.

4.5 Stereochemistry of the photosensitised decomposition

Photosensitised decompositions were carried out analogously to the direct photolyses but adding meta-methoxyacetophenone as sensitiser and irradiating at 300 nm. A typical ^2H NMR spectrum of the products from decomposition of a stereoisomerically pure sample of anti- d_2 -DBO is shown in Figure 4.7.

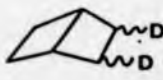
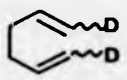
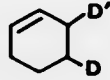
Figure 4.7 ^2H NMR of products from photosensitised decomposition of anti- d_2 -DBO



The spectrum is qualitatively similar to those obtained from direct photolyses. Thus, the BCH is formed with the same predominant double inversion of stereochemistry but has a quantitatively lower exo/endo ratio of deuterium. The diene is formed with an E/Z deuterium ratio of 1. An important difference is that cyclohexenes are not formed in the sensitised photolyses (see Chapter 6).

The stereochemical ratios for direct and sensitised photochemical decompositions of anti-d₂-DBO are summarised in Table 4.5.

Table 4.5 Product stereochemistry of direct and sensitised photochemical decomposition of anti-d₂-DBO.

Source	² H NMR signal ratio's ^{a,b}		
	 <u>exo:endo</u>	 E:Z	 D:D'
direct photolysis ^c	83:17	50:50	~50:50
sensitised photolysis ^c	58:42	50:50	—

a. Integrals $\pm 3\%$

b. signal also observed at 2.09 ppm assigned to diene allylic deuterium.

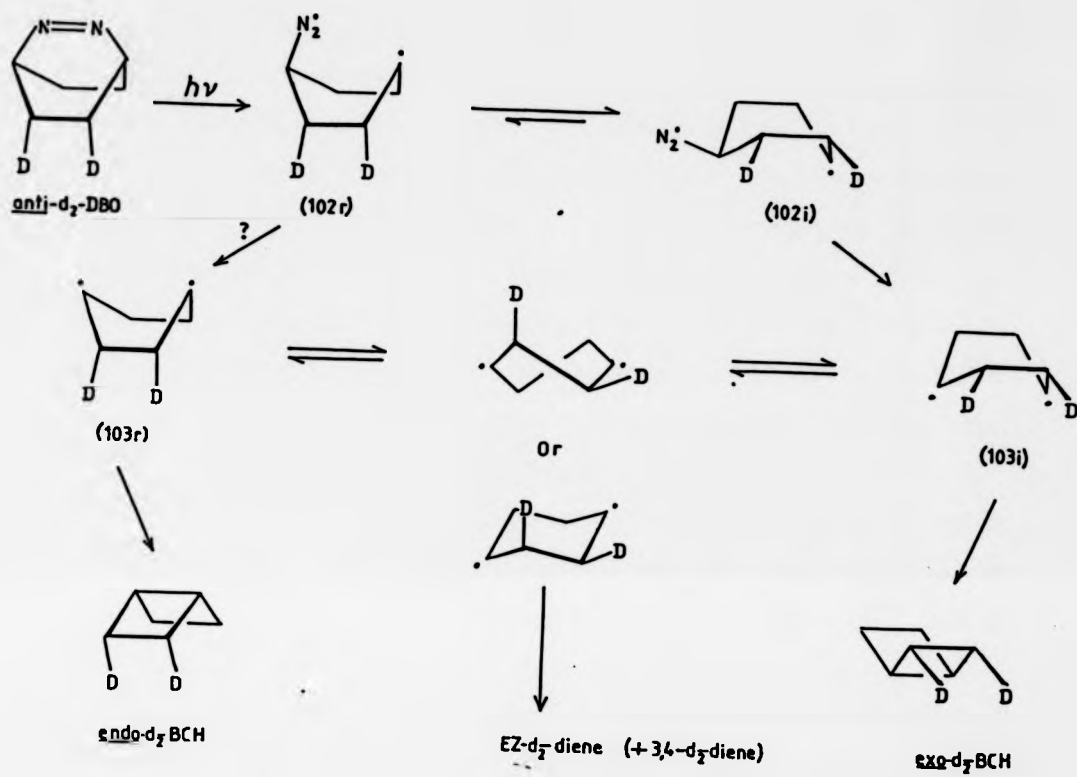
c. 3 runs identical.

4.6 Discussion

It is possible that BCH's derived from $^1(n-\pi^*)$ excited d_2 -DBO are formed exclusively with exo deuterium. The stereochemistry of the direct photolysis could still be explained if ca 40% of the products were derived from $^3(n-\pi^*)$ excited d_2 -DBO, formed by ISC. This is unlikely since direct photolysis is more efficient than sensitised ($\Phi_r^D/\Phi_r^S = 1.29$, where Φ_r is the quantum yield of product formation for direct (D) and sensitised (S) photolysis) while the long fluorescence lifetime ($\tau_f = 434$ ns) suggests that ISC is very slow.¹ Thus, the stereochemical data shown in Table 4.5 represent a "singlet-biradical product distribution" and a "triplet-biradical product distribution", not a combination of the two.

Any mechanism proposed to account for the decomposition of d_2 -DBO must explain the loss of stereochemistry in the hexa-1,5-diene, the predominance of exo deuterium in BCH, and the quantitatively lower degree of double inversion observed in the sensitised photolysis. Our preferred mechanism is given in Scheme 4.2.

Scheme 4.2



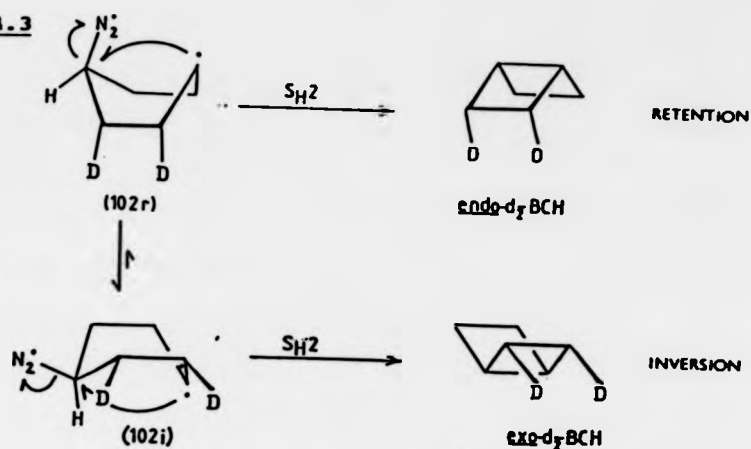
Cleavage of one C-N bond leads to the diazenyl biradical (102r), or the nearby twist-conformer, in which the diazenyl substituent is in the flagpole position. This proposed formation of a diazenyl biradical is in accord with the kinetic studies of Engel *et al*¹ who have shown that stepwise C-N bond cleavage is feasible if the initial cleavage is irreversible (see Section 2.4.3.2, p.88). Conformational inversion of (102r) leads to the more stable (102i), in which the diazenyl substituent is in the bowsprit position. Loss of nitrogen from (102i) affords the boat diyl (103i) which couples to give the preferred, inverted *exo-d*₂-BCH. The alternative *endo-d*₂-BCH may arise in a similar fashion from (102r) if the initial conformational inversion is reversible or incomplete.

Alternatively, *endo-d*₂-BCH could arise by partial back equilibration of (103i). By analogy to BCH pyrolysis,² preferential cleavage from the chair or 90°-twist diyl conformer would lead to *EZ-d*₂-diene.

This mechanism is applicable to both direct and sensitised photolyses, as both give qualitatively similar results. The quantitatively lower coupling stereoselectivity of the sensitised photolysis can be attributed to a SCE operating on either, or both, of the relevant conformational equilibria.

There is a second possible rationale for the predominant double inversion of BCH stereochemistry. We have discussed the evidence for inversion of stereochemistry in free radical substitution reactions (see Section 2.2, p.51). It was suggested that such S_H2-type reactions proceed by a mechanism analogous to S_N2 reactions (*ie* preferred backside attack at an sp³ centre). An S_H2-type reaction in this system, with backside attack, would be more favourable in (102i) than (102r), so inverted BCH's would be formed preferentially (Scheme 4.3).

Scheme 4.3



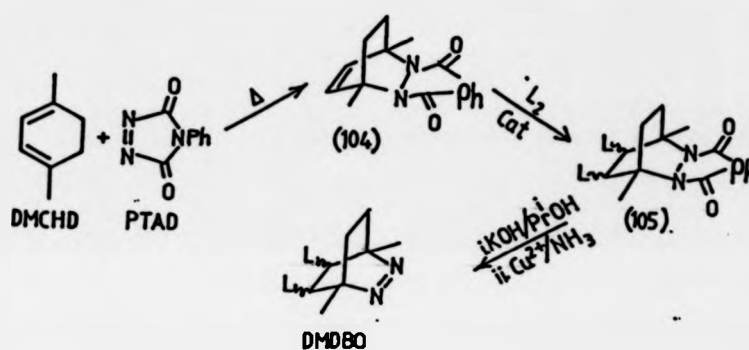
A crucial feature in these mechanisms is the conformational inversion of the first formed diazenyl biradical (102r). Presumably, the driving force for this reaction is the known preference of substituents for the bowsprit position in cyclohexane boat conformations.⁴

In the light of this proposed mechanism, consider the case where the azoalkane has alkyl substituents at the bridgehead positions. Since the alkyl and diazenyl substituents would compete for the bowsprit position, a different stereochemical result would be expected due to perturbation of the conformational equilibria between the diazenyl biradicals and/or cyclohexane-1,4-diyls. To test the effect of bridgehead substituents on stereochemistry we studied the photochemical decomposition of 1,4-dimethyl-2,3-diazabicyclo[2.2.2]oct-2-ene, again using 5,6-deuterio substituents as labels.

4.7 Synthesis of 1,4-dimethyl-2,3-diazabicyclo[2.2.2] oct-2-ene (DMDBO)

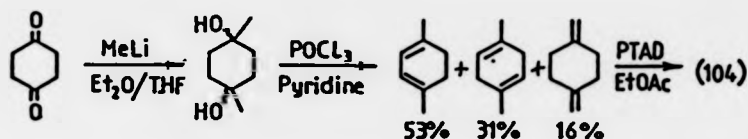
The azoalkane was prepared by analogy to the published procedure⁵ (Scheme 4.4).

Scheme 4.4 L=H,D



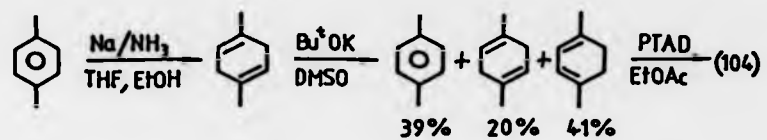
Surprisingly, although several syntheses have been reported,⁶ there was no simple route to 1,4-dimethylcyclohexa-1,3-diene (DMCHD). Since we were not concerned with high yield, regiospecific syntheses (the usual contaminant 1,4-diene will not undergo the Diels-Alder reaction with PTAD), we initially prepared (104) by the route shown in Scheme 4.5.

Scheme 4.5



The yield of (104) from this route was unacceptably low (ca 4% from cyclohexane-1,4-dione). Although this was in part due to the formation of diene isomers, the principle difficulties were encountered in the methylation of the dione (see Experimental Section).

In a second preparation, we attempted to prepare DMCHD by Birch reduction of *p*-xylene following the procedure used for the analogous reduction of the *o*-isomer.⁷ This was initially unsuccessful, probably due to the insolubility of the protic acid (ethanol) in the diethyl ether co-solvent. On changing the co-solvent to THF, high yields of 1,4-dimethyl cyclohexa-1,4-diene were obtained. Isomerisation of the 1,4-diene with potassium *t*-butoxide gave an equilibrium mixture of 1,3- and 1,4-dienes that was used in Diels-Alder reactions with PTAD. The synthesis of (104) is summarised in Scheme 4.6.

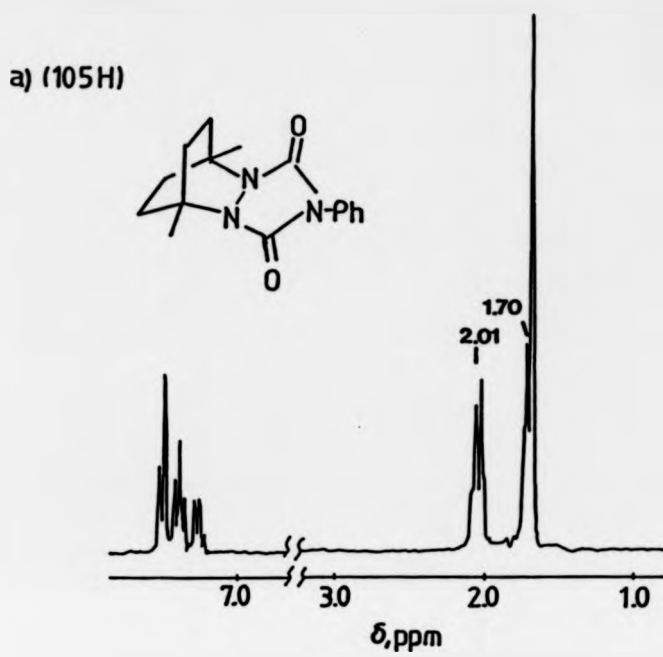
Scheme 4.6

A very similar preparation of DMCHD has recently been reported.⁸

4.8 Stereochemical assignments in DMDBO

The 220 MHz ¹H NMR of DMDBO and its precursor (105H) are illustrated in Figure 4.8.

Figure 4.8 ^1H NMR of DMDBO and its precursor.



b) DMDBO

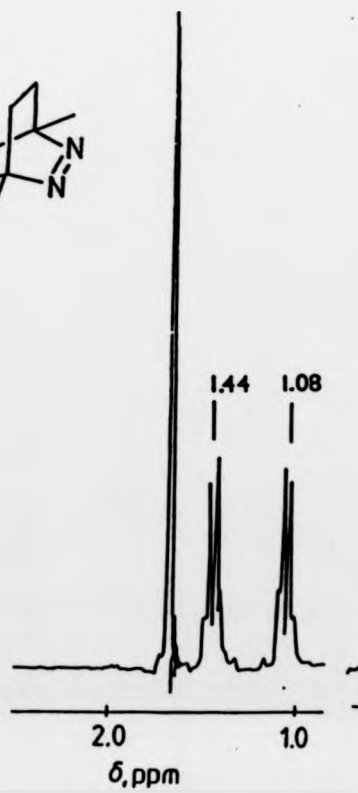
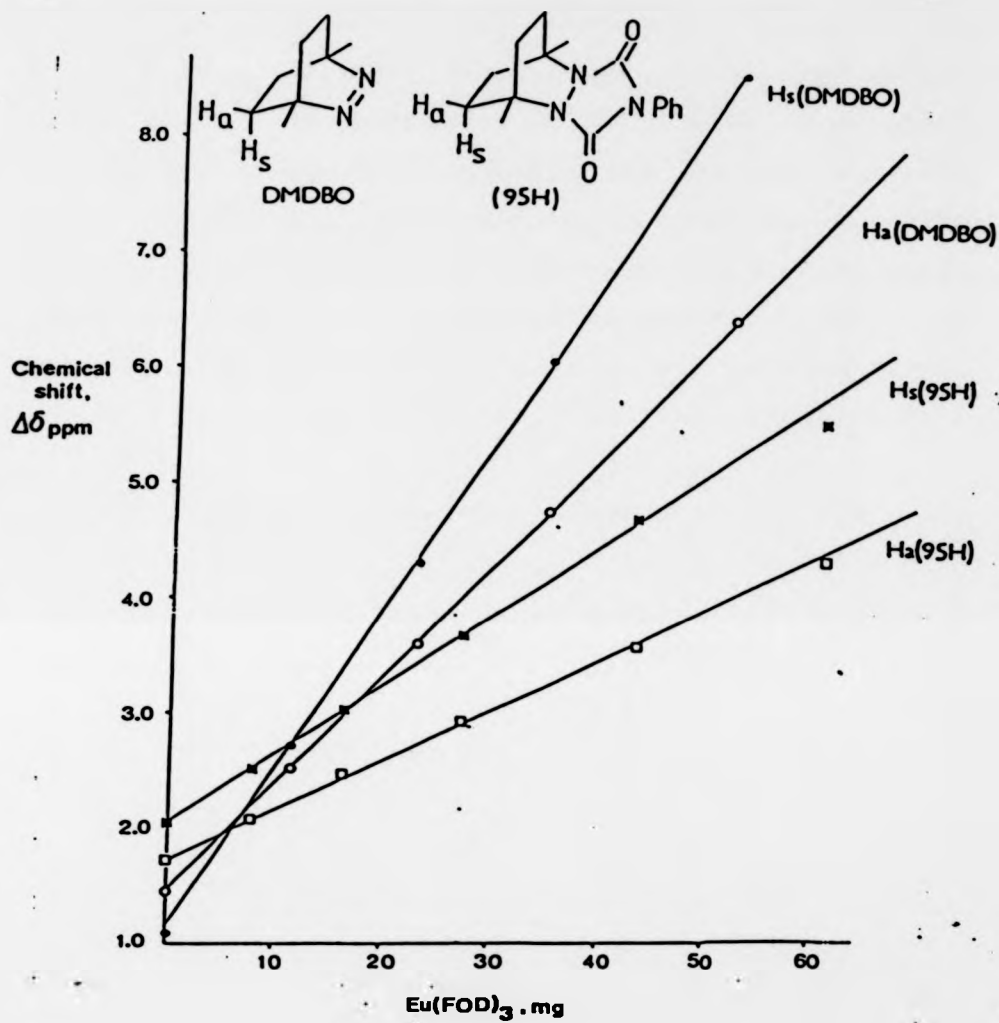


Figure 4.9 Plots of induced $\text{Eu}(\text{FOD})_3$ shifts in DMDBO and (95H)



■ H_s (95H)

● H_s DMDBO

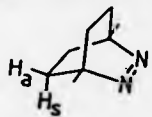
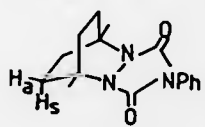
□ H_a (95H)

○ H_a DMDBO

Tables of results can be found in the experimental section.

In both spectra, the syn (H_s) and anti (H_a) protons are part of an AA'BB' spin-spin system. The stereochemical assignments are simplified by assuming that the four syn and four anti protons correspond to two "doublets" centred at 2.01 and 1.70 ppm in (105H), and 1.47 and 1.12 ppm in DMDBO, and ignoring the small signals in between the "doublets". In both cases, the "doublets" can be assigned by appropriate use of $\text{Eu}(\text{FOD})_3$ LSR. Added increments of $\text{Eu}(\text{FOD})_3$ will cause the H_s resonances to shift down-field more rapidly than the H_a resonances. From the graphs shown in Figure 4.9, the stereochemical assignments could be deduced. These are summarised in Table 4.6.

Table 4.6 Stereochemical assignments in DMDBO and (105H).

PRODUCT	^1H NMR signal, ppm	Assignment
	1.47	H_a
	1.12	H_s
	2.01	H_s
	1.70	H_a

4.9 Synthesis of stereoselectively labelled d₂-DMDBO

Replacement of hydrogen by deuterium in the synthesis (Scheme 4.4) led to (105D) and d₂-DMDBO with 5,6-deuterio substituents. Comparison of the ¹H and ²H NMR's of (105D) and integration of the latter, enabled the anti/syn deuterium ratio's to be determined. Unlike our stereochemical study of d₂-DBO, we did not require quantitative determination of the azoalkanes deuterium content. However, this could be qualitatively assessed by integration of their ¹H NMR spectra. The location, and approximate incorporation, of deuterium in samples of (105D) deuterated under several conditions are given in Table 4.7.

Table 4.7 Location and incorporation of deuterium in (105D) for several reducing conditions.

Conditions	² H NMR signals	ratio's ^a	² H incorporation ^b
Pd/C (10%), in benzene, D ₂ (g)	1.76, 2.03	62:38	~90%
PtO ₂ , in EtOAc, D ₂ (g)	1.76, 2.03	90:10	~75%
Wilkinson's catalyst in toluene, D ₂ (g)	1.76, 2.03	30:70	~90%

^a ± 3%

^b estimated from ¹H NMR

The results in Table 4.7 reveal that heterogeneous catalytic reductions result in samples of (105D) in which the deuterium is predominantly anti. Homogeneous catalytic reduction (Wilkinson's catalyst in toluene) results in samples of (105D) in which the deuterium is predominantly syn. This surprising reversal of stereoselectivity proved to be very useful in our stereochemical analysis of cyclohexene formation (see Chapter 6).

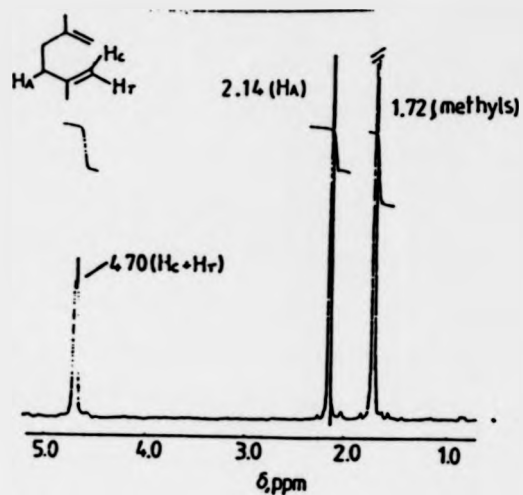
4.10 Photophysics of direct and sensitised photolysis of DMDBO¹

The photophysics of DMDBO are similar to that of DBO. Thus, direct irradiation populates the $^1(n-\pi^*)$ excited state, which decays ($\Phi_D = 0.45$), fluoresces ($\Phi_F = 0.53$), or decomposes via a dissociative state (assumed to be a biradical) with low efficiency ($\Phi_r^1 = 0.02$). Triplet sensitisation behaves analogously, except that the $^3(n-\pi^*)$ excited state does not emit. As in the deazetation of DBO, direct and sensitised photolyses are not coupled and exhibit different Φ_r 's and E_a 's for decomposition.

4.11 Product stereochemical assignments

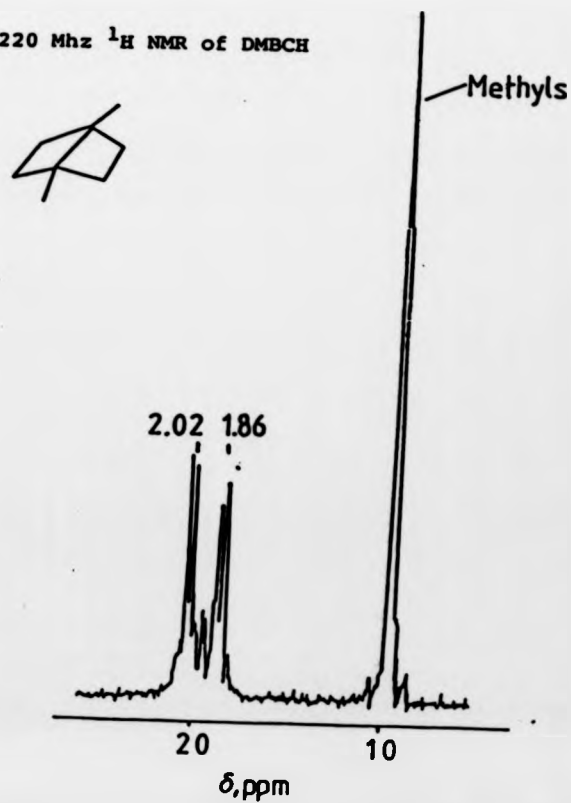
The reported hydrocarbon products from the photochemical decomposition of DMDBO are 1,4-dimethylbicyclo[2.2.0]hexane (DMBCH) and 2,5-dimethylhexa-1,5-diene.¹ Samples of these could be obtained from prep. g.c. of sensitised photolysis mixtures. The 1H NMR of the diene gave only three signals since the cis (H_C) and trans (H_T) resonances were not resolved (Figure 4.10).

Figure 4.10 220 MHz ^1H NMR of 2, 5-dimethylhexa-1,5-diene.



The 220 MHz ^1H NMR of DMBCH is illustrated in Figure 4.11. The exo (H_x) and endo (H_N) protons are part of an AA'BB' spin-spin system.

Figure 4.11 220 Mhz ^1H NMR of DMBCH



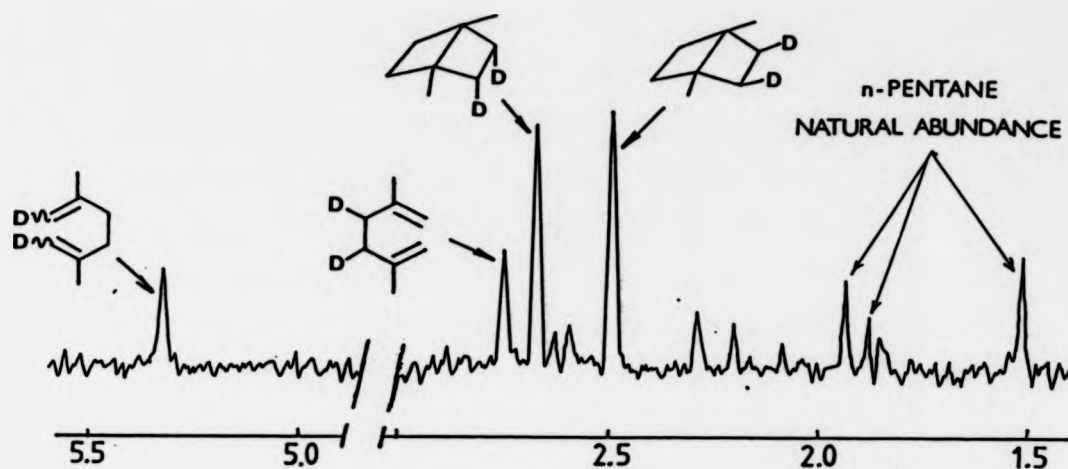
As in our previous stereochemical assignments, we treated the spectrum as a first-order one. Thus, one of the two "doublets" at 2.02 and 1.86 ppm corresponds to the endo (H_N) protons, and the other to the exo (H_X) protons. For simplicity we ignored the small signals in between these "doublets". We assigned the "doublets" by analysis of 400 MHz 1H (1H)nOe difference spectra. Irradiation at the methyl signal (0.97 ppm) caused signal enhancement of both "doublets". However, the signal at 1.86 ppm showed a 2.5 times greater enhancement than the signal at 2.02 ppm. Inspection of Dreiding models reveals that H_X is closer to the methyl group than H_N , enabling the signal at 1.86 ppm to be assigned to H_X .

4.12 Direct and sensitised photolysis of stereoselectively labelled d_2 -DMDBO

Photolyses were carried out analogously to those of DBO. Thus, 1% solutions of the azoalkane were irradiated directly with > 300 nm light, or at 300 nm using *m*-methoxyacetophenone as sensitiser. Removal of polar species, followed by careful concentration, gave solutions of deuterated hydrocarbon products in *n*-pentane which were analysed by 2H NMR.

Direct photolysis of d_2 -DMDBO (90:10 anti/syn deuterium) gave the proton decoupled 2H NMR shown in Figure 4.12.

Figure 4.12 ^2H NMR of products from direct photolysis of $\text{d}_2\text{-DMDBO}^a$

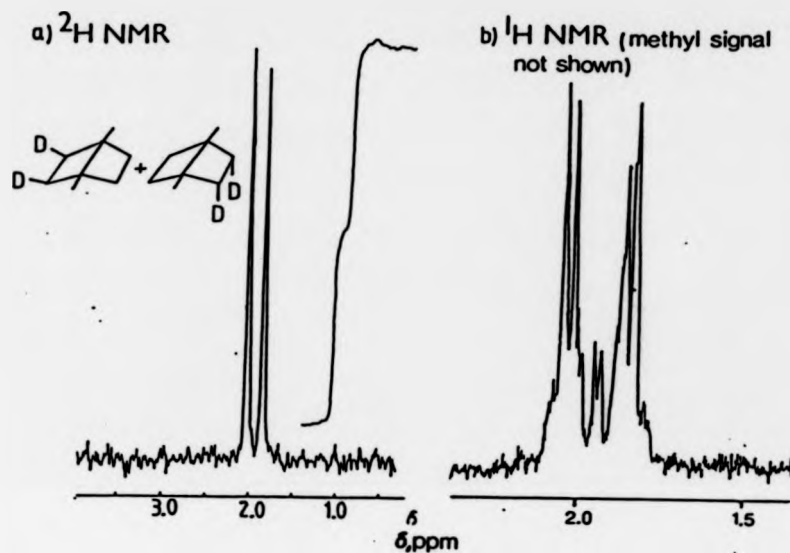


a. 90:10 anti/syn ^2H

Comparison of this spectrum with the ^1H NMR's of 2,5-dimethylhexa-1,5-diene and DMBCH, enabled the major peaks to be assigned. The spectrum also contained a large number of minor peaks which we attributed to deuterated 1,4-dimethylcyclohex-1-ene (cf direct photolysis of $\text{d}_2\text{-DBO}$). This has not previously been observed in the direct photolysis of DMDBO and will be discussed in Chapter 6.

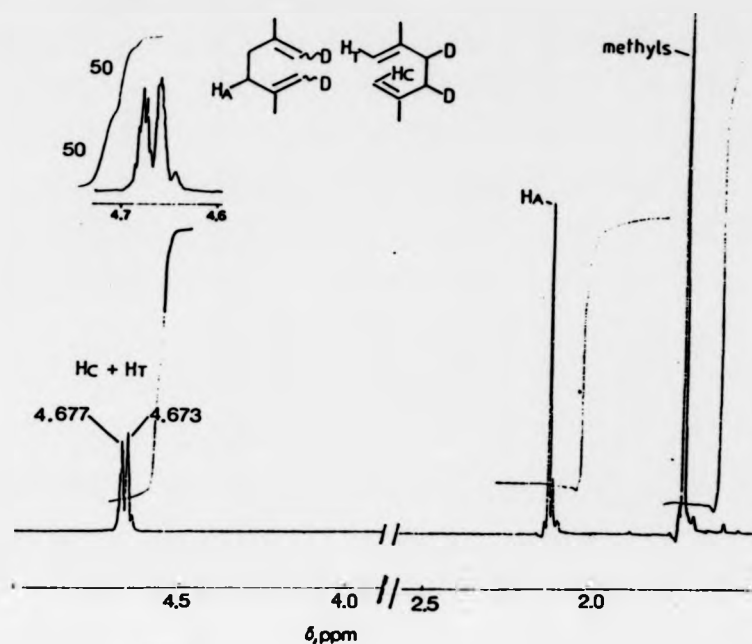
Integration of the major peaks in Figure 4.12 gave the relevant stereochemical ratio. Thus, the ratio of exo to endo deuterium in $\text{d}_2\text{-DMBCH}$ (50:50) shows that the cyclisation is stereorandom. To confirm that the signals were not artificially enhanced, we subjected the hydrocarbon mixture to prep. g.c. The ^1H and ^2H NMR's of the $\text{d}_2\text{-DMBCH}$ collected are shown in Figure 4.13. The spectra confirm that $\text{d}_2\text{-DMBCH}$ is formed stereorandomly.

Figure 4.13 ^1H and ^2H NMR's of d_2 -DMBCH isolated from direct photolysis of d_2 -DMDBO.^a



The proportions of total E- and total Z-deuterium in the 2,5-dimethylhexa-1,5-diene could not be ascertained from Figure 4.13, since their signals were not resolved. However, when the sample was isolated by prep. g.c., sufficient resolution was obtained in the 400 MHz ^1H NMR to measure the ratio (Figure 4.14).

Figure 4.14 400 MHz ^1H NMR of 2,5-dimethylhexa-1,5-dienes isolated from direct photolysis of d_2 -DMDBO. ^{a,b}

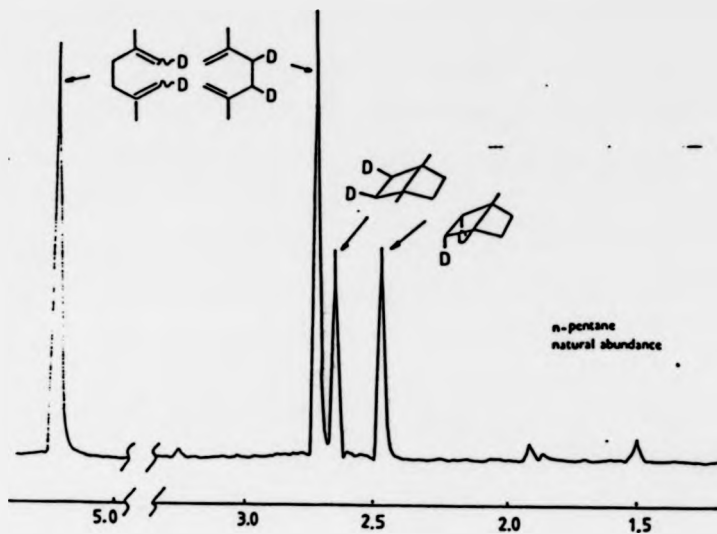


- a. 90:10 anti/syn ^2H
 b. The ^2H NMR of this sample showed equal proportions of allylic to total olefinic deuterium.

The relevant signals are those at 4.677 and 4.673 ppm. One of these corresponds to the cis (H_C) protons and the other to the trans (H_T). Their ratio (inset Figure 4.14) shows that the dienes are formed with an E/Z deuterium ratio of approximately 1.

Sensitized photolysis of d_2 -DMDBO (90:10 anti/syn deuterium) gave identical stereochemical results. Thus, d_2 -DMBCH was formed with an exo/endo deuterium ratio of 1, and deuterated 2,5-dimethylhexa-1,5-dienes contained equal proportions of E- and Z-deuterium. A typical ^2H NMR of the hydrocarbon products from sensitized photolysis of d_2 -DMDBO is given in Figure 4.15.

Figure 4.15 ^2H NMR of products from sensitised photolysis of d_2 -DMDBO.^a



^a 90:10 anti/syn ^2H

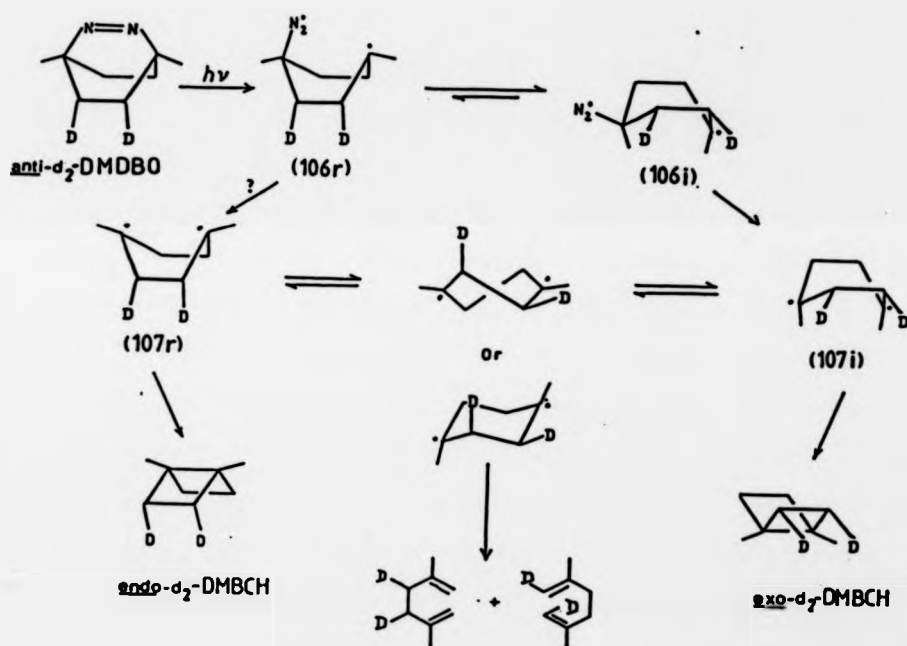
Comparison of this spectrum with that from direct photolysis (Figure 4.12) shows that this spectrum contains very few minor peaks. This is because deuterated 1,4-dimethylcyclohex-1-enes are formed in the direct photolysis, but not the sensitised (cf deazetation of d_2 -DBO).

4.13 Discussion

Direct and sensitised photolysis of d_2 -DMDBO led to d_2 -DMBCH's stereorandomly and 2,5-dimethylhexa-1,5-dienes with an E/Z deuterium ratio of 1 (cf pyrolysis of BCH). While this can be explained for the sensitised photolysis on the basis of a SCE, the

results of the direct photolysis should be compared with those obtained for d_2 -DBO (see Section 4.3, p.126). Certainly the stereorandom formation of products could be explained if they were derived from $^3(n-\pi^*)$ excited d_2 -DMDBO, formed by ISC. However, this is unlikely since ISC is very slow ($\tau_F = 599$ ns).¹ The results are best explained with reference to Scheme 4.7.

Scheme 4.7



Note that this Scheme is very similar to that used to rationalise the decomposition stereochemistry of d_2 -DBO (see Scheme 4.2, p138). Thus, initial cleavage of only one C-N bond leads to the diazenyl biradical (106r). In this system the equilibria between (106r) and (106i), or the diyls (107r) and (107i), must be fully developed. There are several reasons why this could occur.

Firstly, in d_2 -DBO the diazenyl substituent is expected to show a preference over the hydrogen atom for the bowsprit position of a cyclohexane boat conformer. In this system, since the methyl and diazenyl substituents are of similar size, there may be no preference and (106i) and (106r) would be present in equal proportions. Loss of nitrogen, followed by ring closure would lead to equal proportions of exo and endo- d_2 -DMBCH. Preferential cleavage from the chair or 90° -twist diyl would account for the diene stereochemistry.

Secondly, if the lifetime of the diazenyl biradicals, or the diyls, were increased, the relevant equilibria could become fully established leading to random product stereochemistry. This could occur in two ways. The methyls could exert a radical stabilising effect on (106) or (107). Alternatively, steric hindrance of the methyls in the d_2 -DMBCH products may inhibit ring closure in (107), thereby increasing the diyl lifetime.

Another possibility is that the presence of a bridgehead methyl increases the rate of the second C-N bond cleavage. Thus, the decomposition of DMDBO may occur by an S_H1 mechanism with loss of stereochemistry. In DBO, the S_H2 mechanism with inversion is more probable.

4.14 Summary

In this Chapter we have shown that direct and sensitised photolysis of d_2 -DBO proceeds with predominant inversion of BCH stereochemistry. A mechanism was proposed involving stepwise C-N bond cleavage and partial conformational equilibria between diazenyl biradicals and cyclohexane-1,4-diyls. Replacing bridgehead hydrogens by methyls leads to stereorandom BCH formation as the methyl substituents perturb the relevant equilibria. In both d_2 -DBO and d_2 -DMDBO, the hexa-1,5-dienes were formed with an E/Z deuterium ratio of 1. By analogy to BCH pyrolysis it was assumed that this was due to stereoselective formation of EZ- d_2 -diene. However, 2H NMR studies only afford the ratio of total E- to total Z-deuterium, not the proportions of EE-, EZ-, and ZZ- d_2 -diene isotopomers.

Chapter 5

5.1 Introduction

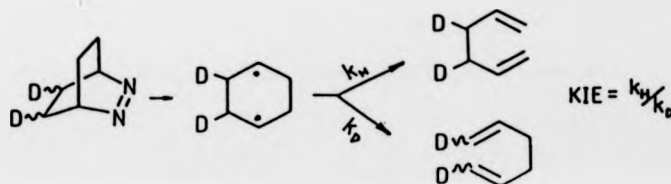
Decomposition of anti-d₂-DBO leads to hexa-1,5-dienes with equal proportions of total E- and total Z-deuterium, a result consistent with exclusive formation of the EZ-isotopomer. However, ²H NMR is unable to distinguish between this situation and the case where, for example, decomposition leads to equal proportions of the EE- and ZZ-isotopomers. This information can be obtained by an indirect chemical method combined with mass spectroscopy (see Section 2.6, p.93). In this chapter we discuss the hexa-1,5-diene stereochemistry in detail and relate the results to our preferred mechanism(s) for d₂-DBO decomposition.

This chapter also contains a discussion of the cleavage kinetic isotope effects (KIE's) for d₂-DBO decomposition, and compares the results with those observed in other systems involving cyclohexane-1,4-diyls as (assumed) intermediates.

5.2 Cleavage kinetic isotope effects

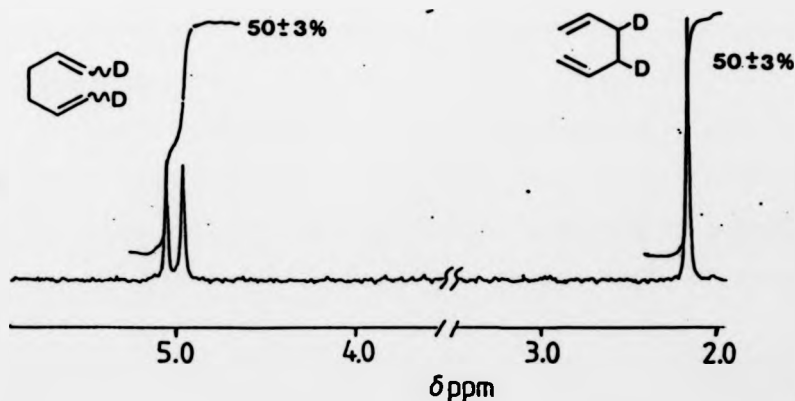
Decomposition of d₂-DBO involves an (assumed) diyl intermediate which can cleave to give dienes with olefinic deuterium (EE-, EZ-, and ZZ-d₂-dienes) or dienes with allylic deuterium (3,4-d₂-diene), as shown in Scheme 5.1.

Scheme 5.1



The ratio of allylic to total olefinic (E+Z) deuterium in the product dienes determines the intramolecular secondary KIE. Its magnitude measures the extent of side-bond cleavage (C2-C3 or C5-C6) in the reactions product determining transition state (PDTST[‡]). Inspection of Figures 4.6 and 4.7 shows that the ratio of total olefinic (E+Z) to allylic deuterium is approximately 1. This suggests that direct and sensitised photolysis of d₂-DBO leads to d₂-dienes with no intramolecular secondary KIE. This was confirmed by isolating samples of d₂-dienes from photolyses mixtures (prep. g.c with an unlabelled carrier) and re-recording ²H NMR's. Figure 5.1 shows the spectrum of dienes isolated from a direct photolysis mixture, with an equal proportion of allylic and olefinic deuterium.

Figure 5.1 ²H NMR of d₂-dienes isolated from direct photolysis of d₂-DBO. a, b

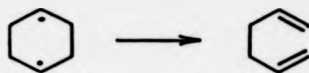


- a. Isolated by prep.g.c. with an unlabelled carrier
 b. Sensitised photolysis samples gave identical results.

A similar analysis of 2,5-dimethylhexa-1,5-dienes isolated from direct and sensitised photochemical decomposition of d_2 -DMDBO gave identical results i.e. absence of intramolecular secondary KIE's.

5.2.1 Discussion

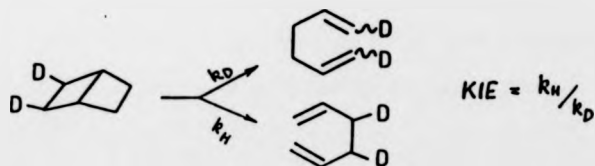
The absence of an intramolecular KIE in the photochemical decomposition of DBO can be rationalised by invoking an intermediate cyclohexane-1,4-diyl. Formation of hexa-1,5-diene from the diyl will be very exothermic. Consequently, the reaction;



is likely to involve an "early" transition state (cf Hammond's postulate). Since an "early" transition state would not be expected to show significant side bond cleavage, the absence of an intramolecular KIE in the decomposition is fully consistent with a biradical mechanism.

In their study of BCH pyrolysis, Goldstein and Benzon¹ measured both intra- and intermolecular KIE's. The intramolecular KIE was defined as on p.159 and was measured¹ by pyrolysis of *exo*- d_2 -BCH and comparison of the appropriate d_2 -diene ¹H NMR signals (Scheme 5.2).

Scheme 5.2

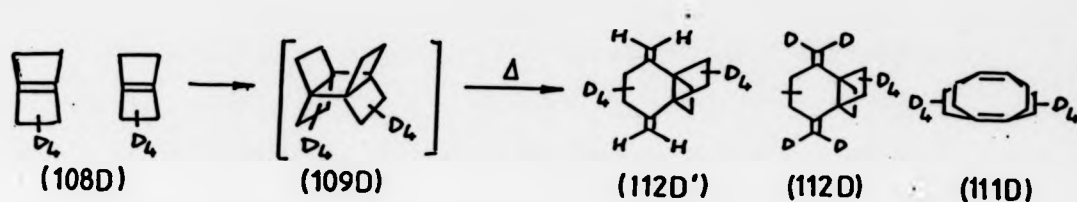


The intermolecular KIE (k_{d_0}/k_{d_4}) was obtained from relative cleavage rate constants (k) of unlabelled (d_0) and tetradeuterated (d_4) BCH¹. Its magnitude measured the extent of side-bond cleavage (C2-C3 or C5-C6) in the reaction's rate determining transition state (RDTST[‡]). Within experimental error, pyrolysis of BCH was shown to lead to hexa-1,5-dienes without inter- or intramolecular KIE's (*ie* $k_{d_0}/k_{d_4} = 1.00 \pm 0.03$ and $k_H/k_D = 1.015 \pm 0.012$).¹ The absence of an intermolecular KIE suggested there was little or no side-bond cleavage in the RDTST[‡]. This is consistent with the involvement of a cyclohexane-1,4-diyl because it places the RDTST[‡] somewhere between the diyl and BCH. However, Goldstein and Benzon found the absence of an intramolecular KIE difficult to explain in terms of a biradical mechanism. This was because thermokinetic estimates at that time put the chair diyl (their assumed biradical intermediate for stereoselective cleavage) some 8-10 kcalmol⁻¹ below the transition state for cleavage. Thus, it was reasoned that if the diyl must climb 8-10 kcalmol⁻¹ to its PDTST[‡] this must have been due, at least in part, to some side-bond cleavage.¹ This argument is now less secure since updated values for $\Delta H_f(\text{chair-diyl})$ place it only 1-2 kcalmol⁻¹ below the PDTST[‡],² while the other possible intermediate for stereoselective cleavage of *exo* deuterated BCH, the 90°-twist diyl, is virtually iso-energetic with the PDTST[‡] (see Section 5.8.1,p210). The absence of an intramolecular KIE in pyrolysis of BCH can readily be rationalised by invoking an identical argument to that used for the decomposition of DBO *ie* cleavage from a cyclohexane-1,4-diyl with an "early" transition state. Such a rationale is complimentary to Goldstein and Benzon's results for the intermolecular KIE in BCH pyrolysis,¹ and is permissive evidence that both pyrolysis of BCH and photochemical

decomposition of DBO form hexa-1,5-dienes from a similar biradical intermediate.

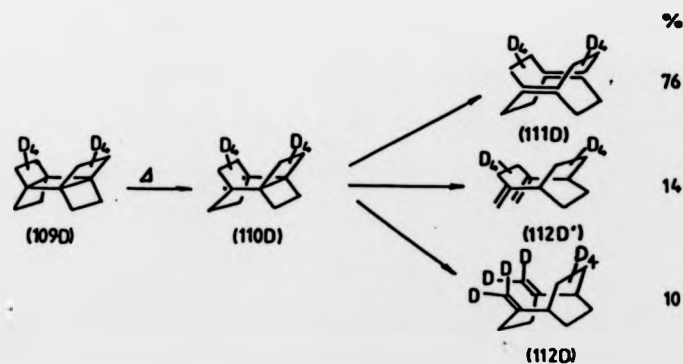
During the course of this work, Wiberg *et al*³ reported a study of a superficially similar BCH system which showed an appreciable secondary intramolecular KIE. Thus, thermal dimerisation of 2,2,3,3-²H₄-bicyclo[2.2.0]hex-2-ene (108D) gave tricyclic hydrocarbons via an (assumed) intermediate propellane (Scheme 5.3).

Scheme 5.3



The propellane (109D) was envisaged to decompose to products through a 1,4-diyli (110),³ (*cf* BCH pyrolysis). The ratio of (112D')/(112D) was measured by ²H NMR and determined the intramolecular KIE for cleavage ($k_H/k_D = 1.4$, Scheme 5.4).

Scheme 5.4



In view of these results we decided to re-investigate the intramolecular KIE's in the pyrolysis of BCH.

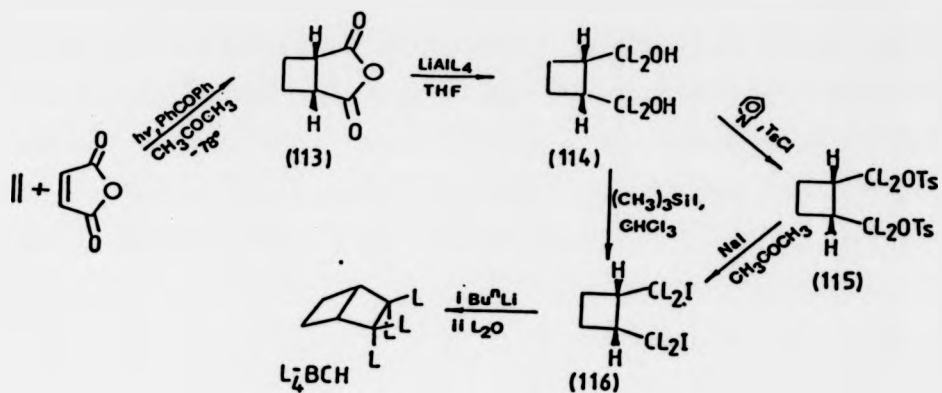
5.2.2 Bicyclohexane Pyrolysis. Measurement of Intramolecular KIE's

If pyrolysis of d_2 -BCH shows the same intramolecular KIE as the superficially similar system of Wiberg *et al.*,³ per deuteron, the ratio of allylic to total olefinic 1H NMR signals will be 48.5: 51.5, respectively (the olefinic and allylic signals contain protons from 3,4- d_2 -diene and EE,-EZ-, and ZZ- d_2 -dienes). Such a small difference in 1H NMR signal integrals may not have been detectable in Goldstein and Benzon's pyrolytic studies.¹ However, in 2H NMR the situation is much better; an intramolecular KIE of 1.2 will translate into a signal integral ratio of 54.5:45.5 for the allylic and total olefinic signals, respectively. This would be readily detected. With 2,2,3,3- d_4 -BCH, an intramolecular KIE of 1.1 per deuteron (*cf* Wiberg *et al.*³) would afford d_4 -dienes with an integral ratio of 58.3:41.7 for allylic and total olefinic 2H NMR signals, respectively. Therefore, we required samples of 2,3- d_2 -BCH, or preferably 2,2,3,3- d_4 -BCH, to determine the intramolecular KIE for BCH pyrolysis by 2H NMR.

5.2.2.1 Synthesis of 2,2,3,3- $[^2H]_4$ bicyclo[2.2.0]hexane(d_4 -BCH)

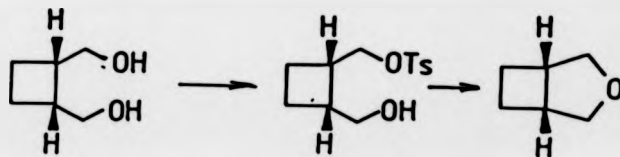
The synthetic strategy for the preparation of d_4 -BCH is outlined in Scheme 5.5. This is analogous to the method previously used to prepare strained bicyclic hydrocarbons.^{4,5}

Scheme 5.5 L = H, D



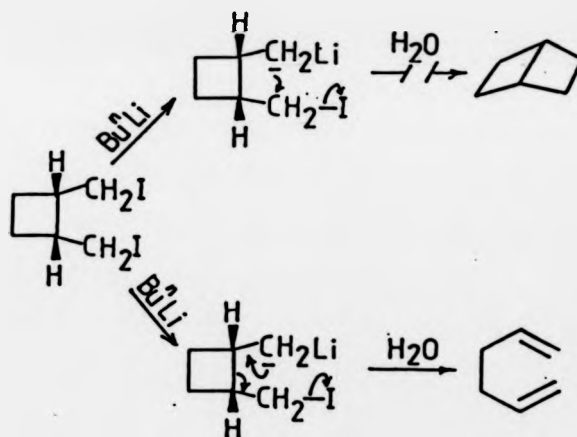
Thus, photochemical [$\pi 2s + \pi 2s$] addition of ethylene and maleic anhydride at -78° gave a mixture containing 78% (113) and 22% oxetane impurity formed by [$\pi 2s + \pi 2s$] addition of maleic anhydride and acetone.⁶ The oxetane was thermally unstable so distillation of the mixture gave pure (113) in 70% yield. Reduction with lithium aluminium hydride led to (114 H), which could be tosylated with tosyl chloride in pyridine. Yields of the bis-tosylate (115H) were poor, possibly due to an intramolecular $\text{S}_{\text{N}}2$ reaction in the mono tosylate (Scheme 5.6).

Scheme 5.6



However, cis-1,2-bis-iodomethylcyclobutane (116H) was obtained in good yield by treating (114H) with trimethylsilyliodide in chloroform. The crucial step in the synthesis was the cyclisation of (116H). Less strained cis-bicyclo[n.2.0] hydrocarbons ($n = 3,4..$ etc) have been synthesised in high yields from the appropriate cyclic cis-1,2-bis-iodomethyl compounds by treatment with *n*-butyl lithium and subsequent hydrolysis^{4,5}. Unfortunately, this treatment of (116H) led only to the ring opened product, hexa-1,5-diene (Scheme 5.7).

Scheme 5.7



As it was not possible to prepare *d*₄-BCH by this route, we sought to obtain samples of *d*₂-BCH for the study from photolysis mixtures.

5.2.2.2 Isolation of 2,3-[²H]₂-bicyclo[2.2.0]hexane from d₂-DBO photolysis mixtures

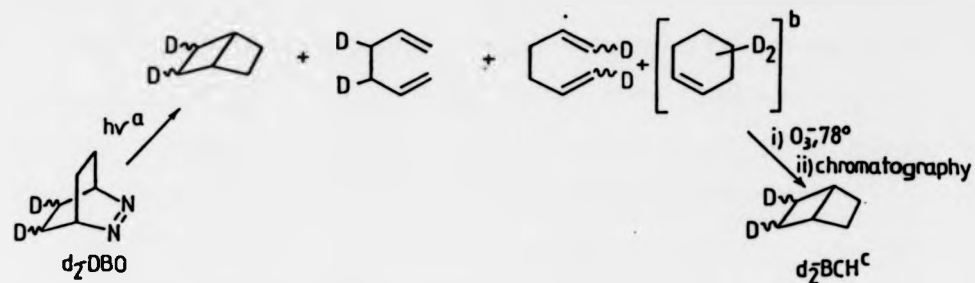
The synthesis of d₂-BCH has been accomplished¹ by a simple variant of Van Tamelen's synthesis⁷ of Dewar benzene (see Scheme 4.1, p132).

However, this method is time consuming, difficult to execute, and gives very low overall yields of d₂-BCH (ca 3%).¹ Consequently we did not attempt the complete synthesis, preferring to isolate samples from d₂-DBO photolysis mixtures.

It was previously noted BCH's formed in direct photolysis of DBO could not be isolated by prep. g.c. as small amounts of cyclohexenes are formed which co-chromatograph. Since cyclohexenes are not produced in sensitised photolyses (see Chapter 6) BCH's could be prep. g.c. isolated from product mixtures. However, in a trial run on protio material, photosensitised decomposition of 341 mg of DBO gave only 10 mg of BCH after prep. g.c.

Samples of d₂-BCH could be obtained more efficiently by a chemical method combined with column chromatography (Scheme 5.8).

Scheme 5.8



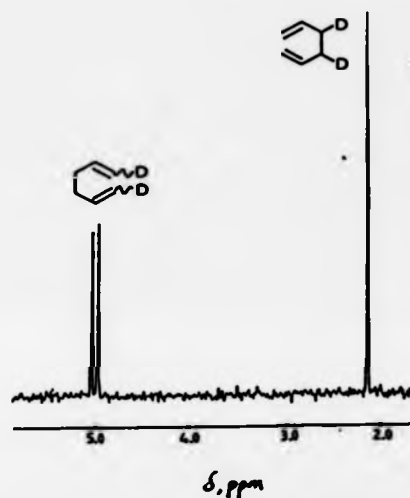
- Direct or sensitised photolysis in *n*-pentane solutions.
- Direct photolysis only.
- As solution in *n*-pentane.

Direct or sensitised photochemical decomposition of d_2 -DBO samples (1% solutions in *n*-pentane) and column chromatography over alumina led to solutions of deuterated hydrocarbons in *n*-pentane. The *n*-pentane solutions were cooled to -78° and treated with ozone. The formation of ozonides was monitored by the disappearance of hexa-1,5-diene (and cyclohexene) olefinic signals in the 1H NMR. When all the unsaturated species had reacted, the solution was passed through an alumina column to remove the oxygenated products. The *n*-pentane eluate was concentrated to afford solutions of d_2 -BCH. Not only does this method have the advantage of being applicable to both photolysis modes, it also leads to d_2 -BCH's stereoselectively, a factor of importance in our later studies (see Section 5.6.1, p.195).

Samples of d_2 -BCH so obtained were pyrolysed at 180° for 21 hrs in sealed glass tubes (10.5 half-lives of BCH decomposition).¹ Subsequent 2H NMR analysis of the pyrolysed solutions showed equal proportions of allylic and total olefinic deuterium (Figure 5.2) in full accord with Goldstein and Benzon's 1H NMR observations.¹

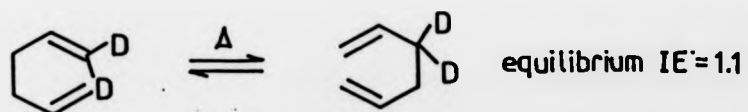
It is important to note that degenerate Cope rearrangement of hexa-1,5-diene was negligible under the conditions of the pyrolysis.⁸ This is important as the preference of deuterium for an sp^3 centre leads to an equilibrium IE in the former reaction (Scheme 5.9).

Figure 5.2 2H NMR of hexa-1,5-dienes from pyrolysis of d_2 -BCH^a



- a. The ratio of exo/endo deuterium is insignificant in studies of the intramolecular KIE.

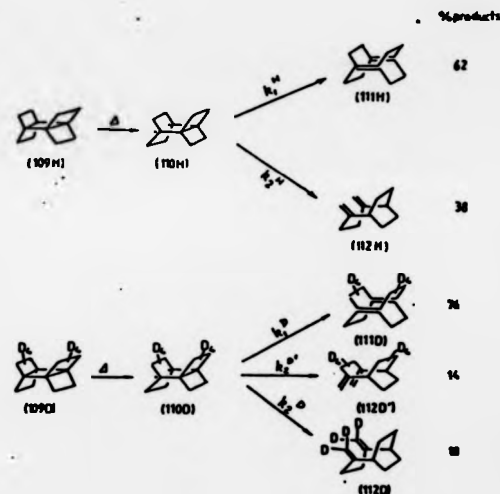
Scheme 5.9



5.2.2.3 Discussion

As pyrolysis of BCH does not involve a significant intramolecular KIE, it is surprising that the superficially similar system of Wiberg *et al*³ exhibits such an appreciable KIE. The product distributions for the reaction of protio and deuterio (109) are shown in Scheme 5.10.

Scheme 5.10 (From ref. 3)



Wiberg *et al*³ assumed that deuteration at, for example, C3 and C4 would not affect cleavage of C1-C6 (ie $k_1^H \sim k_1^D$). Similarly, deuteration at, for example, C3 and C4 should not affect cleavage of C7-C8 and C9-C10. Given the distance of the deuterated sites from the bonds cleaving, both assumptions seemed reasonable. Thus, the products from cleavage of undeuterated bonds in (109D) (ie (111D) and (112D')) should be formed in equal amounts to (111H) and (112H) from the corresponding process in (109H);

$$\frac{(111H)}{\frac{1}{2}(112H)} = \frac{(111D)}{(112D')}$$

Inspection of Scheme 5.10 shows that this is not the case as the relevant ratio's are 62/19 for the protio compounds and 76/14 for the deuterio compounds. Therefore, we conclude that either (a) remote deuteration does affect cleavage rates in (109) or (b) the product proportions (and hence the intramolecular KIE) are not as reported.

The absence of an intramolecular KIE in both BCH pyrolysis and photochemical decomposition of DBO is permissive evidence for the involvement of a common cyclohexane-1,4-diyl intermediate which proceeds to hexa-1,5-diene via an "early" transition state.

5.3 Proportions of EE-, EZ-, and ZZ-1,6-[²H]₂-hexa-1,5-dienes from photochemical decomposition of d₂-DBO

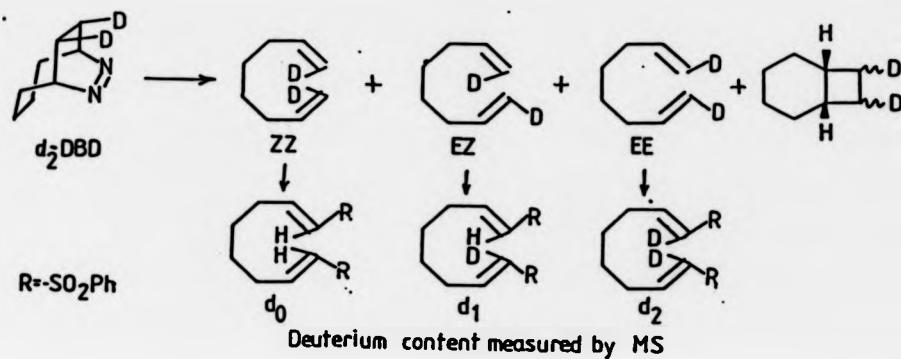
The proportions of d₂-diene isotopomers are inaccessible from ²H NMR studies but can be obtained from an indirect chemical method combined with mass spectroscopy. The method of this analysis was briefly mentioned in Section 2.6, p.93. In this section the analysis is discussed in more detail and the results obtained related to our preferred mechanism for the photochemical decomposition of d₂-DBO.

5.3.1 Method of Analysis

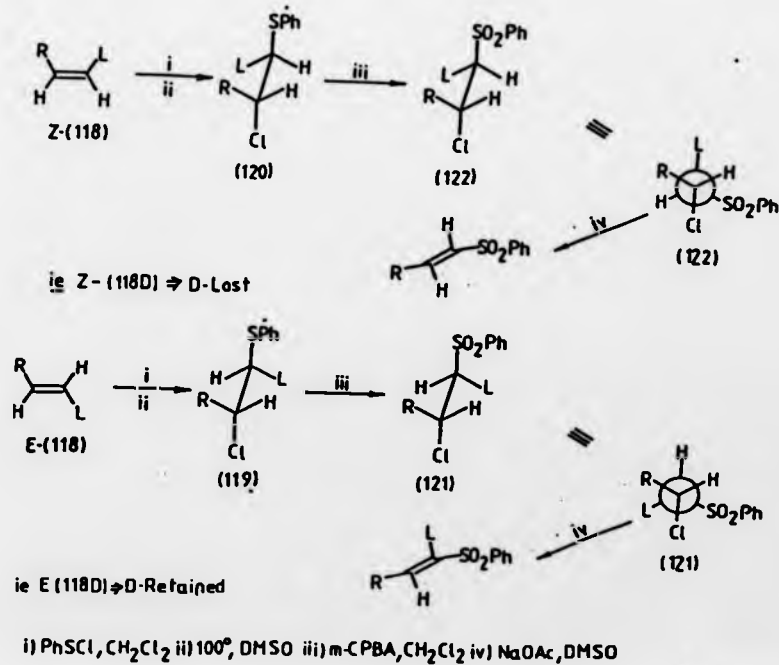
Stereoselective substitution of phenylsulphonyl groups to the terminal positions of the d₂-dienes, in which E-deuterium is retained and Z-deuterium is lost, translates stereochemical information into deuterium content (see Scheme 2.31, p.94). Samuel used a similar analysis to determine the proportions of EE-, EZ-, and ZZ-1,8-[²H]₂-octa-1,7-dienes in the thermal and photochemical decomposition of d₂-DBD (Scheme 5.11).⁹

Stereoselective substitution of phenylsulphonyl groups to terminally deuterated olefins of general structure (118) can be achieved by the sequence of reactions shown in Scheme 5.12.^{9,10}

Scheme 5.11



Scheme 5.12

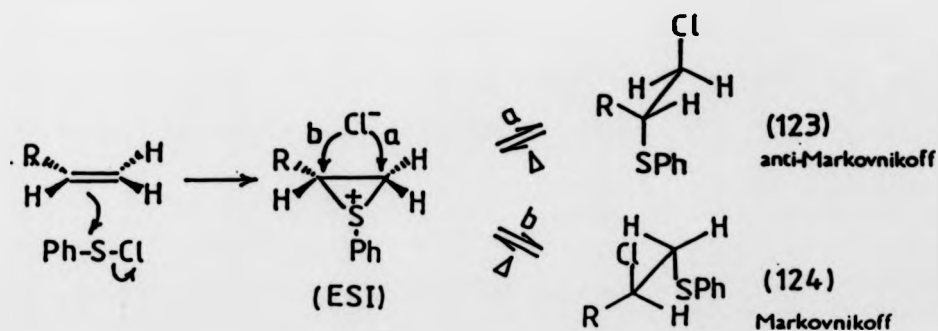


Inspection of Scheme 5.12 shows that E-deuterium will be retained and Z-deuterium lost assuming

- (a) Markovnikoff chlorosulphides (119) and (120) are formed by trans-addition of PhSCL.
- (b) The E-disulphones are formed by trans-coplanar elimination of LCl from (121) and (122), respectively.

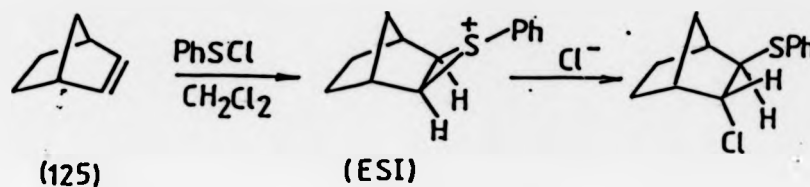
Trans-addition of PhSCL to terminal substituted alkyl olefins would be expected if the reaction involves a bridged sulphur intermediate. There is good evidence that this is the case. For example, Mueller and Butler¹¹ observed high selectivity for the anti-Markovnikoff adducts which increased with the size of the alkyl group. The results were consistent with nucleophilic attack of chloride ion at the least hindered carbon of an intermediate episulphonium ion (ESI). This suggested that the predominance of the anti-Markovnikoff adduct was a kinetic effect. This point was verified since the anti-isomer was readily converted to the thermodynamically more stable Markovnikoff isomer on heating (Scheme 5.13).¹¹

Scheme 5.13



Mueller and Butler obtained further evidence for their proposed mechanism from stereochemical studies.¹¹ It was found that PhSCl addition to norbornene (125) led to 1,2-adduct with exclusive trans-stereochemistry (Scheme 5.14).

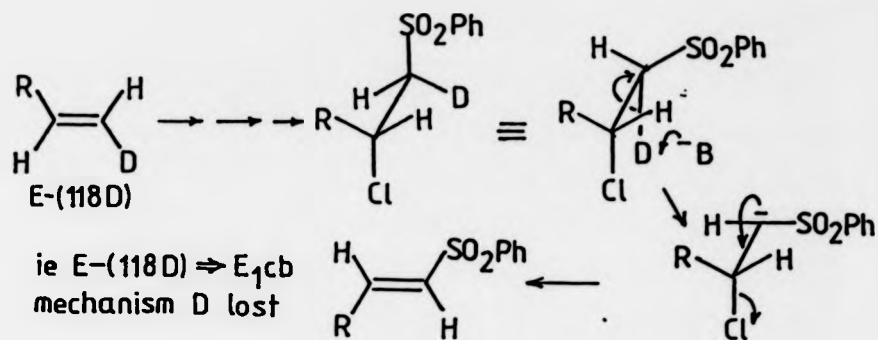
Scheme 5.14



Although the nature of the sulphur intermediate has been questioned,¹² the assumption of trans addition of PhSCl to hexa-1,5-diene is perfectly valid. 48

Dehydrochlorination mechanisms of phenylsulphonyl activated systems are known to vary from essentially E₂ (trans coplanar elimination) to the other extreme of essentially E₁cb.¹³ The E₁cb mechanism usually occurs with syn elimination which would lead to the opposite effect of that depicted in Scheme 5.12 ie retention of Z-deuterium and loss of E-deuterium (Scheme 5.15).

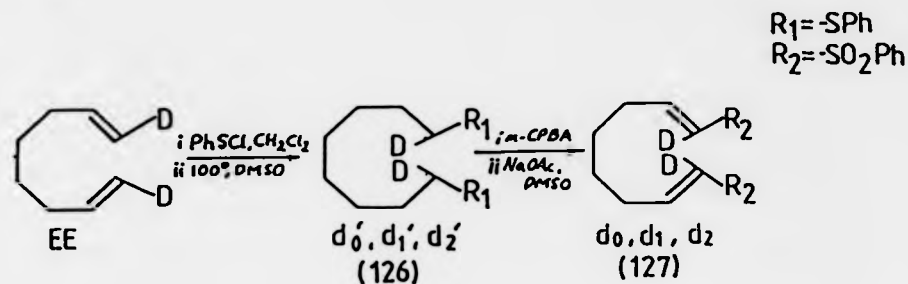
Scheme 5.15



Although our stereochemical analysis would work equally as well if dehydrohalogenation occurred by syn-elimination, competing mechanisms would make it impossible. Previous studies of dehydrochlorination mechanisms in similar phenylsulphonyl activated systems have shown that the use of weak bases in polar aprotic solvents (such as sodium acetate in DMSO) favour trans coplanar elimination by the E₂ mechanism.¹³ Samuel has confirmed that such conditions lead to exclusive trans coplanar elimination in a system very closely related to hexa-1,5-diene by the following control experiment.^{5,9}

Hydroboration of octa-1,7-diyne followed by deuterionolysis led to octa-1,7-diene with > 99% E-deuterium. Subjection of the diene to the sequence of reactions shown in Scheme 5.16 led to EE-disulphone without significant loss of deuterium.

Scheme 5.16



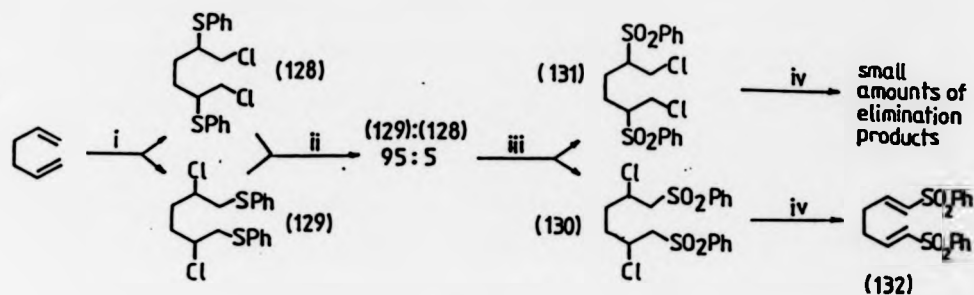
This experiment also confirmed the assumption of trans coplanar addition of PhSCl to the double bonds.^{5,9}

5.3.2 Synthesis of EE-1,6-bis-phenylsulphonylhexa-1,5-diene^{9,10}

Addition of authentic hexa-1,5-diene to PhSCl in dichloromethane gave a mixture of anti-Markovnikoff (128) and Markovnikoff (129) 1,2-adducts. ¹H NMR analysis of the crude material showed the anti-Markovnikoff isomer was formed with ca 70% selectivity. The thermodynamic product mixture (95:5, (129): (128)) was obtained by heating the crude mixture for 1-2 hr in DMSO at 100°. The crude mixture of chlorosulphides was oxidised to the chlorosulphones ((130) and (131)) with *m*-chloroperoxybenzoic acid in dichloromethane and then treated with sodium acetate in DMSO at ambient temperature. The dehydrochlorination step was monitored by ¹H NMR (appearance of olefinic resonances) and was generally complete in 1-3 hr. The ¹H NMR of the crude material showed > 90% of the required EE-disulphone (132) and small amounts of other olefinic species. The minor products were not identified but probably arose from eliminations in the

chlorosulphone (131). All the reactions proceeded in near quantitative yield. The sequence is summarised in Scheme 5.17.

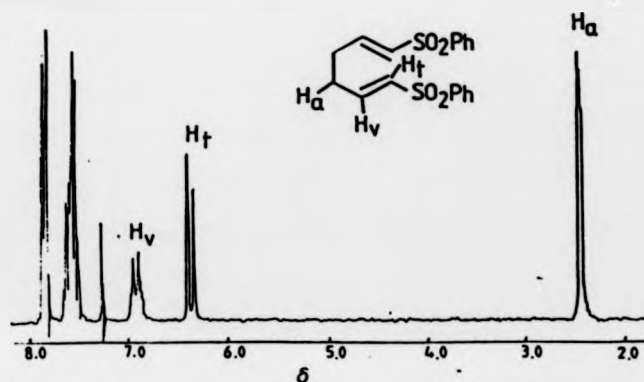
Scheme 5.17



i) PhS₂Cl, CH₂Cl₂ ii) DMSO, 100° iii) m-CPBA, CH₂Cl₂ iv) NaOAc, DMSO

The ¹H NMR of a sample of (132) recrystallised from ethanol is given in Figure 5.3.

Figure 5.3: ¹H NMR of EE-1,6-bis-phenylsulphonylhexa-1,5-diene (132H).



A similar sequence of reactions to that shown in Scheme 5.17 was carried out on 1% n-pentane solutions of hydrocarbon products from direct and sensitised photochemical decomposition of stereoisomerically pure anti-d₂-DBO. The only significant difference occurred in the initial PhSCl addition step, which required 18-24hr. This was because the n-pentane solutions contained low concentrations of hexa-1,5-dienes so the second order reaction with PhSCl in dichloromethane was relatively slow. Samples of (132D) obtained from photolysis hydrocarbon product mixtures were recrystallised from ethanol and their purity verified by ¹H NMR. An example of the synthetic procedure is given in full detail in the experimental section. The deuterium content of the samples of (132D) (disulphones) was measured mass spectrophotometrically.

5.3.3.1 Determination of disulphone deuterium content

In principle, the determination of the deuterium content in samples of (132D) was identical to that used in the determination of d₂-DBO precursors deuterium content (see Section 3.3, p.115). However, in this case EI/MS did not give molecular or fragment ions of sufficient intensity or clarity for the deuterium analysis. The analysis could be performed on protonated molecular ions (MH⁺ + 1, MH⁺ + 2, MH⁺ + 3...etc) formed by chemical ionisation MS (CI/MS) of samples of (132D). Although CI/MS removes the need for self-protonation corrections (see Section 3.3, p.116), reproducibility of results proved to be a problem. This was particularly true when ammonia was used as the ionising gas. Analysing the (MH⁺) ion produced by methane CI was more successful. The ions (MH⁺, 363) were

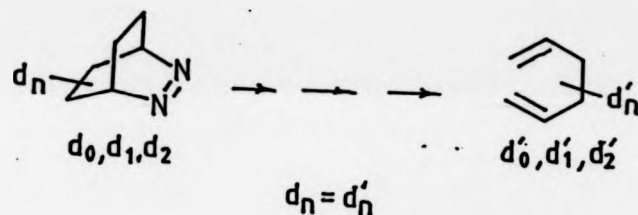
of high intensity and generally satisfied the criteria for deuterium analysis¹⁴ (in particular, absence of $(MH^+ - 1)$ peaks). Thus, deuterated samples of disulphones from direct and sensitised photolyses of anti-d₂-DBO were introduced into the mass spectrometer and scanned six times each. The peak intensities were then used to calculate the relative proportions of d₀-, d₁-, and d₂- disulphones. Correction of $(MH^+ + 1)$, $(MH^+ + 2)$... $(MH^+ + n)$ peaks, arising from natural abundance of heavy isotopes, was achieved using the calculated natural abundancies of unlabelled material (see Appendix 1). Each sample of disulphone was recrystallised and then reanalysed. The process was repeated to obtain three sets of consistent results (see Appendix 5). This ensured that the measured proportions of d₀-, d₁-, and d₂-disulphones were only due to the EE-isomer of (132).

5.3.3.2 Relation of disulphone deuterium content to hexa-1,5-diene stereochemistry

The proportions of d₀-, d₁-, and d₂-disulphones determined mass spectrophotometrically did not represent the proportions of EE-, EZ-, and ZZ-d₂-diene isotopomers. The deuterium content of the disulphones must be corrected for small amounts of d₀- and d₁-dienes, and d₂-disulphone derived from 3,4-d₂-diene. Ideally, this would have been achieved using proportions of d₀-, d₁-, and d₂-dienes (see Scheme 2.31, p.94). However, as reported by Goldstein and Benzon,¹ mass spectrophotometric determination of hexa-1,5-diene deuterium content is not possible as there are significant (M-1) and (M-2) peaks. In this system, the best possible

alternatives are the crude 1,2-adducts derived from treating the dienes with PhSCl . Unfortunately, we were unable to obtain molecular ion or fragmentation peaks for such samples that did not show (M-1) or (M-2) peaks. Consequently, the experimentally determined proportions of disulphones had to be corrected using the deuterium content of the azoalkane precursor (90D). This assumed that a sample of (90D) led to hexa-1,5-dienes without significant loss of deuterium (Scheme 5.18). This assumption is discussed in more detail in Section 5.4.1.

Scheme 5.18


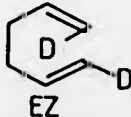
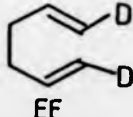


The other information required for the correction procedure is the ratio of allylic to total olefinic deuterium. We had determined this to be 50:50 from ^2H NMR studies (see Section 5.2, 158). Although this value was used in the corrections, note that ^2H NMR would not have detected a ratio $< 53:47$. A worked example of the correction procedure can be found in Appendix 5. The corrected proportions of d_0 -, d_1 -, and d_2 -disulphones are equivalent to the proportions of EE-, EZ-, and ZZ- d_2 -diene isotopomers from photochemical decomposition of anti- d_2 -DBO.

5.4 Results

Two samples of d_2 -DBO (> 99% anti deuterium) were decomposed by direct photolysis and the resultant dienes subjected to the disulphone stereochemical analysis. Both samples of d_2 -DBO used were derived from the same sample of (90D). Two samples of d_2 -DBO (> 99% anti deuterium) were also decomposed by sensitised photolysis but in this case the azoalkanes were derived from samples of (90D) with different deuterium contents. The proportions of EE-, EZ-, and ZZ- d_2 -diene isotopomers (determined as discussed in Section 5.3.3.2) are given in Table 5.1.

Table 5.1 Proportions of EE-, EZ-, and ZZ- $[^2H]_2$ -hexa-1,5-dienes from photochemical decomposition of anti- d_2 -DBO.

Mode of decomposition	% Proportions ^a		
	 ZZ	 EZ	 EE
Direct ^b Run1	3.5 ± 0.5	84.5 ± 0.5	11.5 ± 1.5
	^b Run2	4.0 ± 0.5	84.5 ± 0.5
Sensitised ^c Run1	3.5 ± 1.5	80.5 ± 1.5	16.5 ± 0.5
	^d Run2	9.0 ± 1.0	70.0 ± 2.0

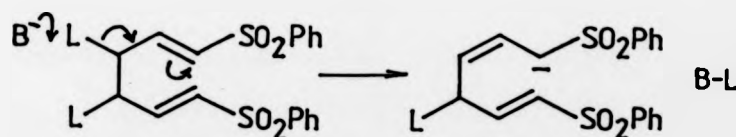
- a. The values are averages of three separate MS experiments for each sample of disulphone obtained in a particular run. The three experiments gave the results within the limits quoted.
- b. From anti- d_2 -DBO with $d_0 = 0$, $d_1 = 4.488$, $d_2 = 95.512$.
- c. From anti- d_2 -DBO with $d_0 = 0.753$, $d_1 = 8.659$, $d_2 = 90.588$.
- d. From anti- d_2 -DBO with $d_0 = 0.083$, $d_1 = 6.762$, $d_2 = 93.200$.

Before considering the mechanistic implications of the results in Table 5.1, two points required further investigation.

Firstly, the results in Table 5.1 were obtained assuming that no secondary KIE's operate in proceeding from the azoalkane to the disulphones. If this were the case, the results for a particular mode of decomposition should be reproducible. While this is true for the direct photolyses, in which samples of d_2 -DBO were derived from the same sample of (90D), the results from sensitised photolyses were significantly different. As the two samples of azoalkanes had different deuterium contents in the latter mode of decomposition, the results suggest that secondary KIE's may be operative. Consequently, we investigated the validity of the assumption that secondary KIE's are negligible.

Secondly, the γ -protons in the disulphones may be acidic as the carbanion formed could be stabilised by the phenylsulphonyl functional group (Scheme 5.19).

Scheme 5.19

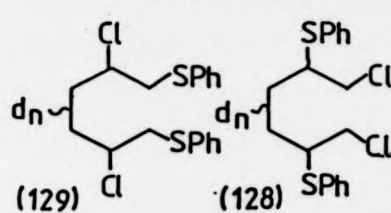
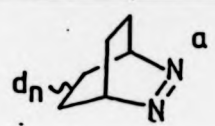


If this process was significant, deuterium wash-out could occur under the basic conditions used in the dehydrochlorination step of the disulphone stereochemical analysis. As this would affect the proportions of d_0 -, d_1 -, and d_2 -disulphones determined by MS, we carried out a control experiment to determine the extent of deuterium wash-out.

5.4.1 Control experiments. Secondary KIE's

We have previously noted that there is no intramolecular KIE for cleavage of the assumed cyclohexane-1,4-diyl intermediate (see Section 5.2, p.158). Thus, photochemical decomposition of d_2 -DBO leads to hexa-1,5-dienes with equal proportions of allylic and total olefinic deuterium. However, as the azoalkane is composed of d_0 -, d_1 -, and d_2 -species a secondary KIE with, for example $k_H/k_D < 1$, would lead to increased proportions of deuterated species. The type of KIE that would lead to this affect is, for example, one in which deuterated azoalkanes gave increased cleavage/coupling ratio's compared with undeuterated azoalkanes. If secondary KIE's are insignificant in the decomposition the proportions of d_0 -, d_1 -, and d_2 -DBO's would be identical to the proportions of d_0 -, d_1 -, and d_2 -dienes. Since the deuterium content of the dienes could not be measured (see p.178) the deuterium content of the compounds at the earliest stage of the disulphone stereochemical analysis should be compared with those of the azoalkane (ie the isomeric mixture of chlorosulphides (128) and (129)). Unfortunately, EIMS of the crude mixture of (128) and (129) showed (M-1) and (M-2) peaks in the MS making them unsuitable for quantitative deuterium analysis. However, as these peaks were small (< 1%) a qualitative estimation of deuterium content could be obtained. The proportions of d_0 -, d_1 -, and d_2 -chlorosulphides obtained from sensitised photolysis of d_2 -DBO are compared with deuterium content of the azoalkane in Table 5.2.

Table 5.2 Comparison of d_2 -DBO deuterium content with resultant chlorosulphides

COMPOUNDS	^2H CONTENT		
	d_0	d_1	d_2
 (129) (128)	1.859	13.518	85.623
 d_n^a	1.156	11.057	87.797

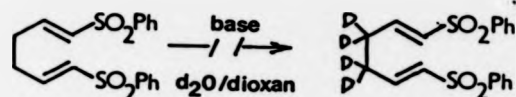
- a. Assuming the deuterium content of the azoalkane is identical to the sample of (90D) from which it was derived.

Assuming the deuterium content of the chlorosulphides is identical to that of the hexa-1,5-dienes (reasonable as all the dienes formed react with PhSCl) the results in Table 5.2 show good qualitative agreement. In view of the qualitative results for the chlorosulphides it is not possible to dismiss the existence of KIE's but the similarity of deuterium contents in Table 5.2 suggests that, if present, they must be small.

5.4.2. Control experiments. Deuterium wash-out

If deuterium wash-out occurred by the mechanism shown in Scheme 5.19, treating a sample of d_0 -disulphone with strong base in D_2O

should, in principle, lead to disulphone deuterated at the allylic positions. This sample could then be subjected to the milder conditions used in the dehydrochlorination step of the stereochemical analysis (sodium acetate in DMSO at ambient temperature). Measurement of the disulphone deuterium content before and after this mild treatment would indicate the extent of deuterium wash-out. This approach was unsuccessful as we were not able to exchange the disulphone allylic protons;

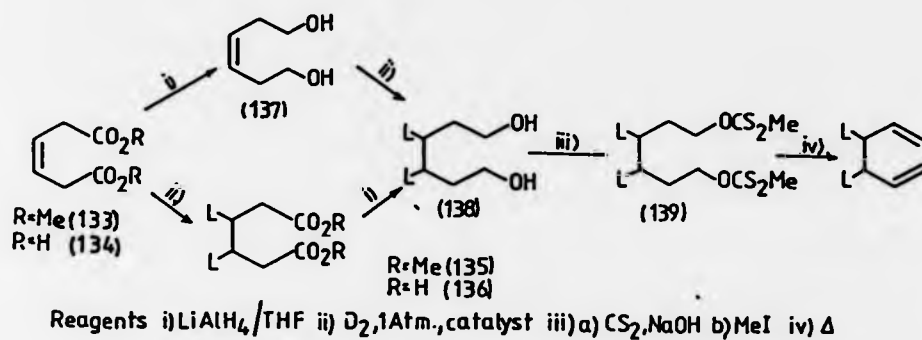


Using NaOD/D₂O/dioxan gave a product whose ¹H NMR showed only aromatic and olefinic signals. Repeating the reaction using NaOH/H₂O/dioxan gave an ¹H NMR spectrum even more complicated, again showing only aromatic and olefinic protons. The unknown products were yellow oils that polymerised on standing. We did not attempt to identify these products.

An alternative approach to this control experiment involves the synthesis of 3,4-[²H]₂-hexa-1,5-diene. Preparation of the disulphone from such a sample, and determination of the deuterium content before and after the elimination step would allow the extent of deuterium wash out to be determined. The general strategy of the synthesis is shown in Scheme 5.20.

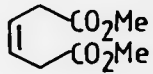
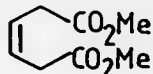
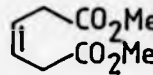
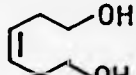

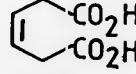
Scheme 5.20

L = H, D



We were able to prepare the xanthate ester (139H) from hexane-1,6-diol (138H) in good yield. Subsequent thermolysis led to moderate yields (30-40%) of hexa-1,5-diene.¹⁵ Problems arose in the preparation of (138D). The unsaturated acid (134) was difficult to reduce because of its poor solubility in organic solvents. Therefore, it was converted to the unsaturated ester (133) by treatment with thionyl chloride and methanol,¹⁶ or reduced to the unsaturated diol (137). These samples were then hydrogenated under a variety of conditions. The results are outlined in Table 5.3 which also contains the data for the diimide reduction of (134) in ethanol.

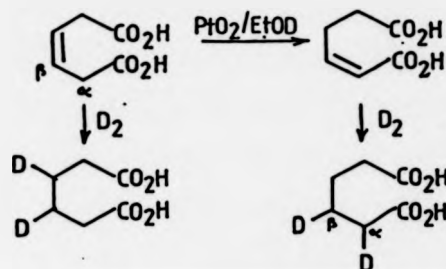
Table 5.3 Hydrogenations of hexa-1,5-diene precursors.

Substrate	Reducing conditions	Comments
	N ₂ H ₂ /EtOH	¹ H NMR indicated very little reduction.
 (133)	Rh[P(Ph ₃) ₃]Cl in toluene	¹ H NMR showed complete reduction.
 (133)	Pd/C/EtOAc	Incomplete reduction. ¹ H NMR showed two olefinic signals and several methyl resonances due to double bond isomerisation.
 (137)	Rh[P(Ph ₃) ₃]Cl in toluene.	¹ H NMR showed incomplete reduction and double bond isomerisation.
 (137)	Pd/C/EtOAc	As above.
 (134)	PtO ₂ /EtOH	¹ H NMR showed complete reduction.

Inspection of the results in Table 5.3 show that double bond migration and slow rates of reduction were a problem in hydrogenations involving Wilkinson's and palladium catalysts. Hydrogenation of (134) with Adam's catalyst in ethanol led to (136H) with no apparent problems, as did Wilkinson's catalyst hydrogenation of (133). However, replacement of hydrogen for deuterium, and product analysis by ²H NMR, showed these two reactions were also plagued by double bond isomerisation. For example, the ²H NMR of (136D) showed a signal integral ratio of 22/78 for the α- and β-deuterons,

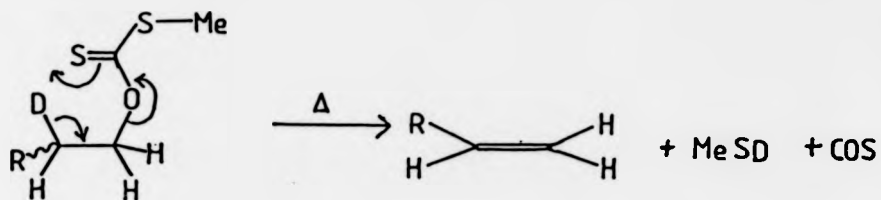
respectively. Although deuterium could have incorporated at the α - and β -positions by exchange, it is more likely to have occurred by the mechanism shown in Scheme 5.21. Similar considerations apply to (135D) synthesised from deuteration of (133).

Scheme 5.21



The presence of deuterium of the α -positions of (136D) or (135D) would lead to hexa-1,5-dienes with deuterium at C2. Since this will be unaffected by the reactions leading to disulphone (see Section 5.3.2., p.175) its presence would not affect the control experiment provided the deuterium content could be qualitatively measured before the elimination step. We have previously noted that the deuterium content of hexa-1,5-dienes, and the chlorosulphides (128D) and (129D), could not be measured quantitatively by mass spectroscopy due to the presence of (M-1) and (M-2) peaks. Consequently, the deuterium content of the hexa-1,5-dienes would have to be determined by measuring the deuterium content of a precursor in its synthesis. This is acceptable provided no deuterium is lost in proceeding from (135D) or (136D) to the diene. However, pyrolysis of (139) is known to occur by syn elimination (Scheme 5.22).¹⁵

Scheme 5.22 R = Alkyl



Therefore, this method could not be used to synthesise samples of (130) of known deuterium content, required for the control experiment. We were eventually able to determine the extent of deuterium wash out in the elimination step of the disulphone synthesis by a less rigorous but logically secure experiment. Photosensitised decomposition of a sample of anti-d₂-DBO, and treatment of the hydrocarbon products with PhSCl led to a mixture of the Markovnikoff and anti-Markovnikoff 1,2-adducts. The reaction mixture was divided into two portions at this point, and each sample carried through the synthesis (Scheme 5.17, p.176), under identical conditions, to the penultimate step. One portion was then treated with sodium acetate in DMSO for 1 hr at room temperature, and the other for 24 hr. If deuterium wash out occurred to any extent in the elimination, the disulphone obtained from the latter reaction would have a much lower deuterium content than the disulphone from the former reaction. If no deuterium wash out occurred, the disulphones would show the same deuterium content. The mass spectrophotometrically determined deuterium content of the two samples are shown in Table 5.4.

Table 5.4 Deuterium content of disulphones obtained under different elimination conditions.

Elimination conditions	Deuterium content ^{a,b}		
	d ₀	d ₁	d ₂
1hr DMSO/NaOAc	4.915	47.847	47.238
24hr DMSO/NaOAc	5.098	47.409	47.493

- a. Uncorrected proportions of d₀-, d₁-, and d₂-disulphones determined by CI/MS.
- b. The values are the average of three separate MS runs, each sample scanned six times in a run.


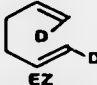
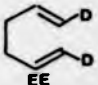
The results in Table 5.4 show that, within experimental error, deuterium is not lost in the elimination reaction. These results can be corrected (See Appendix 5) to give the proportions of EE-, EZ- and ZZ-d₂-dienes formed in the sensitised photolysis. These values are shown in Table 5.5 together with a summary of the earlier results. Also given is the ratio of total E- to total Z-deuterium determined from this analysis.

5.5 Discussion

There are several points to be noted from the results in Table 5.5.

Firstly, the total E- to Z-deuterium ratio measured by chemistry plus MS is qualitatively similar to the ratio determined by ²H NMR (50 ± 3/ 50 ± 3, see p.136). This supports the validity of the analysis.

Table 5.5: Proportions of EE-, EZ- and ZZ-d₂-dienes from photochemical decomposition of anti-d₂-DBO.

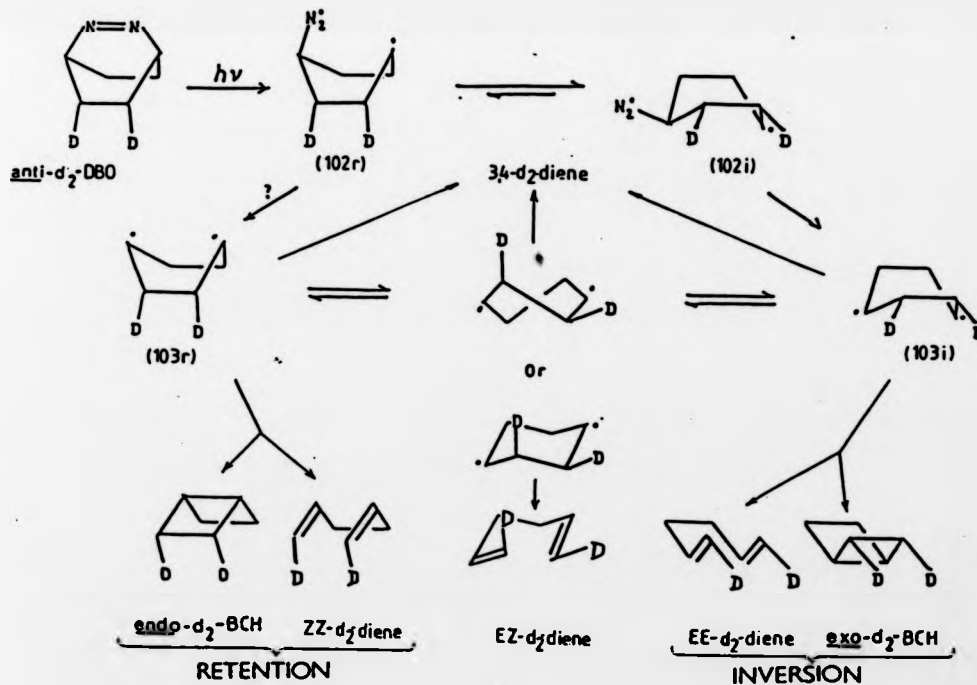
Mode of decomposition	% Proportions ^d			E:Z ratio ^e	
					
Direct	^a Run1	3.5 ± 0.5	84.5 ± 0.5	11.5 ± 1.5	54:46
	^a Run2	4.0 ± 0.5	84.5 ± 0.5	11.0 ± 1.0	53:47
Sensitised	^b Run1	3.5 ± 1.5	80.5 ± 1.5	16.5 ± 0.5	57:43
	^b Run2	9.0 ± 1.0	70.0 ± 2.0	20.5 ± 1.5	55:45
	^c Run3	2.5 ± 0.5	89.5 ± 2.5	8.5 ± 1.5	53:47
	^c Run4	2.5 ± 0.5	89.5 ± 2.5	8.5 ± 1.5	53:47

- From samples of anti-d₂-DBO with identical deuterium content. See Table 5.1.p.180
- From samples of anti-d₂-DBO with different deuterium contents. See Table 5.1.
- From samples of anti-d₂-DBO with $d_0 = 1.156$, $d_1 = 11.089$, $d_2 = 87.797$.
- The errors quoted are explained in the footnote of Table 5.1.
- Values from chemistry plus MS. The ²H NMR value was 50 ± 3%/50 ± 3%.

Secondly, although azoalkanes with different deuterium contents led to product distributions that were quantitatively dissimilar, the qualitative trend was the same for each run. Thus, both direct and sensitised photolyses led to a predominance of the EZ-isotopomer and lesser amounts of the EE- and ZZ-isotopomers. In all cases, the ratio of EE/ZZ isotopomers was > 1 .

The results are most economically rationalised by the mechanism previously discussed relating to the BCH stereochemistry. This is reproduced in Scheme 5.23 including the cleavage products.

Scheme 5.23



Stepwise C-N bond cleavage, conformational inversion of (102r) to the more stable (102i), and loss of nitrogen leads to the inverted boat diyl (103i) (see Section 4.13, p.154). The boat diyl (103r) may arise similarly from (102r) or by back equilibration of (103i). The cleavage stereochemistry requires that (103i) and (103r) predominantly convert to the chair or 90°-twist diyl which ring opens to the EZ-d₂-diene (cf BCH pyrolysis¹). The small amounts of EE- and ZZ-isotopomers arise by cleavage of (103r) and (103i), or their nearby twist conformers. The ratio of EE/ZZ isotopomers suggests that more cleavage occurs from (103i) compared with (103r) (cf the coupling ratio's for (103r) and (103i), Section 4.13, p.154). However, in view of the small amounts that have to be detected (the values shown for the EE- and ZZ-isotopomers are twice the actual amounts formed since 50% of the cleavage product is 3,4-d₂-diene) and the inability to quantitatively assess the affect of secondary KIE's, this conclusion is less precise than any other.

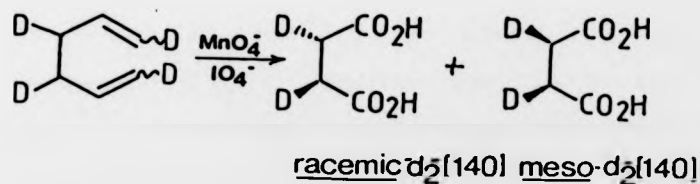
5.6 Comparison of DBO photochemical decomposition with BCH pyrolysis

Pyrolysis of all-exo- d_4 -BCH gives recovered BCH's which contain some endo deuterium.¹ This shows that all-exo- d_4 -BCH can undergo skeletal inversion to all-endo- d_4 -BCH without cleavage to hexa-1,5-diene. Skeletal inversion must involve cleavage of the transannular C-C bond and boat (or nearby twist) conformers of a cyclohexane-1,4-diyl. Cleavage of such diyls would lead to dienes with 1,6-EE or ZZ stereochemistry (see Section 2.4.1). Goldstein and Benzon analysed the product stereochemistry from pyrolysis of all-exo- d_4 -BCH and only detected the EZ diene isotopomer.¹ This suggests that boat diyls can give rise to dienes indirectly via chair or twist conformers, but not directly. A rather surprising result!

We have shown that photochemical decomposition of anti- d_2 -DBO led predominantly to EZ- d_2 -diene and, in contrast to previous reports of BCH pyrolysis, small amounts of EE- and ZZ-isotopomers. The results were rationalised in terms of cleavage from cyclohexane-1,4-diyls (see Section 2.4.1). If BCH pyrolysis involves similar diyl intermediates, EE- and ZZ-isotopomers would be expected from cleavage of deuterated BCH's.

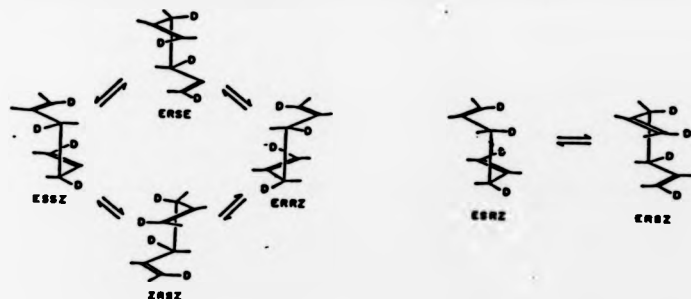
Goldstein and Benzon's stereochemical analysis involved conversion of d_4 -dienes to d_2 -succinic acids (140) by permanganate-periodate oxidation (Scheme 5.24).

Scheme 5.24



Thus, treatment of d_4 -dienes obtained from pyrolysis of exo- d_4 -BCH were oxidised to d_2 -(140). In a parallel experiment isolated d_4 -dienes were heated at 233° for 48 hrs (22 half-lives of a Cope rearrangement).⁸ The two samples of d_2 -(140) were analysed by IR since it was known that racemic and meso isomers could be distinguished.¹⁷ The IR analysis suggested that exclusively meso- d_2 -(140) was obtained from both experiments.¹ Inspection of Scheme 5.25 shows that the Cope rearrangement will equilibrate ESSZ-, ERSE-, ERRZ-, and ZRSZ- d_4 -dienes, assuming it proceeds through a chair transition state (Scheme 5.25).

Scheme 5.25 (from ref. 1)



Permanganate-periodate oxidation of ESSZ-, ERSE-, ERRZ-, and ZRSZ- d_4 -dienes would lead to a mixture of racemic- and meso- d_2 -(140). The observation that meso- d_2 -(140) was formed exclusively from d_4 -dienes before and after equilibration at 233° required that the products of exo- d_4 -BCH pyrolysis were the ERSZ-ESRZ enantiomers since these would be unaffected by such treatment.¹

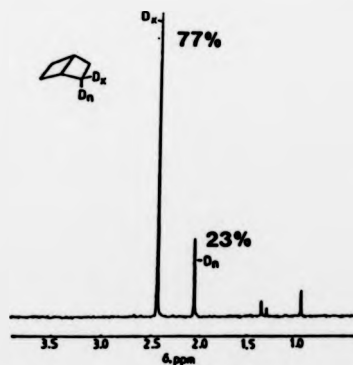
The use of IR spectroscopy makes the succinic acid stereochemical analysis less sensitive than our disulphone technique so small amounts of EE- and ZZ- isotopomers would have been barely

detectable. Thus, in order to compare BCH pyrolysis and DBO photolysis more precisely, we re-investigated the pyrolysis and analysed the diene stereochemistry using our disulphone approach.

5.6.1 Preparation of stereoselectively labelled d_2 -BCH

It was previously noted that samples of d_2 -BCH could be obtained from d_2 -DBO photosylates by a chemical method combined with column chromatography (see Section 5.2.2.2). As direct photochemical decomposition of anti- d_2 -DBO leads to d_2 -BCH's in which the deuterium is predominantly exo (ie double inversion of configuration) stereoselectively labelled samples of d_2 -BCH could be obtained as solutions in n-pentane (see experimental for details). Figure 5.4 shows the ^2H NMR of a sample of d_2 -BCH obtained from this procedure with the expected predominance of exo deuterium.

Figure 5.4 ^2H NMR of d_2 -BCH isolated from direct photolysis of anti- d_2 -DBO



- a. The ratio (77/23) is slightly lower than expected (82/18) probably due to lower stereoselectivity in the azo compound.

A second sample was prepared and gave reproducible results. Isolation of a sample of d_2 -BCH from sensitised photolysis of anti- d_2 -DBO shows an exo/endo deuterium ratio of 58/42 in accord with the results in Table 4.5, p.136.

5.6.2 Pyrolysis of d_2 -BCH

Two samples of d_2 -BCH, obtained from direct photolyses of anti- d_2 -DBO, were pyrolysed at 180° for 20 hrs (10 half-lives of the cleavage reaction)¹. The Cope rearrangement of hexa-1,5-diene is negligibly slow under these conditions which is important since it involves an equilibrium isotope effect of 1.2^8 (see Section 5.2.2.2, p168) and would cause errors in the disulphone stereochemical analysis (see Appendix 5). The 2H NMR's of the samples after pyrolysis showed equal proportions of allylic and total olefinic deuterium and, within experimental error, an E/Z ratio of 1 (see Figure 5.2, p168). Both pyrolysis samples were then subjected to the disulphone stereochemical analysis. The proportions of EE-, EZ- and ZZ- d_2 -diene obtained after appropriate correction (See Appendix 5) are shown in Table 5.6.

Table 5.6 Proportions of EE-, EZ- and ZZ-d₂-dienes from pyrolysis of d₂-BCH.

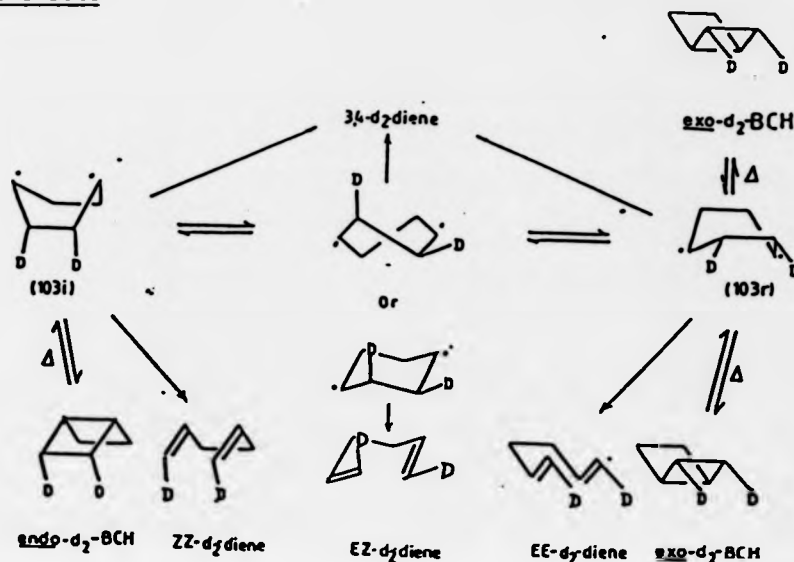
BCH sample <u>exo/endo</u>	% d ₂ -diene proportions ^c			E/Z ^d ratio
	ZZ	EZ	EE	
75/25 ^a	3.5 ± 0.5	78.5 ± 2.5	18 ± 2.0	55/45
77/23 ^b	4.0	82.5 ± 1.5	13.5 ± 1.5	55/45

- a. From sample of precursor (90D) with $d_0 = 0.736$, $d_1 = 15.675$, $d_2 = 83.589$.
- b. From sample of (90D) with $d_0 = 0.031$, $d_1 = 5.960$, $d_2 = 94.279$.
- c. Average of two MS runs. Computed identically to the example given in Appendix 5.
- d. The ²H NMR ratio is $50 \pm 3/50 \pm 3$.

5.6.3 Discussion

Inspection of the results in Table 5.6 shows that pyrolysis of d₂-BCH with predominantly exo deuterium led to EZ-d₂-diene as the major product, and the EE- and ZZ-isotopomers as minor products. Note that the minor products were not detected in Goldstein and Benzon's succinic acid analysis of deuterium labelled BCH.¹ The results also show an EE/ZZ ratio > 1. The observations can be rationalised by a mechanism involving conformations of a cyclohexane-1,4-diyl (Scheme 5.26).

Scheme 5.26



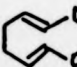


Exo- d_2 -BCH ring opens to give a boat (or nearby twist) diyl with retained configuration (103r). This can cleave to the EE- d_2 -diene or convert to the more stable chair or 90° -twist diyls. These predominantly ring open to yield the EZ- d_2 -diene as major product. The chair or 90° -twist diyl must convert to the boat diyls ((103r) and (103i)) as incomplete pyrolysis showed BCH exo/endo isomerisation occurred.¹ The ZZ- d_2 -diene can arise similarly from endo- d_2 -diene or by equilibration of (103r). Since the EE/ZZ ratio is > 1 and the d_2 -BCH was predominantly exo, the pyrolysis appears to proceed with overall retention of stereochemistry. This implies that the first-formed boat diyl from d_2 -BCH shows some cleavage before complete conformational equilibration. However, in view of the small amounts of EE- and ZZ- d_2 -dienes that have to be detected (the values shown for these compounds are twice the actual amounts since 50% of the cleavage product is the 3,4- d_2 -diene) this conclusion is less precise than any other (cf Section 5.5, p189).

5.6.4 BCH pyrolysis and DBO photolysis. Common biradical intermediates

The stereochemical study of d_2 -BCH pyrolysis has shown that small amounts of EE- and ZZ- d_2 -dienes were produced, in contrast to the studies of Goldstein and Benzon.¹ This suggested that the first-formed boat diyls can cleave, as well as convert to the chair or 90°-twist diyl. Near identical results were observed in the photochemical decomposition of d_2 -DBO. Table 5.7 summarises our stereochemical results for cleavage of d_2 -BCH and photochemical decomposition of d_2 -DBO.

Table 5.7 Comparison of d_2 -BCH and d_2 -DBO cleavage stereochemistries

Precursor	Mode of decomposition	% Products		
				
DBO ^a	hv(D) Run 1	4	84	12
	Run 2	4	85	11
	hv(S) Run 1	4	80	16
	Run 2	9	70	21
	Run 3 ^c	2	89	9
BCH ^b	Δ Run 1	4	79	18
	Run 2	4	82	13

a See Table 5.1.

b See Table 5.6.

c Average of runs 3 and 4, Table 5.4.

The near identity of product distributions from both precursors is evidence that the two reactions occur on the same (or very similar) diyl potential energy surface.

5.6.5 The cyclohexane-1,4-diyl potential energy surface

Our stereochemical studies have shown that both photochemical decomposition of d_2 -DBO and pyrolysis of d_2 -BCH lead predominantly to EZ- d_2 -diene with lesser amounts of EE- and ZZ- isotopomers. This suggested that both reactions occur on the same C-6 potential energy surface, the major product arising from cleavage of a chair or 90° -twist diyl and the minor products from cleavage of boat diyls. To understand why cleavage is more favoured from chair or 90° -twist diyls than boat diyls, through-space and through-bond interactions of the radical centres have to be considered.

5.6.5.1. Through-bond and through-space interactions in biradicals

Since Hoffman *et al* introduced the dissection of interactions between orbitals into TS and TB interactions, a number of chemical consequences have been discussed.¹⁸ This concept can be used to explain why chair or 90° -twist diyls cleave more readily than boat diyls, and why the latter preferentially couple.

Pyrolysis of BCH leads to fission of the central C-C bond and formation of a species (141) containing two electrons (spins paired) in degenerate atomic orbitals (ϕ_A and ϕ_B). The singly occupied atomic orbitals can interact directly across space (TS) or hyperconjugatively via the intervening σ -bonds (TB);

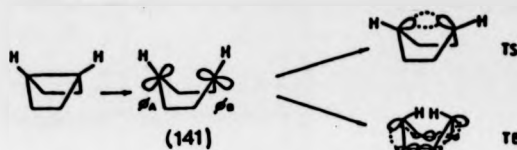
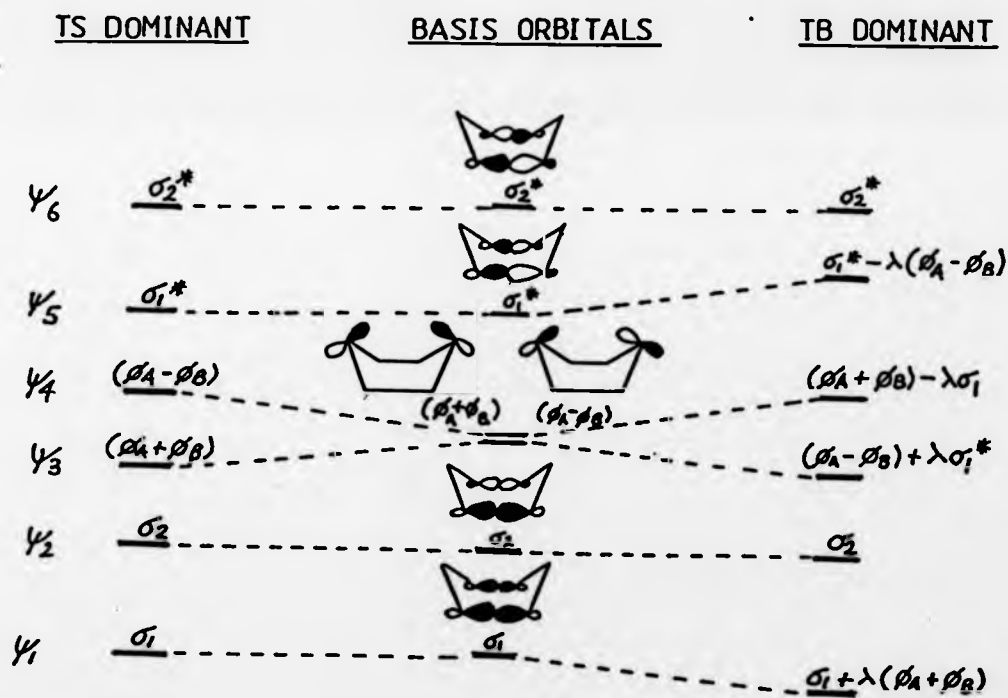


Figure 5.5 shows the orbital interaction diagram for the boat diyl in which the symmetric combination of atomic orbitals lies below the antisymmetric if TS interactions are dominant, and the reverse effect if TB interactions are dominant.

Figure 5.5 TB and TS interactions in a boat cyclohexane-1,4-diyl.

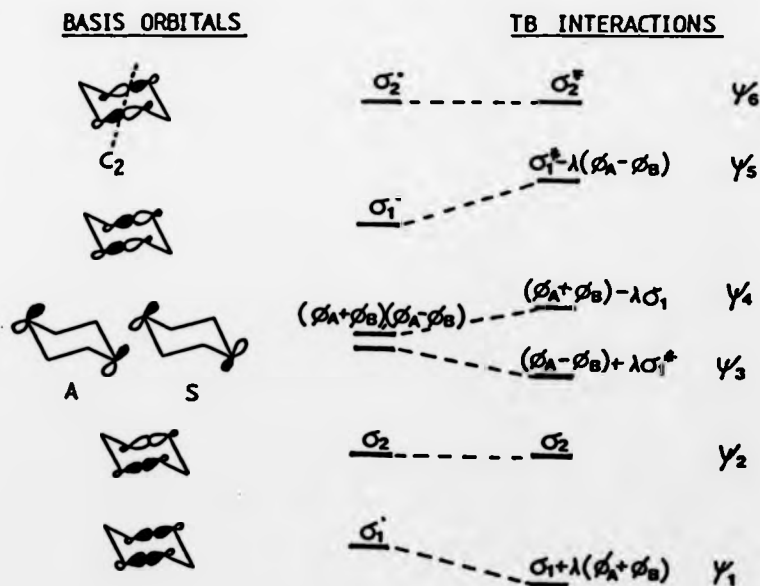


The relevant symmetry is a mirror plane dissecting C_2-C_3, C_5-C_6 .

It can be seen that if TS interactions are dominant, the HOMO (ψ_3) is 1,4-bonding and so should preferentially couple. If TB interactions are dominant, the HOMO is 1,4 anti-bonding and also has σ^* character. Thus, it should preferentially cleave. The boat diyl represents the extreme case of TS interactions and thus it couples in preference to cleaving. This is supported by Dewar *et al.*'s MINDO/3 calculations¹⁹ in which the calculated geometry of the boat diyls shows a pyrimidalisation at the radical centres which further increases the TS interaction.

If the boat diyl undergoes a pseudorotation which removes the TS interaction (i.e. conversion to a chair or 90°-twist diyl) TB interactions should become dominant. Figure 5.6 shows the orbital interaction diagram in which TB interactions are dominant.

Figure 5.6 TB interactions in a chair diyl.^a



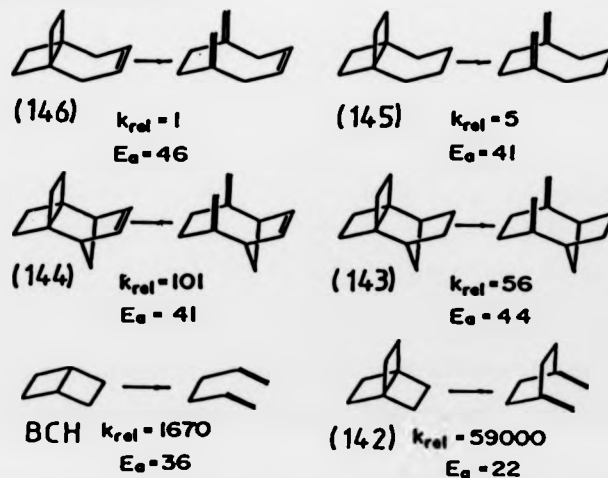
^a The symmetry is relative the C₂ axis

In this case the HOMO (ψ_3) has zero-bonding between C1-C4 and has σ^* character at C2-C3. Thus, it cleaves readily. Similar effects apply to the 90° -twist as in Figure 5.6. The distortions of radical centres calculated by Dewar *et al.*'s MINDO/3 studies increase the TB interactions for the chair and 90° -twist diyls making cleavage very favourable.¹⁹

The TS and TB interactions discussed also apply to the biradical generated photochemically. However, the differences in electron distribution between S_0 and S_1 biradicals can affect cleavage/coupling ratio's (see Chapter 6).

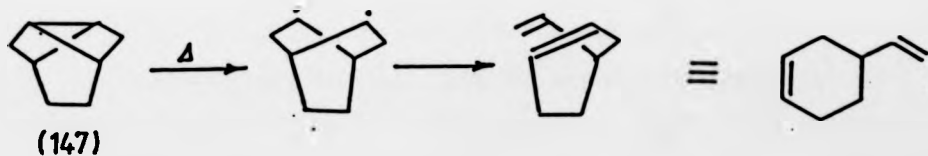
The discussion of TS and TB interactions in cyclohexane-1,4-diyls suggests that zero-bonding between C1-C4 must be achieved for facile cleavage. In BCH this can readily be achieved by twisting or conversion to a chair conformer. If bridges are incorporated into the BCH system this should interfere with the achievement of the zero-bonded conformer, so the activation energy should rise so it is greater than that for cleavage of BCH. Wiberg *et al.*²⁰ have studied the series of [n.2.2] propellanes shown in Scheme 5.27.

Scheme 5.27 (from ref. 20)



Inspection of Scheme 5.27 shows that systems in which conformational flexibility is restricted have greater activation energies than the parent system (ie (143) \rightarrow (146)) and must involve cleavage from biradicals in boat (or nearby twist) conformations). The increase in activation energies from BCH \rightarrow (146) are not ground state effects as all the tricyclic compounds are less strained than BCH.²⁰ The facile cleavage of the [2.2.2] propellane (142), which would also be restricted from forming a 1,4-zero-bonded conformer, is probably a ground state effect as replacing the six-membered ring in the tricyclic compounds for the four-membered ring increases the strain energy above that of BCH.²⁰ An interesting example of a diyl conformationally restricted from forming a 1,4-zero-bonded conformer was reported by Kaufmann and de Meijère.²¹ They found that cleavage of nortwistbrendane (147) has an activation energy 14.6 kcal mol⁻¹ higher than that of BCH. It was suggested that cleavage of the central C-C bond led to a 1,4-diyl geometrically constrained from cleaving from any other conformation than the 90°-twist (Scheme 5.28).²¹

Scheme 5.28



The higher activation energy compared with BCH was suggested to be evidence that the latter reaction involves the chair diyl.²¹ However, inspection of Dreiding models reveals that the first formed conformer is the 30°-twist, not the 90°-twist. The 30°-twist is not a

favourable conformer for cleavage as the orbitals at the radical centres are not well situated for TB interactions with the edge bonds. Furthermore, it is not certain that the higher activation energy of (147) compared to BCH is not a ground state effect since the strain energy of (147) is unknown.

5.6.5.2 Stereoselective cleavage; Chair or 90°-twist diyl intermediates

Our stereochemical studies suggest that pyrolysis of BCH and photochemical decomposition of DBO occur on the same C-6 potential energy surface. Thus, both reactions involve small amounts of cleavage from boat (or nearby twist) diyl conformers with most of the cleavage arising from chair or 90°-twist diyls. Cleavage of the latter conformers is more favoured than the boat conformers due to interactions of the radical centres with the edge-bonds. The exo and endo disubstituted boat diyls must be interconvertible since skeletal inversion is known in exo-d₄-BCH¹ and anti-d₂-DBO gives both exo and endo-d₂-BCH. The question arises whether cleavage and/or conformational equilibration, occur from a chair or 90°-twist diyl.

If the diyl shows the same conformational preferences as cyclohexane (as the Gaussian 80 at STO-3G level calculations of Lloyd et al²² suggest) the 90°-twist diyl is the energetically preferred species linking the boat diyls. This is apparent on inspection of Figure 2.1, p.69. Conversion of a boat to a chair cyclohexane conformation requires 5-6 kcal mol⁻¹. As the chair conformer is thermodynamically preferred, the reverse process (chair → boat) requires an E_a of some 10-11 kcal mol⁻¹. Thus, for boat-chair-boat equilibration, a cyclohexane-1,4-diyl would have to lie in a potential energy minimum of 10-11 kcal mol⁻¹. This is much deeper than the minimum estimated

thermokinetically for a chair diyl in BCH pyrolysis (see Section 5.8.1.). Interconversion of boat conformations through twist conformations, on the other hand, requires only 1-2 kcal mol⁻¹.

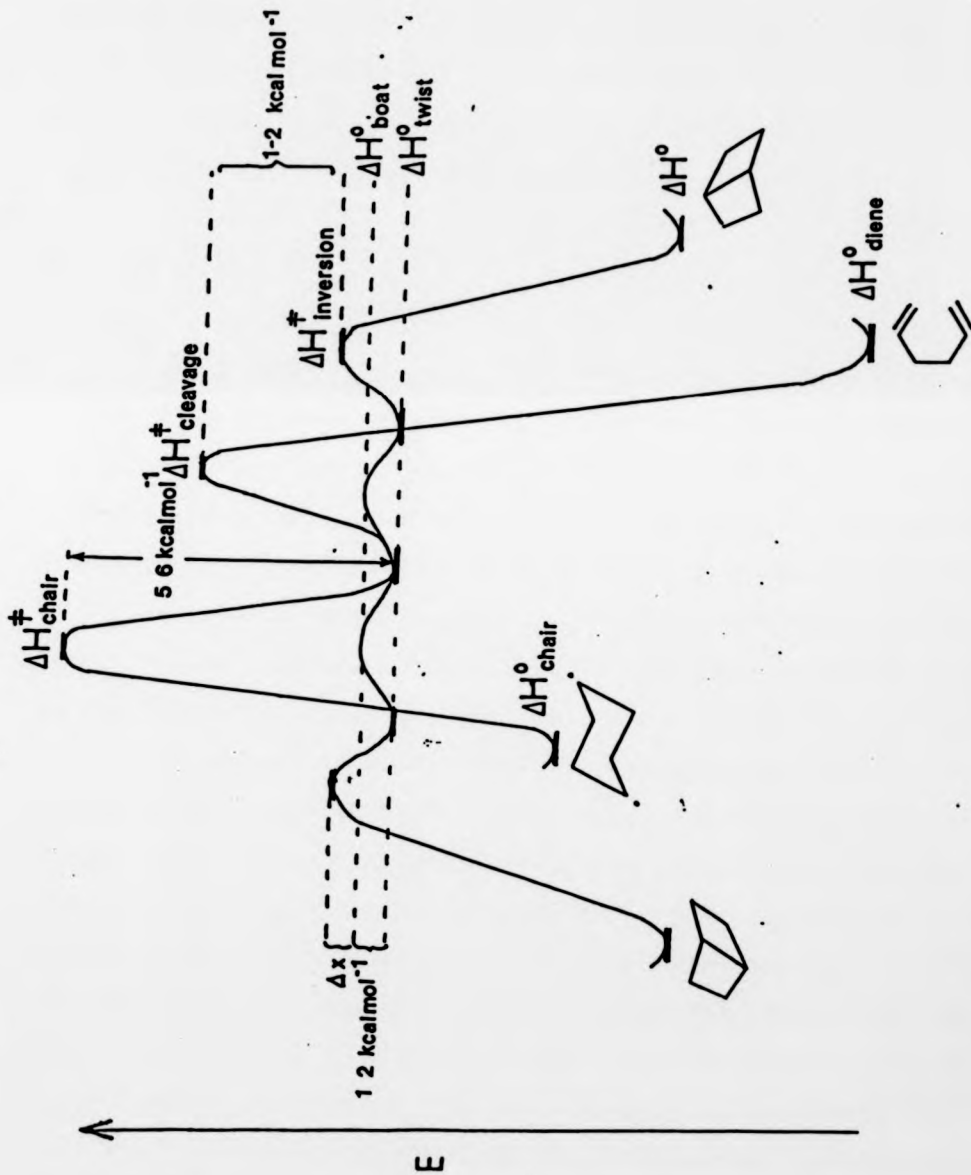
A combination of our stereochemical studies with energetic considerations, suggest that a chair diyl is inaccessible in BCH pyrolysis and photochemical decomposition of DBO. The argument assumes that;

- (a) BCH pyrolysis and DBO photolysis occur on the same C-6 potential energy surface.
- (b) Cyclohexane-1,4-diyl and cyclohexane show the same conformational preferences.

It is known from Goldstein and Benzon's kinetic study¹ of BCH pyrolysis that $\Delta H^\ddagger_{\text{cleavage}} - \Delta H^\ddagger_{\text{inversion}}$ is ca 1-2 kcal mol⁻¹. From assumption (b) and Figure 2.1, p.69, we also have;

- (a) $\Delta H^\circ_{\text{twist}} \rightarrow \Delta H^\circ_{\text{boat}} \approx 1-2 \text{ kcal mol}^{-1}$.
- (b) $\Delta H^\ddagger_{\text{chair}}$ (i.e. the energy required to convert a twist conformer to a chair conformer) $\approx 5-6 \text{ kcal mol}^{-1}$.

Photochemical decomposition of DBO leads to BCH with predominant double inversion of stereochemistry. Thus, the energy of the transition state for ring closure ($\Delta H^\ddagger_{\text{inversion}}$) must be only slightly higher than $\Delta H^\circ_{\text{boat}}$ otherwise the BCH stereochemistry would be random. Since the energy of the cleavage transition state ($\Delta H^\ddagger_{\text{cleavage}}$) is 1-2 kcal mol⁻¹ above $\Delta H^\ddagger_{\text{inversion}}$, the chair diyl appears to be energetically inaccessible. This implies that the 90°-twist diyl is the reactive conformer for cleavage. These points are summarised in the energy diagram of Figure 5.7.

Figure 5.7 C_6H_{10} potential energy surface

NB $\Delta H_{inversion}$ is only slightly higher than ΔH_{boat}° (Δx is small)

The assumption that the two reactions occur on the same C6 potential energy surface appears to be valid since both reactions lead to near identical hexa-1,5-diene product distributions. Although there is theoretical support that the diyl shows the same conformational preferences to cyclohexane, the argument summarised in Figure 5.7 is based on small energy differences. Thus, although a 90°-twist diyl appears the energetically favoured intermediate for cleavage, the chair diyl cannot be unambiguously dismissed.

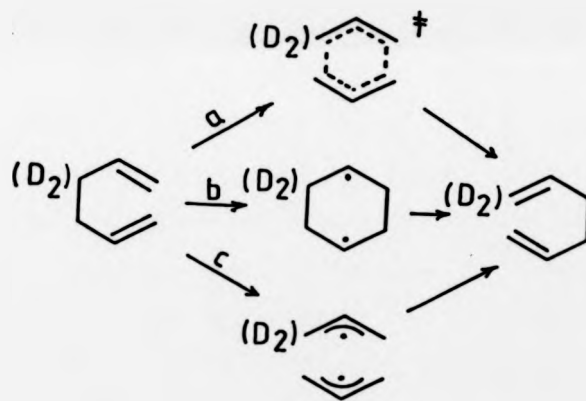
5.7 Summary

In this chapter we have shown that direct and sensitised photochemical decomposition of anti-d₂-DBO leads predominantly to EZ-d₂-diene. The result was rationalised in terms of an intermediate cyclohexane-1,4-diyl which cleaves from a chair or 90°-twist conformation. Significant amounts of EE- and ZZ-d₂-dienes were formed in the decomposition which demonstrated that boat diyl conformers can cleave as well as couple to BCH's. Both the cleavage stereochemistry and the coupling stereochemistry were rationalised by the same mechanistic scheme. We also studied the cleavage stereochemistry of d₂-BCH pyrolysis and found it to be nearly identical to that of d₂-DBO. Thus, BCH pyrolysis does not lead exclusively to EZ-d₂-diene as reported. The near identity of product distributions suggests both reactions occur on the same C6 potential energy surface. This conclusion was also consistent with our cleavage KIE studies. It was found that both BCH pyrolysis and photochemical decomposition of d₂-DBO gave hexa-1,5-dienes with no detectable intramolecular KIE. This result was permissive evidence for a common diyl intermediate that cleaves via an "early" transition state.

5.8 The Cope rearrangement of hexa-1,5-diene

The mechanism of the Cope rearrangement has been subject to intense investigation.²³ In addition to a concerted 3,3-sigmatropic shift mechanism there are two possible non-concerted mechanisms. One involves σ -bond cleavage to afford two allyl radicals and the other involves σ -bond formation to involve a cyclohexane-1,4-diyl (Scheme 5.29).

Scheme 5.29



The mechanism involving initial σ -bond cleavage and then recombination of two allyl radicals (path c) can be dismissed on the basis of thermokinetic arguments (see Section 1.4.4., p.35). Distinction between the other possible mechanisms, a concerted 3,3-sigmatropic shift (path a) and initial σ -bond formation and then cleavage of an intermediate cyclohexane-1,4-diyl (path b) is much less straightforward. It is important to consider which mechanism is

involved in this study because if a diyl is involved its properties should be related to BCH pyrolysis and photochemical decomposition of DBO.

5.8.1 Concerted versus stepwise mechanisms. Thermokinetic Studies

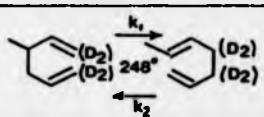
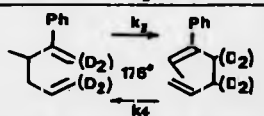
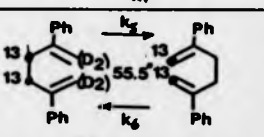
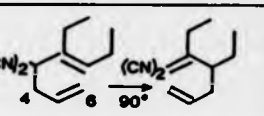
Stereochemical studies have firmly established that a Cope rearrangement requires a chair-like arrangement of six carbons in the lowest energy pathway.²³ In principle it should be possible to distinguish between the mechanistic alternatives on the basis of thermokinetic arguments. Doering originally estimated ΔH_f^\ddagger of the chair diyl for the parent system to be 38 kcal mol⁻¹ above hexa-1,5-diene and 3.5 kcal mol⁻¹ below the energy of the concerted transition state.⁸ The estimated value for ΔH_f° chair diyl was also below the transition state enthalpies for BCH skeletal inversion and cleavage, implying both reactions could involve a common diyl intermediate. Using the updated values for ΔH_f° (CH₃)₂CH[•] raised the estimated value for ΔH_f° chair diyl to 6-7 kcal mol⁻¹ above the Cope transition state, but still an energetically acceptable intermediate in BCH pyrolysis.² This was the first indication that BCH pyrolysis and the Cope rearrangement of hexa-1,5-diene do not share a similar potential energy surface. Considering the usual uncertainties in thermokinetic arguments the chair diyl was still energetically accessible in the Cope rearrangement. Using Tsang's most recent value for ΔH_f° chair diyl²⁴ the biradical appears to be energetically inaccessible as it is 10-11 kcal mol above the energy of the Cope transition state. However, using this most recent value for ΔH_f° chair diyl renders its involvement in BCH pyrolysis uncertain as it becomes nearly iso-energetic with the transition states for cleavage

and skeletal inversion. Clearly, thermokinetic arguments are unable to unambiguously establish the mechanism of the Cope rearrangement.

5.8.2 Concerted versus stepwise mechanisms. Use of secondary KIE's to locate transition states

In the Cope rearrangement one σ -bond is broken and a new one is formed. Secondary KIE's on each bond change should be independent. For example, deuterium substitution at the terminal carbons should not affect cleavage of C3-C4. The secondary KIE's would be expected to relate to the extent of bond making or bond breaking in the reaction transition state. The inverse KIE's resulting from deuterium substitution at the terminal carbons of various hexa-1,5-diene derivatives have been measured and compared with the normal KIE's resulting from substitution at the internal carbons of the same dienes (Table 5.8).^{22,24}

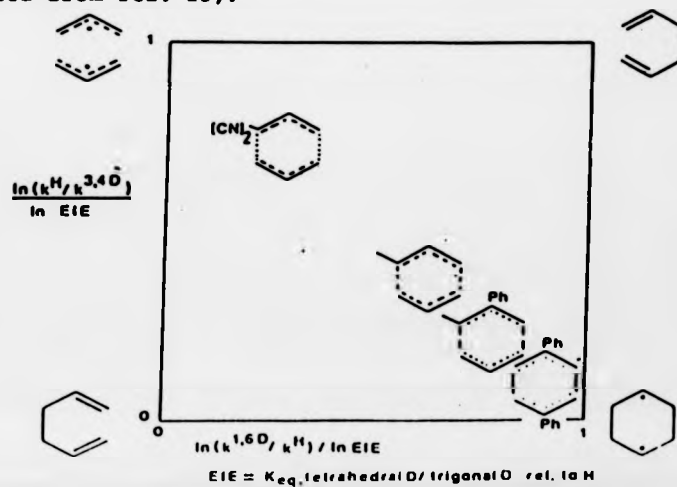
Table 5.8: Secondary KIE's in the Cope rearrangement of various 1,5-dienes (modified from refs. 22 and 24).

Hexa-1,5-diene derivative	KIE	
	BM ^a	BB ^b
	$\frac{k_1^{D_4}}{k_1^H} = 1.13$	$\frac{k_2^H}{k_2^{D_4}} = 1.07$
	$\frac{k_3^{D_4}}{k_3^H} = 1.30$	$\frac{k_4^H}{k_4^{D_4}} = 1.09$
	$\frac{k_5^{D_4}}{k_5^H} = 1.57$	$\frac{k_6^H}{k_6^{D_4}} = 1.07$
	$\frac{k_7^{6-D_2}}{k_7^H} = 1.06$	$\frac{k_8^H}{k_8^{4-O_2}} = 1.19$

^a Bond making KIE
^b Bond breaking KIE

Inspection of the data in Table 5.8 shows that the KIE's vary dramatically with substitution suggesting the transition state also changes with substitution. Gajewski *et al*^{23,25} have depicted the range of transition states occurring in these Cope rearrangements with a More O'Ferrall-Jencks diagram (Figure 5.8). This two-dimensional reaction co-ordinate has structural co-ordinates connecting the reactant and product to the non-concerted extremes (*i.e.* two allyl radicals and a cyclohexane-1,4-diy1). Ideally, the structural co-ordinates would be the bond orders or bond lengths of the various transition states. However, such values have not been measured. The structural co-ordinate used was the ratio of the BMKIE or BBKIE to the equilibrium isotope effect (EIE).²³ These values were experimentally accessible and meaningful since the KIE's result only from some bonding change at the reacting centre and represent some fractional change in bonding relative to the complete change that the EIE represents. The EIE's for the systems shown in Table 5.8 were measured and, together with KIE's, enabled representation of the reaction transition state structures (Figure 5.8).

Figure 5.8 More O'Ferrall-Jencks diagram representing the range of transition states in the Cope rearrangement of various 1,5-dienes (modified from ref. 23).



All the transition states represented in Figure 5.8 lie on the diagonal connecting the two biradical extremes (ie the transition states are symmetrical and have equal C1-C6 and C3-C4 bond orders). the parent system could not be placed on the diagram as measurement of deuterium KIE's would require a further isotopic label. However, Gajewski et al^{23,25} noted that the transition state for the parent system would be very similar to that of the monomethyl derivative. Assuming that the relationship between bond order and KIE's is linear they suggested the parent system would have ca two-thirds of a bond between C1-C6 and two-thirds of a bond between C3-C4. The 3,3-dicyano derivative, on the other hand, has a transition state that resembles two allyl radicals, while increasing phenyl substitution at C2 and C5 leads to a tight (diyl-like) transition state^{23,25}. The tight transition states of the mono- and diphenyl substituted hexa-1,5-dienes explains why there is a constant multiplicative experimental rate increase for their Cope rearrangements.

5.8.3 Summary

Thermokinetic arguments using updated values for ΔH_f° chair diyl suggest that a Cope rearrangement proceeds via a concerted mechanism. This has been confirmed by Gajewski et al^{23,25} who found that the parent (unsubstituted) system is only partially bonded between C3-C4 and C1-C6. This conclusion has theoretical support. Although Dewar's MINDO/3 calculations suggest that cyclohexane-1,4-diyl is a common intermediate in both BCH pyrolysis and the Cope rearrangement of hexa-1,5-diene¹⁹, higher level calculations by Borden et al (MCSCF with 3-21G basis sets) have provided strong computational evidence

that the Cope rearrangement follows the concerted path.²⁶ Since it is well established that pyrolysis of BCH and photochemical decomposition of DBO occur via biradical mechanisms, the Cope rearrangement can not occur on the same C6 potential energy surface.

CHAPTER 6

6.1 Introduction

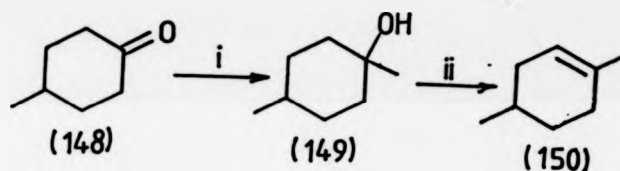
The ^2H NMR spectra of products from direct photochemical decomposition of $\text{d}_2\text{-DBO}$ and $\text{d}_2\text{-DMDBO}$ contained resonances that were attributed to cyclohexene. This conclusion was based on the fact that the ^2H NMR resonances were very similar to the ^1H NMR resonances of authentic material. The cyclohexenes are envisaged to arise from a hydrogen (or deuterium) shift in an intermediate cyclohexane-1,4-diyl. In this chapter we give further evidence for the involvement of cyclohexenes in the direct photochemical decomposition of DBO's and their occurrence in other reactions involving cyclohexane-1,4-diyls. We also discuss the stereochemistry of cyclohexene formation and the mechanistic significance thereof.

6.2 Occurrence of cyclohexenes

To establish whether cyclohexenes are formed in decompositions of DBO's and pyrolysis of BCH's they should, ideally, be isolated and their spectral and chromatographic properties compared to authentic material. Gas chromatographic studies of the parent cyclohexene established that it had identical retention times to that of BCH even on capillary columns. Consequently, it could not be isolated from photolysis or pyrolysis mixtures. Thus, the only direct evidence for its occurrence in decomposition of DBO and pyrolysis of BCH was the NMR spectral characteristics. For the dimethyl derivatives, the only possible cyclohexene product from a hydrogen (or deuterium) shift in an intermediate diyl is 1,4-dimethylcyclohex-1-ene (150). This had

different gas chromatographic properties to DMBCH and 2,5-dimethylhexa-1,5-diene and so could be isolated from such hydrocarbon product mixtures by prep. g.c. Comparison of the spectral and chromatographic properties of isolated (150) with a sample independently synthesised (as shown in Scheme 6.1¹) enabled us to establish the occurrence of (150) in DMBCH pyrolysis and decomposition of DMDBO.

Scheme 6.1



i) MeLi, Et₂O. ii) POCl₃, C₆H₅N.

6.2.1 Direct photochemical decomposition of DMDBO and DBO

Samples of DMDBO (1% solutions in n-pentane) were photolysed and the products analysed by gas chromatography. The minor product (< 10% of total hydrocarbon mixture from chromatograph signal integrals) was isolated by prep. g.c. Its ¹H NMR and gas chromatographic properties were identical to samples of (150) independently synthesised. Direct photolysis of d₂-DBO samples (1% solution in n-pentane) and analysis of the hydrocarbon products by ²H NMR suggested cyclohexene was formed (see Section 4.3). As it is firmly established that (150) is produced in the photochemical decomposition of DMDBO this suggestion is confirmed.

6.2.2 Photosensitised decomposition of DMDBO and DBO

Photosensitised decomposition of d_2 -DBO and d_2 -DMDBO and subsequent analysis of the hydrocarbon products by 2H NMR only showed the signals assigned to DMBCH and the diene (see Figure 4.7, p.135 and Figure 4.15). Gas chromatographic analysis of product mixtures from the decomposition of DMDBO confirmed that cyclohexenes were not formed in these reactions.

6.2.3 Pyrolysis reactions

The pyrolysis of d_2 -BCH was discussed in Section 5.6.1., p195. Inspection of the pyrolysed solution's 2H NMR (Figure 5.2, p168) shows that hexa-1,5-dienes are the only products. We showed that (150) was not formed in the decomposition of DMBCH by pyrolysing samples in sealed tubes (1% solutions in n-pentane, 170° for 8 hr ca 4 half-lives of the cleavage reaction)² and analysis of the products by gas chromatography. The analysis showed ca 96% diene, 4% DMBCH, (150) being absent. Control experiments showed that if (150) had been formed it would have survived the pyrolysis conditions.

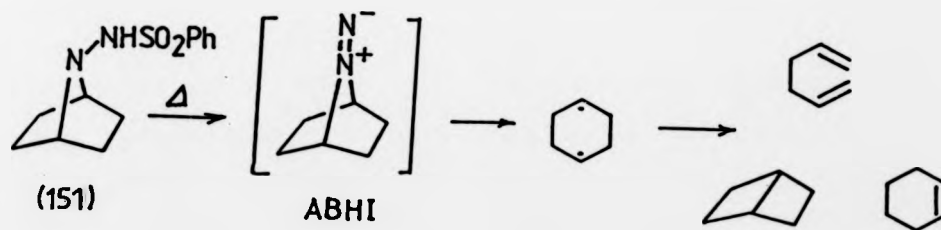
For completeness we also pyrolysed samples of DMDBO and DBO. DMDBO samples were pyrolysed for 2.5 hr at 240° (ca 10 half-lives of the decomposition reaction)³ and the products analysed by gas chromatography. The major product was the diene but trace amounts of DMBCH were also present. Samples of (150) were not detected although control experiments showed they would have survived the pyrolysis conditions. To confirm that cyclohexenes were not formed in the pyrolysis of DBO we pyrolysed d_2 -DBO (25 mg samples in 1% solutions of n-pentane) at 230° for 17 hr (ca 5 half-lives of the decomposition

reaction).³ Analysis of the pyrolysed solution by ²H NMR showed hexa-1,5-diene was the only product. Control experiments showed that if cyclohexene had been formed it would have survived the pyrolysis conditions.

6.3 Discussion

Cyclohexene has not been reported as a product from DBO but from the isomeric 7-azabicyclo[2.2.1]heptane N-imide (ABHI). This 1,1-diazene is the proposed intermediate from the thermal decomposition of the benzene sulphonamide derivative (151) of N-amino-7-azabicyclo[2.2.1]heptane.⁴ Thermal decomposition of the presumed intermediate (ABHI) leads to hexa-1,5-diene, BCH, and cyclohexene, consistent with (though not proof of) the intermediacy of a cyclohexane-1,4-diyl (Scheme 6.2).⁴

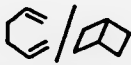
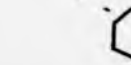
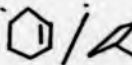

Scheme 6.2



The results in Section 6.2 suggest that cyclohexenes are formed in direct photochemical decomposition of DBO, but not sensitised decomposition or pyrolysis of BCH (ie the reactions lead to different product distributions). The results may seem surprising since all the

reactions appear to involve similar cyclohexane-1,4-diyyl intermediates. The difference between product distributions from direct and sensitised photolysis can be attributed to a SCE. More surprising is the difference between direct photolysis and BCH pyrolysis since both are nominally singlet processes. This is also true for the thermal decomposition of ABHI although this decomposition does lead to cyclohexenes. Table 6.1 compares the product ratio's formed from ABHI with those from direct photolysis of DBO and illustrates the difference in cleavage/coupling ratio's.

Table 6.1 Product ratio's from DBO and ABHI

Precursor	Decomposition mode, temp.	Product ratio's	
		 / 	 / 
DBO	hr (D), 25°	1.38 ^b	-
ABHI ^a	B, 25°	3.17 ^c	0.042 ^c
	,120°	3.04 ^c	0.125 ^c

a assumed intermediate from decomposition of (151) in diglyme with BuⁿOCH₂CH₂ONa at the temperature stated.

b calculated from ref. 5


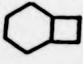

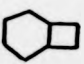
c calculated from ref. 4.

Another interesting feature of the results in Table 6.1 is the effect of temperature on ABHI decomposition. The results show that the proportion of cyclohexene from ABHI increases with increasing

temperature. Assuming this reaction does involve a cyclohexane-1,4-diyl intermediate, we would expect pyrolysis of BCH (and thermolysis of DBO) to lead to more cyclohexene than the other nominally singlet process, direct photolysis. Since this is the reverse of what we observe, formation of cyclohexenes can not be due to a temperature effect.

Similar differences in product distributions from two nominally singlet processes have been observed by Samuel in the thermal and direct photochemical decomposition of DBD.⁶ The product ratio's for the decompositions are shown in Table 6.2.

Table 6.2 Product ratio's from DBD decomposition

DBD Decomposition conditions	Products, ratio's	
	 / 	 / 
Δ , 30° ^a	0.981 ± 0.064	0.551 ± 0.042
hv, direct ^b	4.751 ± 0.030	0.300 ± 0.003

a Extrapolated from higher temperatures

b Estimated 30°.

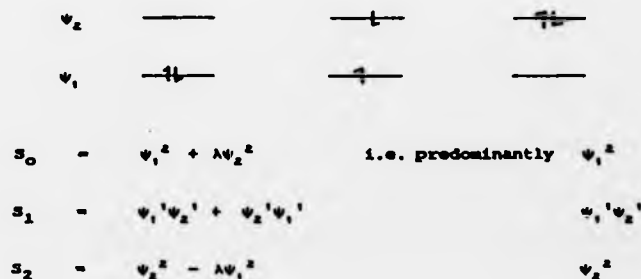
The differences in product distributions formed from the two nominally singlet cyclooctane-1,4-diyls were attributed to differences in electronic states (ie S_1 versus S_0 reactivity).⁶ The consequences of different electronic states in 1,4-biradical reactions are discussed in the following section.

6.3.1 Different electronic states of a biradical. TS and TB interactions.⁷

We have previously discussed the effect of TS and TB interactions on relative cleavage rates of boat and chair cyclohexane-1,4-diyls. The effect of TS and TB interactions in biradicals can also lead to differences in product distributions from two nominally singlet processes (ie direct photolysis and pyrolysis of precursors). Figure 5.5, p.201 shows the energetic ordering of molecular orbitals formed by the TS and TB interactions of the basis orbitals (ϕ_A and ϕ_B). The diagram is strictly that of a boat diyl but has the same energetic ordering of molecular orbitals as any 1,4-diyl. Inspection of Figure 5.5 shows that the anti-symmetric combination of basis orbitals lies below the symmetric combination if TB interactions are dominant, and vice-versa if TS interactions are dominant. Salem's analysis (see Section 1.2, p.3) shows that there are three low-lying singlet states for a biradical and if the orbital degeneracy is slightly lifted (ie by TS or TB interactions) the ordering and orbital character of the states is as shown in Scheme 6.3.

Scheme 6.3

FIGURE 2: Singlet biradicals



Thus, the lowest singlet (S_0), which has its electrons paired, has predominantly ψ_1 character and the second singlet (S_1), which has its electrons paired but anti-parallel, has reduced ψ_1 and increased ψ_2 character. Inspection of Figure 5.5 shows that if TB interactions are dominant in a 1,4-diyl, ψ_1 has $(\phi_A - \phi_B)$ character and is 1,4-antibonding. It also has σ^* character and thus reduced bonding between C2-C3. Consequently an S_0 biradical would be expected to cleave rather than couple. In contrast, ψ_2 has $(\phi_A + \phi_B)$ character and is therefore 1,4-bonding. It also has σ character which strengthens C2-C3. Thus, relative to S_0 , S_1 should show less C2-C3 cleavage relative to coupling at C1-C4. If TS interactions are dominant the situation is reversed. Thus, S_0 has $(\phi_A + \phi_B)$ character and should couple preferentially relative to S_1 which has $(\phi_A - \phi_B)$ character. If the different electronic states of a biradical could be generated independently they would therefore be expected to show different cleavage/coupling ratio's.

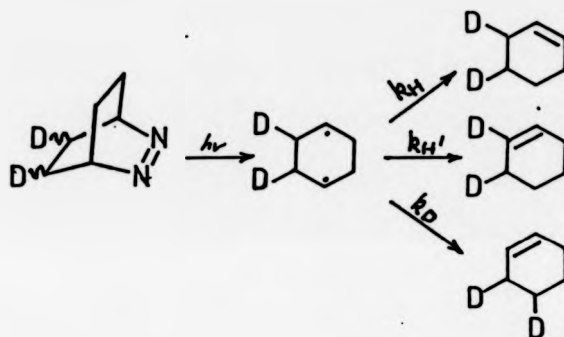
Thermolysis of ABHI, DBD, or BCH would be expected to lead to an S_0 biradical while direct photolysis of DBO or DBD might lead to an S_1 biradical via the singlet excited state of the azo compound. The differences in electronic state may therefore explain the difference in cleavage/coupling ratios in DBD thermolysis and direct photolysis, and ABHI thermolysis and DBO direct photolysis.

6.4 Stereochemistry and mechanism of formation

It is likely that cyclohexenes in the direct photochemical decomposition arise from hydrogen (or deuterium) shift(s) in an intermediate cyclohexane-1,4-diyl. Direct photolysis of d_2 -DBO (68)

anti, 32% syn deuterium) and analysis of the products by ^2H NMR (see Figure 4.3, p126) showed a 1:1 ratio for the allylic and total sp^3 plus olefinic deuterium. Inspection of Scheme 6.4 shows that this is entirely consistent with a 1,3-shift mechanism in an intermediate cyclohexane-1,4-diyl.

Scheme 6.4

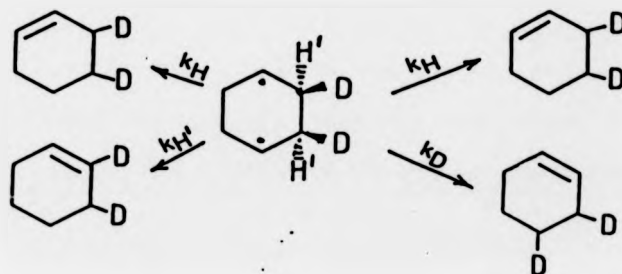


More surprisingly, direct photolysis of d_2 -DBO with > 99% anti deuterium led to cyclohexenes with a 1:1 ratio of sp^3 to allylic deuterium, but no olefinic deuterium (see Figure 4.6, p.134). Inspection of Scheme 6.5 shows that olefinic deuterium will be absent if the shift occurs from only one face (the "upper" face in Scheme 6.5) of a diyl with a cis arrangement of deuteriums.

Scheme 6.5

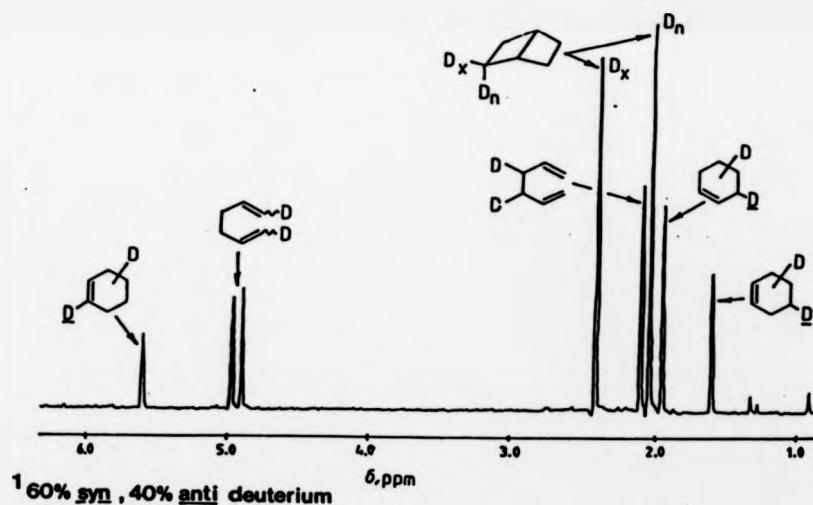
"Lower" face only

"Upper" face only



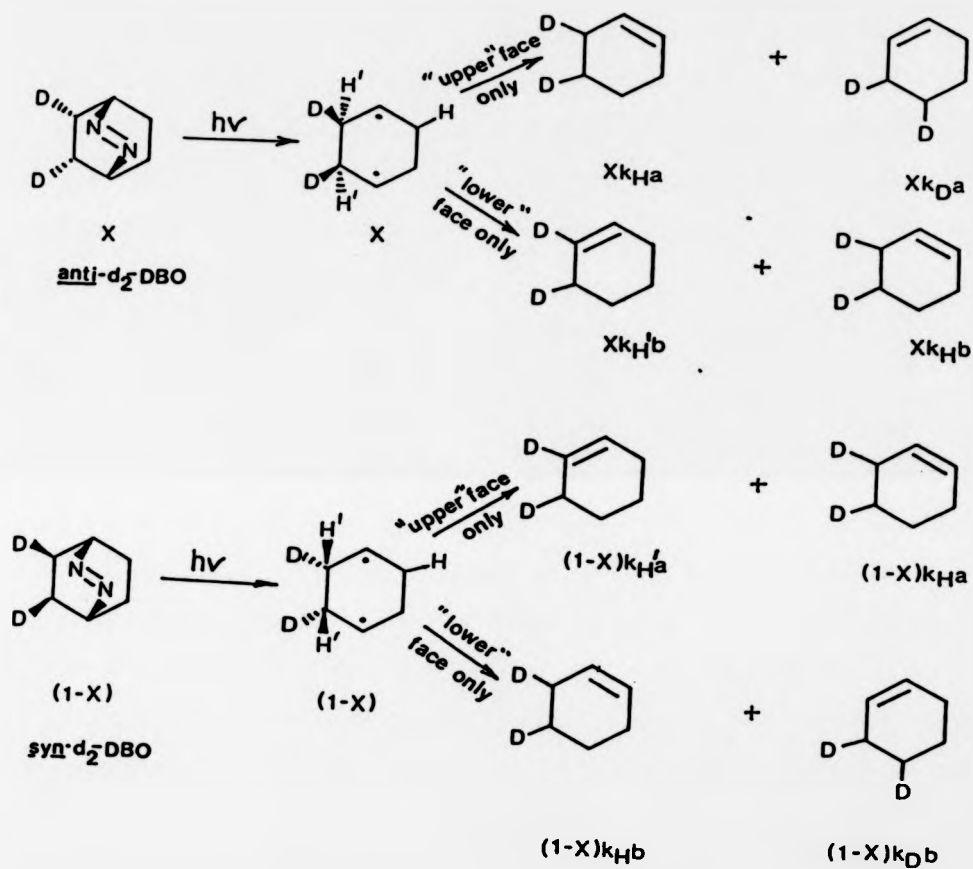
If a diyl is generated with the opposite stereochemistry of the diyl in Scheme 6.5 (*ie* deuterium on the "lower" face) the ratio of olefinic deuterium to sp^3 and allylic deuterium will increase. This was realised by photolysing a sample of d_2 -DBO in which the deuterium was predominantly *syn* (prepared by deuteration of (85) in toluene with Wilkinson's catalyst). The 2H NMR of the products from photolysis of this sample (60% *syn*, 40% *anti* deuterium) gave the 2H NMR shown in Figure 6.2.

Figure 6.2 2H NMR of products from direct photolysis of d_2 -DBO¹



Inspection of Figure 6.2 shows that the ratio of olefinic deuterium to sp^3 and allylic deuterium is greatly increased confirming that the 1,3-shift is stereoselective. Since we had two samples of d_2 -DBO with different *anti/syn* ratio's it was possible to quantify the degree of stereoselectivity and determine the primary KIE. The general method is outlined in Scheme 6.6.

Scheme 6.6



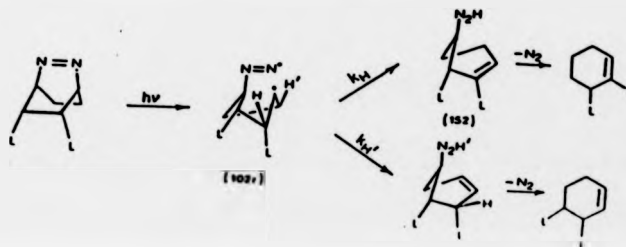
- x : proportion of *anti* d_2
 $(1-x)$: proportion of *syn* d_2
 a : proportion of shift which occurs from "upper" face
 b : proportion of shift which occurs from "lower" face
 k_H : H-shift
 $k_{H'}$: H'-shift
 k_D : D-shift
 assume $k_H \approx k_{H'}$

The ratio's of syn/anti deuterium in two different samples of d_2 -DBO and those of allylic, sp^3 , and olefinic cyclohexene deuterium can be obtained by integration of the appropriate 2H NMR's. This enables calculation (see Appendix 6) of the primary KIE (k_H/k_D) and the reaction stereoselectivity (the quantities a and b in Scheme 6.6). Solution gives $k_H/k_D \cong 2.5 - 3.0$, $a \cong 1$, and $b \cong 0$. The magnitude of the KIE is consistent with an H/D-shift in a cyclohexane-1,4-diyl. The value of a and b reflect the high stereoselectivity of the reaction. The shift only occurs from the "upper" face of the diyl formed from d_2 -DBO.

6.4.1 Discussion

The discussions so far have been based on the assumption that the 1,3-shift occurs from a cyclohexane-1,4-diyl. However, a stereoselective shift is possible if a diazenyl biradical were the intermediate. For example, stepwise cleavage of the C-N bonds, as proposed in Section 4.6, p137, would lead to a boat, or nearby twist, conformation of a diazenyl biradical (102r). This species (102r) could collect either of the two closest syn protons to give a nitrogen compound (152) which would be expected to readily decompose to the observed 1,3-shift product.⁸ This mechanism cannot be involved since anti- d_2 -DBO would lead to cyclohexenes with olefinic deuterium, (Scheme 6.7) the opposite result to the one we observed.

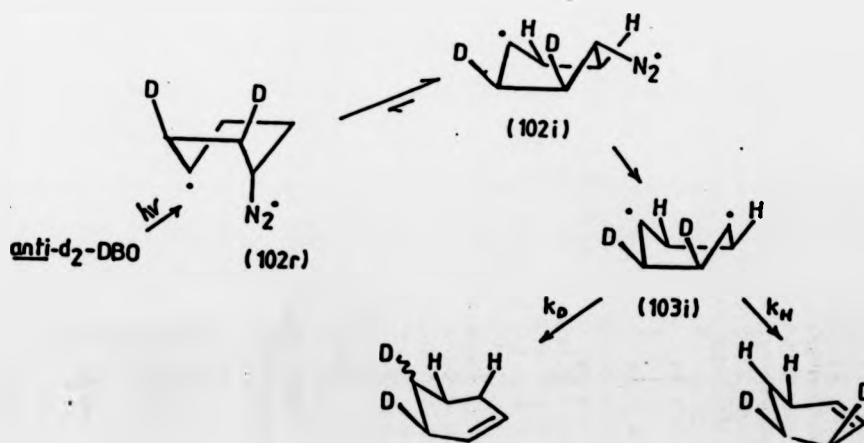
Scheme 6.7 L = H, D L = D = anti- d_2 -DBO



The same mechanism could not occur in the more stable (102i) as the diazenyl substituent in the bowsprit position is too far away to collect the proton (deuterium). Thus, the assumption that the 1,3-shift occurred in a cyclohexane-1,4-diyl is valid.

The high stereoselectivity observed in the 1,3-shift reaction of d_2 -DBO requires that the two faces of the diyl can be differentiated. This rules out the involvement of chair, 90° -twist, and planar arrangements of six carbon atoms. A boat diyl conformer formed from d_2 -DBO does satisfy this criterion. Our mechanism for the decomposition of anti- d_2 -DBO suggests an inverted boat diyl conformer (103i) would be formed preferentially (see Section 4.6, p.137). A 1,3-shift from the "upper" face of (103i) would lead to the preferred cyclohexenes without olefinic deuterium (Scheme 6.8).

Scheme 6.8



A 1,3-shift from the "upper" face of (103i) satisfies the stereochemical observation and is consistent with our preferred decomposition mechanism. However, a 1,3-shift requires the orbitals involved to be nearly co-linear. In the boat diyl the orbitals are nearly perpendicular. If (103i) relaxes to the more stable 30°-twist conformer, a shift from the "upper" face rationalises the stereochemical results and is more likely since the orbitals involved are nearly co-linear (this is readily verified with Drieding molecular models).

6.5 Summary

Cyclohexenes are formed in the direct photochemical decomposition of DBO, but not the photosensitised decomposition, or BCH pyrolysis. We have shown that cyclohexenes are formed stereoselectively from d₂-DBO, an observation that could be rationalised by a 1,3-shift mechanism in a 30°-twist conformer of an intermediate cyclohexane-1,4-diyl.

The absence of cyclohexene products in the pyrolysis of BCH does not require that direct photolysis of DBO and BCH pyrolysis involve different intermediates. Similar differences have been observed in other systems and may be rationalised by TS and TB interactions in the different singlet electronic states of the biradical.

Chapter 7

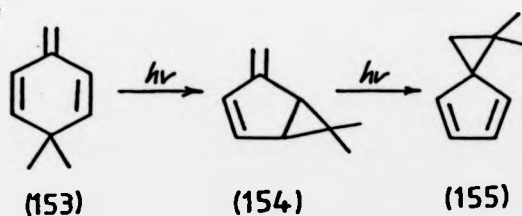
7.1 Introduction

In this chapter we discuss our attempts to trap a hypothetical singlet diyl intermediate in the unimolecular photochemical rearrangement of a cyclic triene.

7.2 Photochemical rearrangement of 3,3-dimethyl-6-methylenecyclohexa-1,4-diene (153)

Zimmerman *et al*¹ have reported that irradiation of 3,3-dimethyl-6-methylenecyclohexa-1,4-diene (153) led to 2-methylene-6,6-dimethylbicyclo[3.1.0]hex-3-ene (154) as a primary photoproduct and 1,1-dimethyl-spiro[2,4]hepta-4,6-diene (155) as a secondary photoproduct² (Scheme 7.1).

Scheme 7.1

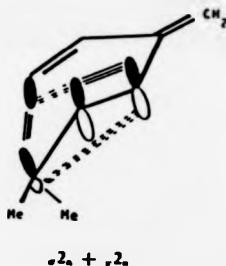


Photophysical studies have shown that when the ³(π-π*) excited state of (153) is generated independently by sensitised photolysis the unimolecular rearrangement is 50 times less efficient than that observed for direct photolysis. This indicates that the reaction

occurs from the $^1(\pi-\pi^*)$ excited state of (153)¹.

The structural change (153) \rightarrow (154) is formally of the di- π -methane type.³ The di- π -methane rearrangement can occur by a symmetry allowed concerted pathway or via biradical intermediates. The concerted mechanism for the reaction (153) \rightarrow (154) can be envisaged as an excited state - allowed $\pi 2a$ and $\sigma 2a$ process (Figure 7.1).

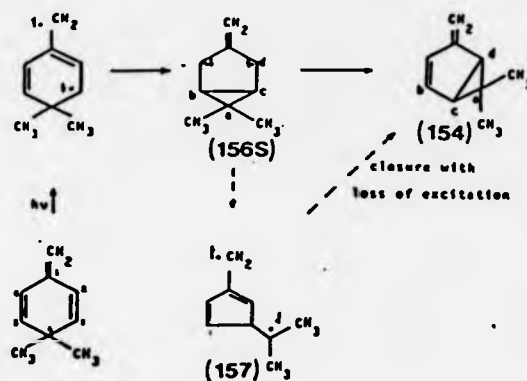
Figure 7.1 Orbital symmetry considerations for photochemical rearrangement of (153) from ref. 1.



\equiv bonds being made $---$ bonds being broken

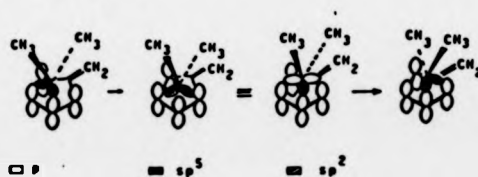
Although the $\pi 2a + \sigma 2a$ process accommodates the structural change, studies on other di- π -methane rearrangements suggest that the process requires more than just a σ and a π bond.³ The biradical mechanism begins with bridging between C2 and C4 in the excited state, as shown in Scheme 7.2, to give the singlet diyl (156S). It has been suggested that (156S) could simply then ring open to give (157) followed by reclosure with loss of electronic excitation to give (154).¹

Scheme 7.2 (from ref. 1)



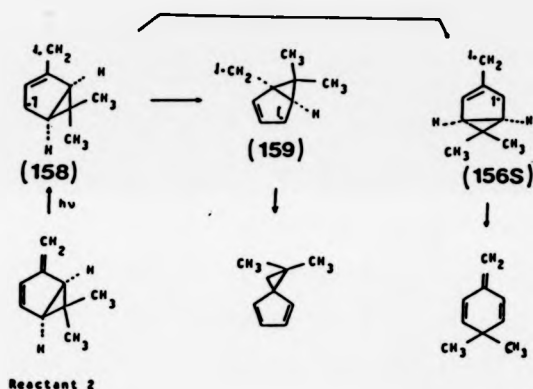
Alternatively, Zimmerman *et al*¹ suggested that (156S) transforms to product by a one step slither of the dimethyl divalent carbon a from carbons b and c of the original skeleton to carbons c and d (note Schemes 7.2 and 7.3).

Scheme 7.3 (from ref. 1).



The slither mechanism also accommodates the rearrangement of (154) to (155).² Slither can occur in either direction from the excited state of (154) to give the product. This is depicted in valence bond terms in Scheme 7.4.

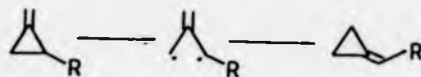
Scheme 7.4 (from ref. 2).



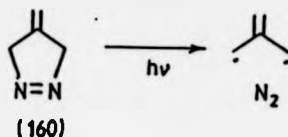
Although the species (158) and (159) are not envisaged to be discrete intermediates, the singlet diyl (156S) in Schemes 7.2 and 7.4 is a member of a special class of biradicals known as trimethylenemethanes (TMM's).

7.3 Trimethylenemethanes (TMM's)

TMM's have been proposed as the likely intermediates in the pyrolysis of methylenecyclopropanes;⁴



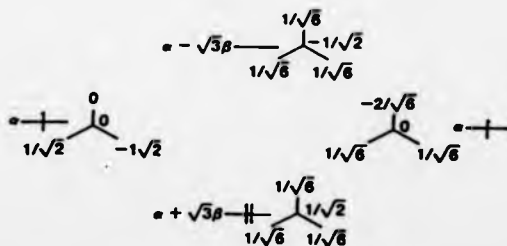
Dowd⁵ has generated the same (or very similar) intermediate by irradiating 4-methylenepyrazoline (160) at 77 K;



The TMM was ESR active and the triplet subsequently shown to be the ground state by a Curie-law analysis. The low $|E|$ parameter ($|E|/hc \text{ cm}^{-1} < 0.001$) and $|D|$ parameter ($|D|/hc \text{ cm}^{-1} = 0.024$) were fully consistent with the proposed planar TMM structure,^{5,6}

A planar TMM can be analysed by simple Hückel molecular orbital theory.⁷ This treatment leads to the set of π -electron energies and symmetry adapted orbitals shown in Figure 7.2.

Figure 7.2 HMO's of TMM (from ref. 9).



π -Electron energies and MO coefficients of the TMM system derived from simple Hückel theory. The occupation scheme represents the triplet ground state predicted from Hund's Rule.

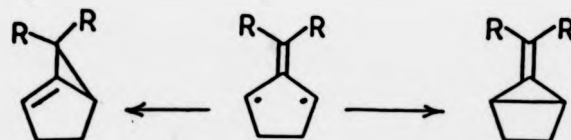
Insertion of the four π -electrons and application of Hund's rule predicts the triplet ground state experimentally observed by Dowd.

The triplet ground state of TMM increases its unimolecular lifetime enhancing the chances of it being intermolecularly intercepted. Indeed, TMM is known to undergo intermolecular reactions such as dimer formation.⁸ However, the yields of such reactions are low, the main reaction being cyclisation to MCP. If the cyclisation of TMM's could be inhibited, the lifetime may be sufficiently increased to allow the triplet to be more easily trapped. Furthermore, since TMM precursors are ground or excited state species with electrons paired, the principle of spin conservation requires that the triplet biradical can only be obtained via a singlet biradical. Thus, if ring closure is sufficiently inhibited the possibility of singlet biradical trapping exists.

7.3.1 Strain protected TMM's⁹

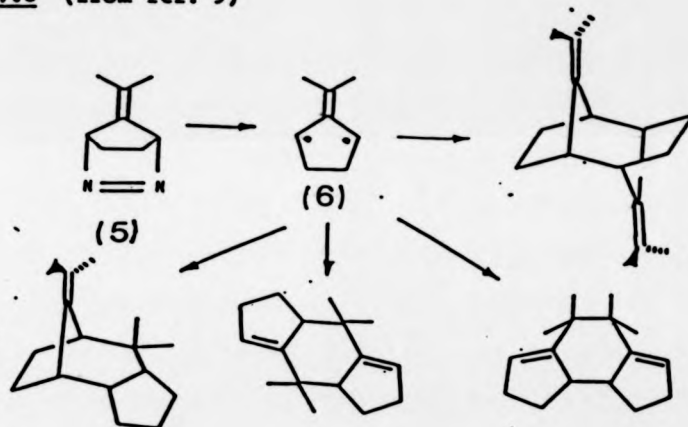
Incorporation of a TMM into a small ring should increase the activation energy to cyclisation due to incipient product ring strain. This has been found to be true for the 2-alkylidene-cyclopentane-1,3-diyl series of TMM's which can only cyclise to the highly strained bicyclic hydrocarbons shown in Scheme 7.5.⁹

Scheme 7.5



The strain energy of the [2.1.0] system (R=H) is estimated to be at least 68 kcal mol^{-1} .⁹ The [3.1.0] system would be expected to be even more strained. The inhibition of ring closure increases the unimolecular lifetime of the diyls to an extent that they undergo intermolecular reactions in quantitative yield. For example, thermal and photochemical decomposition of the precursor (5) occurs smoothly above about 40° to give near quantitative yields of the TMM dimers shown in Scheme 7.6.¹⁰

Scheme 7.6 (from ref. 9)



The formation of dimers is accompanied by strong CIDNP of the product protons observed as emissions in the $^1\text{H NMR}$,⁹ and ESR kinetic studies have shown that the bulk of the reaction is due to triplet plus triplet species.¹¹

7.3.1.1 Singlet 2-alkylidene-cyclopentane-1,3-diyls

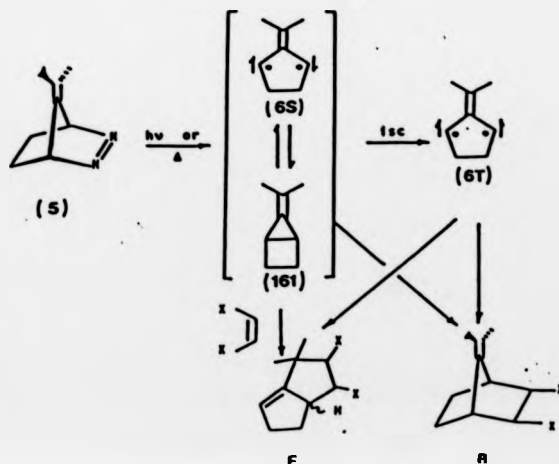
The 2-alkylidene-cyclopentane-1,3-diyl series have triplet ground states but as they are formed from precursors with spins paired, the singlet diyl must be the first formed intermediate. The inhibition of

ring closure and the presence of conjugation make the singlet 2-alkylidene-cyclopentane-1,3-diyls the most stable singlet biradicals known. This is exemplified by the fact that excited states of the singlet diyl ($6S^*$) have been detected by picosecond LFP (see Section 1.4.1., p18). There is also substantial evidence that the singlet diyl can be intercepted by olefins.

7.3.1.2 Trapping of singlet diyls

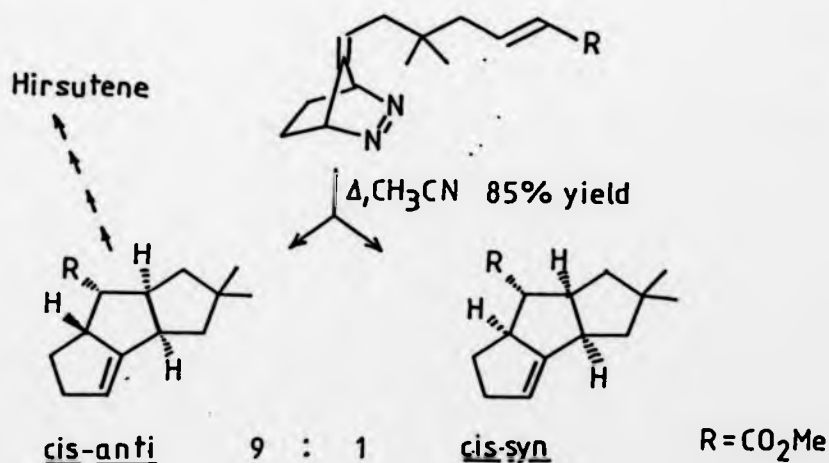
When the thermal and direct photochemical decomposition of the diazene diyl-precursors is carried out in the presence of high concentrations of olefins with electron-withdrawing substituents, dimer formation is suppressed and near quantitative yields of olefin-diyl adducts are produced.⁹ There is substantial evidence that there are two sequentially formed interceptable singlet species (a diyl and a strained hydrocarbon) but kinetic studies have established that it is the diyl that is being intercepted.¹² The major mechanistic conclusions are outlined for 2-isopropylidene-cyclopentane-1,3-diyl (6) in Scheme 7.7

Scheme 7.7 (from ref. 9)



The first trappable intermediate is the singlet diyl (6S) which reversibly interconverts with (16I) at temperatures above -60° . If no olefins are present, (6S) undergoes ISC to the triplet diyl (6T) which ultimately dimerises. If high concentrations of diylophilic olefins (*ie* olefins with conjugating substituents) are present, (6S) is intercepted before ring closure to (16I) and ISC to (6T).⁹ There are two possible types of diyl-olefin adducts, bridged (B) and fused (F). The singlet diyl-olefin reaction occurs with high regioselectivity. For example, decomposition of (5) in the presence of high concentrations of dimethyl fumarate leads to singlet diyl-olefin adducts with a F/B ratio of 67.¹³ In fact the yield and regioselectivity of singlet diyl-olefin adducts are so high they are synthetically useful. For example, Little *et al*¹⁴ have used intramolecular trapping techniques in natural product syntheses (Scheme 7.8).

Scheme 7.8



7.4 Involvement of TMM biradicals in the photochemical rearrangement of (153)

The structure of the proposed singlet intermediate (156S) in the photochemical rearrangement of (153) is formally a TMM incorporated into a five-membered ring and as such, is related to the 2-alkylidene-cyclopentane-1,3-diyls;

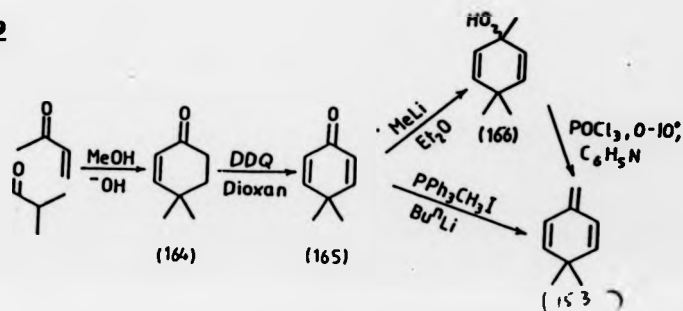


As the 2-alkylidene-cyclopentane-1,3-diyl singlets can be intermolecularly intercepted by diylphilic olefins, the hypothetical intermediate (156S) may show similar behaviour. If (156S) could be trapped by olefins, this would provide a rare example of singlet diyl trapping and also distinguish between concerted and stepwise mechanisms in the photochemical rearrangement of (153). The aim of this work was to photolyse (153) in the presence of diylphilic olefins in attempts to trap the hypothetical singlet diyl (156S).

7.4.1 Synthesis of 3,3-dimethyl-6-methylene-cyclohexa-1,4-diene

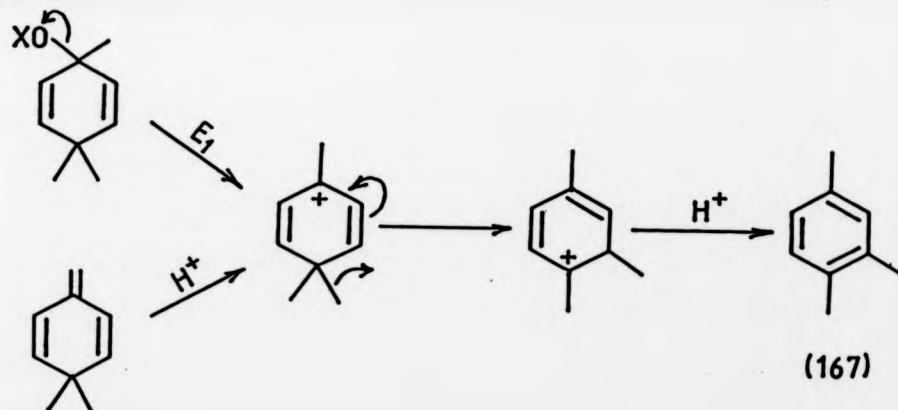
The synthesis of (153) has been reported by Zimmerman *et al*¹ (Scheme 7.9).

Scheme 7.9



The Wittig reaction is reported to give (153) in 60% yield.¹ However, our attempts to synthesise (153) using the Wittig reaction were very inefficient, mainly due to the occurrence of substantial tautomerisation. Thus, the synthesis was accomplished by dehydration of the carbinol (166), which could be produced in quantitative yield from the dienone (165). The reaction conditions were chosen so that the elimination proceeded by an E2-mechanism under basic conditions since a facile rearrangement of (153) would predominate if the elimination occurred by the E1-mechanism, or if acid was present (Scheme 7.10).

Scheme 7.10



The elimination was accomplished using phosphoryl chloride in pyridine at low temperatures. This gave good yields of (153) contaminated with small amounts of (167). The samples of (153) were purified by prep. g.c. before photolysis.

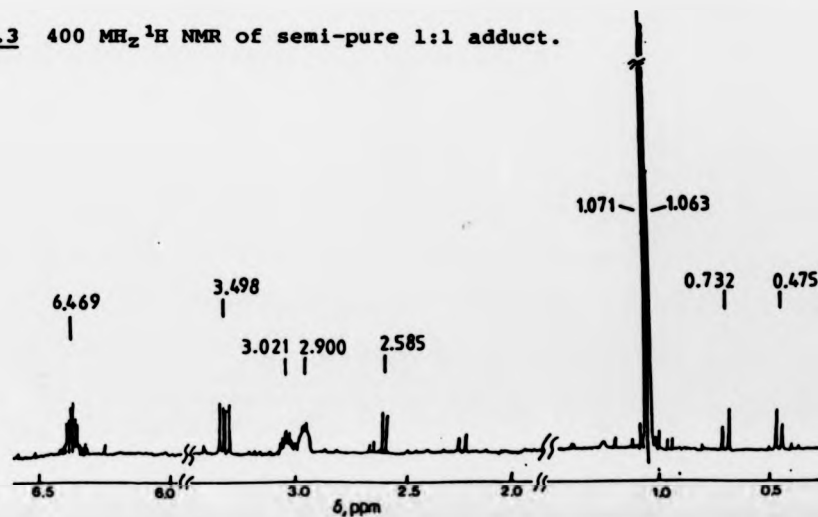
7.4.2 Photolysis of triene in the presence of olefin biradical traps

Exploratory photolyses involved irradiation (at 254 nm) of (153)

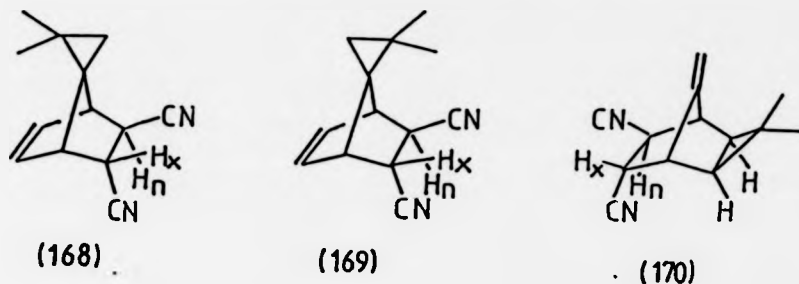
(0.3 ml of a 1% stock solution in CH_3CN) in the presence of high concentrations of dimethyl fumarate or fumaronitrile. The reactions were monitored by gas chromatography at low temperatures for consumption of (153) and at higher temperatures for the appearance of products. The new products were analysed for 1:1 olefin-triene adducts by EI and NH_3/CI mass spectroscopy. The GC/MS analysis of the experiment using dimethyl fumarate as the trapping olefin showed 1:1 adduct formation had occurred (CI GC/MS MH^+ 265). The GC/MS indicated at least three 1:1 adducts. Since a control experiment showed dimethyl fumarate underwent photochemical *cis/trans* isomerisation at 254 nm, at least two 1:1 adducts would have been expected. The experiment using fumaronitrile as the trapping olefin showed at least two 1:1 adducts of the correct molecular weight by GC/MS (M^+ , 199). Fewer adducts were expected for the fumaronitrile experiment as a parallel photolysis showed a smaller degree of olefin *cis/trans* isomerisation occurred.

A preparative scale photolysis was carried out irradiating (153) (0.06 mol dm^{-3}) in CH_3CN in the presence of fumaronitrile (0.14 mol dm^{-3}). A crude 1:1 adduct was isolated and gave the ^1H NMR shown in Figure 7.3.

Figure 7.3 400 MHz ^1H NMR of semi-pure 1:1 adduct.



The ^1H NMR spectrum and spin-decoupling experiments were consistent with the following structures;

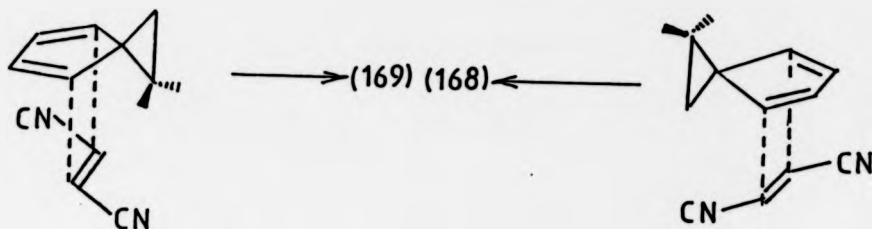


Thus, the AB quartet (doublets at 0.475 and 0.732 ppm) corresponds to the cyclopropyl protons, and the two singlets at 1.063 and 1.071 ppm to the non-equivalent methyls. The protons α to the carbonitrile function show a double doublet at 3.498 ppm and a doublet at 2.585 ppm. The α -proton showing the doublet corresponds to H_N as the dihedral angle between H_N and the bridgehead proton is ca 90° (Karplus analysis shows that no coupling is expected for this situation). The olefinic protons (in (168) and (169)) or exo-methylene protons (in (170)) appear as a multiplet at 6.469 ppm (AB part of an ABXY spin-spin system) while the bridgehead protons are complicated multiplets at 2.900 and 3.021 ppm.

7.5.3 Discussion

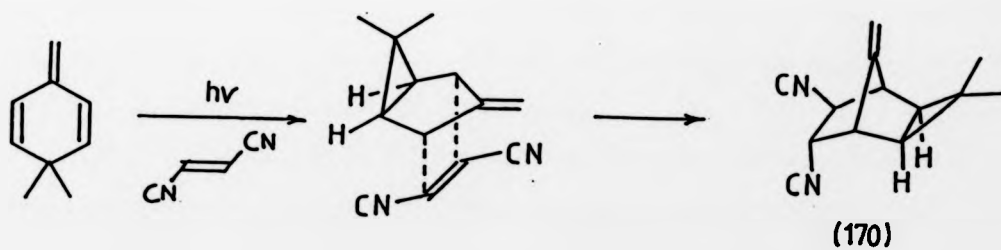
The structures (168) and (169) would arise from a Diels-Alder reaction of the secondary photoproduct (155) with the olefin. The most likely product from such a reaction is (168) as the transition state leading to it is less sterically crowded than the alternative transition state leading to (169), (Scheme 7.11).

Scheme 7.11



The structure (170) would be the expected product from trapping of the bridged diyl intermediate in a 1,3 manner (Scheme 7.12).

Scheme 7.12

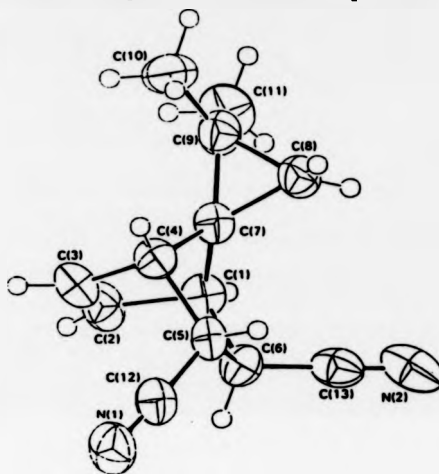


The chemical shift of the protons attached to an sp^2 carbon (see Figure 7.3) is more consistent with olefinic than exo-methylene protons. However, the methylene protons in (170) lie in the deshielding zone of the cyclopropane ring.¹⁵ Methyl steric compression is also likely to deshield the exo-methylene protons.¹⁶

We were able to obtain crystals of the semi-purified photoadduct

and thus solved the structural dilemma by X-ray analysis. This gave the structure shown in Figure 7.4.

Figure 7.4 ORTEP diagram of isolated product



View of the molecule, showing the atomic numbering.

Inspection of Figure 7.4 shows that the 1:1 adduct isolated from the crude photolysis mixture was the Diels-Alder adduct of the secondary photoproduct (155) with the olefin.

The product isolated from the crude reaction mixture was of little mechanistic significance. However, other adducts may have been present in the crude mixture. Thus, we analysed the crude product obtained from photolysis of (153) in the presence of fumaronitrile and fumarate in more detail.

7.4.4 Detailed analysis of photoadduct mixtures

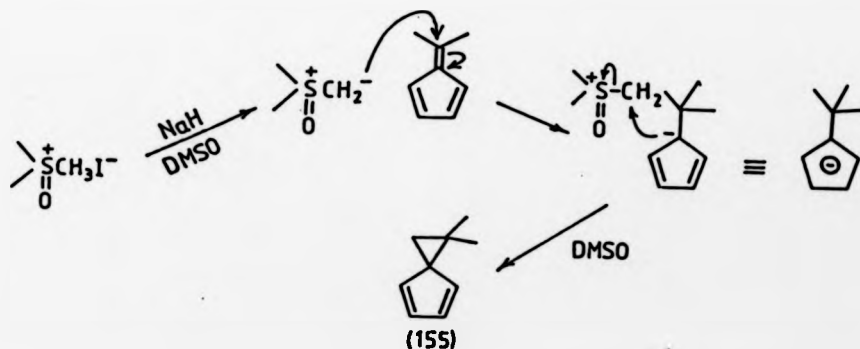
The detailed analysis required independent synthesis of samples of the possible Diels-Alder olefin adducts and then comparison of their capillary gas chromatographic properties with those of the

crude triene-olefin product mixtures. Any long retention-time peak unidentified by capillary g.c. could be analysed by capillary GC/MS to determine if the compound was a 1:1 triene-olefin adduct.

7.4.4.1 Independent synthesis of Diels-Alder adducts

The synthesis of the spiro-diene (155) was accomplished by the reaction of trimethyloxosulphonium iodide with dimethyl fulvene. The reaction involves a sulphur ylid reacting with the fulvene as shown in Scheme 7.13.

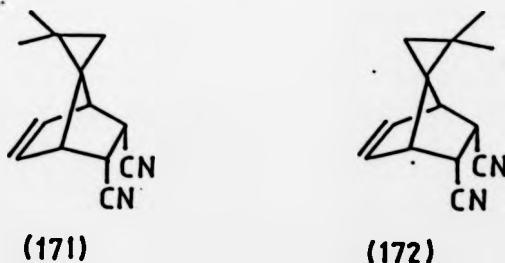
Scheme 7.13



Refluxing (155) in ethanol with fumaronitrile led to (168) as the major product which could be isolated in crystalline form. This had identical spectral properties to the product isolated from photolysis mixtures. Capillary g.c. (OV101, 140°) showed the sample had a retention time of 420s. Capillary g.c. analysis of the mother liquor showed long retention time peaks at 420s and 450s. The peak at 450s (< 5%) is most likely the other trans-adduct (169) as the ^1H NMR showed an AB quartet centred at 0.474 ppm (the cyclopropyl H's).

We were not able to obtain pure samples of maleonitrile to prepare the cis Diels-Alder adducts. However, we obtained approximately a 1:1 mixture of fumaro- and maleonitrile by photolytic isomerisation of the trans-isomer. The cis/trans mixture of olefins was refluxed with (155) in ethanol to give the Diels-Alder products. Crystals isolated from the crude mixture, were shown by ^1H NMR analysis to be a mixture of (168) and a cis adduct. We were able to separate the cis adduct by crystal picking. Its ^1H NMR spectrum (400 MHz) showed broad singlets for all the protons except the olefinic protons (a double doublet which appeared as a triplet with $J = 2\text{Hz}$). The possible cis-isomers (noting that exo-isomers are not expected in Diels-Alder reactions)¹⁷ are shown in Scheme 7.14.

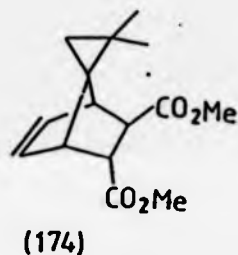
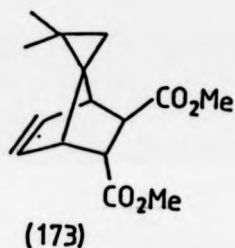
Scheme 7.14



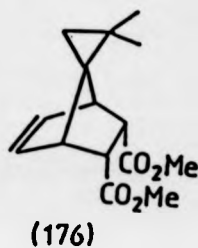
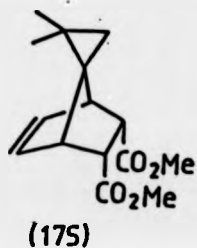
We established the structure of the isolated cis adduct by analysis of its $^1\text{H}\{^1\text{H}\}\text{nOe}$ difference spectrum. This showed an nOe at the $\alpha\text{-CN}$ proton signals on irradiation at the cyclopropyl proton signals, and no nOe at these $\alpha\text{-protons}$ when the methyl signals were irradiated. This is consistent with (171) but not (172). Preferential formation of (171) over (172) is expected on the basis of differences in steric crowding in their transition states (cf the argument on p.240). The ^1H NMR of the mother liquor suggested the

presence of (172) as a minor product. Capillary g.c. analysis of the pure cis adduct (OV101, 140°) showed one long retention time peak at 990s. Identical analysis of the crude cis/trans adduct mixture showed long retention time peaks at 420s, 450s, 828s, and 990s.

Similar treatment of the Diels-Alder reactions of (155) with maleate and fumarate showed the formation of four adducts. The reaction of (155) with fumarate led to two trans adducts;



¹H NMR analysis of the crude mixture indicated these were formed in a 95:5 ratio. The major adduct was assumed to be (173) by involving the argument that the transition state leading to it would be less sterically crowded, and thus lower in energy, than the alternative. Capillary g.c. analysis (OV101, 150°) of the crude mixture showed there to be a major long retention time peak at 552s, and a minor one at 570s. ¹H NMR analysis of the crude product from reaction of maleate and (155) showed the formation of two cis-adducts in the ratio of 68:32;

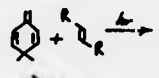

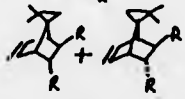

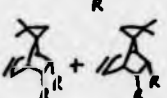


The major adduct was crystalline and was isolated from the mixture. Its ^1H (^1H) nOe difference spectrum showed an nOe at the ester α -protons upon irradiation of the signal for the cyclopropyl hydrogens, and a small nOe for the olefinic signal upon irradiation at the methyl signal. This is consistent with (175) but not (176). The ratio of (175)/(176) shows that the two possible transition states are of similar energy. Capillary g.c. analysis (OV101, 150°) showed (175) and (176) to have retention times of 648s and 660s, respectively.

7.4.4.2 Analysis of photoproduct mixtures

Photolysis of (153) (1% solution in CH_3CN) in the presence of fumarate led to a crude mixture of 1:1 adducts. The excess fumarate was removed by vacuum sublimation and the residue analysed by capillary g.c (OV101, 150°). The long retention peaks were identified by co-injections with independently synthesised pure Diels-Alder adducts, or mixtures of adducts (Table 7.3).

Table 7.3 Comparison of capillary g.c retention times.^a

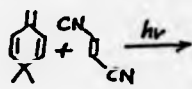
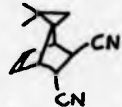
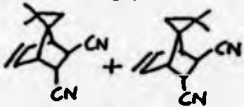

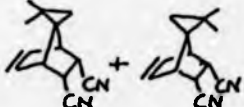
Adducts	Relative retention times (s)			
	552	570	648	660
	552	—	—	—
	552	570	—	—
	—	—	648	—
	—	—	648	660

^aOV101, 150° . R = CO_2Me

Inspection of Table 7.3 shows that the Diels-Alder adducts were the only ones formed.

Similar treatment of the photolysis of (153) in the presence of fumaronitrile gave the results shown in Table 7.4.

Table 7.4 Comparison of capillary g.c retention times.^a

Adducts	Relative retention times (s)			
	420	450	828	990
	420	—	—	—
	420	450	—	—
	—	—	—	990
	420	450	828	990

^a OV101, 140°

Inspection of Table 7.4 suggests that the Diels-Alder adducts are the only ones formed. Capillary GC/MS of the photolysis mixture confirmed that the four peaks observed were 1:1 adducts with $M^+ = 198$.

7.4.5 Discussion

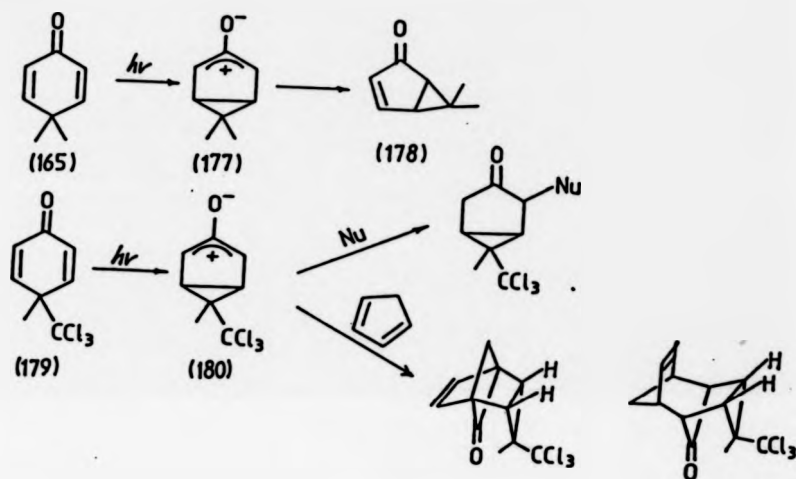
Our studies have shown that the proposed bridged singlet diyl intermediate (156S) in the photochemical rearrangement of (153) cannot be intercepted by diylphilic olefins. As the olefins were present in high concentrations this result suggests that such a biradical would have a lifetime shorter than the diffusion controlled rate limit (ca 100 ps) or that the photochemical rearrangement of (153) proceeds via the $\pi 2a + \sigma 2a$ concerted mechanism.

If the bridged singlet diyl does exist as an intermediate, the question arises as to why it cannot be intercepted whereas the superficially similar 2-alkylidene-cyclopentane-1,3-diyls give adducts in near quantitative yields. The major difference between the two systems are the unimolecular reactions available to them. The 2-alkylidene-cyclopentane-1,3-diyls can only couple, a reaction only inhibited by incipient product ring strain. The hypothetical intermediate (156S) will be much shorter-lived since it can undergo the unimolecular walk rearrangement.

If the walk rearrangement of (153) could be inhibited it may be possible to intercept (156S). This could be achieved by carrying out the photolysis at lower temperatures. However, this may lead to practical problems such as inefficient formation of (156S) and olefin solubility. A second possibility would be to have a sterically bulky substituent at C3 of (153). This should slow the walk rearrangement thereby increasing the unimolecular lifetime of (156S). Reducing the efficiency of walk rearrangements is known to increase the chances of intercepting short-lived intermediates. For example, in the related photochemical reaction of cross-conjugated cyclohexadienones¹⁸ the proposed zwitterionic intermediate can be intercepted by olefins if

the walk rearrangement is inhibited. An example of such a case is shown in Scheme 7.15.

Scheme 7.15



The dimethyl substituted product (165) proceeds to product (178) through a presumed zwitterionic intermediate (177) which cannot be intercepted. As the walk proceeds from (177) to (178) a positive charge develops on C4. Thus, an electron withdrawing substituent at C4 should reduce the efficiency of the process, enabling capture of the zwitterionic intermediate. This has been confirmed for the trichloromethyl substituted system (179) in which the zwitterionic intermediate (180) has been intercepted by nucleophiles¹⁹ and olefins²⁰ (Scheme 7.15).

Experimental

General Notes

All melting points are uncorrected and were determined in open capillaries using a Gallenkamp instrument. Elemental analyses were carried out by Butterworth Laboratories Ltd., Teddington, Middlesex.

^1H NMR spectra were recorded on a Perkin Elmer R34 220MHz continuous wave spectrometer. ^1H NMR peaks are designated by their chemical shift(s) in p.p.m. relative to TMS, followed by their relative integral, multiplicity (s = singlet, br s = broad singlet, d = doublet, t = triplet, q = quartet, m = multiplet), and assignment.

^2H NMR spectra were recorded at 61.4 MHz on a Bruker WH400 Fourier transform spectrometer. All ^2H NMR peaks are designated by their chemical shift(s) relative to an internal standard of CDCl_3 , or otherwise ghost referenced. Samples analysed in aqueous solution were referenced with HOD.

Infra-red spectra were recorded on a Perkin Elmer 680B spectrophotometer as either liquid films or mulls (nujol). UV/Vis measurements were recorded on a Perkin Elmer 552 spectrophotometer using the solvents quoted.

Mass spectra and GC/MS were recorded on a Carlos Erba-Kratos MS80 instrument. The peaks are designated relative mass of ion, percentage intensity. Only the major intensity peaks are quoted.

Analytical g.l.c. spectra were recorded on a Pye Unicam 204 instrument using N_2 as the carrier gas. Capillary g.l.c. were recorded on a Carlos Erba 2450TP instrument using He as the carrier gas. The details of the g.l.c. work given in the text refer to the column used, oven temperature, and relative retention time of peaks of

interest. Integrations were performed automatically using a Pye Unicam DP88 computing integrator. Preparative g.l.c. were also carried out using the Carlos Erba 2450TP instrument with the column and oven temperature conditions stated in the text.

Analytical and preparative t.l.c. were carried out using F254 and PF254 (Merck) plates. The compounds were visualised under UV light or developed in iodine. Mobilities are quoted as R_f values (distance moved by compound/distance moved by solvent).

Column chromatography employed either neutral Alumina (activity grade I, 100-200 mesh) or silica gel (230-400 mesh) as the solid phase with the solvents quoted in the text.

Solvents were AR grade unless otherwise stated in the text. n-Pentane was purified by washing with concentrated H_2SO_4 , water, and then passing through an alumina column and distillation.

Experimental for Chapter 3

4-phenyl-1,2,4-triazoline-3,5-dione (PTAD)

A solution of 4-phenyl-1,2,4-triazolidine-3,5-dione (4.4 g, 25 mmol) in EtOAc (25 ml) was stirred under nitrogen at 0°C during the dropwise addition of t-butyl hypochlorite (5 ml, 46 mmol). The bright red reaction mixture was allowed to warm to room temperature and stirred for 1 hr. The solvent was removed in vacuo at ambient temperature to give 4.2 g (96%) of PTAD as bright red crystals. The product was not purified further but immediately taken up in 25 ml of EtOAc for use in Diels-Alder cycloadditions with cyclohexa-1,3-diene.

4-Phenyl-2,4,6-triazatricyclo[5.2.2.0^{2,6}]undec-8-ene-3,5-dione (85)

The procedure was modified from that reported by Gillis and Haggarty.¹ A suspension of PTAD (4.2 g, 24 mmol) in EtOAc (25 ml) was stirred at room temperature and treated with cyclohexa-1,3-diene until the red colour had completely discharged. The white product was filtered at the pump and washed with ice-cold EtOAc. The yield of product was 4.36 g and it required no further purification. Further product was obtained from the filtrate on standing. This was filtered at the pump and recrystallised from EtOAc. The total yield of (85) was 5.51 g (90%). M.p. 170-172° (lit.¹ 170-171°). ¹H NMR δ (CDCl₃): 1.61 - 2.23 (4H, AA'BB' part of AA'BB'XX' spin-spin system, 2 x anti-H, 2 x syn-H); 4.79 (2H, br s, bridgeheads); 6.51 (2H, t, J = 2Hz, - CH = CH-); 7.30 - 7.48 (5H, m, aromatics). IR ν max: 1760, 1700 cm⁻¹ (C=O).

4-Phenyl-2,4,6-triazatricyclo[5.2.2.0^{2,6}]undecane-3,5-dione (86H).

Heterogeneous catalytic reductions of (85)

Heterogeneous catalytic reductions of (85) were carried out using the following general procedure: A solution of (85) (2.55 g, 10 mmol) in anhydrous benzene (250 ml) with 100 mg of 10% palladium on charcoal was attached to an atmospheric hydrogenation apparatus. The solution was stirred vigorously at ambient temperature until uptake of hydrogen ceased. The solution was filtered through celite and concentrated in vacuo to give (86H) in quantitative yield. A sample recrystallised from EtOH had m.p. 211 - 212° (lit.¹ 211 - 212°). ¹H NMR δ (CCl₄): 1.80 - 2.20 (8H, AA'BB' part of AA'BB' XX' spin-spin system, 4 x syn, 4 x anti-H); 4.43 (2H, br s, bridgeheads); 7.31 - 7.58 (5H, m, aromatics). IR ν max: 1760, 1700 cm⁻¹ (C=O). MS m/z (EI): 257 (M, 35%); 228 (26); 119 (100); 91 (17); 81 (23); 67 (28).

2,3-Diazabicyclo[2.2.2]oct-2-ene (DBO)

The procedure used for the hydrolysis and oxidation was modified from the general procedure reported by Adam et al¹. A suspension of (86) (0.76 g, 3 mmol) and KOH (1.71 g, 30 mmol) in IPA (10 ml) was refluxed for 3 hrs under nitrogen. After cooling to room temperature a fast stream of nitrogen was bubbled through the solution and ca 5 g of crushed-ice added. The mixture was made strongly acidic with concentrated HCl (gas evolution) and warmed at 40° for 5 minutes. After neutralising with 5 M NH₄OH, a 3M aqueous solution of CuCl₂·2H₂O was added, dropwise, leading to precipitation of a brick-red copper complex. This was isolated by filtration and the filtrate neutralised with 5M NH₄OH. The cycle was repeated until the brick-red product

failed to precipitate (2 cycles were usually sufficient). The brick-red precipitate was dissolved in 5 M NH_4OH , and the resultant royal blue aqueous solution extracted with CH_2Cl_2 (3 x 50 ml). The combined organic extracts were washed successively with brine (50 ml) and H_2O (50 ml) and then dried over anhydrous MgSO_4 . The solution was filtered and concentrated in vacuo at ambient temperature. The crude product was chromatographed over silica-gel (1 x 20 cm column) eluting with CH_2Cl_2 . The product was located in the eluent by UV spectroscopy, and the solvent removed in vacuo at ambient temperature. The azoalkane was further purified by sublimation (70-80°, 15-20 mm Hg) to give DBO (263 mg, 81%) as a white crystalline solid. M.P. 141-142° (lit.⁶ 141.4°). ^1H NMR δ (CCl_4): 121 - 1.60 (8H, AA'BB' part of AA'BB'XX' spin-spin system, 4 x syn-H, 4 x anti-H); 5.10 (2H, br s, bridgeheads).

The "doublets" corresponding to the syn and anti protons in DBO and (86H) were assigned by LSR studies as discussed in the text. Thus, 20 mg samples of DBO and (86H) were dissolved in 0.5 ml of CCl_4 in an NMR tube. The chemical shift of the "doublets" was recorded and then subsequently on each addition of approximately 10 mg portions of $\text{Eu}(\text{FOD})_3$. This gave the following data;

Eu(FOD) ₃ , mg:	0	10	20	30	48	52	
(86H) Chemical shift, $\Delta\delta$ ppm:	1.84	2.04	2.13	2.24	2.36	2.40	
Chemical shift, $\Delta\delta$ ppm:	2.10	2.41	2.60	2.77	3.00	3.10	
Eu(FOD) ₃ , mg:	0	13	23.5	40	47	55	70
(DBO) Chemical shift, $\Delta\delta$ ppm:	1.27	1.74	2.08	2.49	2.72	2.96	3.34
Chemical shift, $\Delta\delta$ ppm:	1.55	1.87	2.08	2.37	2.50	2.67	2.94

The data were then plotted as shown in figures 3.2 and 3.4.

Heterogeneous catalytic deuteration of (85)

Heterogeneous catalytic deuteration of (85) were carried out using the procedure discussed for the preparation of (86H). The solvents and heterogeneous catalysts used have been given in Section 3.12. The syn/anti ratio's of deuterium were measured by electronic integration of the sample ^2H NMR, and their deuterium content measured mass spectroscopy. The ratio's and deuterium content of samples of (86D) so prepared are given in Table 3.7.

2,3-Diazabicyclo[2.2.2]oct-5-ene-2,3-dicarboxylic acid diisopropyl ester (88)

This was prepared by a Diels-Alder reaction of diisopropylazodicarboxylate (DIAD) and cyclohexa-1,3-diene using Askani's⁸ photochemical modification; A solution of freshly distilled cyclohexa-1,3-diene (3.5 g, 44 mmol) and DIAD (7.96 g, 39 mmol) in 300 ml of spectroscopic grade cyclohexane was photolysed using a 500 W medium pressure mercury vapour lamp which was immersed in the solution in a water-cooled pyrex well. When the orange colour of the DIAD had completely discharged (ca 24 hr) the solvent was removed in vacuo to give 10.5 g (95%) of crude (88) as a pale yellow oil. On standing, large colourless prism-like crystals formed which were filtered and washed with ice-cold EtOH. The sample required no further purification before use in preparation of (90). Recrystallisation of a sample from hexane/ CHCl_3 had m.p. 101.5-102.5°. (Found: C, 59.52; H, 8.04; N, 9.91. $\text{C}_{14}\text{H}_{22}\text{N}_2\text{O}_4$ requires C, 59.55; H, 7.85; N, 9.92%). ^1H NMR δ (CCl_4): 1.24 (12H, d, $J = 6\text{Hz}$, 2 x $\text{CH}(\text{CH}_3)_2$); 1.37 - 2.10 (4H, m, ABCD part of an ABCDXY spin-spin system, 2 x anti-H, 2 x

syn-H); 4.89 (2H, br s, bridgeheads); 4, 94 (2H, septet, $J = 6\text{Hz}$, 2 x $\text{CH}(\text{CH}_3)_2$); 6.57 (2H, br s, - $\text{CH} = \text{CH}$ -). IR ν max: 1740, 1720 cm^{-1} (C=O). MS m/z (EI): 282 (M^+ , 23%); 196 (32); 154 (76); 126 (38); 109 (23); 81 (84); 80 (32); 79 (25); 43 (100).

Heterogeneous catalytic reduction of (88). Preparation of 2,3-diazabicyclo[2.2.2]octane-2,3-dicarboxylic acid diisopropyl ester (90H).

Heterogeneous catalytic reductions of (88) were carried out using the procedure discussed for the preparation of (86). A sample of (88) reduced with hydrogen gave (90H) as a white solid in quantitative yield. The sample required no further purification before being used in the preparation of DBO. A sample recrystallised from hexane/ CHCl_3 had m.p. 83-84°. (Found: C, 59.19; H, 8.72; N, 9.82. $\text{C}_{14}\text{H}_{24}\text{N}_2\text{O}_4$ requires C, 59.13; H, 8.50; N, 9.85%). ^1H NMR δ (CCl_4): 1.28 (12H, d, $J=6\text{Hz}$, 2 x $\text{CH}(\text{CH}_3)_2$); 1.32 - 2.20 (8H, m, ABCD part of an ABCDX spin-spin system, 4 x syn-H, 4 x anti-H); 4.14 (2H, br s, bridgeheads); 4.89 (2H, septet, $J = 6\text{Hz}$, 2 x $\text{CH}(\text{CH}_3)_2$). IR ν max: 1740, 1720 cm^{-1} (C=O). MS m/z (EI): 284 (M^+ , 5%); 198 (14); 197 (5); 183 (9); 157 (8); 136 (100); 111 (53); 83 (23); 51 (8); 43 (24).

Heterogeneous catalytic deuteration of (88)

Heterogeneous catalytic deuteration of (88) were carried out using the procedure given for the reduction of (85). The solvents and catalysts used are given in Table 3.7. The syn/anti ratio's of deuterium in samples of (90D) were measured by integration of their ^2H NMR spectra as discussed in Section 3.2, and their deuterium content

was measured by mass spectroscopy. The stereochemical ratio's and deuterium content of samples prepared are given in Tables 3.7 and 3.8.

Homogeneous catalytic deuteration of (88)

A solution of (88) (2.82 g, 10 mmol) in dry toluene (250 ml) was deuterated at 1 atmosphere pressure in the presence of Wilkinson's catalyst (100 mg). When uptake of deuterium ceased, the solution was passed through a florisil column (2 x 50 cm) and the product eluted with Et₂O (400 ml). The solvent was removed in vacuo and the crude product recrystallised from hexane/CHCl₃ to give 2.35 g (82%) of (90D) as a white solid m.p. 83 - 85°. A sample analysed by ²H NMR had 80% anti and 20% syn-deuterium. The deuterium content, as measured by EIMS, was d₀ 0.000, d₁ 1.081, and d₂ 98.763%.

Deutero-dilimide reduction of (88)

The procedure was analogous to that reported by Baird et al.¹⁴ Potassium azodicarboxylate (PADA) was slurried with EtOD and stored in vacuo at 0°C over anhydrous CaSO₄ for 20 hr. The EtOD was removed in vacuo and the PADA redried over P₂O₅. All the apparatus was carefully dried and (88) was washed with ice-cold EtOD before use.

A suspension of PADA (2.078g, 10.6 mmol) and (88) (1.20 g, 4.26 mmol) in EtOD (5 ml) was stirred under nitrogen and treated with CH₃CO₂D using a syringe pump (150 μl hr⁻¹) until the yellow colour had completely discharged. The mixture was diluted with H₂O (15 ml) and extracted with CH₂Cl₂ (3 x 15 ml). The combined organic extracts were washed successively with aqueous NaHCO₃ and H₂O, and then dried over anhydrous MgSO₄. The solution was filtered and concentrated in vacuo

to give 1.12 g of a white solid. ^1H NMR analysis showed the material to be a mixture of the reduced material (72%) and the unsaturated starting material (28%). The sample was subjected to the reduction on a further three occasions until ^1H NMR analysis showed the reduction was complete. The overall yield of (90D) was 1.04 g (85%). A sample recrystallised from CHCl_3 /hexane had m.p. 84 - 85°. Integration of the ^2H NMR showed the sample had 40% anti and 60% syn deuterium. The deuterium content, as measured by EIMS, was d_0 2.999, d_1 26.885, and d_2 70.142%.

2,3-Diazabicyclo[2.2.2]oct-2-ene (DBO) (2)

A solution of (90H) (0.5 g, 1.76 mmol) in 2 ml of CDCl_3 was stirred under nitrogen in the dark. Trimethylsilyliodide (1.056 g, 5.28 mmol) was added, dropwise, and the reaction mixture heated for 3 hr at 60°, monitoring the course by ^1H NMR. When complete, the solvent was removed in vacuo at ambient temperature and the residue treated with deoxygenated MeOH (5 ml, excess). A fast stream of nitrogen was bubbled through the solution and ca 5 g of crushed-ice added. The procedure was then identical to that used to prepare DBO from (86H). The yield of DBO after purification was 81 mg (42%), m.p. 141 - 142°. The spectral characteristics have been discussed previously.

2,3-Diazabicyclo[2.2.2]oct-2-ene (DBO) (3)

The procedure was identical to that discussed for the preparation of DBO from (86H) except that the samples were refluxed under nitrogen for 70 hr. Using 10 mmol samples of (90H) gave, on

average, 70-80% yields of DBO after purification. Samples of d_2 -DBO were obtained from (90D) and (86D) by the appropriate method. Deuterated samples had m.p. 142 - 143° and the syn/anti deuterium ratio's given in Tables 3.7 and 3.8.

Experimental For Chapter 4

Direct photolysis of DBO

Direct photolysis of DBO and d_2 -DBO was carried out according to the following general procedure: A sample of DBO (200 mg, 1.82 mmol) was dissolved in 20 ml of purified n-pentane. The solution was placed in the photolysis cell, a 0.5 cm x 5 cm pyrex annulus encircling the water-cooled light source. The solution was irradiated with a 500 W medium pressure mercury lamp. The reaction was monitored by DBO consumption using UV spectroscopy ($\lambda_{\text{MAX}}^{\text{Pentane (DBO)}}$ 375 nm). After 2-3 hr the solution became cloudy due to the known formation of the singlet excited state quencher. The time required for complete DBO consumption varied from 4-7 days. When the photolysis was complete, the solution was passed through an alumina column (100-200 mesh, 1 cm x 20 cm) and eluted with 100 ml of purified n-pentane. The eluent was carefully concentrated through a 20 cm x 1 cm glass-helix column until the volume of colourless residue was 1-2 ml. The pentane solution could be analysed by ^1H NMR to check the presence of hexa-1,5-diene, cyclohexene and BCH (identified by their olefinic and bridgehead resonances, respectively). When protio samples of DBO were photolysed, prep. g.c. (10 mm 20% SE30 column at 80°) of the residue enabled hexa-1,5-diene to be isolated (retention time 9.6 min). BCH and cyclohexene co-chromatographed under these conditions (retention time 18.9 min). When deuterated samples of DBO were photolysed, the pentane residue was analysed by ^2H NMR. The spectra have been discussed in the text.

Sensitised photolysis of DBO

Sensitised photolyses of DBO and d_2 -DBO were carried out according to the following general procedure. A sample of DBO (200 mg, 1.82 mmol) was dissolved in purified n-pentane (20 ml) with m-methoxyacetophenone (60 mg, 0.4 mmol) as sensitiser. The solution was placed in a quartz test-tube fitted with a rubber septum cap and irradiated in a Rayonet apparatus fitted with 300 nm medium pressure mercury lamps. Quantitative UV spectroscopy showed that the sensitiser had an extinction coefficient (ϵ) of 3,047 at 300 nm whereas DBO absorption at this wavelength is minimal. The course of the photolysis was monitored by withdrawing aliquots and measuring the consumption of DBO as discussed for direct photolysis runs. When the reaction was complete (4-7 days) the solution was chromatographed and concentrated as in the direct photolysis. When protio samples of DBO were photolysed, the concentrated residues were subjected to prep. g.c. (10 mm 20% SE30 80°). This enabled the products, BCH and hexa-1,5-diene, to be isolated. Isolated BCH (retention time 18.9 min) was shown to be uncontaminated by cyclohexene. When d_2 -DBO samples were photolysed the concentrated n-pentane residue was analysed by ^2H NMR. The spectra have been discussed in the text.

cis-exo-Bicyclo[2.2.0]hex-5-ene-2,3-dicarboxylic anhydride (100)

The procedure was modified from that reported by McDonald and Reineke.² A solution of cis-1,2-dihydrophthalic anhydride (99) (202 mg, 1.35 mmol) in anhydrous Et_2O (20 ml) was placed in a quartz test tube and irradiated at 254 nm in a Rayonet apparatus fitted with medium pressure mercury vapour lamps. The reaction was monitored by ^1H NMR

(disappearance of (99) olefinic signals (δ 6.05 and 5.71 ppm) and appearance of a sharp singlet (δ 6.45) for the olefinic protons of (100)) and was complete after 44 hr. The solvent was removed in vacuo to give crude product. This was purified by vacuum sublimation (50-60°, 0.01 - 0.04 mm Hg) to give 112 mg (55%) of the title compound as a white solid. This did not require further purification before use in the preparation of (101H). A sample recrystallised from hexane had m.p. 161-162° (lit.² 162-163°). ¹H NMR δ (CDCl₃): 3.39 (2H, s, bridgeheads); 3.68 (2H, s, 2 x α -H); 6.47 (2H, s, -CH=CH-).

cis-exo Bicyclo[2.2.0]hexane-2,3-dicarboxylic anhydride (101H)

cis-Bicyclo[2.2.0]hex-5-ene-2,3-dicarboxylic anhydride (92 mg, 0.61 mmol) was dissolved in 50 ml of EtOAc in a 100 ml flask. Palladium on charcoal (10%) (20 mg) was added and the flask attached to an atmospheric pressure hydrogenation apparatus and stirred vigorously at ambient temperature. When hydrogen uptake had ceased, the solution was filtered through celite and concentrated in vacuo to give (101H) in quantitative yield. A sample recrystallised from 1:1 Et₂O: pentane had m.p. 85-86° (lit.² 79-84°). The ¹H NMR was assigned by 400 MHz ¹H{¹H}nOe studies as described in Section 4.4. δ (CDCl₃): 2.23-2.32 (2H, m, 2 x endo-H); 2.70 - 2.79 (2H, m, 2 x exo-H); 3.10 - 3.14 (2H, m, bridgeheads); 3.54 (2H, s, 2 x α -H).

1,7-dimethyl-4-phenyl-2,5,6-triazatricyclo[5.2.2.0^{2,6}]undec-8-ene-3,5-dione (104). (1)

Cyclohexane-1,4-dione (15 g, 134 mmol) was dissolved in dry THF (50 ml) and stirred under nitrogen during the dropwise addition of 2.2

equivalents of methyl lithium in Et₂O (197 ml of a 1.5 M solution) at 0°. The mixture was allowed to warm to room temperature and then stirred for a further 2 hr under nitrogen. The mixture was then cooled to 0° and the excess methyl lithium quenched with H₂O. The ether layer was decanted and the THF/H₂O phase concentrated in vacuo to remove THF. The aqueous residue was then continuously extracted with EtOAc for 7 days. The combined organic extracts were concentrated in vacuo to give 11.42 g of an off-white solid. ¹H NMR analysis (CDCl₃) indicated the presence of two cis/trans isomers (methyl signals at δ 1.21 and 1.26 ppm) and about 20% unreacted dione (methylene singlet at δ 2.70 ppm). The IR spectrum showed O-H stretching at 2900-3450 cm⁻¹ and the C=O stretching of unreacted dienone. The crude mixture (11.4 g) was dissolved in 100 ml of pyridine and vigorously stirred during the dropwise addition of phosphoryl oxychloride (18.3 g, 119 mmol). The dark brown reaction mixture was warmed to 100° and the course of the reaction monitored by ¹H NMR (appearance of olefinic resonances). The reaction was complete after 3 hr and the pyridine solution was then poured onto ice and extracted with 30-40° petrol (3 x 100 ml). The combined petrol extracts were washed with H₂O (3 x 100 ml) and then passed down an alumina column (100-200 mesh, 2 x 50 cm). A further 100 ml of 30-40° petrol was passed down the column and the whole then concentrated through a 2 x 30 cm vigreux column until the volume of residue was 8-10 ml. ¹H NMR analysis of the residue (CDCl₃) showed the presence of three elimination products with olefinic signals at δ 4.71, 5.40, and 5.58 ppm, with integral ratio's of 16, 31, and 53%, respectively. The major product was the required 1,3-diene, the minor products being the 1,4-diene (31%) and the 1,4-exomethylene diene (16%). The petrol residue was treated with a solution of PTAD in EtOAc (4.2 g in 25 ml,

prepared as described for the synthesis of (85)) until the red colour of the PTAD just persisted. The solution was stirred for 15 hr and then concentrated in vacuo. The crude product was recrystallised from MeOH/CHCl₃ to give the title compound as white crystals. The yield of crystals was 1.52 g (4% from cyclohexane-1,4-dione). M.p. 171-172°. ¹H NMR δ (CDCl₃): 1.45-1.55 (2H, apparent d, J=8.8Hz, 2 x syn-H or 2 x anti-H); 1.95 (6H, s, 2 x CH₃); 2.10-2.20 (2H, apparent d, J=8.8Hz, 2 x syn-H or 2 x anti-H); 6.30 (2H, s, -CH=CH-); 7.30-7.46 (5H, m, aromatics).

1,7-dimethyl-4-phenyl-2,5,6-triazatricyclo[5.2.2.0^{2,6}]undec-8-ene-3,5-dione (104). (2)

The synthesis of (104) was analogous to that reported by Engel et al⁵ and the Birch reduction of p-xylene was modified from the procedure reported for the O-isomer: A three necked round bottom flask, fitted with a dry-ice condenser and surrounded by cotton-wool, was charged with 150 ml of liquid NH₃ and then mechanically stirred while 25 ml of dry THF, 25 ml of absolute EtOH, and p-xylene (15.9 g, 150 mmol) were added in that order. The milky-white solution was then slowly treated with finely cut pieces of sodium (10.35 g, 450 mmol in total). On each addition the solution turned blue and then milky-white as the sodium was consumed. When the addition was complete the NH₃ was allowed to evaporate (ca 4 hr) and the flask then fitted with a reflux condenser. The residue was then carefully treated with 50 ml of ice-water to dissolve the salts. The aqueous solution was extracted with 30-40° petrol (3 x 100 ml) and the combined organic extracts dried over anhydrous MgSO₄. The solution was filtered and concentrated through a 2 x 30cm vigreux column. The residue was

distilled to yield 11.85 g of colourless liquid (B.p. 40-43°, 15-20 mm Hg). ¹H NMR analysis showed the product to be a mixture of starting material (25%) and the required 1,4-diene (75%). The 1,4-diene had the following ¹H NMR data: δ (CDCl₃): 1.69 (6H, s, 2 x -CH₃); 2.58 (4H, s, 2 x CH₂); 5.40 (2H, s, 2x=CH). The distilled mixture (11.8g) was dissolved in 150 ml of DMSO (distilled from CaH₂) and treated with a 1:1 complex of Bu^tOK:Bu^tOH (2.07 g, 11.07 mmol) under nitrogen. The reaction mixture was heated to 100° and the progress of the isomerisation monitored by withdrawing aliquots and recording ¹H NMR spectra. The relevant signals were the olefinic resonances at δ (DMSO): 5.43 (1,4-diene); 5.58 (1,3-diene); and the aromatic resonance of p-xylene. After 2 hrs the reaction had reached equilibrium (ca 41% 1,3-diene) and the dark yellow solution was cooled in an ice-bath and diluted with H₂O (300 ml). The mixture was extracted with 30-40° petrol (3 x 150 ml) and the combined extracts dried over anhydrous MgSO₄, filtered, and concentrated through a 2 x 30 cm vigreux column. The residue was treated with PTAD in EtOAc as described previously. The yield of recrystallised (104) was 6.1 g (14% from p-xylene). The sample had m.p. and spectral properties previously described.

Hydrogenation and deutero-genation of (104). Preparation of 1,7-dimethyl-4-phenyl-2,4,6-triazatricyclo[5.2.2.0^{2,6}]undec-ane,3,5-dione (105H), and (105D)

The procedure for the reduction of (104) was identical for that described for (85) in the experimental for Chapter 3. A sample of (105H) recrystallised from EtOH had m.p. 157-158°. IR ν max: 1705, 1760 cm⁻¹ (C=O). The ¹H NMR was discussed in Section 4.8. The

apparent doublets at 2.01 and 1.70 ppm corresponding to the syn and anti proton resonances were assigned by $\text{Eu}(\text{FOD})_3$ LSR studies identical to those discussed for (86) in Chapter 3. The relevant data for the graphs in Figure 4.9 were:

$\text{Eu}(\text{FOD})_3$ mg	0	7.8	17.0	27.5	43.3
61.3					
Chemical shift $\Delta\delta$ ppm	1.70	2.07	2.47	2.91	3.56
4.28					
Chemical shift $\Delta\delta$ ppm	2.01	2.51	3.03	3.62	4.67
5.45					

Samples of (105D) were prepared by atmospheric deuteration of (104) using the catalysts and solvents given in Table 4.7. The procedure using Wilkinson's catalyst in toluene was identical to that described in the Experimental for Chapter 3. The syn/anti deuterium ratio's in samples of (105D) were measured by ^2H NMR, and the deuterium incorporation estimated from ^1H NMR spectra.

1,4-Dimethyl-2,3-diazabicyclo[2.2.2]oct-2-ene (DMDBO)

The preparation of DMDBO from (105H) was identical to that described for the hydrolysis and oxidation of (86H) in the experimental for Chapter 3. A purified sample had m.p. $71-72^\circ$ (lit.⁵ $70.5 - 71.5^\circ$). The ^1H NMR was described in Section 4.8. The two apparent doublets at 1.47 and 1.12 ppm were assigned by $\text{Eu}(\text{FOD})_3$ LSR studies. The relevant data for the graphs in Figure 4.9 were;

$\text{Eu}(\text{FOD})_3$ mg	0	11.5	23.0	35.0	53.1
Chemical shift $\Delta\delta$ ppm	1.12	2.73	4.34	6.03	8.48
Chemical shift $\Delta\delta$ ppm	1.47	2.52	3.60	4.73	6.36

Samples of d_2 -DMDBO were prepared from samples of (105D) in the same manner. Their syn/anti ratio's of deuterium were determined from 2H NMR spectra.

Direct and sensitised photolyses of DMDBO and d_2 -DMDBO

The photolyses were carried out using the same procedure described for DBO. The course of the photolyses was monitored by consumption of DMDBO ($\lambda_{\text{max}}^{\text{Pentane}}$ 380 nm) by UV spectroscopy. The pentane residues from d_2 -DMDBO photolyses were analysed by 2H NMR and gave the data given in Section 4.12. The hydrocarbon products could be isolated by prep. g.c. (10 mm 20% SE30 column, 100°). The products had the following retention times: DMBCH, 15.5 min; 1,4-dimethylcyclohexa-1,3-diene, 19.4 min; 1,4-dimethylcyclohex-1-ene, 28.6 min. The latter product was only formed in the direct photolysis.

Experimental for Chapter 5cis-Cyclobutane-2,3-dicarboxylic anhydride (113)

The procedure was similar to that reported by Owsley and Bloomfield.⁶ A solution of maleic anhydride (15.0 g, 150 mmol) and benzophenone (0.8 g, 4.4 mmol) in AR acetone was degassed with nitrogen for 15 min. The solution was saturated with ethylene, cooled to -78° , and irradiated with a 500 W medium pressure mercury lamp immersed in the solution in a water-cooled quartz well which was insulated by a high vacuum. Ethylene was bubbled through the solution at a rate of 125 ml min^{-1} and the extent of reaction monitored by ^1H NMR (maleic anhydride consumption). After the reaction was complete (12.5 hr) nitrogen was bubbled through the solution for 15 min. The solvent was removed in vacuo to give 23.88 g of a white residue. ^1H NMR analysis showed this to be a mixture of product (78%) and oxetane impurity formed by 2+2 addition of acetone and ethylene (22%). The residue was distilled to give the title compound as pure product (B.p. $98-110^{\circ}$, 0.1 - 0.5 mm Hg). The yield was 12.85 g (68%). A sample recrystallised from Et_2O /pentane had m.p. $142-144^{\circ}$. ^1H NMR δ (CDCl_3): 2.31 - 2.49 (2H, m, 2 x endo-H or 2 x exo-H); 2.71 - 2.92 (2H, m, 2 x endo-H or 2 x exo-H); 3.51 - 3.60 (2H, m, 2 x α -H). IR ν max: 1800, 1700 cm^{-1} (C=O).

cis-1,2-bis-hydroxymethylcyclobutane (114)

A suspension of lithium aluminium hydride (0.88 g, 23 mmol) in dry THF (30 ml) was stirred under nitrogen at 0° during the dropwise addition of a solution of cis-cyclobutane-2,3-dicarboxylic anhydride

(1.26 g, 10 mmol) in dry THF (20 ml). The mixture was allowed to warm to room temperature and then refluxed for 1.5 hr. After this time, the reaction mixture was treated with sufficient quantities of a 1:1 celite/ $\text{Na}_2\text{SO}_4 \cdot 10\text{H}_2\text{O}$ mixture to hydrolyse the aluminium salts. The mixture was filtered at the pump and the solid washed with 50 ml of THF. The THF solution was dried with anhydrous MgSO_4 , filtered, and concentrated in vacuo to give 0.96 g (83%) of the title compound as a colourless oil. $^1\text{H NMR } \delta$ (CDCl_3): 1.60 (2H, m, 2 x endo-H or 2 x exo-H); 1.81 (2H, m, 2 x endo-H or 2 x exo-H); 2.49 (2H, br s, 2 x OH); 3.41 (2H, m, 2 x CHH'OH); 3.60 (2H, m, 2 x CHH'OH). IR ν max: 3050-3600 cm^{-1} (O-H).

Cis-1,2-bis-*p*-toluenesulphonate methyl cyclobutane (115)

A solution of *p*-toluenesulphonyl chloride (1.80 g, 9.45 mmol) in dry pyridine (20 ml) was treated with (114) (0.5 g, 4.31 mmol) at 0°. The solution was stirred at 0° for 20 hr and then poured on to ice. The solid was filtered at the pump and recrystallised from MeOH to give the title compound (0.45 g, 25%) as white rhomboid crystals. M.p. 56-57°. $^1\text{H NMR } \delta$ (CDCl_3): 1.64 (2H, m, 2 x endo-H or 2 x exo-H); 2.01 (2H, m, 2 x endo-H or 2 x exo-H); 2.45 (6H, s, 2 x $-\text{CH}_3$); 2.71 (2H, m, bridgeheads); 4.04 (4H, m, 2 x CH₂ OTs); 7.54 (8H, AB quartet, $J = 8.6\text{Hz}$, aromatics).

Cis-1,2-bis-iodomethylcyclobutane (116). (1)

Sodium iodide (0.375 g, 2.5 mmol) and (115) (0.42 g, 1 mmol) were refluxed in acetone and the reaction monitored by t.l.c. (9:1 CH_2Cl_2 /pentane). After 2 hr, t.l.c. analysis showed all the tosylate

had reacted (R_f 0.43) and the presence of a new compound at R_f 0.70. The solvent was removed in vacuo and the residue subjected to prep t.l.c. (9:1 CH_2Cl_2 /pentane). The fastest moving band (263 mg, 78%) was the title compound. A sample recrystallised from EtOH gave white flakey crystals m.p. 32-33° (Found: C, 21.76; H, 2.82; I, 75.42. $\text{C}_6\text{H}_{10}\text{I}_2$ requires C, 21.45; H, 3.00; I, 75.55%). $^1\text{H NMR } \delta$ (CDCl_3): 1.60 (2H, m, 2 x endo-H or 2 x exo-H); 2.10 (2H, m, 2 x endo-H or 2 x exo-H); 2.81 (2H, m, bridgeheads); 3.22 (2H, t (overlapping dd), $J = 9.4 \text{ Hz}$, 2 x $-\text{CH}_2\text{H}'\text{I}$); 3.40 (2H, dd, $J = 9.4, 6.6 \text{ Hz}$, 2 x $-\text{CHH}'\text{I}$).

Cis-1,2-bis-iodomethylcyclobutane (116). (2)

A solution of (114) (0.3 g, 2.59 mmol) in chloroform (3 ml) was treated, dropwise, with trimethylsilyliodide (1.28 g, 6.43 mmol). The reaction flask was fitted with a rubber septum-cap and stirred in the dark. The reaction was monitored by withdrawing aliquots for t.l.c. analysis (9:1 CH_2Cl_2 /pentane). When the reaction was complete (22 hr) the reaction mixture was poured into 10 ml of saturated aqueous NaHCO_3 . The aqueous solution had 20 ml of CH_2Cl_2 added to it and the organic phase decanted. This was then washed with water and dried over anhydrous MgSO_4 . The solution was filtered and concentrated in vacuo to give the crude product. This was purified by silica-gel column chromatography (2 x 20 cm column) eluting with 9:1 CH_2Cl_2 /pentane. The yield of (116) was 0.63 g (72%). The spectral characteristics were as previously given.

Reaction of cis-1,2-bis-iodomethylcyclobutane with n-butyllithium

A sample of the iodide (0.315 g, 0.94 mmol) was dissolved in 1 ml of dry Et_2O and stirred under nitrogen during the dropwise addition

of n-butyllithium in n-pentane (0.5 ml of a 2M solution). The reaction was stirred at room temperature and the consumption of the iodide monitored by t.l.c. (9:1 CH₂Cl₂/pentane, R_F 0.70). After 1 hr t.l.c. analysis showed there was still some iodide present. A further 0.6 ml of the n-butyl lithium in pentane solution was added and the reaction stirred for a further 1 hr (t.l.c. analysis showed all the iodide had been consumed). The reaction mixture was refluxed for 1 hr and then treated with H₂O (0.054 ml, 3.0 mmol). The solution was passed through an alumina column (100-200 mesh, 1 x 5 cm) eluting with a further 20 ml of n-pentane. The solution was concentrated through a glass helix column until the volume of residue was approximately 0.5 ml. The residue was analysed by ¹H NMR and shown to contain only the resonances characteristic of hexa-1,5-diene.

Chemical isolation of d₂-BCH from d₂-DBO photolysates

The general procedure used to isolate d₂BCH from d₂-DBO photolysates was as follows: A sample of d₂-DBO (252 mg, 2.25 mmol) was subjected to direct photolysis in n-pentane as discussed in the experimental for Chapter 4. The n-pentane solution obtained after alumina column chromatography (ca 125 ml total volume) was placed in a three neck roundbottomed flask fitted with an adaptor to allow ozone to be passed into the solution and an outlet. The solution was cooled to -78° and ozone (generated with an arc-lamp from oxygen in a BOC mark II ozoniser) was bubbled into the solution until all the hexa-1,5-diene and cyclohexene had formed ozonides (disappearance of olefinic resonances by ¹H NMR analysis). The solution was allowed to warm to room temperature and then passed through an alumina column (100-200 mesh, 1 cm x 20 cm) eluting with a further 100 ml of

n-pentane. The eluent was concentrated through a glass helix column (1 x 20 cm) until the volume of residue was approximately 2 ml. Analysis of the residue by ^2H NMR showed that $\text{d}_2\text{-BCH}$ was the only deuterated hydrocarbon present (see Section 5.6.1). Samples of $\text{d}_2\text{-BCH}$'s were isolated from sensitised photolysis mixtures using an identical procedure.

Pyrolyses of $\text{d}_2\text{-BCH}$

All the pyrolyses of $\text{d}_2\text{-BCH}$ samples were carried out using 1-2 ml of the concentrated n-pentane solutions obtained from the ozonolysis and column chromatography procedure. The samples were sealed under nitrogen in glass tubes and heated in an oven at 180° for 21 hr (10.5 half-lives of the BCH decomposition reaction). The solutions were then analysed by ^2H NMR to determine secondary kinetic isotope effects for the cleavage reaction as discussed in Section 5.2.2.2, or converted to disulphones for the stereochemical analysis (see later).

2,5-Dichloro-1,6-bis-phenylthiohexane (129)

N-chlorosuccinimide (1.34 g, 10 mmol) was suspended in CH_2Cl_2 (10 ml) with stirring under nitrogen. Thiophenol (1.10 g, 10 mmol) was added dropwise over 0.5 hr and the white suspension immediately turned orange. The solution was allowed to stir under nitrogen for a further 0.5 hr and then hexa-1,5-diene added to the orange suspension until the colour was completely discharged. The solution was concentrated in vacuo and the residue shaken with 20 ml of CCl_4 . The solution was filtered, dried with anhydrous MgSO_4 , refiltered and

concentrated in vacuo to give 2.38 g of a yellow oil. ^1H NMR analysis showed this to be a 70:30 mixture of anti-Markovnikoff (128) and Markovnikoff (129) 1,2-adducts, respectively ($-\text{CHCl}$ and $-\text{CH}_2\text{Cl}$ resonances at δ 3.91 and 3.20, respectively). The crude sample was dissolved in 5 ml of DMSO and heated at 100° . The isomerisation was most conveniently monitored by ^1H NMR, comparing the integrals of the α -chloro proton signals. The reaction was complete after 2 hrs and the mixture poured into 10 ml of H_2O . The aqueous solution was extracted with CH_2Cl_2 (3 x 15 ml) and the combined organic extracts washed with H_2O (25 ml). The solution was dried over anhydrous MgSO_4 , filtered, and concentrated in vacuo to give 2.54 g of the title compound as a yellow oil. This was not purified further. ^1H NMR δ (CDCl_3): 1.65 - 2.40 (4H, m, 2 x $-\text{CH}_2\text{CHClCH}_2\text{SPh}$); 3.12 (2H, dd, $J=14.5, 8.3$ Hz, 2 x $-\text{CHH}'\text{SPh}$); 3.31 - 3.43 (2H, m, 2 x $-\text{CHH}'\text{SPh}$); 3.91 (2H, br s, 2 x $-\text{CHCl}$); 7.18 - 7.47 (6H, m, m-, p-aromatics); 7.50 (4H, d, $J=7.3$ Hz, o-aromatics). MS m/z (EI): 374, 372, 370 (M, 4.0, 16.6, 23.4%); 227 (50.7), 225 (82.3) (M-PhSCL); 123 (100).

2,5-Dichloro-1,6-bis-phenylsulphonyl hexane (130)

The crude sample of (129) from the previous experiment (2.54 g, 6.9 mmol) was dissolved in 25 ml of CH_2Cl_2 and stirred in an ice-bath. The solution was treated with 85% m-chloroperoxybenzoic acid (5.68 g, 28.0 mmol) portionwise over 0.5 hr. The reaction was allowed to warm to room temperature and stirred for a further 1 hr. The reaction mixture was then poured into saturated aqueous NaHCO_3 (50 ml) and NaHSO_3 (10 ml), and extracted with CH_2Cl_2 (2 x 20 ml). The combined organic extracts were dried over anhydrous MgSO_4 , filtered, and concentrated in vacuo to give 2.194 g of crude title compound. This

did not require further purification for the dehydrochlorination step. This was especially true when disulphones were being prepared for the stereochemical analysis as isotopic fractionation could occur. A crude sample of the protio material formed crystals of one diastereoisomer on standing. They were isolated and recrystallised from EtOH to give white needle-like crystals m.p. 157.5 - 158°. ^1H NMR δ (CDCl_3): 1.86 - 2.40 (4H, m, $2 \times \text{CH}_2\text{CHH}'\text{SO}_2\text{Ph}$); 3.14 (2H, dd, $J=14.6$, 4.9Hz , $2 \times \text{-CHH}'\text{SO}_2\text{Ph}$); 4.38 (2H, br s, $2 \times \text{-CHCl}$); 7.60 - 7.81 (6H, m, m-, p-aromatics); 7.93 (4H, d, $J=7.3\text{Hz}$, o-aromatics). MS m/z (EI): 401, 399 (M-Cl, 1.2, 4.0%); 363 (M-2HCl, 3); p 297, 295, 293 (M-SO₂Ph, 2.4, 11.6, 16.8); 221 (17); 195 (34); 143 (59); 141 (24); 125 (68); 115 (45); 79 (60); 77 (100).

EE-1,6-bis-phenylsulphonylhexa-1,5-diene (132)

A crude sample of (130) prepared as discussed in the previous experiment (2.10 g, 4.82 mmol) was dissolved in DMSO (10 ml) containing anhydrous NaOAc (1.58 g, 19.3 mmol). The reaction was stirred at room temperature and monitored by ^1H NMR (appearance of olefinic resonances). When the reaction was complete (2 hr) the solution was diluted with H₂O (20 ml) and extracted with CH₂Cl₂ (3 x 20 ml). The combined organic extracts were washed with H₂O (2 x 20 ml), dried over anhydrous MgSO₄, filtered and concentrated in vacuo to give 2.0g of crude product as a yellow oil. Crystals formed on standing, which were removed and recrystallised from EtOH to constant m.p. The white needle-like crystals had m.p. 123 - 123.5°. (Found: C, 59.57; H, 5.01; S, 17.52. C₁₈H₁₈O₄S₂ requires: C, 59.65; H, 5.00; S, 17.69%). ^1H NMR δ (CDCl_3): 2.40 (4H, m, $2 \times \text{-CH}_2\text{CH=CHSO}_2\text{Ph}$); 6.34 (2H, d, $J=14.6\text{Hz}$, $2 \times \text{-CH=CHSO}_2\text{Ph}$); 6.91 (2H, m, $\text{-CH}_2\text{CH=CHSO}_2\text{Ph}$); 7.49

- 7.68 (6H, m, p-, m-aromatics); 7.84 (4H, d, J=7.3Hz, o-aromatics).
MS m/z CI (CH₄): 363 (MH⁺, 100%); 221 (28); 143 (19); 125 (14); 111
(16).

Preparation of EE-1,6-bis-phenylsulphonylhexa-1,5-dienes from d₂-DBO
photosylates and d₂-BCH pyrolyses samples

The general procedure used to obtain samples of disulphones for the stereochemical analysis was as follows: A concentrated n-pentane solution of deuterated hydrocarbons from direct or photosensitised decomposition of d₂-DBO (obtained as discussed in the experimental for Chapter 4) or from pyrolysis of d₂-BCH (obtained as discussed on p.271) was treated with a solution of PhSCl in CH₂Cl₂ (prepared as noted previously) until the yellow colour just persisted. The sample was allowed to stir over night and then analysed by ¹H NMR. If the spectrum showed olefinic resonances, more PhSCl/CH₂Cl₂ solution was added and stirring continued until all the olefinic species had reacted. When the reaction was complete the procedure was identical to that given earlier, monitoring all reactions by ¹H NMR. Samples of disulphones were recrystallised from EtOH to constant m.p. (123-123.5°) and then analysed for deuterium content by CIMS (CH₄) as discussed in Section 5.3.3.1 and Appendix 1. The sample was then recrystallised and reanalysed to ensure consistent data. The proportions of d₀-, d₁- and d₂-disulphones obtained from three such MS runs were corrected (see Appendix 5) and gave the stereochemical results shown in Tables 5.7.

O,O-hexenyl-1,6-bis-S-methyldithio carbonate (139)

Freshly ground NaOH (3.24 g, 81.0 mmol) and hexane-1,6-diol (4.76 g, 40.4 mmol) were dissolved in anhydrous THF (24 ml) and CCl₄ (2 ml). The mixture was stirred under nitrogen during the dropwise addition of carbon disulphide (6.31 g, 82.0 mmol). The yellow suspension was stirred for 3 hr under nitrogen and then treated with freshly distilled methyl iodide (11.36 g, 80.0 mmol). The mixture was refluxed for 14 hr, cooled, and then diluted with Et₂O (200 ml). The inorganic salts were filtered at the pump, and the Et₂O washed with H₂O (5 x 100 ml). The organic phase was dried over anhydrous MgSO₄, filtered, and concentrated in vacuo to give 11.40 g (94%) of the title compound as a pale yellow oil that crystallised on standing. A sample recrystallised from EtOH had m.p. 30.5 - 31°. ¹H NMR δ (CDCl₃): 1.41 (4H, m, 2 x -CH₂CH₂CH₂OCS₂CH₃); 1.78 (4H, m, 2 x -CH₂CH₂OCS₂CH₃); 2.50 (6H, s, methyls); 4.59 (4H, t, J=7.2Hz, 2 x -CH₂CH₂OCS₂CH₃). IR ν max: 1120 cm⁻¹ (C=S). MS m/z (CI, NH₃): 2.99 (MH⁺, 72.4%); 191 (M⁺-COS, MeSH, 100); 163 (43.9); 131 (20.0); 99 (14.3); 91 (19.0).

Pyrolysis of O,O-hexenyl-1,6-bis-S-methyldithiocarbonate

A three neck round bottom flask fitted with thermometer, dropping funnel and vigreux column, was charged with 50 ml of diphenyl ether. A liquid nitrogen cooled cold trap was attached to the end of the vigreux column and the diphenyl ether brought to its boiling point under a nitrogen atmosphere. A crude sample of O,O-hexenyl-1,6-bis-S-methyldithiocarbonate (1.49 g, 5.0 mmol) was added dropwise to the boiling solvent and the volatile products collected in the cold trap. The weight of volatile product collected

was 0.85 g. ^1H NMR analysis showed that methyl thiol and hexa-1,5-diene were the major products. The crude product was passed through an alumina column (100-200 mesh, 1 x 20 cm) and the hexa-1,5-diene eluted with n-pentane. The pentane solution was concentrated through a glass helix column until the volume of residue was approximately 3 ml. ^1H NMR analysis showed the residue only contained hexa-1,5-diene. The pentane solution could then be treated with $\text{PhSCl}/\text{CH}_2\text{Cl}_2$ solutions to prepare disulphones as discussed earlier.

Trans-hex-3-ene-1,6-dioic acid dimethyl ester (133)

Trans-hex-3-ene-1,6-dioic acid (2.0 g, 13.9 mmol) was placed in a three neck round bottom flask fitted with a dropping funnel, reflux condenser, and a drying tube. Freshly distilled thionyl chloride (3.64 g, 30.56 mmol) was added to the flask and the resultant orange solution treated with a catalytic amount of dimethyl formamide (0.223 g, 3.06 mmol). The solution became a deeper orange and gases were evolved. The solution was stirred for 0.5 hr at room temperature and then for 0.5 hr at 70° . The dark brown solution was cooled and then treated with excess MeOH and quenched with saturated aqueous NaHCO_3 . The solution was extracted with CH_2Cl_2 (3 x 50 ml) and the combined organic extracts washed with H_2O (50 ml), dried over anhydrous MgSO_4 , filtered, and concentrated in vacuo. The crude product was distilled to give 1.40 g (59%) of the title compound as a pale yellow liquid (B.p. $110 - 115^\circ$, 15 - 20 mm Hg). ^1H NMR δ (CDCl_3): 3.05 (4H, m, 2 x $-\text{CH}_2\text{CO}_2\text{CH}_3$); 3.65 (6H, s, methyls); 5.54 (2H, m, $-\text{CH}=\text{CH}-$). IR v max: 1740 cm^{-1} (C=O).

Hydrogenations of trans-hex-3-ene-1,6-dioic acid, trans-hex-3-ene-1,6-dioic acid dimethyl ester, and trans-hex-3-ene-1,6-diol

All the catalytic hydrogenations were carried using the general procedure given for the hydrogenations of (85) or (88) in the experimental for Chapter 3, using the solvents and catalysts given in Table 5.3. The crude products were analysed by ^1H NMR and IR (see Table 5.3). The diimide reduction of (133) was achieved by the procedure given for (88) in the experimental for Chapter 3. The results in Table 5.3 show that only the reduction of (134) in EtOH/PtO₂ and (133) in toluene/Wilkinson's catalyst proceeded smoothly. The products hexane-1,6-dioic acid (136) and hexane-1,6-dioic acid dimethyl ester (135) had the following ^1H NMR data: (135) δ (CDCl₃): 1.60 (4H, m, β -H's); 2.28 (4H, m, α -H's); 3.60 (6H, s, methyls). (136) δ (D₂O): 1.57 (4H, m, β -H's); 2.35 (4H, m, α -H's).

Replacement of hydrogen for deuterium (and EtOD for EtOH in the reduction of (134)) led to samples of (136D) and (135D). The samples were analysed by ^1H NMR and ^2H NMR. The ^2H NMR of (136D) showed that 22% of the incorporated deuterium was located at the α -carbons, and 78% at the β -carbons. The ^1H NMR of (135D) showed approximately 90% deuterium incorporation. The ^2H NMR of (135D) showed that 31% of the deuterium was located at the α -carbons and 69% at the β -carbons.

Trans-hex-3-ene-1,6-diol (137)

A suspension of lithium aluminium hydride (0.23 g, 6.05 mmol) in anhydrous THF (100 ml) was stirred under nitrogen at 0° during the

dropwise addition of trans-hex-3-ene-1,6-dioic acid dimethyl ester (0.50 g, 2.91 mmol) in THF (50 ml). The reaction was allowed to warm to room temperature and then refluxed for 2.5 hr. The sample was cooled and treated with sufficient 1:1 celite/ $\text{Na}_2\text{SO}_4 \cdot 10\text{H}_2\text{O}$ to hydrolyse the aluminium salts, filtered, and concentrated in vacuo to give 0.27 g (80%) of the title compound as a colourless oil. This required no further purification. ^1H NMR δ (CDCl_3): 2.36 (4H, m, 2 x $-\text{CH}_2\text{CH}_2\text{OH}$); 3.71 (4H, t, $J=7.3$ Hz, 2 x $-\text{CH}_2\text{CH}_2\text{OH}$); 5.56 (2H, m, $-\text{CH}=\text{CH}-$). IR ν max: 3700-3100 (O-H); 1610 cm^{-1} (C=C).

Experimental for Chapter 61,4-Dimethylcyclohexane-1-ol (149)

4-Methylcyclohexanone (11.8 g, 105 mmol) was dissolved in anhydrous Et₂O (150 ml) and stirred under nitrogen during the dropwise addition of a solution of methyl lithium in Et₂O (90 ml of a 1.5 M solution). The solution was stirred at room temperature for 1 hr and then quenched with H₂O. The organic layer was decanted, washed with water (100 ml) and then dried over anhydrous MgSO₄. Filtration and concentration of the solution *in vacuo* gave 12.22 g (91%) of the title compound as a colourless liquid. ¹H NMR analysis showed the product to be a mixture of *cis* and *trans* isomers (2 methyl signals at 1.10 and 1.15 ppm (*cis* and *trans* -C(OHCH₃)) and two doublets (J=4.9Hz) at 0.81 and 0.92 ppm (*cis* and *trans* -CHCH₃)). The product was not purified further before being used to prepare 1,4-dimethyl cyclohex-1-ene.

1,4-Dimethylcyclohex-1-ene (150)

1,4-Dimethylcyclohexane-1-ol (12.0 g, 93.75 mmol) was dissolved in dry pyridine (150 ml) and treated, dropwise at 0°, with POCl₃ (18.0 g, 227.8 mmol). The temperature was then raised to 100° and the course of the reaction monitored by ¹H NMR (appearance of olefinic signals). The reaction was complete after 1.5 hr and the solution was carefully poured onto ice. The aqueous solution was extracted with 30-40° petrol (3 x 150 ml) and the combined organic extracts washed successively with aqueous 2M HCl (150 ml), H₂O, aqueous saturated NaHCO₃, and water. The petrol solution was then passed through an

alumina column (100-200 mesh, 2 x 30 cm) eluting with a further 100 ml of 30-40° petrol. The eluent was concentrated through a short vigreux column until the volume of residue was approximately 10 ml. Distillation of the residue gave 6.30 g (61%) of the title compound as a colourless liquid (b.p. 30-40°, 15-20 mm Hg). Samples used as analytical g.c. standards were further purified by prep. g.c. (10% SE30, 120°, retention time 4.75 min). ¹H NMR δ (CDCl₃): 0.94 (3H, d, J=4.9Hz, -CHCH₃); 1.24-2.15 (7H, complex multiplets, aliphatics); 1.65 (3H, s, -C=CCH₃); 5.34 (1H, br s, -C=CH).

Direct photolysis of DBO and DMDBO

These photolyses were carried out analogously to the procedures discussed in the experimental for Chapter 4. Thus, direct photolyses of DMDBO were carried out using 1% solutions of the azoalkane in purified n-pentane. On large scale photolyses (200 mg of azoalkane) it was possible to isolate the products by prep.g.c. (10 mm, 20% SE30 column). The relative retention times were given in the experimental for Chapter 4. The fraction collected with retention time 28.6 min had identical g.c. and spectroscopic properties to independently synthesised 1,4-dimethylcyclohex-1-ene. Analytical g.c. analysis of DMDBO product mixtures were carried out using a 3% SE30 column at 70°. The products had relative retention times of 124, 235, and 319 s for DMBCH, 1,4-dimethylhexa-1,5-diene, and 1,4-dimethylcyclohex-1-ene, respectively. Integration of the signal suggested that the cyclohexene was at least 10% of the product distribution. Direct photolyses of DBO were carried out using 1% solutions of the azoalkane in n-decane in order to analyse the products by g.c. Product analysis by capillary g.c. (OV101, 50°) showed that BCH co-chromatographed with authentic cyclohexene at 141s.

Sensitised photolysis of DBO and DMDBO

These were carried out as discussed in the experimental for Chapter 4. Cyclohexenes were shown to be absent by ^2H NMR analysis and also by g.c. analysis (3%, SE30, 70°) for DMDBO samples.

Pyrolysis of DMBCH and BCH

Samples of d_2 -BCH were pyrolysed in sealed glass tubes and the products analysed by ^2H NMR as discussed in the experimental for Chapter 5. DMBCH samples (obtained from prep. g.c.) were pyrolysed as 1% solutions in n-pentane in sealed glass tubes for 8 hr at 170° (4 half-lives of the cleavage reaction). Analytical g.c. (3% SE30, 70°) showed that 1,4-dimethylcyclohex-1-enes were not produced.

Pyrolysis of DMDBO and d_2 -DBO

The pyrolysis were carried out in sealed glass tubes and the products analysed by analytical g.c. in the case of DMDBO, and ^2H NMR for d_2 -DBO. DMDBO samples (10 mg) were pyrolysed in 1% solutions in pentane for 2.5 hr at 240° (10.5 half-lives of the decomposition reaction) while d_2 -DBO samples (25 mg) were pyrolysed in 2ml of n-pentane for 17 hr at 230° (5 half-lives of the decomposition reaction). The solution from the latter reaction was analysed directly by ^2H NMR after the pyrolysis without further treatment. Both reactions were shown not to produce cyclohexenes.

All the pyrolysis experiments had control samples of the appropriate cyclohexenes which were pyrolysed under the same conditions and shown to be unaffected by the treatment.

Wilkinson's catalyst deuteration of 4-phenyl-2,4,6-triazatricyclo
[5.2.2.0^{2,6}]undec-8-ene-3,5-dione (85)

The deuteration was carried out using the procedure discussed for the Wilkinson's catalyst reduction of (88) in the experimental for Chapter 3. The sample of (86D) obtained was shown to contain 60% syn and 40% anti deuterium by integration of its ²H NMR. The sample was subsequently converted to d₂-DBO using the procedure discussed in the experimental for Chapter 3. Direct photolysis of the sample and product analysis by ²H NMR enabled the stereoselectivity of cyclohexene formation to be deduced (see Section 6.4 and Appendix 6).

Experimental for Chapter 73,6,6-Trimethylcyclohexa-1,4-dien-3-ol (166)

A solution of 4,4-dimethylcyclohexa-2,5-dienone (9.0 g, 73.0 mmol) in anhydrous Et₂O (40 ml) was stirred under nitrogen at 0° during the dropwise addition of methyl lithium in ether (60 ml of a 1.6 M solution). When the addition was complete the reaction was allowed to warm to room temperature and stirred for 1 hr. The flask was cooled in an ice-bath and the reaction quenched with H₂O. The organic layer was decanted, dried over anhydrous MgSO₄, filtered and concentrated in vacuo to give the title compound as an orange oil (9.57 g, 95%). This did not require further purification. ¹H NMR δ (CCl₄): 1.00 (3H, s, C(6)-CH₃); 1.05 (3H, s, C(6)-CH₃); 1.18 (3H, s, C(3)-CH₃); 5.55 (4H, AB quartet, J=9.7Hz, olefinics).

3,3-Dimethyl-6-methylenecyclohexa-1,4-diene (153)

A solution of (166) (5.0 g, 36.0 mmol) in pyridine (75 ml) was stirred under nitrogen at 0° during the dropwise addition of POCl₃ (8.0 g, 52.0 mmol). The reaction was allowed to warm to room temperature and monitored by ¹H NMR (analysis of the olefinic region). The reaction was usually complete in 2 hr. The mixture was then poured onto ice and extracted with 30-40° petrol (3 x 50 ml). The combined petrol extracts were washed with H₂O (3 x 20 ml) and then passed through an alumina column (2 x 30 cm) eluting with a further 100 ml of petrol. The eluent was concentrated through a glass-helix column until the volume of residue was approximately 5 ml. The residue was distilled to give 3.9 g of a colourless liquid (B.p.

38-40°, 15-20 mm Hg). ^1H NMR showed that the product was contaminated with 1,2,4-trimethyl benzene (see Section 7.4.1). Further purification for photolysis was accomplished by prep. g.l.c. (10 mm Carbowax column, 160°). The ^1H NMR spectral data were δ (CCl_4): 1.14 (6H, s, methyls); 4.69 (2H, s, $=\text{CH}_2$); 5.80 (4H, AB quartet, $J=10.0\text{Hz}$, olefinics).

Exploratory photolyses

A stock solution of triene (0.06 M) in acetonitrile was irradiated in the presence of freshly sublimed dimethyl fumarate or fumaronitrile (0.14 M) in 0.3 ml quartz cells fitted with rubber septum caps. The irradiations were carried out using a Rayonet apparatus fitted with 254 nm medium pressure mercury lamps. The photolyses were monitored by g.c. at low temperatures (80°, 10% SE30) for triene consumption and higher temperatures (10% SE30, 180° for fumaronitrile adducts, 200° for dimethyl fumarate adducts) and then analysed by GC/MS, using the same high temperature chromatographic conditions, to determine if 1:1 adducts had been formed (see Section 7.4.2).

Preparative scale photolyses

A stock solution of triene (25 ml, 0.06 M in acetonitrile) was irradiated in the presence of freshly sublimed fumaronitrile (0.14 M) in quartz test tubes fitted with rubber-septum caps. The light source was a Rayonet apparatus fitted with 254 nm medium pressure mercury lamps and the reactions were monitored by low and high temperature g.c. analysis as previously described. When complete the solvent was

removed in vacuo and unreacted diylophile removed from the residue by vacuum sublimation (60-70°, 15-20 mm Hg). The remaining residue (0.49 g) was analysed by GC/MS (EI) (180°, 10% SE 30) and shown to contain 1:1 adducts (m/z, M 199). The crude product was subjected to column chromatography (200-400 mesh silica gel, 2 cm x 30 cm) eluting with 5% MeOH/CH₂Cl₂ and collecting 25 ml fractions. The fractions were analysed by g.c. (180°, 10% SE 30) and the adduct shown to have eluted after 250 ml. Removal of the solvent in vacuo gave the ¹H NMR (400 MHz) shown in Figure 7.3. Crystallisation from IPA gave colourless flakey-crystals (m.p. 102-103°) which were analysed by x-ray diffraction and shown to be 2',2'-dimethylspiro[bicyclo[2.2.1]hept-5-ene-7,1'-cyclopropane]-2-endo-3,exo-dicarbonitrile (168).

1,1-Dimethylspiro[4.2]hepta-4,6-diene (155)

A suspension of sodium hydride (0.523 g, 21.80 mmol) in dry DMSO (15 ml) was stirred under nitrogen with trimethyloxosulphonium iodide (4.809 g, 21.86 mmol) for 1 hr. After this time dimethylfulvene (2.0 g, 18.80 mmol) was slowly added to the grey-white suspension until the orange colour of the fulvene just persisted. The mixture was poured onto ice and extracted with 30-40° petrol (3 x 50 ml). The combined petrol extracts were dried over anhydrous MgSO₄, filtered, and concentrated through a glass-helix column until the volume of residue was approximately 3 ml. This was distilled to give 1.73 g (77%) of the title compound as a colourless liquid (B.p. 45-47°, 15-20 mm Hg). ¹H NMR δ (CDCl₃): 1.40 (6H, s, methyls); 1.76 (2H, s, cyclopropyl H's); 6.30 (2H, m, 4-H, 7-H or 5-H, 6-H); 6.51 (2H, m, 4-H, 7-H or 5-H, 6-H).

Photolysis of fumaronitrile

Freshly sublimed fumaronitrile (3.25 g, 41.7 mmol) was dissolved in acetonitrile (25 ml) and irradiated in a quartz test-tube with 254 nm light from medium pressure mercury lamps in a Rayonet. The isomerisation was monitored by ^1H NMR (δ (CDCl_3) olefinic signals at 6.20 and 6.27 ppm for fumaronitrile and maleonitrile, respectively) and shown to be a 1:1 mixture of cis and trans isomers after 72 hrs irradiation. The solvent was removed in vacuo and the residue sublimed at 60-70° (15-20 mm Hg) to give 2.61 g of a 1:1 fumaronitrile maleonitrile mixture.

Reaction of 1,1-dimethylspiro[4.2]hepta-4,6-diene with olefins

The general procedure for the reaction of the spirodiene with fumaronitrile, 1:1 maleonitrile and fumaronitrile, dimethylmaleate, and dimethyl fumarate was as follows: A solution of the spirodiene (0.40 g, 3.33 mmol) and freshly sublimed olefins (1.1 mole equivalents) in EtOH (15 ml) was refluxed with stirring until all the spirodiene had reacted (^1H NMR analysis). When the reaction was complete the solvent was removed in vacuo and excess olefin removed by vacuum sublimation. The residue was analysed by ^1H NMR and capillary g.c. The products were identified by $^1\text{H}\{^1\text{H}\}_n\text{Oe}$ studies as discussed in the text. The following results were obtained:

Reaction with fumaronitrile

^1H NMR δ (CDCl_3): The residue was shown to contain two trans adducts (capillary g.c. retention times 420 s and 450 s, OV101, 140°).

The major adduct was crystallised on standing. Isolation and recrystallisation from IPA gave white-flakey crystals m.p. 102-103°. The sample had identical spectroscopic properties to (168) isolated from the photolysis of the triene in the presence of fumaronitrile. (Found: C, 78.64; H, 7.35; N, 13.76. $C_{13}H_{14}N_2$ requires C, 78.75; H, 7.12; N, 14.13%). 1H NMR δ ($CDCl_3$): 0.48 (1H, d, $J=5.7$ Hz, 3'-H); 0.73 (1H, d, $J=5.7$ Hz, 3'-H); 1.06 (3H, s, methyl); 1.07 (3H, s, methyl); 2.59 (1H, d, $J=4.3$ Hz, 2-H); 2.90 (1H, m, 1-H or 4-H); 3.02 (1H, m, 1-H or 4-H); 3.50 (1H, dd, $J=4.3, 4.2$ Hz, 3-H); 6.47 (2H, m, 5-H, 6-H). IR ν max: 2240 cm^{-1} ($C \equiv N$). MS m/z (EI): 198 (M, 1.3%); 171 (M-HCN, 2); 156 (8); 120 (21); 105 (100); 78 (10).

Reaction with fumaronitrile and maleonitrile mixture

1H NMR analysis showed the presence of the trans adducts and two cis adducts, (171) and (172). Crystals formed in the crude residue which were isolated and recrystallised from EtOH. 1H NMR analysis showed the crystals to be a mixture of (168) and a cis adduct. The isomers could be separated by crystal picking, the clusters of needle-like crystals of the cis adduct being clearly distinguishable from the plate-like crystals of (168). The cis adduct was shown to be (171) by $^1H\{^1H\}nOe$ studies (see Section 7.4.4.1). The properties of 2',2'-dimethylspiro[bicyclo[2.2.1]hept-5-ene-7,1'-cyclopropane]-2-endo-3-endo-dicarbonitrile (171) were as follows. M.p. (EtOH) 198-200°. (Found C, 78.33; H, 7.24; N, 14.16. $C_{13}H_{14}N_2$ requires C, 78.75; H, 7.12; N, 14.13%). 1H NMR δ ($CDCl_3$): 0.26 (2H, s, 2 x 3'-H); 1.20 (6H, s, methyls); 2.98 (2H, s, 2-H, 3-H); 3.38 (2H, s, 1-H, 4-H); 6.57 (2H, s, 5-H, 6-H). IR ν max: 2245 cm^{-1} ($C \equiv N$). MS m/z (EI): 198 (M, 1.1%); 171 (M-HCN, 1); 120 (16); 105 (100); 91 (10); 78 (13); 77 (11).

The cis adduct not isolated was 3',3'-dimethylspiro[bicyclo[2.2.1]hept-5-ene-7,1'-cyclopropane]-2-endo-3-endo-dicarboinitrile (172) and had the following ^1H NMR data: δ (CDCl_3); 0.41 (2H, s, 2 x 2'-H); 1.20 (6H, s, methyls); 3.00 (2H, s, 2-H, 3-H); 3.20 (2H, s, 1-H, 4-H); 6.34 (2H, s, 5-H, 6-H).

Reaction with dimethylfumarate

^1H NMR and capillary g.c. analysis of the crude reaction mixtures indicated two 1:1 adducts formed in the ratio of 95:5. The major adduct crystallised and was shown to be 2',2'-dimethylspiro[bicyclo[2.2.1]hept-5-ene-7,1'-cyclopropane]-2-endo-3-exo-dicarboxylic acid dimethyl ester (173) by $^1\text{H}\{^1\text{H}\}\text{nOe}$ studies. A sample recrystallised from EtOH had m.p. 78-78.5°. ^1H NMR δ (CDCl_3): 0.38 (1H, d, $J=5.4$ Hz, 3'-H); 0.40 (1H, d, $J=5.4$ Hz, 3'-H); 0.93 (3H, s, methyl); 0.97 (3H, s, methyl); 2.76 (1H, d, $J=4.4$ Hz, 2-H); 2.87 (1H, m, 1-H or 4-H); 2.88 (1H, m, 1-H or 4-H); 3.63 (1H, apparent d (probably dd masked by ester methyl), $J=4.4$ Hz, 3-H); 3.65 (3H, s, methyl); 3.69 (3H, s, methyl); 6.10 (1H, dd, $J=2.6, 5.6$ Hz, 5-H or 6-H); 6.34 (1H, dd, $J=2.6, 5.6$ Hz, 5-H or 6-H). IR ν max: 1760 cm^{-1} (C=O). MS m/z (EI): 264 (m, 0.8%); 232 (M-MeOH, 13); 204 (11); 173 (21); 145 (52); 120 (35); 113 (32); 105 (100); 91 (18); 78 (112); 77 (14). CI (NH_3): 265 (MH^+ , 8.7).

Reaction with dimethyl maleate

^1H NMR analysis of the crude reaction mixture showed the presence of two cis adducts formed in the ratio 68:32. The major adduct was crystalline and could be isolated from the mixture.

$^1\text{H}(^1\text{H})\text{nOe}$ studies (Section 7.4.4.1) established that it was 2',2'-dimethylspiro[bicyclo[2.2.1]hept-5-ene-7,1'-cyclopropane]-2-endo-3-endo-dicarboxylic acid dimethyl-ester (175). Recrystallisation from EtOH gave white flakey crystals m.p. 79.5 - 80.5° (Found: C, 68.18; H, 7.88. $\text{C}_{15}\text{H}_{20}\text{O}_4$ requires: C, 68.16; H, 7.63%). ^1H NMR δ (CDCl_3): 0.22 (2H, s, 2 x 3'-H); 1.04 (6H, s, methyls); 2.79 (2H, s, 1-H, 4-H); 3.47 (2H, s, 2-H, 3-H); 3.62 (6H, s, methyls); 6.35 (2H, s, 5-H, 6-H). IR ν max: 1745 cm^{-1} (C=O). MS m/z (EI): 232 (M-MeOH, 2.7%); 204 (14); 149 (17); 145 (74); 120 (44); 113 (41); 105 (100); 91 (21); 78 (12) 77 (16); 59 (16). CI (NH_3): 265 (MH^+ , 8.1).

The product not isolated was an oil identified by $^1\text{H}(^1\text{H})\text{nOe}$ studies and ^1H NMR to be 3',3'-dimethylspiro[bicyclo[2.2.1]hept-5-ene-7,1'-cyclopropane]-2-endo-3-endo-dicarboxylic acid dimethyl ester (176). ^1H NMR δ (CDCl_3): 0.30 (2H, s, 2 x 2'-H); 1.05 (6H, s, methyls); 2.79 (2H, s, 1-H, 4-H); 3.30 (2H, s, 2-H, 3-H); 3.80 (6H, s, methyls); 6.26 (2H, s, 5-H, 6-H).

References for Chapter 1

1. R.B. Woodward and R. Hoffmann, *Angew. Chem. Int. Ed. Eng.*, **8**, 781 (1969).
2. L. Salem and C. Rowland, *Angew. Chem. Int. Ed. Eng.*, **11**, 92 (1972).
3. W. Kirmse "Carbene Chemistry", A.T. Blomquist, Ed., Academic Press, New York, 1964.
4. For a review see T. Bailey and S. Masamune, *Tetrahedron*, **36**, 343 (1980).
5. N.J. Turro, "Modern Molecular Photochemistry", Benjamin/Cummings, California, 1978.
6. Azulene and its derivatives give S_2-S_0 fluorescence which has an absorption maxima at ca 370 nm while the absorption spectra have maxima at ca 580 nm. S_2 emission occurs because the relatively large S_2-S_1 energy gap slows down the normally very rapid internal conversion. See M. Beer and H.C. Longuet-Higgins, *J. Chem. Phys.*, **23**, 1390 (1955).
7. M. Simmons, "Chemical and Biochemical Applications of Electron Spin Resonance Spectroscopy", Van Norstrand Reinhold, London, 1978.
8. For an example see M.S. Platz in "Diradicals", W.T. Borden, Ed., Wiley, New York, 1982, p. 208.
9. E. Wasserman, V.J. Kuck, R.S. Hutton and W.A. Yager, *J. Amer. Chem. Soc.*, **92**, 7491 (1970).
10. P. Dowd, *J. Amer. Chem. Soc.*, **88**, 2587 (1966).
11. M.S. Platz, J.M. McBride, R.D. Little, J.J. Harrison, A. Shaw, S.E. Potter and J.A. Berson, *J. Amer. Chem. Soc.*, **98**, 5725 (1976).

12. C.R. Watson, Jr., R.M. Pagni, J.R. Dodd and J.E. Bloor, *J. Amer. Chem. Soc.*, 98, 2551 (1976).
13. G. Kothe, K.H. Denkel and W. Simmermann, *Angew. Chem. Int. Ed. Eng.*, 9, 906 (1970).
14. S.L. Buchwalter and G.L. Closs, *J. Amer. Chem. Soc.*, 97, 3857 (1975).
15. S.L. Buchwalter and G.L. Closs, *J. Amer. Chem. Soc.*, 101, 4688 (1979).
16. M.P. Conrad, R.M. Pitzer and H.F. Schaefer III, *J. Amer. Chem. Soc.*, 101, 2245 (1979).
17. H.R. Ward in "Free Radicals", Vol. I, J.K. Kochi, Ed., Wiley, New York, 1973, p239-273.
18. R. Kaptein, F.J.J. De Kanter and G.H. Rist, *Chem. Commun.*, 499 (1981).
19. R. D. Small, Jr., J.C. Sciaino, *Chem. Phys. Letts.*, 50, 431 (1977).
20. D.F. Kelley, P.M. Rentzepis, M.R. Uazur and J.A. Berson, *J. Amer. Chem. Soc.*, 104, 3764 (1982).
21. (a) M. Demuth, D. Lemmer and K. Schaffner, *J. Amer. Chem. Soc.*, 102, 5409 (1980). (b) M. Demuth, W. Amrein, C.O. Bender, S.E. Braslavsky, U. Burger, M.V. George, D. Lemmer and K. Schaffner, *Tetrahedron*, 37, 3245 (1981).
22. See R.M. Wilson, S.W. Wunderly, T.F. Walsh, A.K. Mussur, R. Outcalt, F. Geiser, S.K. Gee, W. Brabender, L. Yerino, Jr., and G.A. Thorp, *J. Amer. Chem. Soc.*, 104, 4429 (1982) and references cited therein.
23. J.C. Sciaino, *J. Amer. Chem. Soc.*, 99, 1494 (1977).
24. P.J. Wagner and K.C. Liu, *J. Amer. Chem. Soc.*, 96, 5952 (1974); P.J. Wagner, K.C. Liu and Y. Noguchi, *ibid*, 103, 3837 (1981).

25. B.J. Caulsson and T.A. Hillard, *J. Amer. Chem. Soc.*, 94, 7047 (1972).
26. R.M. Wilson and F. Geiser, *J. Amer. Chem. Soc.*, 100, 2225 (1978).
27. W. Adam, K. Hannemann and R.M. Wilson, *J. Amer. Chem. Soc.*, 106, 7646 (1984).
28. W.T. Borden and E.R. Davidson, *J. Amer. Chem. Soc.*, 102, 5409 (1980).
29. P.D. Bartlett and R. Wheland, *J. Amer. Chem. Soc.*, 92, 3822 (1970).
30. P.D. Bartlett, *Quart. Rev. Chem. Soc.*, 24, 473 (1970).
31. B.S. Rabinovitch, E.W. Schlag and K.B. Wiberg, *J. Chem. Phys.*, 28, 504 (1958).
32. P.D. Bartlett and N.A. Porter, *J. Amer. Chem. Soc.*, 90, 5317 (1968).
33. S.W. Benson, "Thermochemical Kinetics", 2nd Ed., Wiley, New York, 1976.
34. H.E. O'Neal and S. W. Benson, *J. Phys. Chem.*, 72, 1866 (1968).
35. H. Fischer, in "Free Radicals", Vol. II, J.K. Kisti, Ed. Wiley, New York, 1973, p.483.
36. W. Von E. Doering, *Proc. Natl. Acad. Sci. USA*, 78, 5279 (1981).
37. F. Bernardi, A. Bottoni, M.A. Robb, H.B. Schleger and G. Tonachini, *J. Amer. Chem. Soc.*, 107, 2260 (1985).
38. J.J. Gajewski, "Hydrocarbon Thermal Isomerizations", Academic Press, New York, Chapter 3, p27, 1981.
39. F.T. Smith, *J. Chem. Phys.*, 29, 235 (1958).
40. H. Kollmar, *J. Amer. Chem. Soc.*, 95, 966 (1973).
41. R. Hoffmann, *J. Amer. Chem. Soc.*, 90, 1475 (1968).

42. See P.B. Dervan and D.A. Dougherty in "Diradicals", W.T. Borden, Ed., Wiley, New York, 1982, p.122 and references cited therein.
43. (a) K. Humski, R. Malojeic, S. Borcic, and D.E. Sunko, J. Amer. Chem. Soc., 92, 6534 (1970). (b) W. Van E. Doering, V.G. Toscano, and G.H. Beasley, Tetrahedron 27, 5299 (1971).
44. (a) P.B. Dervan and T. Uyehara, J. Amer. Chem. Soc., 98, 1262 (1976). (b) P.D. Dervan, T. Uyehara, and D.S. Santilli, ibid; 101, 2069 (1979).
45. G. Scacci, C. Richard and M.H. Back, Int. J. Chem. Kinet., 9, 513 (1977); 9, 525 (1977).
46. H.R. Gerberich and W.D. Walters, J. Amer. Chem. Soc., 83, 3935 (1961); 83, 4884 (1961).
47. P.B. Dervan and T. Uyehara, J. Amer. Chem. Soc., 101, 2076 (1979).
48. L.U. Stephenson and J.I. Brauman, J. Amer. Chem. Soc., 93, 1988 (1971).
49. (a) P.B. Dervan and D.S. Santilli, J. Amer. Chem. Soc., 101, 3663 (1979); 102, 3863 (1980).
50. J.A. Berson, D.C. Tompkins, and G. Jones, II, J. Amer. Chem. Soc., 92, 5799 (1970).
51. C.P. Casey and R.A. Boggs, J. Amer. Chem. Soc., 94, 6457 (1972).
52. L.M. Stephenson and T.A. Gibson, J. Amer. Chem. Soc., 96, 5624 (1974).

References for Chapter 2

1. For a review see; P.S. Engel, Chem. Rev., 80, 99 (1980).
2. W.R. Roth and M. Martin, Ann. der. Chemie., 702, 1 (1967).
3. R.B. Woodward and R. Hoffman, Angew. Chem. Int. Ed. Eng., 8, 781 (1969).
4. W.R. Roth and M. Martin, Tet. Lett., 4695 (1967).
5. J.H. Incremona and C.J. Upton, J. Amer. Chem. Soc., 94, 301 (1972).
6. G.G. Mayes and D.E. Applequist, J. Amer. Chem. Soc., 95, 856 (1973).
7. E.L. Allred and R.L. Smith, J. Amer. Chem. Soc., 89, 7133 (1967); 91, 6766 (1969).
8. P.S. Engel, R.A. Hayes, L. Keifer, S. Szilagyi, and J.W. Timberlake, J. Amer. Chem. Soc., 100, 1876 (1978).
9. R.G. Bergman in "Free Radicals", Vol. 1, J.G. Kochi, Ed., Wiley, New York, 1973, p.214.
10. W. Adam, T. Oppenlander, and G. Zarrg, J. Org. Chem., 50, 3303 (1985).
11. W. Adam, W.D.G. Gillaspey, E-M. Peters, R. J. Rosenthal, and H.G. Van Schnering, J. Org. Chem., 50, 580 (1985).
12. L.A. Paquette and L.M. Leichter, J. Amer. Chem. Soc., 92, 1765 (1970).
13. W.P. Lay, K. Mackenzie, and J.R. Telford, J. Chem. Soc. (C), 3199 (1971).
14. M.H. Chang, R. Jain, and D.A. Dougherty, J. Amer. Chem. Soc., 106, 4211 (1984).
15. K.B. Wiberg and J.U. Lavenish, J. Amer. Chem. Soc., 88, 5272 (1966).
16. For a review see; P.B. Dervan and D.A. Dougherty in "Diradicals", W.T. Borden, Ed., Wiley, New York, 1982, p.107.

17. T.C. Clarke, L.A. Wendling, and R.G. Bergman, *J. Amer. Chem. Soc.*, 99, 2471 (1977).
18. C.J. Samuel, *Chem. Commun.*, 131 (1982).
19. C.J. Samuel, *Chem. Commun.*, submitted for publication.
20. T. Uyehara, M. Takahashi, and T. Kato, *Tet. Lett.*, 1241 (1985).
21. The "only cleavage product is 3-methylhepta-1,6-diene which affords no stereochemical information.
22. S. Cremer and R. Srinivasan, *Tet. Lett.*, 24 (1960).
23. C. Steel, R. Zands, P. Hurwitz, and S.G. Cohen, *J. Amer. Chem. Soc.*, 86, 679, (1964).
24. L.A. Paquette and J.A. Schwartz, *J. Amer. Chem. Soc.*, 92, 3215 (1970).
25. Similar conclusions were reached by Cain and Solly; E.N. Cain, *Tet. Lett.* 1965 (1971); E.N. Cain and R. K. Solly, *J. Amer. Chem. Soc.*, 94, 3830 (1972); *Int. J. Chem. Kinet.*, 4, 159 (1972); *Aust. J. Chem.*, 25, 1443 (1972).
26. M.J. Goldstein and M.S. Benzon, *J. Amer. Chem. Soc.*, 94, 5119 (1972); 94, 7147 (1972).
27. For a relevant review see; G. M. Kellie and F.G. Riddell, "Non-Chair conformations of six-membered rings", in *Topics in Stereochemistry*, Vol. 8, E.L. Eliel and N.L. Allinger, Eds., Interscience, New York, 1974, p.225.
28. R.V. Lloyd, J.G. Causey, and F.A. Mamary, *J. Amer. Chem. Soc.*, 102, 2260 (1980).
29. A. Sinnema, F. Van Rantwijk, A.J. de Koning, A.M. Van Wijk, and H. Van Bekkum, *Chem. Commun.*, 364 (1973); *Tetrahedron*, 32, 2269 (1976).
30. B. Anderson and R. Srinivasan, *Acta. Chem. Scand.*, 26, 3468 (1972).

31. M.J.S. Dewar, G.P. Ford, M.L. McKee, H.S. Rzepa, and L.E. Wade, *J. Amer. Chem. Soc.*, 99, 5069 (1977).
32. H.C. Ramsperger, *J. Amer. Chem. Soc.*, 51, 2134 (1929).
33. This equation is derived assuming k_{rel} for (76) is the average of the rate constants for DBO and (75).
34. P.S. Engel, C.J. Nalepa, D.W. Horsey, D.E. Keys, and R.T. Gow, *J. Amer. Chem. Soc.*, 105, 7102 (1983).
35. W.R. Roth and M. Martin, *Tet. Lett.*, 3865 (1967).
36. W.R. Roth, unpublished data, cited by R.G. Bergman in "Free Radicals", Vol. 1, J.G. Kochi, Ed., Wiley, New York, 1973, p.229.
37. The calculated percentage of endo-(81) formed from syn-(79) (including the percentage of exo-(81) formed from syn-(79) (11.7%)) is $(96.1 - 11.7)/100 \times 7.1$, which gives 6.0% of endo-(81). Similarly, the percentage of exo-(81) formed from anti-(79) (7.0%) is $(97.7 - 7.0)/100 \times 17.1$, giving 15.5% of exo-(81). Thus, the exo-(81)/endo-(81) ratios calculated to arise from syn-(79) and anti-(79) are 11.7/6.0 and 15.5/7.0, giving 1.95 and 2.21, respectively.
38. W.D.K. Clark and C. Steel, *J. Amer. Chem. Soc.*, 93, 6347 (1971).
39. P.S. Engel, D.W. Horsey, D.E. Keys, C.J. Nalepa, and L.R. Soltero, *J. Amer. Chem. Soc.*, 105, 7108 (1983).
40. (a) H. Tanida, S. Terataki, Y. Hata, and M. Watanabe, *Tet. Lett.*, 5345 (1969).
(b) L.A. Paquette and L.M. Leichter, *J. Org. Chem.*, 39, 461 (1974).
41. (a) N.J. Turro, J-M. Liu, H-D. Martin, and M. Kunze, *Tet. Lett.*, 1299 (1980).
(b) H-D. Martin, E. Eisenmann, M. Kunze, and V. Bonacic-Kontecky, *Chem. Ber.*, 113, 1153 (1980).
42. H-D. Martin and M. Heckman, *Tet. Lett.*, 1183 (1978).

References for Chapter 3

1. For the Diels-Alder reaction see; B.T. Gillis and J.D. Hagarty, *J. Org. Chem.* 32, 330 (1967). The hydrolysis and oxidation of triazolinediones has been reported by W. Adam, O. de Lucchi, and I. Erden, *J. Amer. Chem. Soc.*, 102, 4806 (1980). The general procedure is analogous to that of P.S. Engel, R.A. Hayes, L. Keifer, S. Szilagyi, and J.W. Timberlake, *J. Amer. Chem. Soc.*, 100, 1876 (1978).
2. For a review see; A.F. Cockerill, G.L.O. Davies, R.C. Harden, and D.M. Rackham, *Chem. Rev.*, 73, 553 (1973).
3. D.J. Chadwick and D.H. Williams, *J. Chem. Soc., Perkin II*, 1202 (1974).
4. P.N. Rylander, *Aldrichimica Acta*, 12, 53 (1979).
5. O. Diels, J. H. Blom, and W. Kohl, *Annalen*, 443, 243 (1925).
6. (a) J. Pirsch and J. Jörgl, *Ber.*, II, 68, 1324 (1935). (b) S.G. Cohen and R. Zand, *J. Amer. Chem. Soc.*, 84, 586 (1962).
7. R.C. Cookson, S.S.H. Gilani, and I.D.R. Stevens, *J. Chem. Soc.*, (c), 1905 (1967).
8. R. Askani, *Chem. Ber.*, 98, 2551 (1965).
9. R.B. Woodward and R. Hoffmann, *Angew. Chem. Int. Ed. Engl.*, 8, 781, (1969).
10. Similar effects are observed for the diethyl analogues, See: J.M. Lehn and J. Wagner, *Tetrahedron*, 25, 677 (1969); J.E. Anderson and J.M. Lehn, 24, 123 (1968).
11. P.G. Gassman, P.K. Hodgson and R.J. Balchunis, *J. Amer. Chem. Soc.*, 98, 1275 (1976).
12. E.A. Wildi and B.K. Carpenter, *Tet. Let.*, 2469 (1978).

13. M.E. Jung and M.A. Lyster, *J. Chem. Soc. Chem. Commun.*, 315 (1978).
14. Electronic effects are also more important than steric effects in the diimide reductions of 7-substituted norborgenes; W.C. Baird, Jr., B. Franzus and J.H. Surridge, *J. Amer. Chem. Soc.*, 89, 410 (1967).
15. For a detailed discussion see; K. Bieman, "Mass Spectroscopy; Organic Chemical Applications", McGraw-Hill, New York, 1962, Chapter 5, p. 204.

References for Chapter 4

1. (a) P.S. Engel, D.W. Horsey, D.E. Keys, C.J. Nalepa and L.R. Soltero, *J. Amer. Chem. Soc.*, 105, 7180 (1983). (b) C. Steel and W.D. Clark, *ibid*, 93, 6347 (1971).
2. M.J. Goldstein and M.S. Benzon, *J. Amer. Chem. Soc.*, 94, 5119 (1971).
3. For a recent review of nitrogen NMR see; M. Witanowski, E.A. Webb, and L. Stefaniak, *Ann. Rep. NMR Spec.*, 11B, 1 (1981).
4. E.L. Eliel "Stereochemistry of Carbon Compounds", McGraw-Hill, New York, 1962, Chapter 8.
5. P.S. Engel, R.A. Hayes, L. Keifer, S. Szilagyi, and J.W. Timberlake, *J. Amer. Chem. Soc.*, 100, 1876 (1978).
6. (a) A. Ruttiman, A. Wick, and A. Eschenmopser, *Helv. Chim. Acta.*, 58, 1450 (1975). (b) W.G. Dauben, D.J. Hart, J. Ipartschi, and A.P. Kozikowski, *Tet. Lett.*, 4425 (1973). (c) K. Alder and H. Van Brachel, *Liebigs, Ann. Chem.*, 608, 195 (1957).
7. L.A. Paquette and J.H. Barrett in "Organic Synthesis", Col. Vol. V, 467 (1973).
8. W.T. Brady, S.D. Norton and J. Ko, *Synthesis*, 704 (1985).

References for Chapter 5

1. M.J. Goldstein and M.S. Benzon, *J. Amer. Chem. Soc.*, 94, 5119 (1972); M.S. Benzon, Ph.D. Thesis, Cornell University, 1971.
2. W. von E. Doering, *Proc. Natl. Acad. Sci. USA*, 78, 5279 (1981).
3. K.B. Wiberg, M.G. Matturo, P.J. Okarama, and M.E. Jason, *J. Amer. Chem. Soc.*, 106, 2194 (1984).
4. E. Casadevall, C. Largeau, and P. Moreau, *Bull. Soc. Chim. Fr.*, 1514 (1968).
5. C.J. Samuel, *Chem. Commun.*, 131 (1981).
6. D.C. Owsley and J.J. Bloomfield, *J. Org. Chem.*, 36, 3768 (1971).
7. E.E. van Tamelen, S.P. Pappas and K.L. Kirk, *J. Amer. Chem. Soc.*, 92, 6092 (1971).
8. W. von E. Doering, V.G. Toscano, and G.H. Beasley, *Tetrahedron*, 27, 5299 (1971).
9. C.J. Samuel, *Chem. Commun.*, submitted for publication.
10. P.B. Hopkins and P.L. Fuchs, *J. Org. Chem.*, 43, 1208 (1978).
11. W.H. Mueller and P.E. Butler, *J. Amer. Chem. Soc.*, 88, 2866 (1966); 90, 2075, (1968).
12. W.A. Smit, N.S. Zevirov, I.V. Bodrikov, and M.Z. Krimer, *Acc. Chem. Res.*, 12, 282 (1979).
13. V. Fiandanese, C.V. Maffeo, G. Marchese, and F. Naso, *J. Chem. Soc. Perkin II*, 221 (1975); J.C. Phillips and L.C. Hernandez, *Tet. Lett.*, 4461 (1977).
14. K. Biemann, "Mass Spectroscopy. Organic Chemical Applications", McGraw-Hill, New York, 1962, Chapter 5.
15. C.H. de Puy and R.W. King, *Chem. Rev.*, 60, 431 (1960); E.R. Nace in, "Organic Synthesis", Vol. 12, 57, Wiley, New York (1964).

16. H.H. Bosshard, R. Mory, M. Schmid, and H. Zollinger, *Helv. Chim. Acta*, 42, 1653 (1959).
17. C.R. Childs and K. Bloch, *J. Org. Chem.*, 26, 1630 (1961).
18. R. Hoffmann, A. Imamura, and W.J. Hehre, *J. Amer. Chem. Soc.*, 90, 1499 (1968); R. Hoffman, *Acc. Chem. Res.*, 15, 245 (1982).
19. M.J.S. Dewar, G.P. Ford, M.L. McKee, H.S. Rzepa, and L.E. Wade, *J. Amer. Chem. Soc.*, 99, 5069 (1977).
20. K.B. Wiberg and M.G. Matturo, *Tet. Lett.*, 3481 (1981).
21. D. Kaufmann and A. de Meijère, *Chem. Ber.*, 117, 3134 (1984).
22. R.V. Lloyd, J.G. Causey, and F.A. Momary, *J. Amer. Chem. Soc.*, 102, 2260, (1980).
23. For a summary of the arguments see J.J. Gajewski in "Hydrocarbon Thermal Isomerisations", Academic Press, New York, 1981, Chapter 6.
24. W. Tsang, *J. Amer. Chem. Soc.*, 107, 2872 (1985).
25. J.J. Gajewski and N.D. Conrad, *J. Amer. Chem. Soc.*, 100, 6269 (1978); 101, 6693 (1979).
26. Y. Osamura, S. Kato, K. Morokuma, D. Feller, E.R. Davidson, and W.T. Borden, *J. Amer. Chem. Soc.*, 106, 3362, (1984).

References for Chapter 6

1. The procedure was modified from that of J.F. Savage, R.H. Baker, and A.S. Hussey, *J. Amer. Chem. Soc.*, 82, 6090 (1960).
2. R. Srinivasan, *Int. J. Chem. Kinet.*, 1, 133 (1969).
3. P.S. Engel, C.J. Nalepa, D.W. Horsey, D.E. Keys, and R.T. Gow, *J. Amer. Chem. Soc.*, 105, 7102 (1983).
4. P.B. Dervan and T. Uyehara, *Chem. Commun.*, 469 (1979).
5. P.S. Engel, D.W. Horsey, D.E. Keys, C.J. Nalepa, and L.R. Soltero, *J. Amer. Chem. Soc.*, 105, 7108 (1983).
6. C.J. Samuel, *Chem. Commun.*, submitted for publication, 1986.
7. A number of chemical consequences of TS and TB interactions have been discussed, see; R. Hoffmann, A. Imamura, and W.J. Hehre, *J. Amer. Chem. Soc.*, 90, 1499 (1968); R. Hoffmann, *Acc. Chem. Res.*, 4, 1 (1971); M.N. Paddon-Row, *Acc. Chem. Res.*, 15, 245 (1982).
8. The mechanism is analogous to that proposed to account for the formation of peroxide and eneone in the oxygen trapping study of cyclohexane-1,4-diyl from the photosensitised decomposition of DBO. See; W. Adam, K. Hannemann, and R. Marshall-Wilson, *J. Amer. Chem. Soc.*, 106, 7646 (1984).

References for Chapter 7

1. H.E. Zimmerman, P. Hackett, D.F. Juers, J.M. McCall, and B. Schroder, *J. Amer. Chem. Soc.*, 93, 3653 (1971).
2. H.E. Zimmerman, P. Hackett, D.F. Juers, J.M. McCall, and B. Schröder, *J. Amer. Chem. Soc.*, 93, 3662 (1971).
3. For a review see H.E. Zimmerman in "Rearrangements in Ground and Excited States", Vol. 3, P.de Mayo, Ed., Academic Press, New York, 1980, p.146.
4. For a review see J.A. Berson in "Rearrangements in Ground and Excited States", Vol., P. de Mayo, Ed., Academic Press, New York, 1980, p.311.
5. P. Dowd, *J. Amer. Chem. Soc.*, 88, 2587 (1966); *Acc. Chem. Res.*, 5, 242 (1972).
6. R.J. Baseman, D.W. Pratt, M. Chow, and P. Dowd, *J. Amer. Chem. Soc.*, 99, 6438 (1977).
7. H.C. Longuet-Higgins, *J. Chem. Phys.*, 18, 265 (1950).
8. R.J. Crawford and D.M. Cameron, *J. Amer. Chem. Soc.*, 88, 2589 (1966); J.J. Gajewski, A. Yeshurun, and E.J. Bair, *J. Amer. Chem. Soc.*, 94, 2138 (1972).
9. For a review see J.A. Berson in "Diradicals", W.T. Borden, Ed., Wiley, New York, 1982, Chapter 4.
10. J.A. Berson, R.J. Bushby, J.M. McBride, and M. Tremelling, *J. Amer. Chem. Soc.*, 93, 1544 (1971).
11. M.S. Platz and J.A. Berson, *J. Amer. Chem. Soc.*, 98, 6743 (1973); 102, 2358 (1980).
12. M.R. Mazur and J.A. Berson, *J. Amer. Chem. Soc.*, 103, 684 (1981); 104, 2217 (1982).

13. J.A. Berson, C.D. Duncan, and L.R. Corwin, *J. Amer. Chem. Soc.*, 96, 6175 (1974); J.A. Berson, L.R. Corwin and J.H. Davis, *J. Amer. Chem. Soc.*, 96, 6177 (1974).
14. R.D. Little, G.W. Muller, M.G. Venegas, G.L. Carroll, A. Bukhari, L. Patton, and K. Stone, *Tetrahedron*, 37, 4371 (1981).
15. For examples of magnetic anisotropic effects of cyclopropane rings in tricyclo[3.2.1.0^{2,4}] systems see; J. Haywood-Farmer, R.E. Pincock, and J.I. Wells, *Tetrahedron*, 22, 2007 (1966), and references cited therein.
16. For examples see; S. Winstein, P. Carter, F.A.L. Anet, and A.J.R. Bourne, *J. Amer. Chem. Soc.*, 87, 5243 (1965); C.G. Cardenas, *Tet. Lett.*, 4013 (1969); W. Nagata, T. Terasawa and K. Tori, *J. Amer. Chem. Soc.*, 86, 3764 (1964).
17. R.B. Woodward and R. Hoffmann, "The Conservation of Orbital Symmetry", Academic Press, New York, 1970, p.145.
18. D.I. Schuster, *Acc. Chem. Res.*, 11, 65 (1978).
19. D.I. Schuster and V.Y. Abraitys, *Chem. Commun.*, 419 (1969).
20. C.J. Samuel, *J. Chem. Soc. Perkin II*, 736 (1981).

Appendix 1

The natural isotope contributions to the azo precursors ((86H) and 90H) and protio disulphone were calculated using the following BASIC program on a Hewlett Packard 9845 B computer.

```

10 OPTION BASE 1
20 DIM Hght2(0:100),F(5),Elements(2),Formulas(70)
30 COM Hght1(0:100),Ip
40 INTEGER Nf,Mass,Nis,A
50 Dummy: DATA 0,0
60 H: DATA 2,01,.99985,.00015
70 C: DATA 2,12,.9889,.0111
80 N: DATA 2,14,.9964,.0036
90 O: DATA 3,16,.99761,.00039,.00200
100 F: DATA 1,19,1.0
110 Si: DATA 3,28,.9223,.0467,.0310
120 P: DATA 1,31,1.0
130 S: DATA 5,32,.9500,.0076,.0422,0,.0002
140 Cl: DATA 3,35,.7577,0,.2423
150 MAT Hght1=ZER
160 Hght1(I)=1
170 Ip=1
180 Nf=0 !this is the first line of a loop executed for each element
190 INPUT "Element symbol,Number of atoms",Elements,Nf
200 IF Nf=0 THEN 520 ! implies no input before "continue" ie calc finished
210 RESTORE Dummy ! this is to cope with unknown elements or errors
220 IF Elements="H" THEN RESTORE H
230 IF Elements="C" THEN RESTORE C
240 IF Elements="N" THEN RESTORE N
250 IF Elements="O" THEN RESTORE O
260 IF Elements="F" THEN RESTORE F
270 IF Elements="Si" THEN RESTORE Si
280 IF Elements="P" THEN RESTORE P
290 IF Elements="S" THEN RESTORE S
300 IF Elements="Cl" THEN RESTORE Cl
310 MAT F=ZER
320 READ Nis,A
330 IF Nis=0 THEN 650 !this is only true if dummy has been read
340 IF Nis=1 THEN 500 !jumps over calculation for monoisotopics
350 FOR I=1 TO Nis
360 READ F(I)
370 NEXT I
380 FOR I=1 TO Nf
390 Ip=Ip+Nis-1
400 FOR J=1 TO Nis
410 FOR K=J TO Ip
420 Hght2(K)=Hght2(K)+F(J)*Hght1(K-J+1)
430 NEXT K
440 NEXT J
450 MAT Hght1=Hght2
460 GOSUB 680 !tests for low intensity high mass peaks and discards them
470 MAT Hght2=ZER
480 NEXT I
490 Formulas=Formulas&Elements&","&VALS(Nf)&","
500 Mass=Mass+Nf*A
510 GOTO 100
520 PRINTER IS 8
530 PRINT LIN(3),CHR$(132),Formulas,CHR$(128),LIN(1)
540 FOR I=1 TO Ip
550 PRINT Mass-I*1,
560 FIXED 5
570 PRINT Hght1(I)
580 STANDARD
590 NEXT I
600 PRINTER IS 16
610 DISP "Do you want to use this to correct LABELS? Continue or Stop"
620 PAUSE
630 LINK "LABELS"
640 STOP
650 DISP "Unknown Element, Press continue"
660 PAUSE
670 GOTO 100
680 FOR J=Ip TO 1 STEP -1
690 IF Hght1(J)>1E-6 THEN 710
700 NEXT J
710 Ip=J
720 RETURN

```

The program calculates the relative abundance of isotopes in the molecular ion group using typical values for the relative abundance of the isotopes. Whenever possible experimental values (obtained directly from MS ion intensities of the molecular ion group) were used or, if the higher mass peaks are not detected by MS, experimental values corrected to take into account the undetected peaks. For example, the calculated natural isotope contributions for the molecular ion group of (90H) were;

(M) 284, (M+1) 285, (M+2) 286, (M+3) 287, (M+4) 288, (M+5) 289
 %83.807, 14.208, 1.801, 0.170, 0.013, 0.001.

The experimental values from MS for the same precursor (6 scans) were;
 % 83.677, 14.309, 2.014.

The experimental values are corrected to take into account any (M+3), (M+4), and (M+5) peaks not detected by MS. This was achieved by assuming the missing values were present but not detected and multiplying the experimental values by the fraction; $1 - (0.170 + 0.013 + 0.001)/100$. For example, the experimental values for a sample of (90H) were:

(M),	(M+1)	(M+2)	(M+3)	(M+4)	(M+5)
%83.677,	14.309,	2.014	-	-	-

the "preferred" values were:

%83.523,	14.283,	2.010,	0.170,	0.013,	0.001
----------	---------	--------	--------	--------	-------

Appendix 2

The deuterium content of the azo precursors (86D) and (90D), and disulphones from the stereochemical analysis was determined as follows;

Let the measured MS molecular ion group intensities be M, M+1, M+2, ... M+n. M arises from molecules containing no deuterium atoms (d_0) and no other heavy atoms (h_0) such as ^{13}C . Thus;

$$M = h_0 d_0 \text{ where } h_0 \text{ and } d_0 \text{ are expressed as fractions.}$$

M+1 can arise from molecules containing no deuterium atoms (d_0) and one heavy atom (h_1) or one deuterium atom (d_1) and no heavy atoms (h_0). Thus;

$$M+1 = h_0 d_1 + h_1 d_0$$

Similarly;

$$M+2 = h_2 d_0 + h_1 d_1 + h_0 d_2$$

In general;

$$M+n = h_n d_0 + h_{n-1} d_1 + h_{n-2} d_2 \dots h_0 d_n$$

Since the ion intensities of deuterated samples can be obtained by MS, and the percentage values $h_0 + h_n$ can be calculated or measured as discussed in Appendix 1 the set of equations;

$$M = h_0 d_0$$

$$M+1 = h_1 d_0 + h_0 d_1$$

$$M+2 = h_2 d_0 + h_1 d_1 + h_0 d_2$$

$$M+n = h_n d_0 + h_{n-1} d_1 + h_{n-2} d_2 \dots h_0 d_n$$

can be solved by a least squares analysis to obtain percentage values for $d_0, d_1, d_2 \dots d_n$. The equations were solved using the following BASIC program on a Hewlett Packard 9845B computer;

```

10   DIM H(9),A(9,9),P(9,9),Q(9,9),R(9,9),S(9,9),T(9),D(9),V(9),C(9),W(9),X(9),
Y(9)
20   COM Hght1(100),Ip
30   M=Ip-1
40   FOR I=0 TO M
50   H(I)=Hght1(I+1)
60   NEXT I
70   INPUT "Maximum number of labels per molecule",N
80   INPUT "Highest mass peak in the unlabelled compound is parent+",M
90   INPUT "Highest mass peak in the labelled compound is parent+",L
100  FOR I=M+1 TO 9
110  H(I)=0
120  NEXT I
130  INPUT "Ion intensities at natural abundance",H(*)
140  REDIM A(L,N)
150  MAT A=ZER
160  FOR I=0 TO N
170  FOR J=I TO L
180  A(J,I)=H(J-I)
190  NEXT J
200  NEXT I
210  REDIM D(L),P(N,L),Q(N,N),R(N,N),S(N,L),T(N),V(N),C(L),W(L),X(L),Y(L)
220  INPUT "Ion intensities in the labelled compound",D(*)
230  MAT P=TRN(A)
240  MAT Q=P*A
250  MAT R=INV(Q)
260  MAT S=R*P
270  MAT T=S*D
280  MAT C=A*T
290  MAT X=C/(SUM(C)/100)
300  MAT W=D/(SUM(D)/100)
310  MAT V=T/(SUM(T)/100)
320  MAT Y=W-X
330  Error=SQR(DOT(Y,Y)/(L-N))
340  FIXED 3
350  PRINTER IS 0
360  FOR I=0 TO N
370  PRINT V(I);
380  NEXT I
390  PRINT TAB(70),Error,LIN(1)
400  PRINTER IS 16
410  PRINT PAGE,"EXPERIMENTAL          RECALCULATED          DIFFERENCE",LIN(1)
420  FOR I=0 TO L
430  PRINT W(I),X(I),W(I)-X(I)
440  NEXT I
450  PRINT LIN(2),H(*);
460  PRINT D(*);
470  DISP "DO YOU WANT TO CONTINUE OR STOP?"
480  PAUSE
490  DISP "TYPE IN ONLY DATA TO BE CHANGED. OTHERWISE CONTINUE"
500  PAUSE
510  GOTO 70
520  END

```


As the solution is achieved by a least squares analysis, for each set of experimental MS intensities input, the computer prints out a value for the square root of the sum of squares of errors together with the computed percentage proportions of d_0 , d_1 and d_2 molecules. The square root of the sum of squares of errors represents a "goodness of fit" for the input data (the lower the value, the better the data "goodness of fit"). The "goodness of fit" was normally < 1 .

Appendix 3

In Chapter 3 it was noted that precursors (86) and (90) undergo significant self-protonation in the mass spectrometer. This can lead to errors in the computed proportions of d_0 , d_1 , and d_2 molecules. We were initially alerted to the phenomenon by the "goodness of fit" values, which were significantly > 1 . For example a sample of (90D) prepared by Wilkinson's catalyst deuteration of (88) gave the following d_0 , d_1 , d_2 , and "goodness of fit" values for an MS run (5 scans).

	% Proportions			"Fit"
	d_0	d_1	d_2	
-0.005	1.106	98.899	7.316	
-0.005	1.195	98.810	7.299	
-0.005	0.873	99.132	7.706	
-0.005	1.356	98.649	7.390	
-0.005	1.043	98.962	7.007	

Self-protonation was shown to be occurring by analysing the experimental isotope abundancies of unlabelled precursors (see Section 3.3).

If the EIMS data of a labelled precursor are analysed as if d_3 material were present, self-protonation can be corrected for as follows.

If x_0 , x_1 , x_2 are the actual percentage abundances of d_0 , d_1 , d_2 after correction.

If y_0, y_1, y_2, y_3 are the erroneous percentage abundances of d_0, d_1, d_2, d_3 given by the procedure in Appendix 2 (assuming on chemical grounds that d_3 is absent and is only apparently present because of self-protonation) then

	§ Proportions			
	d_0	d_1	d_2	d_3
(1- λ) unprotonated	(1- λ) x_0	(1- λ) x_1	(1- λ) x_2	
λ protonated		λx_0	λx_1	λx_2

(where λ is the fraction of self-protonation). Adding gives:

$$y_0 = (1-\lambda)x_0$$

$$y_1 = (1-\lambda)x_1 + \lambda x_0$$

$$y_2 = (1-\lambda)x_2 + \lambda x_1$$

$$y_3 = \lambda x_2$$

$$x_0 = y_0/(1-\lambda)$$

$$(1-\lambda)x_1 + \alpha y_0 = y_1 \quad (\alpha = \lambda/1-\lambda)$$

$$\therefore x_1 = y_1/(1-\lambda) - \alpha y_0/(1-\lambda)$$

$$(1-\lambda)x_2 + \alpha y_1 - \alpha^2 y_0 = y_2$$

$$\therefore x_2 = -\alpha y_1/(1-\lambda) + \alpha^2 y_0/(1-\lambda) + y_2/(1-\lambda)$$

$$y_3 = \lambda x_2 = -\alpha^2 y_1 + \alpha^3 y_0 + \alpha y_2$$

$$\underline{\alpha^3 y_0 - \alpha^2 y_1 + \alpha y_2 - y_3 = 0}$$

Thus, once α is found, λ follows and x_0, x_1 and x_2 are easily calculated. The equation was solved using the following BASIC program on a Hewlett Packard 9854B computer:

```

10 INPUT "ABUNDANCES",Y0,Y1,Y2,Y3
20 A0=Y3/100
30 F=A0^3*Y0-A0^2*Y1+A0*Y2-Y3
40 G=3*A0^2*Y0-2*A0*Y1+Y2
50 A1=A0-F/G
60 IF ABS(A1-A0)<1E-4 THEN 90
70 A0=A1
80 GOTO 30
90 L=A1/(1+A1)
100 DISP "PERCENT PROTONATION =",L*100
110 X0=Y0/(1-L)
120 X1=(Y1-L*X0)/(1-L)
130 X2=Y3/L
140 FIXED 3
150 PRINT X0,X1,X2
160 STOP
170 END

```

Using the procedure to correct the d_0 , d_1 , d_2 values given earlier:

% Proportions					
erroneous	d_0	d_1	d_2	d_3	"Fit"
	0	1.082	87.300	11.617	0.112
	0	1.163	87.173	11.664	0.259
	0	0.872	86.857	12.271	0.212
	0	1.307	86.878	11.815	0.271
	0	1.026	87.765	11.209	0.293
% Proportions					
corrected	d_0	d_1	d_2	% Protonation	
	0	1.226	98.773	11.161	
	0	1.319	98.681	11.820	
	0	0.995	99.005	12.394	
	0	1.485	98.515	11.993	
	0	1.157	98.843	11.340	

Appendix 4

An examples of the procedure used to compute the data in Table was as follows:

A sample of (90D) obtained by Pd/C catalysed deuteration of (88) in EtOAc was introduced into the mass spectrometer and the M+n ion intensities of five scans recorded. These were analysed for d₀, d₁, d₂, d₃ as discussed in Appendix 2, using the calculated natural isotope abundances obtained as discussed in Appendix 1. The erroneous values of d₀, d₁, d₂, and d₃ were corrected for self-protonation as discussed in Appendix 3 to give the following data:

d ₀	% Proportions		% Protonation
	d ₁	d ₂	
0.741	9.551	89.707	2.135
0.750	9.243	90.008	2.123
0.702	9.661	89.637	2.056
0.739	9.868	89.394	2.366
0.729	9.391	89.881	2.128

Average: 0.732 9.543 89.725

The procedure was repeated on a second occasion and gave the following average (five scans) corrected d₀, d₁, d₂ values:

d ₀	d ₁	d ₂
0.732	9.398	89.870%

The data given in Table 3.7 were taken as the average value of the two results:

d ₀	d ₁	d ₂
0.732	9.471	89.798

Appendix 5

The general procedure used to compute the proportions of EE-, EZ-, and ZZ-d₂-diene isotopomers from the measured deuterium content of disulphones (see Appendix 2) is given in the following example:

A sample of disulphone obtained from direct photolysis of anti-d₂-DBO was analysed by CIMS (CH₄) and shown to have the following average (six scans) deuterium content;

d₀ 3.129 d₁ 44.460 d₂ 52.411%

The d₂-DBO was derived from a sample of precursor with the following deuterium content:

d₀ 0.000 d₁ 4.488 d₂ 95.512%

Given that EE-, EZ-, and ZZ- isotopomers only arise from 1,6-d₂-dienes, while the disulphone deuterium content arises from 1,6-d₂-dienes, 3,4-d₂-dienes, E- and Z-d₁-dienes, 3-d₁-diene, and d₀-diene, the measured content must be corrected by appropriate subtraction to give values for 1,6-d₂-dienes only. The figures obtained after correction can be expressed as percentages thus translating disulphone deuterium content into 1,6-d₂-diene stereochemical information. Thus:

1. d₂-disulphone (52.411%) arises from 3,4-d₂-diene and EE-1,6-d₂-diene (in the stereochemical analysis, E-deuterium is

retained and Z-deuterium is lost). ^2H NMR of the hydrocarbon products shows that 50% of the d_2 -diene is the 3,4-isotopomer. Assuming the deuterium content of the precursors (90D) is the same as the deuterium content of the diene, and since the proportion of d_2 -(90D) is 95.512%, the expected proportion of d_2 -disulphone from 3,4- d_2 -diene is $0.5 \times 95.512 = 47.756$. Thus of the 52.411% of d_2 -disulphone measured experimentally, $52.411 - 47.756$ arises from EE-1,6- d_2 -diene.

2. d_1 -disulphone arises from EZ-1,6- d_2 -diene, E-1- d_1 -diene, and 3- d_1 -diene. ^2H NMR analysis shows that 50% of the d_1 -diene (with the same deuterium content as d_1 -(90D)) is 3- d_1 -diene, and 50% 1- d_1 -diene. Of the 1- d_1 -diene there is a 50% probability that the deuterium is E. Thus, the total proportion of E-1- d_1 -diene and 3- d_1 -diene is $0.5 \times 0.5 \times 4.488$ (E-1- d_1 -diene) plus 0.5×4.488 (3- d_1 -diene). The measured proportion of d_1 -disulphone is 44.460% so the fraction arising from EZ-1,6- d_2 -diene is $44.460 - [(0.5 \times 0.5 \times 4.488) + (0.5 \times 4.488)]$.

3. d_0 -disulphone arises from ZZ-1,6- d_2 -diene, Z-1- d_1 -diene, and d_0 -diene. The proportion of Z-1- d_1 -diene is identical to the proportion of E-1- d_1 -diene calculated in (2). The proportion of d_0 -diene is equivalent to the proportion of d_0 -precursor (0.000%). The measured proportion of d_0 -disulphone is 3.129% so the fraction arising from ZZ-1,6- d_2 -diene is $3.129 - [(0.5 \times 0.5 \times 4.488) + (0.000)]$.

Performing the subtractions in (1), (2) and (3) gives the following data, equivalent to the fractions of d_1 -disulphones arising from EE-, EZ-, and ZZ-1,6- d_2 -dienes:

- (1) $52.4111 - 47.756 = 4.655 \equiv \text{EE}$
- (2) $44.460 - [(0.5 \times 0.5 \times 4.488) + (0.5 \times 4.488)]$
 $= 41.094 \equiv \text{EZ}$
- (3) $3.129 - [(0.5 \times 0.5 \times 4.488) + (0.000)] = 2.007$
 $\equiv \text{ZZ}$

The values were expressed as percentages giving the following stereochemical results:

%	ZZ-	EZ-	EE-1,6-d ₂ -diene
	4	86	10

The CIMS analysis of the same sample of disulphone was repeated on two further occasions and led to the following measured disulphone deuterium contents:

run 2	d ₀	2.785	d ₁	44.343	d ₂	52.872%
run 3	d ₀	2.981	d ₁	43.021	d ₂	53.998%

Correcting the measured values to take into account disulphones formed from d₀- and d₁-diene, and 3,4-d₂-diene (as discussed above) gave the following values;

run 2	d ₀	1.663	d ₁	40.977	d ₂	5.116
run 3	d ₀	1.859	d ₁	39.665	d ₂	6.242

Expressing these values as percentages gave the following stereochemical data:

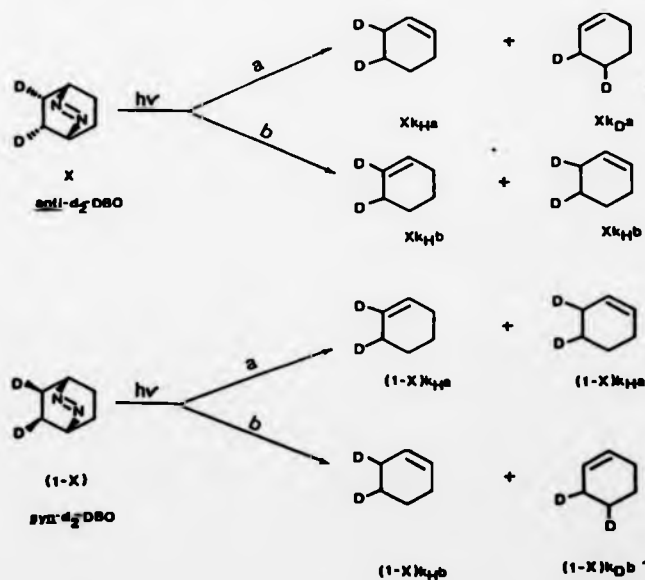
	ZZ-	EZ-	EE-1,6-d ₂ -diene
run 2	3	86	11
run 3	4	83	13

The three runs were quoted as one value with the percentage deviation from the mid-value:

ZZ-	EZ-	EE-1,6-d ₂ -diene
3.5 ± 0.5	84.5 ± 1.5	11.5 ± 1.5%

Appendix 6

In Chapter 6 it was shown that direct photochemical decomposition of d_2 -DBO led to cyclohexene, a 1,3-shift product. From ^2H NMR integrals of cyclohexenes obtained from samples of d_2 -DBO with different syn/anti ratio's we were able to determine the primary KIE for the 1,3-shift and the degree of stereoselectivity with which it occurred. The calculation does not require involvement of biradical intermediates thereby avoiding mechanistic bias. The relevant parameters are given in the following scheme;



x is the proportion of anti- d_2 -DBO and $(1-x)$ the proportion of syn- d_2 -DBO from integration of ^2H NMR spectra. The nitrogen leaves from the "upper" face depicted in the scheme so a represents the proportion of shift which occurs from the anti-face and b the

proportion of shift from the syn-face (relative to the -N=N- in d_2 -DBO). The values k_H and k_D represent the proportions of H-shift (k_H) and D-shift (k_D) and are related to the rate of H- and D- shift. The ratio k_H/k_D is the primary KIE for the reaction. The other information required is the ratio's of sp^3 (C4, C5) and olefinic cyclohexene 2H NMR integrals. From the scheme we have;

Olefinic 2H NMR signals arising from:

$$k_H x b + k_H (1-x) a$$

but $a+b=1 \therefore b=1-a$ so olefinic 2H NMR signals arise from:

$$\begin{aligned} k_H x - k_H x a + k_H (1-x) a \\ = \underline{k_H x + k_H a (1-2x)}. \end{aligned}$$

Similarly, sp^3 2H NMR signals arise from:

$$k_H x a + k_D x a + k_H (1-x) a + k_H x b + k_H (1-x) b + k_D (1-x) b.$$

Substituting b for $1-a$ and simplifying gives:

$$\underline{k_H - k_D (1-2x) a + k_D (1-x)}$$

CASE 1 d_2 -DBO (68% anti, 32% syn-deuterium) leads to cyclohexenes with an sp^3 /olefinic 2H NMR signal integral ratio of 3.933. Thus;

$$\begin{aligned} 3.933 = \frac{k_H - k_D (1-1.36) a + 0.32 k_D}{0.68 k_H + k_H (1-1.36) a} \end{aligned}$$

$$\therefore 3.933 (0.68 k_H - 0.36 k_H a) = k_H + 0.36 k_D a + 0.32 k_D$$

$$2.674 k_H - 1.416 k_H a = k_H + 0.36 k_D a + 0.32 k_D$$

$$1.674 k_H - 1.416 k_H a - 0.36 k_D a = 0.32 k_D$$

let $k_H/k_D = \alpha$

thus:

$$1.674\alpha - 1.416\alpha a - 0.36a = 0.32 \quad (1)$$

CASE 2 d_2 -DBO (40% anti- and 60% syn-deuterium gives cyclohexene with an sp^3 /olefinic 2H NMR integral ratio of 1.907. Thus:

$$1.907 = \frac{k_H - k_D(1-0.8)a + 0.6k_D}{0.4k_H + k_H(1-0.8)a}$$

$$\therefore 1.907 (0.4k_H + 0.2k_H a) = k_H - 0.2k_D a + 0.6 k_D$$

$$\therefore 0.763k_H + 0.381k_H a = k_H - 0.2 k_D a + 0.6 k_D$$

$$\therefore -0.237k_H + 0.381k_H a + 0.2k_D a = 0.6k_D$$

let $k_H/k_D = \alpha$

thus:

$$-0.237\alpha + 0.381\alpha a + 0.2a = 0.6 \quad (2)$$

The simultaneous equations (1) and (2) can be solved for a in terms of α to give

$$a = -2.07\alpha + 6.658$$

substituting a into equation (1) gives:

$$2.931\alpha^2 - 7.009\alpha - 2.717 = 0$$

Solution of this quadratic equation gives $\alpha = 2.73$ or -0.34 . Since α is the primary KIE for the 1,3-shift it must have a value ≥ 0 . Thus $k_H/k_D = 2.73$.

The degree of stereoselectivity is found by substituting the calculated α value into equation (1). This leads to a value for α of $1.006 \approx 1.0$ ie the shift occurs exclusively from the anti-face of d_2 -DBO. This was confirmed experimentally since d_2 -DBO with $> 99\%$ anti-deuterium led to cyclohexene with no olefinic deuterium, fully consistent with a 1,3-shift occurring only from the anti-face of the anti- d_2 DBO. The mechanism of the reaction was discussed in Section 6.4.